Technical Report
RAL-TR-96-005

Particle Physics Experiments Report 1995

B A Roberts (Compiler)

February 1996

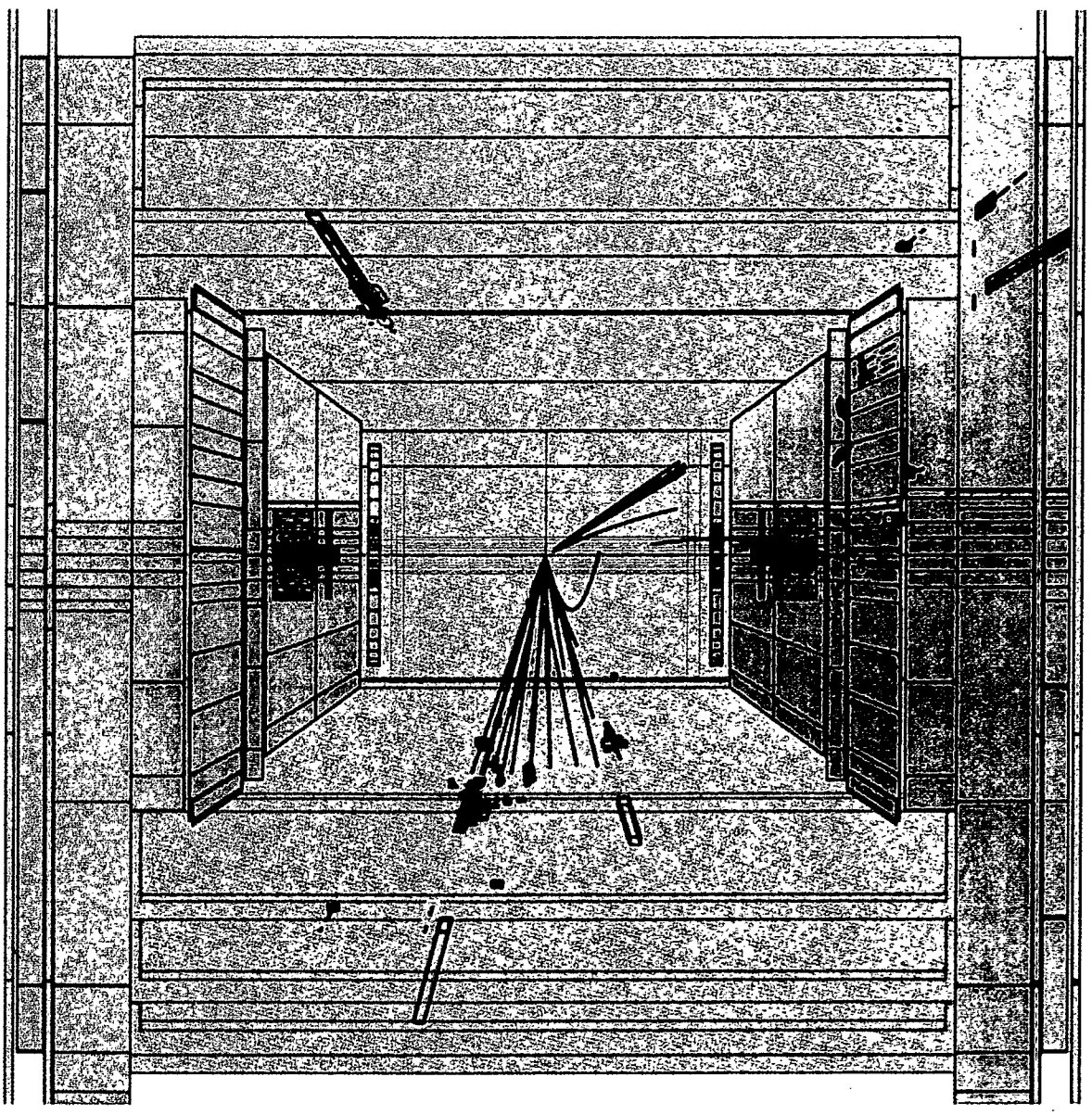

COUNCIL FOR THE CENTRAL LABORATORY OF THE RESEARCH COUNCILS

PARTICLE PHYSICS EXPERIMENTS

1995

COMPILED BY: B A ROBERTS

INTRODUCTION

This report describes work carried out in 1995 on experiments approved by the Particle Physics Experiments Selection Panel. The contents consist of unedited contributions from each experiment.

Rutherford Appleton Laboratory
Chilton
Didcot
OXON
OX11 0QX

FRONT COVER

One of the highest energy e^+e^- collisions ever, recorded by DELPHI at LEP in November 1995

The event is the associated production of a photon and a Z^0, followed by the decay of the Z^0 into two jets and the detection of the photon in the top left, a process which will be quite common at LEP 2. Measurement of the photon momentum allows the identification of the Z^0, even when the Z^0 decays to unobservable particles. Thus the rate of such decays can be measured.

Particle Physics and Astronomy Research Council

PARTICLE PHYSICS EXPERIMENTS

Accelerator	Year of Running	Status (Dec 1995)	Spokesman	Experiment Code
Reactor ILL	1980-1995	Running and Analysis	K F Smith	PN5
	1987-1995	Running and Analysis	D H Perkins	SOUDAN II
ISIS	1988-1995	Running and Analysis	J Kleinfeller	KARMEN
SPS	1982-1995	Running and Analysis	J B Kinson	WA76/WA91
FNAL	1985-1988	Analysis	G T Jones	E632
SLAC	1994-1995	Running and Analysis	M Breidenbach	SLD
LEAR	1991-1995	Running and Analysis	E Gabathuler	PS195

Accelerator	Year of Running	Status (Dec 1995)	Spokesman	Experiment Code
LEAR	1989-1995	Running and Analysis	H Koch	PS197
	1994-1995	Running and Analysis	P F Smith	
SPS	1990-1995	Complete	G Romano D H Davis	NA34/P213 EMU09
SPS	1987-1995	Running and Analysis	J Kinson	WA85/WA94
		Preparation	N W Tanner	SNO
	1991 - 1995	Running and Analysis	J Lowe	AGS E813, 836, 886
SPS	1992 - 1995	Running and Analysis	D M Websdale	WA92
	1993 - 1995	Running and Analysis	N E Booth	

Accelerator	Year of Running	Status (Dec 1995)	Spokesman	Experiment Code
SPS	1993 - 1995	Running	K Peach	NA48
SPS	1994 - 1995	Running	J B Kinson	WA97
ILL	1993-1995	Running	K Green	
SPS	1993	Running and Analysis	V Smith	WA89
SPS	1995	Running	J B Kinson	WA102
PEP-II	1994 - 1995	Preparation	J Fry	BABAR
LEP	1989-1995	Running and Analysis	J Steinberger J C Thompson	ALEPH
LEP	1989-1995	Running and Analysis	A Michelini R M Brown	OPAL

Accelerator	Year of Running	Status (Dec 1995)	Spokesman	Experiment Code
LEP	1989-1995	Running and Analysis	U Amaldi W Venus	DELPHI
HERA	1992-1995	Running and Analysis	F Eisele J Dainton	H1
HERA	1992-1995	Running and Analysis	G Wolf R J Cashmore	ZEUS

Accelerator	Year of Running	Status (Dec 1995)	Spokesman	Experiment Code
LHC		Development	F Dydak P Jenni P Norton	ATLAS
LHC		Development	M Della Neggra T Virdee R M Brown	CMS
HERA		Running	G Court	HERMES
		Development	G Stefanini F Vasey I Kenyon	RD-23
		Development	G Hall	RD-20

Accelerator	Year of Running	Status (Dec 1995)	Spokesman	Experiment Code
		Development	J Hassard	RD-42
		Development	R M Brown D J A Cockerill	
		Development	C Danson C B Edwards	-

Electric Dipole Moment of the Neutron

PF2, TGV at Niveau D, ILL, Grenoble. Proposal 157

University of Sussex, RAL, ILL, Harvard, Washington.

For particles to have electric dipole moments (EDMs), the forces concerned in their structure must be asymmetric with regard to space-parity (P) and time reversal (T). P-violation is a well-known intrinsic feature of the weak interaction, but CP- (and hence T-) violation, which is believed to be responsible for the baryon asymmetry of the universe, has thus far been found only in the neutral kaon system. Such limited information leaves open a wide range of possibilities for competing theories attempting to explain the origin of T-violation. Experimental measurements of particle EDMs, and in particular that of the neutron, are providing some of the strongest additional constraints on these theories. The Standard Model of the electroweak interaction gives a contribution to the neutron EDM of the order of 10^{-31} to 10^{-33} e cm which, because it is second order in the weak interaction coupling constant, is very small. However, extensions to the Standard Model, such as additional Higgs fields, right-handed currents or supersymmetric partners, invariably give rise to dipole contributions which are of first order. These are necessarily much larger, and are typically of order 10^{-25} to 10^{-27} e cm. Large dipole moments might also come from CP-violation in the QCD sector of the strong interaction.

This experiment uses the Ramsey resonance technique to measure with very high precision the precession frequency of ultracold neutrons in a small magnetic field. The precession frequency will change in the presence of an electric field if the neutron has an EDM. The most recent result from our collaboration, published in 1990, was $d_n = -(3\pm2\pm4) \times 10^{-26}$ e cm; that of LNPI in Russia was $d_n = +(3\pm4\pm2) \times 10^{-26}$ e cm. During the last five years, the ILL reactor in Grenoble has been rebuilt and refurbished, and (as of Spring 1995) it is once again providing neutrons. Our collaboration is now the only group in the world able to improve upon this critical measurement.

As has been reported in previous years, we took the opportunity presented by the reactor shutdown to make significant changes to the hardware. During this past year, many of these changes have been completed, and we are now once again on the verge of taking data. The following paragraphs summarise the highlights of the progress made during 1995.

A new, large storage cell, machined in Russia from a single fused quartz boule, has been installed. This provides a sidewall suitable for containing both the neutrons and the polarised mercury atoms from our magnetometer, whilst acting as an excellent insulator for the applied high voltage. Using this bottle, we have demonstrated what we believe to be the first ever co-storage of hot polarised atoms with ultracold polarised neutrons. We have achieved excellent spin relaxation times of 170 s for the neutrons, and over 200 s for the mercury, which will allow us to measure the precession frequencies with unprecedented precision.

A new set of HV electrodes, designed and built at RAL, has also been installed. Their improved design, together with that of our new HV feedthrough, will allow us to apply very high voltages (perhaps up to 250 kV) without breakdown. We have successfully developed a technique for coating the electrodes with teflon; this has a considerably higher Fermi potential than aluminium, and is thus better able to contain the neutrons. The installation of NiMo-coated guide tubes has likewise improved the transmission efficiency of neutrons entering the storage cell.

Our new PC-based data acquisition (DAQ) system, written using the LabView software package, has been considerably upgraded. It is now possible to see online an enormous number of parameters that previously had to be extracted slowly offline, and correlations between different quantities that might be indicative of systematic errors should be significantly easier to uncover. The DAQ software also includes a data simulation facility, in order to test any data analysis procedures for hidden biases. A new central data storage facility at RAL will allow easy access to the data by our collaborators around the world.

Perhaps our most important milestone has been the convincing demonstration that the resonant frequencies of neutrons and mercury follow one another as the magnetic field drifts. Prior to this, it was necessary to measure the neutron frequency by fitting the neutron counts (as a function of applied rf frequency) over several cycles, and trying to compensate for the average change in field as seen by the (relatively crude) external magnetometers. Our new philosophy is to use the measured precession frequency of the mercury atoms to calculate the expected (i.e., zero EDM) resonant frequency of the neutrons on a cycle-by-cycle basis, and then to fit the neutron counts to a "mobile" Ramsey lineshape which moves in the appropriate way as the magnetic field drifts. The net effect is to fit the ratio of the two precession frequencies; it is this ratio which will be directly sensitive to the neutron EDM. The cycle-by-cycle fluctuations in field, clearly visible in the magnetometer data, are thus eliminated. This is demonstrated in the graphs below.

Overall, 1995 has been an extremely successful year, seeing the final installation of several major component upgrades to this experiment. Following a few more tests of the new high voltage system, we expect to begin preliminary data taking late in 1995 or early in 1996. We believe that we have now reduced the systematic errors to the point that they will contribute only about 2×10^{-27} e cm to the uncertainty of the measurement of the neutron EDM, and that several years' running will be needed before the statistical uncertainty can be reduced to a comparable level. We are now investigating various possibilities to try to improve our counting statistics, such as diamond-coating the inside of the storage cell (to increase its Fermi potential), and the installation of more ^{58}NiMo-coated guide tubes to transport the neutrons to our experiment.

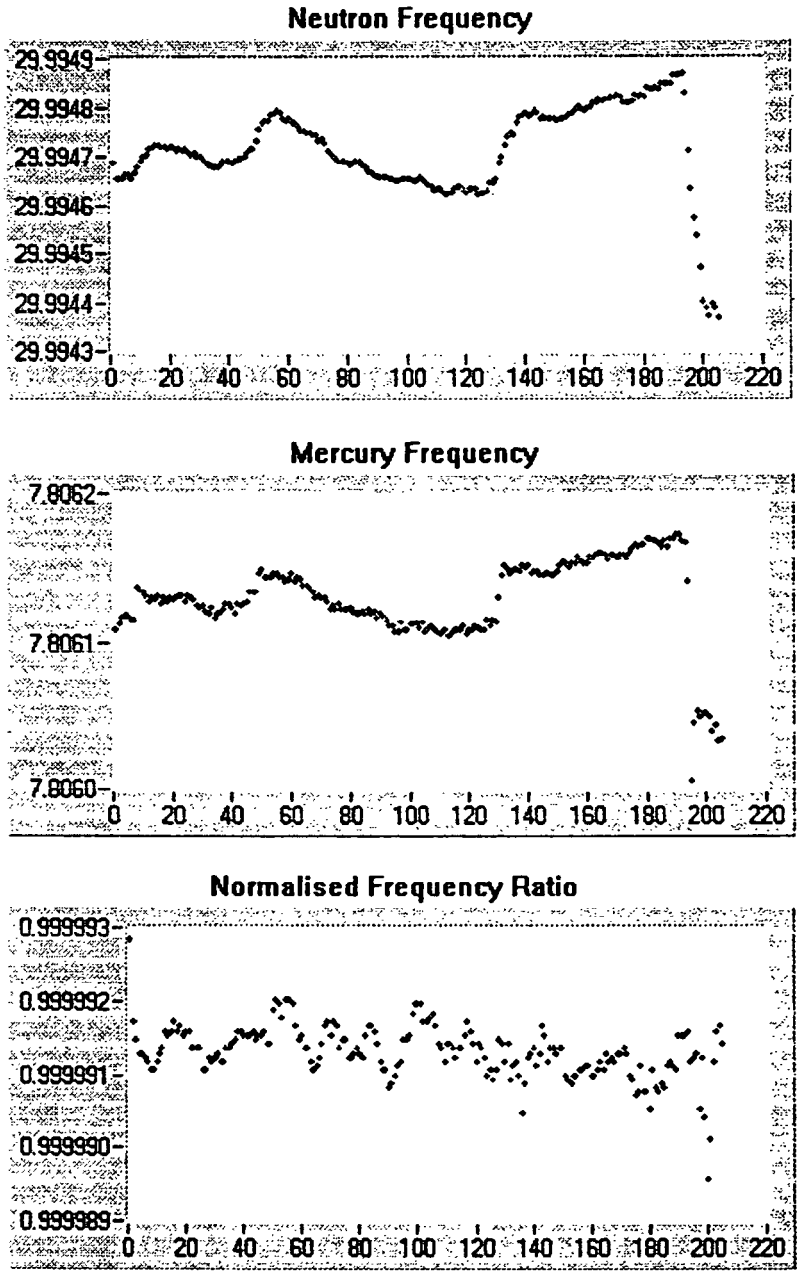

Figure 1. Graphs showing how the precession frequencies of neutrons and mercury change as the magnetic field drifts. Each point represents a counting time (cycle) of approximately 3 minutes. The point-to-point fluctuations seen in the mercury frequency are somewhat reduced in the case of the neutron frequency measurements by a 4-cycle integration period. The ratio of frequencies (normalised to the ratio of gyromagnetic ratios) stays constant to within a few parts in 10^7, corresponding to field shifts at the nanogauss level.

Publications

"Opportunities from the Restart of the ILL Reactor: Fundamental Physics with Neutrons at the ILL", J.M. Pendlebury, proceedings of a one-day meeting on the Future Prospects for Fundamental Physics with Super Low Energy Neutrons, University of Kyoto, 3rd Jan 1995, pp 1-16.

"Conclusion of the $n\bar{n}$ Experiment: Grand Unification Must Wait", D. Dubbers and J.M. Pendlebury, ILL Annual Report for 1994, May 1995, p. 34.

"Summary Talk on Precision Clocks", J.M. Pendlebury, Proceedings of the XVth Moriond Workshop, "Dark Matter in Cosmology, Clocks and Tests of Fundamental Laws", Villard-sur-Ollon, 21st-28th Jan 1995, Editions Frontieres, 91192 Gif-sur-Yvette, France.

"The Neutron EDM Experiment in Preparation at the ILL", J.M. Pendlebury *et al.*, Proceedings of the XVth Moriond Workshop, "Dark Matter in Cosmology, Clocks and Tests of Fundamental Laws", Villard-sur-Ollon, 21st-28th Jan 1995, Editions Frontieres, 91192 Gif-sur-Yvette, France.

"Observation of $\phi\phi$ Production in the Reaction $\bar{p}p \rightarrow 4K^{\pm}$ at 1.4 GeV/c Incident $\bar{p}$ Momentum", L. Bertolotto, A. Buzzo, P.T. Debevec, D. Drijard, S. Esao, R. Eisenstein,...P.G. Harris *et al.*, Phys. Lett. B **345**, 25 (1995).

Proposal 240

SOUDAN II experiment
Argonne - Minnesota - Oxford - DRAL - Tufts Collaboration

The Soudan 2 Experiment is designed to concentrate on the search for failures of the conventional picture as described by the Standard Model of Particle Physics. There are a number of questions about unusual processes on which, it has been speculated, this model might well fail or require major extension.

Searching for rare signals at the level of one or two per year requires that background signals are minimised and that the "fiducial volume" of the detector is surrounded with an efficient shield to sense when signals are due to radiation entering from outside. The apparatus consists of a 960-ton iron calorimeter 2700 feet deep at the lowest level in the Soudan iron mine, northern Minnesota. One third of the 4.3 ton modules of which it is composed was made in the UK by the Oxford and DRAL groups. The designing and planning of the experiment started in 1981; the first modules started taking data in 1988; the full detector was completed in November 1993. Since then data taking has continued 70-80% of the time. The small "down time" has allowed a major refurbishment programme in which many of the earlier modules were rebuilt or repaired to raise their performance to the same specification as the final ones. This rebuild, funded in part by UK contributions through DRAL, was completed in 1995. The main detector is surrounded on all sides by a shield to detect incoming particles and radiation. A UK-funded addition to this was made in 1995 by the Oxford group; an extra double plane of chambers covering the top of the detector has been constructed using redundant detectors from the TASSO experiment. The final section of this will be completed in 1996.

Leaving aside the constant low-level background from natural radioactivity, which is easily recognised and dismissed, there are three possible sources of signals in the main detector:

1. the passage of downward going muons from cosmic rays together with any secondary radiation caused by them;

2. the interaction of neutrinos coming from the decay of π, K and μ produced in the atmosphere by cosmic rays;

3. the decay of protons and neutrons with violation of baryon number conservation.

Each of these is sensitive to departures from the Standard Model; the counting rates per year are several million, about a hundred and zero respectively. For this reason each needs to be understood before meaningful conclusions on the lower rate processes can be drawn.

The study of cosmic ray muons has included:

- a survey of their directions mapped onto the celestial sphere to search for "hotspots" or point sources, reflecting on the origin, propagation and interaction of cosmic rays;

- a study of muon showers deep underground in coincidence with scintillator and surface arrays, reflecting on the question of the composition of cosmic rays at very high energy;

- a search for highly ionising magnetic monopoles;

- a study of energetic horizontal muons and their possible sources including neutrinos from Active Galactic Nuclei.

The most exciting results from Soudan 2 concern the neutrino interaction data. These are data where there is no evidence of an incoming particle in the outer 50cm of the detector and no signal in the envelopping shield either. Much work is being done to show that this successfully excludes all events induced by cosmic muons. The remaining "contained events" (CEV) are examined and classified as muon-like, shower-like or multiprong, according as they have a single characteristically long muon track, a shower structure, or a number of tracks and showers. The success of this classification is now monitored with a stream of Monte Carlo generated events which are combined into the data stream at the mine. Both the large water cherenkov experiments, Kamioka and IMB, have reported significant anomalies in the ratio of muon-like to shower-like events. In principle the ratio is well understood, derived largely from the raw 2:1 mix of muon and electron neutrinos that result from lepton conservation in the decay of charged pions. These experiments quote their result as the ratio,

$$R = \frac{(muon/electron)_{data}}{(muon/electron)_{MC}}.$$

As the first four symbols on figure 1 show their ratio R is quite incompatible with unity. Despite having quite different systematic errors from these experiments the current (preliminary) Soudan 2 result,

$$R = 0.63 \pm 0.15$$

is some two standard deviations from unity and compatible with them. The statistical error given is still larger than systematic uncertainties and more data is needed; the collaboration expects to run until a sensitivity of 5,000 ton-years is reached. In the meantime we are developping other methods of analysis which use computed event shape and which do not make use of event-by-event judgement by a physicist.

Since it appears unlikely that the effect is the result of a systematic error, the possibility of neutrino flavour oscillations has to be seriously considered. This implies that at least one neutrino has mass and that the mass eigenstates are not eigenstates of flavour. While the atmospheric neutrino experiment in Soudan 2 may establish the effect, it can do no more then place bounds on the several parameters required to describe the general three-flavour mixing of the mass eigenstates. (Of course the now well-established solar neutrino deficit, if due to neutrino oscillations, also describes part of this matrix.) During 1995 the UK Soudan groups joined by the University of Sussex submitted a far-reaching proposal to Fermilab to carry out an accelerator neutrino oscillation experiment with a beam from Fermilab to Soudan, MINOS. The neutrino oscillation phase is dependant on L/E and such a beam with L of 700km and E around 10 GeV covers the same range of L/E as the atmospheric experiment. However such an experiment is superior to the atmospheric one in three ways: the beam can be controlled and has a single initial flavour; a 'near station' experiment at Fermilab will study the unoscillated beam; the energy E is above threshold for ν_τ charged current events, permitting the detection of neutrinos of all three flavours. This experiment has now been strongly endorsed by a special HEPAP panel and has been approved as part of the Fermilab program. In the UK the proposal has been presented to the PPESP which has approved the initial allocation of some R & D resources.

As the questions surrounding the understanding of neutrino induced events have clarified, the collaboration has turned its attention back to the search for Nucleon Decay - which was the original motivation for the Soudan 2 Experiment. While the water cherenkov experiments have reported no

signal in simple channels, there are many channels for which some or all of the decay products would be below cherenkov threshold including $p \rightarrow K^{+}\nu$. With an analysed data sample of 1.7×10^{3} ton-years there are a small number of events that can be interpreted as due to nucleon decay. A group within the collaboration is studying the possible interpretations of these events and conclusions about nucleon decay that can be drawn from them.

References

- A new calculation of atmospheric neutrino fluxes, D. H. Perkins, Astroparticle Physics 2(1994)249-256
- Ultrahigh energy cosmic ray composition from surface air shower and underground muon measurements at Soudan 2, N. P. Longley et al., Phys. Rev. D52 (1995)2760
- A sensitive honeycomb calorimeter module for the Soudan 2 nucleon decay experiment, W. W. M. Allison et al., Nucl. Inst. & Meth. (to be published)
- A study of cosmic ray composition in the knee region using multiple muon events in the Soudan 2 detector, S. M. Kasahara et al. (to be submitted to Phys. Rev. D)

Thesis

- The construction and analysis of a whole-sky map using underground muons, G. L. Giller, University of Oxford, April 1994

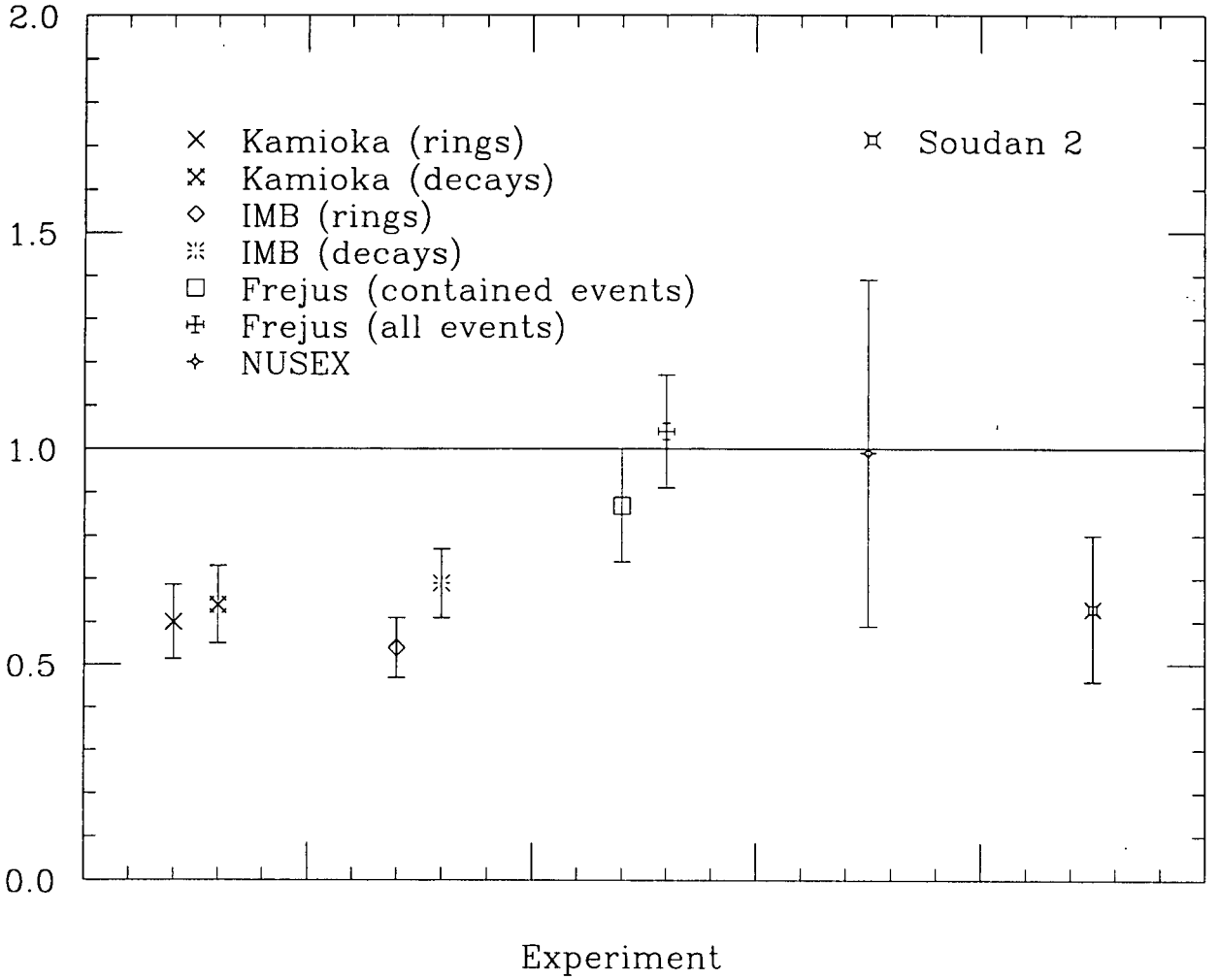

Figure 1 All published values of the ratio R from underground experiments.

KARMEN: Neutrino Spectroscopy at ISIS

Forschungszentrum Karlsruhe, University of Karlsruhe
University of Erlangen, University of Bonn
Queen Mary and Westfield College
University of Oxford
Rutherford Appleton Laboratory

The KARMEN experiment was commissioned for long term data taking in summer 1990. Since then 2000 neutrino interactions have been recorded and analysed. Half way through this data acquisition period the energy dependence of the $^{12}C(\nu_e , e^-)^{12}N_{g.s.}$ cross section and the first observation of the neutral current process $^{12}C(\nu , \nu')^{12}C^*$ (1^+1) induced by ν_e and $\bar{\nu}_\mu$ have been published. Recently statistics for the neutral current reaction $^{12}C(\nu_\mu , \nu_\mu')^{12}C^*$ reached a level sufficient to deduce a reliable cross section and to determine the isovector-axialvector coupling of neutral currents directly from a set of data acquired in the same experiment for three neutrino flavours. In addition the first reliable cross section of neutrino induced transitions to excited nuclear levels in the reaction $^{12}C(\nu_e , e^-)^{12}N^*$ has been determined. These cross sections are of interest for astrophysics in connection with the origin of light elements in the universe.

For all cross section measurements on ^{12}C in the KARMEN experiment the systematics errors due to the flux normalization are now larger than the statistical errors. The cross sections measurements for ν_e-absorption on ^{13}C and ^{56}Fe are still dominated by their statistical errors and require continuing data taking to achieve equivalent precision.

The main emphasis of future measurements with the KARMEN detector will be focused on the search for neutrino oscillations and the investigation of the anomaly observed in the time distribution relative to beam-on-target of isolated neutral events. Observation of neutrino oscillations would contradict the Standard Model of the electro-weak interactions and imply at least one of the neutrino types involved to be

a massive particle. Verification of the highly speculative interpretation of the anomaly in the time distribution of the isolated neutral events as a evidence for the existence of a massive weakly interacting particle emerging from the spallation source would be a major breakthrough in the search for this type of particles.

The search for neutrino oscillations between electron type and muon type neutrinos has received a considerable boost of interest after the LSND claim of positive evidence for the $\bar{\nu}_\mu \rightarrow \bar{\nu}_e$ appearance oscillation. Since 1990 KARMEN has been investigating the very same oscillation channel with high precision and has found no evidence for oscillations. The current result of the KARMEN experiment excludes already a significant part of the parameter space allowed for oscillations in the LSND experiment.

Evidence for $\bar{\nu}_\mu \rightarrow \bar{\nu}_e$ appearance oscillation in the KARMEN detector is a delayed coincidence of an energetic positron from the inverse β-decay on free protons of the liquid scintillator with capture gamma rays from absorption of the thermalized neutron from this process in gadolinium or by hydrogen. Although this delayed coincidence signature is very stringent , there is a significant background from cosmic rays. Even after exploiting the unique time structure of ISIS application of shape analysis to the oscillation signal and background energy distributions and very sophisticated stopped muon tracking this background is irreducible.

The current level of background induced by cosmic rays limits the sensitivity of the KARMEN experiment in the oscillation parameter space. Significantly increased neutron detection efficiency from 20% to 53% and major changes in the trigger system during 1995 would allow KARMEN to probe further into the parameter space of the LSND claim after another three years of data taking, but the area of highest sensitivity of the LSND experiment would remain unchecked.

The nature of the limiting background has been clearly identified as high energy neutrons generated by cosmic muons in spallation processes in the iron of the shielding blockhouse surrounding the detector. These neutrons can easily penetrate

the iron shielding inside the first layer of the veto system without leaving a trace in the veto and create a signature in the central detector which could be mistaken for an oscillation event.

This background could be greatly reduced if most of the muons entering the shielding blockhouse could be identified doing so. An additional veto system very similar to the existing system that surrounds the inner passive iron shield of the detector but buried inside the massive walls and the roof of the shielding blockhouse can achieve just this. Extensive Monte Carlo simulations and special measurements during the last months have revealed that such an additional veto will reduce the high energy neutron background to 2.5% of its current level. The parameter space then accessible after three years of data taking includes the area of the LSND claim and would set new limits on neutrino oscillations if no positive evidence is found. The current most stringent limits (BNL E776) on $\bar{\nu}_\mu \rightarrow \bar{\nu}_e$ oscillations are shown in figure 1 together with the region of parameter space allowed by the LSND result, the present limits of the KARMEN experiment and estimated limits for KARMEN after another three years of data taking with and without the veto upgrade.

The significant background reduction by this new veto system will also greatly benefit further investigation of the anomaly in the time distribution of the isolated neutral events. The observed anomaly is still present despite the changes in the KARMEN detector during the last year. The Kolmogorov-Smirnov test on the data agree with the previous χ^2 tests underlining the presence of a signal with a Gaussian distribution at around 3.6 μs after beam on target. Increased neutrino statistics will of course strengthen the significance of this finding but, as statistics can only be doubled in the next three years, a background reduction for neutral events to 2.5% of its present level around beam-on-target time is more effective. The new veto will also reduce the background due to bremsstrahlung from decay positrons of muons stopping undetected in the inner passive iron shield since the overall detection efficiency for muons entering the volume surrounded by the existing veto increases.

The signal to background ratio for the anomaly time region will improve by a factor of 2.

The reduction of bremsstrahlung background also eliminates the major background component for the measurement of ν_e-absorption on ^{13}C and ^{56}Fe and will enable the KARMEN experiment to determine for the first time the cross section of these reactions with high precision

The proposal for the veto upgrade of the KARMEN detector has been accepted and funding is secured. The upgrade is scheduled to start in January 1996. Data acquisition is scheduled to be resumed in late Autumn 1996. First results for a stringent test of the LSND claim are expected during 1998.

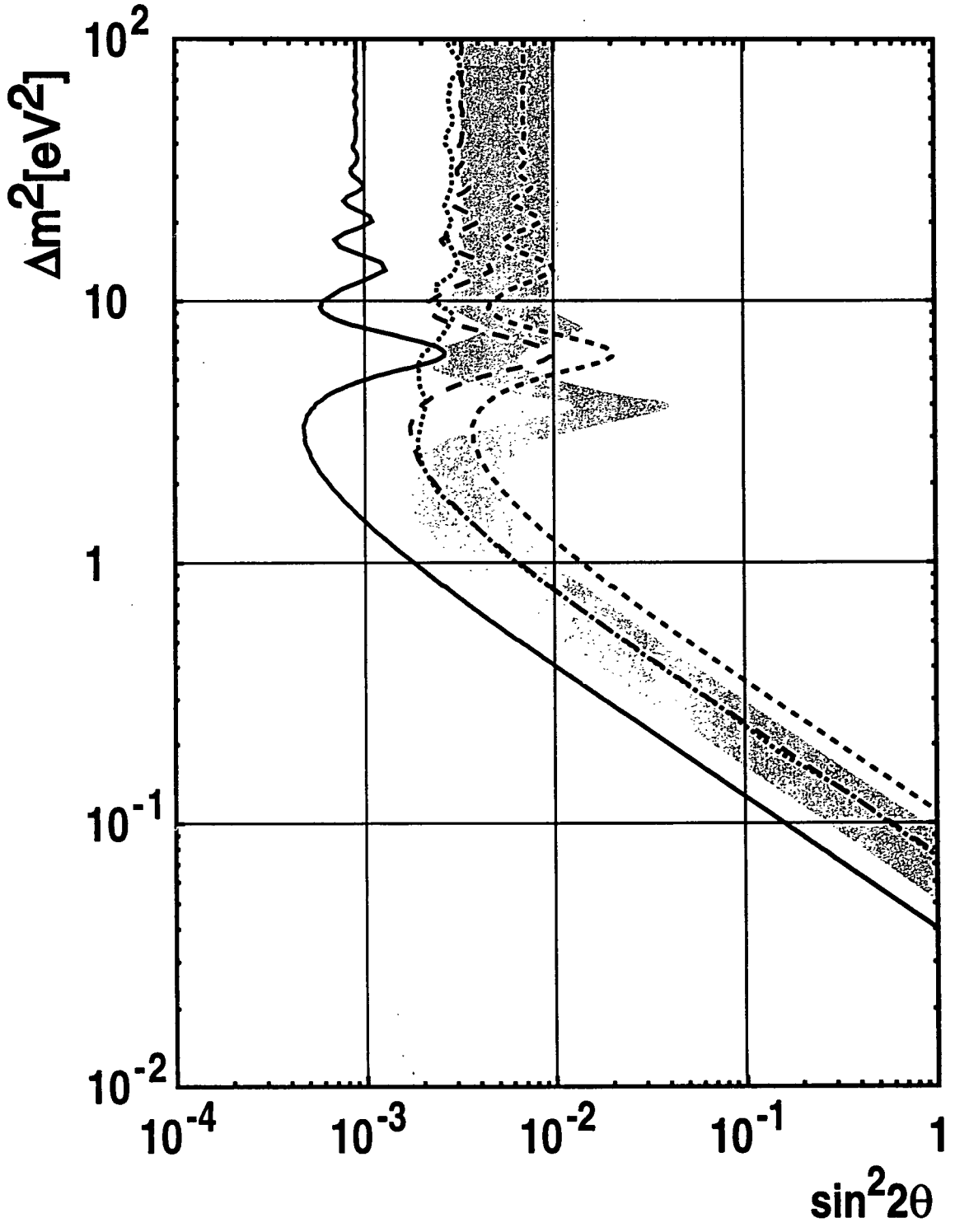

Figure 1: Limits for oscillation parameters Δm^2 and $\sin^2 2\theta$ 90% confidence level contours from the KARMEN experiment for $\bar{\nu}_\mu \rightarrow \bar{\nu}_e$ oscillations as in August 1995 (short dashes) estimated limits after three more years of data taking without veto upgrade (long dashes) and estimated limits after three years of data taking with the veto upgrade implemented (solid line). The shaded area is the parameter space allowed by the LSND experiment. The currently most stringent limit of BNL E776 (dotted line).

Publications since October 1994

G. Drexlin, B. Zeitnitz
Das Neutrinoexperiment KARMEN
KfK-Nachrichten, Jahrg. 26, 2/94, p. 117-127.

B.A. Bodmann et al. (KARMEN Collaboration)
Neutrino interactions with carbon: recent measurements and a new test of ν_e , ν_μ *universality*
Phys. Lett. **B 332** (1994) 251-257.

B.A. Bodmann et al. (KARMEN Collaboration)
Determination of a nuclear weak axial charge radius from the $^{12}C(\nu_e,e^-)^{12}N_{gs}$ *reaction*
Phys. Lett. **B 339** (1994) 215-218.

G. Drexlin, B. Zeitnitz
Anomalie im Zeitspektrum von "beam stop" -Neutrinos
Physikalische Blätter 51 (1995) Nr. 2.

B. Armbruster et al. (KARMEN Collaboration)
Anomaly in the time distribution of neutrinos from a pulsed beam stop source
Phys. Lett. **B 348** (1995) 19-28.

A SEARCH FOR GLUEBALLS IN THE CENTRAL REGION

WA76/WA91 Proposal 246

Athens : Bari : Birmingham : CERN : Dubna : Paris.

Experiment WA76 and its successor WA91 have been designed to study exclusive final states formed in the reaction

$$pp \rightarrow p_f(X^0)p_s \quad (1)$$

where the subscripts f and s indicate the fastest and slowest particles in the laboratory respectively, and X^0 represents the central system. The central system is presumed to be produced by double exchange processes. At high centre-of-mass energies the contribution of Double Pomeron Exchange (DPE) to such processes becomes increasingly large. The Pomeron is believed to have a large gluonic content, and as a result it is thought that Pomeron Pomeron scattering could be a good source of gluonic states, glueballs and hybrids.

The WA76 experiment was run in two stages. Data taken with π^+ and p incident beams at 85 GeV/c allowed good separation of many exclusive channels [1]. Several resonances suggested as gluonium candidates were seen with good signal to background ratios whereas well-known $q\bar{q}$ states were seen less prominently than in peripheral production. A second period of data taking using a 300 GeV/c p beam yielded 12 million triggers. The layout of the apparatus is shown in fig. 1. In addition to the Omega MWPC and drift chambers, two threshold Cerenkov counters were used for charged particle identification, and a fine grain electromagnetic calorimeter was used for neutral particles. The fast track measurement system [2], shown in fig. 2, is of particular interest. In order to achieve good momentum resolution, which is essential for the separation of exclusive channels, a system of microstrip detectors was used to measure the beam particle and the fast track. The reconstructed beam momentum distribution from the WA76 data is shown in fig. 3, and corresponds to a precision $\delta p/p = 3 \times 10^{-5} p$ (Subsequently $\delta p/p = 1 \times 10^{-5} p$ was achieved using a similar layout and finer pitch microstrips in WA91.)

The WA91 experiment aims to investigate central production at 450 GeV/c with a significant increase in statistics over WA76 [3]. The first phase of the experiment, performed in 1992, used the refurbished OLGA calorimeter brought close to the Omega magnet to improve acceptance for neutral particles. Slow protons were detected in WA76 on the left side of the target only, while the WA91 setup, shown in fig. 4, also allows for slow proton detection on the right. The right hand slow proton setup uses a new hodoscope (SPCR) built by the Birmingham group. The 1992 exposure yielded 67 million triggers. The second phase of the experiment was completed on June 8th 1994 and 42 million triggers were taken. The threshold Cerenkov counters C1 and C2 were used for charged particle identification and the same arrangement of fast and slow particle detectors was employed as for the first phase of the experiment. The GAMS

electromagnetic calorimeter and OLGA were also used, placed behind the Cerenkov counters, to study their use for a future phase of the experiment (WA102).

The analysis of the WA76 data is now essentially complete, while results from the WA91 data are still coming. The principal results from the experiment programme are summarized below.

A detailed study of the $\pi^+\pi^-$ mass spectrum has been performed for the 300 GeV/c data [4]. The spectrum is shown in fig. 5, and shows clear evidence for S*/$f_0(975)$ production. A good description of the $\pi^+\pi^-$ mass spectrum was obtained using a coupled channel (Flatté) formalism, and allowing the S*/$f_0(975)$ to interfere coherently with the S-wave background. The S*/$f_0(975)$ parameters were determined to be $m_0 = 979 \pm 4$ MeV, $g_\pi = 0.28 \pm 0.4$, $g_K = 0.56 \pm 0.18$, giving a pole position on sheet II at $(1001 \pm 2) - i(36 \pm 4)$ MeV.

The principal interest in the $K\overline{K}$ spectrum lies in the observation of the $\theta/f_2(1720)$ [5], the first such observation in hadroproduction. The K^+K^- spectrum is shown in fig. 6, where a peak corresponding to the $\theta/f_2(1720)$ is clearly seen. As a signal is also seen in the $K^0_SK^0_S$ mass spectrum, it is concluded that the spin of the object is either 0^{++} or 2^{++}. The decay angular distributions for the $f'(1525)$ and the $\theta/f_2(1720)$ are found to be qualitatively similar, suggesting that the $\theta/f_2(1720)$ and the $f'(1525)$ have the same spin.

The $K\overline{K}\pi$ mass spectrum in the 1.4 GeV mass region has been of long standing interest in this experiment [1,6,7]. The $K^0_SK^\pm\pi^\mp$ mass spectrum is shown in fig. 7, and shows very prominent signals for the D/$f_0(1285)$ and E/$f_1(1420)$ mesons. While the status of the D/$f_0(1285)$ is not controversial, that of the E/$f_1(1420)$ has aroused much interest in recent years. It now appears that there are three states in this mass region. The one seen by WA76 has been found to have $M = 1429 \pm 3$ MeV and $\Gamma = 58 \pm 8$ MeV. A Dalitz plot analysis has shown its J^{PG} to be 1^{++}, decaying to $K^*\overline{K}$ [5]. More recently [7], its observation in our $K^0_SK^0_S\pi^0$ data has fixed its C-parity to be +, from which we deduce its isospin to be zero. We have searched for the E/$f_1(1420)$ in our $\pi^+\pi^-\pi^+\pi^-$ [8], $\eta\pi^+\pi^-$ [9] and $\rho^0\gamma$ [10] channels. Although the D/$f_0(1285)$ is clearly seen in all channels, as can be seen from fig. 8, there is no evidence for production of the E/$f_1(1420)$ in any of them [11].

Results on the vector-vector final states centrally produced at 300 GeV/c have been reported in [12] and [13], involving the associated production of $\omega\rho, \omega\omega, \omega\phi$.

The $\pi^+\pi^-\pi^+\pi^-$ spectrum has been analysed at both 300 GeV/c and 450 GeV/c [14]. The $\pi^+\pi^-\pi^+\pi^-$ mass spectrum is shown in fig. 9 for the 450 GeV/c data with superimposed fit [15]. The values of the parameters obtained are shown in table 1. In addition to the D/$f_0(1285)$ two further resonances are seen, the X(1450) and the X(1900), with masses and widths $M = 1446 \pm 5$ MeV, $\Gamma = 56 \pm 12$ MeV, and $M = 1926 \pm 12$ MeV, $\Gamma = 370 \pm 70$ MeV respectively. These resonances were first seen in the WA76 300 GeV/c data, but were not seen at 85 GeV/c[8]. The energy dependence and t dependence of the X(1450) show that it is not a decay channel of the E/$f_1(1420)$ seen in the $K\overline{K}\pi$ spectrum. A new spin analysis of the X(1450) [15,16] finds its spin parity to be $J^{PC} = 0^{++}$, decaying to $\rho(\pi\pi)_{Pwave}$. The X(1900) is found to be a $J^{PC} = 2^{++}$ object decaying to $a_2\pi$ and $f_2(1270)(\pi\pi)_{Swave}$. As the X(1900) is

a broad object and the peaks in the $a_2\pi$ and $f_2(1270)(\pi\pi)_{Swave}$ channels are slightly displaced, it could be that there are two resonances present. The analysis method used was not available when the original WA76 study was performed, but a re-analysis of these data shows that the two data samples yield the same J^{PC} assignments for these two resonances.

A further study of the combined WA76 and WA91 data [17] in $\pi^+\pi^-\pi^+\pi^-$ and $\pi^+\pi^-$ channels discusses possible interpretations of the above- mentioned final states in the light of the Crystal Barrel results [18]. In our $\pi^+\pi^-\pi^+\pi^-$ channnel there are two new states, $f_0(1450)$ and $f_2(1900)$. There is another new state in the $\pi^+\pi^-$ channel with $M = 1497 \pm 30$ MeV and $\Gamma = 199 \pm 30$ MeV which is compatible with the $f_0(1520)$ observed in the Crystal Barrel experiment. We propose [17] an interpretation where the 1450 and 1497 MeV structures are explained as being due to an interference between $f_0(1365)$ and $f_0(1520)$ states observed by the Crystal Barrel experiment at CERN.

A natural continuation and extension of the WA91 experiment is the experiment WA102, combining the excellent charged particle reconstruction of the Omega Spectrometer with the multiphoton detection facility of the GAMS-4000 Calorimeter. For details see this volume, Proposal 291.

REFERENCES

1. T.A. Armstrong et al., Phys. Lett. **146B** (1984) 273.
   T.A. Armstrong et al., Phys. Lett. **166B** (1986) 245.
   T.A. Armstrong et al., Phys. Lett. **167B** (1986) 133.
   T.A. Armstrong et al., Z. Phys. C **34** (1987) 23.
   T.A. Armstrong et al., Z. Phys. C **35** (1987) 167.
2. T.A. Armstrong et al., Nucl. Inst. and Meth. **A274** (1989) 165.
3. S. Abatzis et al., CERN SPSC/90-2/P249 (1990).
4. T.A. Armstrong et al., Z. Phys. C **51** (1991) 351.
5. T.A. Armstrong et al., Phys. Lett. **227B** (1989) 186.
6. T.A. Armstrong et al., Phys. Lett. **221B** (1989) 216.
7. T.A. Armstrong et al., Z. Phys. C **56** (1992) 29.
8. T.A. Armstrong et al., Phys. Lett. **228B** (1989) 536.
9. T.A. Armstrong et al., Z. Phys. C **52** (1991) 389.
10. T.A. Armstrong et al., Z. Phys. C **54** (1992) 371.
11. T.A. Armstrong et al., Proceedings of the 26th Int.Conf.on High Energy Physics,Dallas, Texas,August 1992,AIP Conf.Proc.No.**272** (1993) 544.
12. T.A. Armstrong et al.,Z.Phys.**C 58** (1993) 257.
13. T.A. Armstrong et al., Proceedings of the Hadron'93 Conf., Como,Italy,June 1993,Nuovo Cimento **107A** (1994) 1841.
14. F. Antinori et al., Proceedings of the Hadron'93 Conf., Como,Italy,June 1993, Nuovo Cimento **107A** (1994) 1857.
15. S. Abatzis et al., Phys.Lett. **324B** (1994) 509.
16. F. Antinori et al., Proceedings of the ICHEP'94 27th Int.Conf. On High Energy Physics,Glasgow,UK,July 1994,IOP Publ.(1995) 1403.
17. F. Antinori et al.,Phys.Lett. **353B** (1995) 589.
18. V.V. Anisovitch et al., Phys.Lett. **323B** (1994) 233.

PUBLICATIONS (OCT.1994 - SEPT.1995)

1. Study of vector-vector final states centrally produced in pp interactions at 300 GeV/c.
   IJ Bloodworth, JN Carney, CJ Dodenhoff, JB Kinson, O Villalobos Baillie and MF Votruba with Athens, Bari, CERN and Paris.
   Nuovo Cimento **107 A** (1994) 1841-1845.

2. First results from the experiment WA91 at the CERN Omega Spectrometer.
   RP Barnes, A Bayes, JN Carney, S Clewer, JP Davies, CJ Dodenhoff, D Evans, JB Kinson, O Villalobos Baillie and MF Votruba with Athens, Bari, CERN and Dubna.
   Nuovo Cimento **107 A** (1994) 1857-1865.

3. Observation of new states in the reaction $pp \rightarrow p_f(\pi^+\pi^-\pi^+\pi^-)p_s$ at 300 and 450 GeV/c.
   RP Barnes, A Bayes, JN Carney, S Clewer, JP Davies, CJ Dodenhoff, D Evans, JB Kinson, K Norman, O Villalobos Baillie, MF Votruba with Athens, Bari, CERN and Dubna. Proc. of the ICHEP'94 27th Int. Conf. on High Energy Physics, Glasgow, July 1994; IOP Publ. (1995) 1403-1405.

4. A further study of the centrally produced $\pi^+\pi^-$ and $\pi^+\pi^-\pi^+\pi^-$ Channels in pp interactions at 300 and 450 GeV/c.
   A Bayes, JN Carney, S Clewer, JP Davies, CJ Dodenhoff, D Evans, JB Kinson, K Norman, O Villalobos Baillie and MF Votruba with Athens, Bari, CERN and Dubna.
   Phys.Lett. **B353** (1995) 589-594.

5. A further study of the $\pi^+\pi^-$ and $\pi^+\pi^-\pi^+\pi^-$ channels in pp interactions at 300 and 450 GeV/c.
   A Bayes, JN Carney, S Clewer, JP Davies, CJ Dodenhoff, D Evans, JB Kinson, A Kirk, K Norman, O Villalobos Baillie and MF Votruba with Athens, Bari, CERN and Dubna. Proc. of the Hadron'95 Int. Conf., Manchester, July 1995, to be published.

6. Preliminary results from the second phase of the WA91 experiment.
   A Bayes, JN Carney, S Clewer, JP Davies, CJ Dodenhoff, D Evans, JB Kinson, A Kirk, K Norman, O Villalobos Baillie and MF Votruba with Athens, Bari, CERN and Dubna. Proc. of the Hadron'95 Int. Conf., Manchester, July 1995, to be published.

THESES (PhD)

7. CJ Dodenhoff, A study of the centrally produced $\eta\pi^+\pi^-$ and $\pi^+\pi^-\pi^0$ systems at 450 GeV/c.
   University of Birmingham, Nov.1994 (RAL-TH-95-007).

8. S Clewer, Analysis of the central $K^0_S K^\pm\pi^\mp$ system and determination of $f_1(1285)$ branching ratio at 450 GeV/c.
   University of Birmingham, Dec.1994 (RALT-032-95).

	Mass (MeV)	Width (MeV)	Observed decay mode	$I(J^{PC})$	Mass and Width from ref. [8]. (MeV)
$f_1(1285)$	1280 ± 2	40 ± 5	$\rho\pi\pi$	$0(1^{++})$	M 1281 ± 1 Γ 31 ± 5
X(1450)	1446 ± 5	56 ± 12	$\rho\pi\pi$	$0(0^{++})$	M 1449 ± 4 Γ 78 ± 18
X(1900)	1926 ± 12	370 ± 70	$a_2(1320)\pi$ $f_2(1270)\pi\pi$	$0(2^{++})$	M 1901 ± 13 Γ 312 ± 61

Table 1. Parameters of resonances in the fit to the $\pi^+\pi^-\pi^+\pi^-$ mass spectrum.

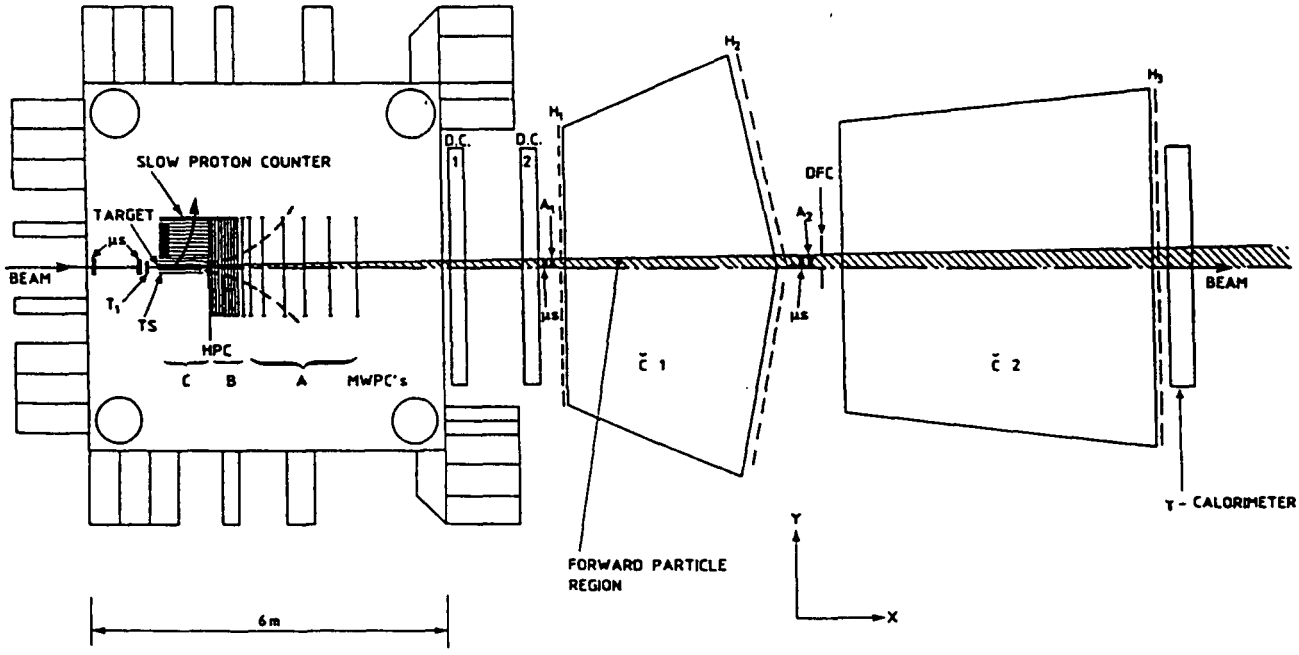

Fig. 1. Layout of the CERN Ω Spectrometer as used for the WA76 experiment.

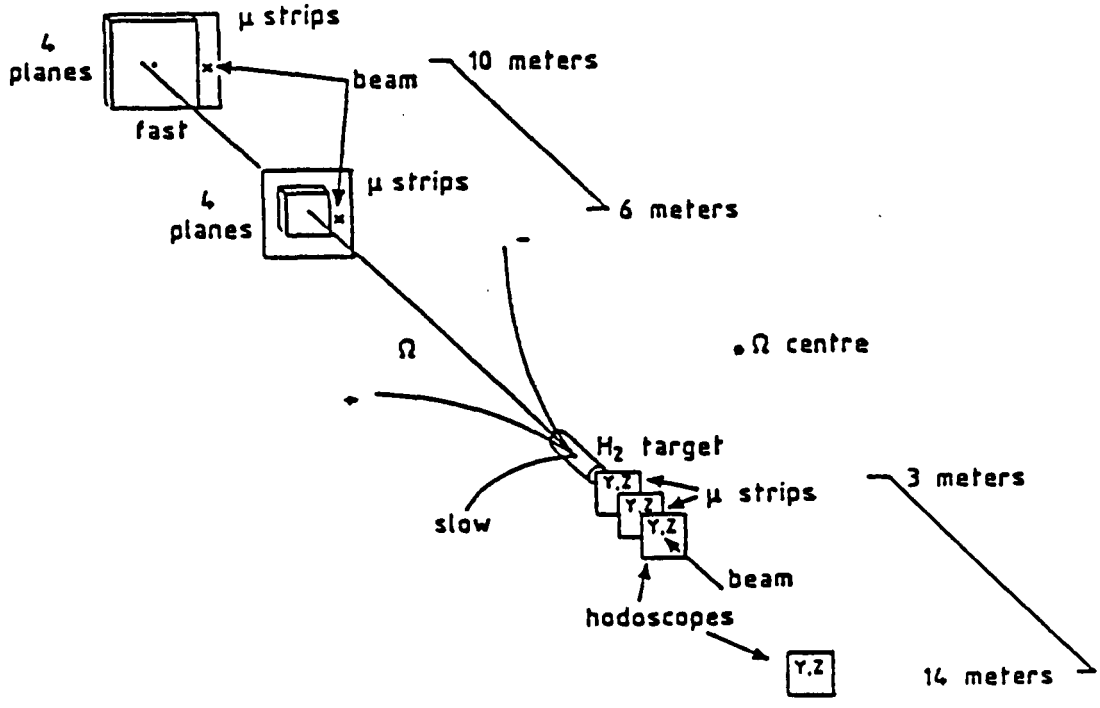

Fig. 2 Layout of the μ-strips and scintillators used to measure the beam and the fast particle.

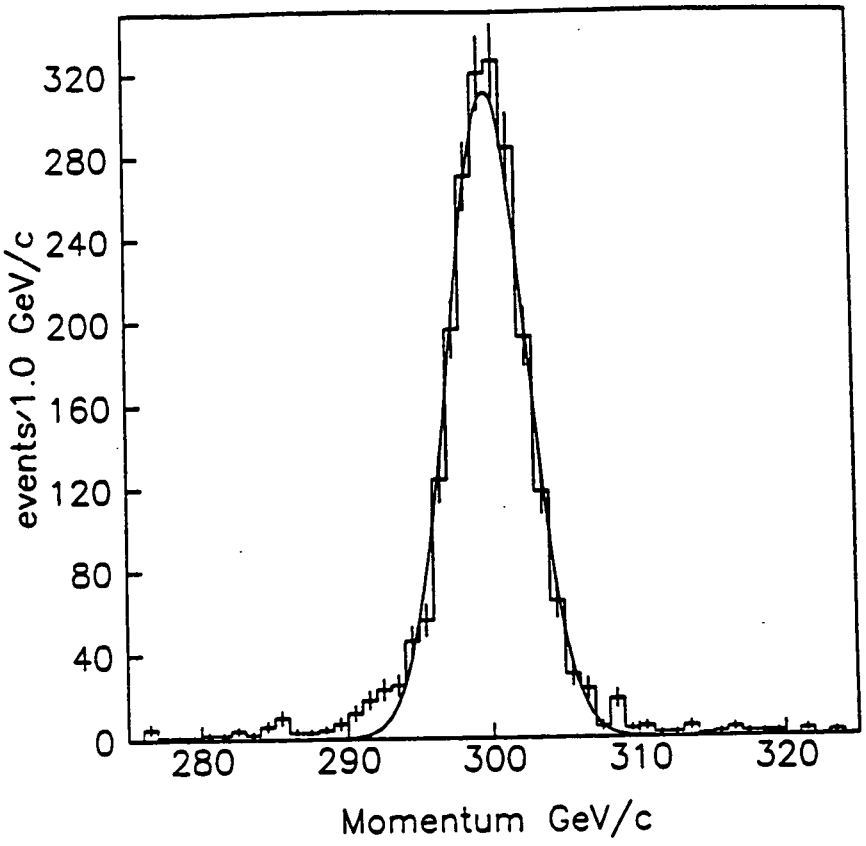

Fig. 3. Reconstructed beam momentum at 300 GeV/c.

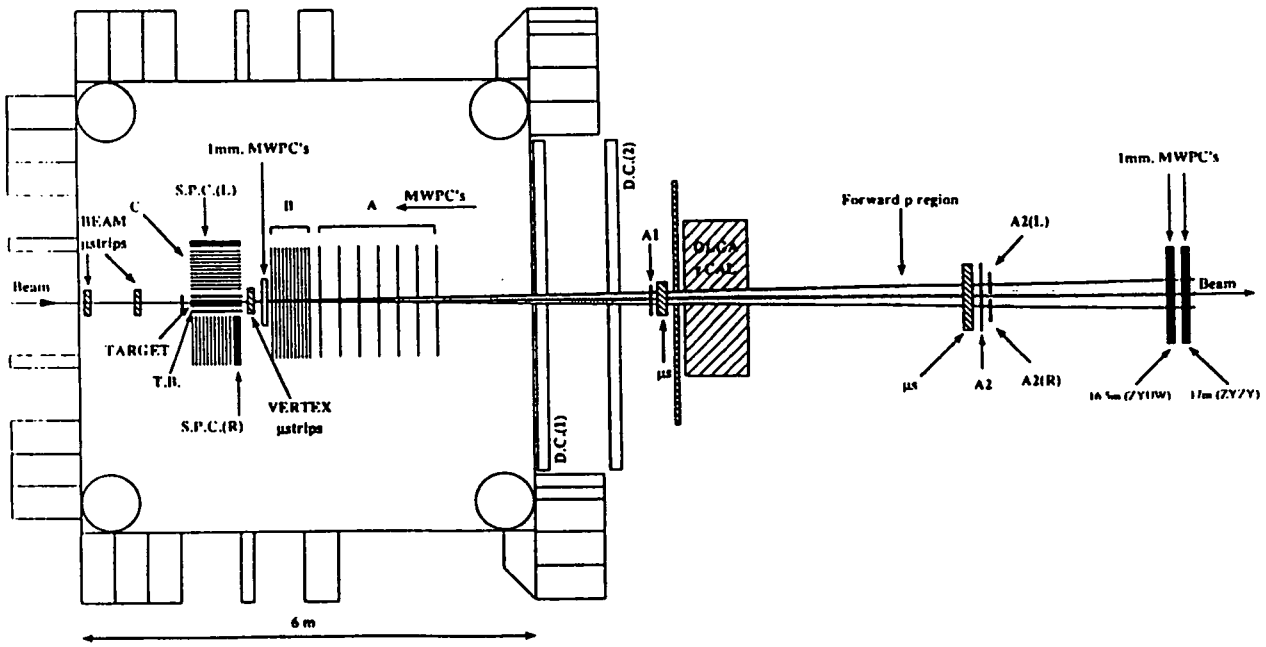

Fig. 4. WA91 apparatus (1992) configuration.

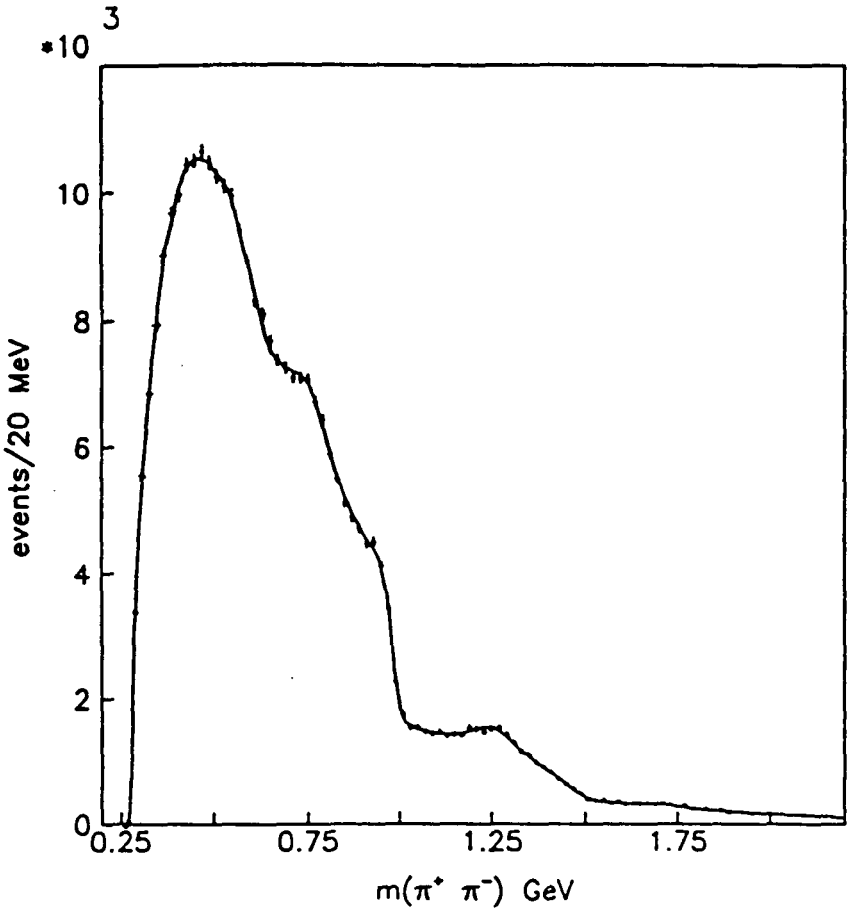

Fig. 5. $\pi^+\pi^-$ effective mass distribution at 300 GeV/c. The fit is described in the text.

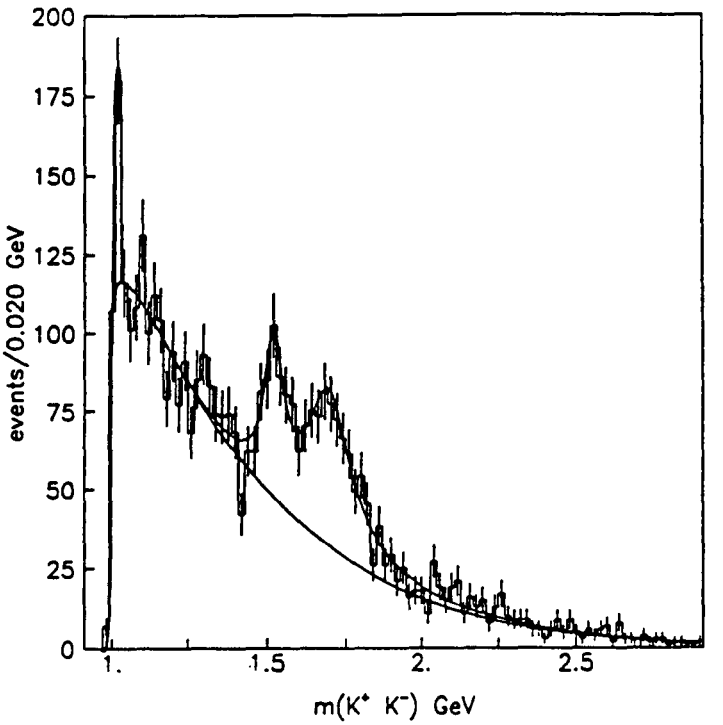

Fig. 6. K^+K^- effective mass distribution at 300 GeV/c. The fit is described in reference 4.

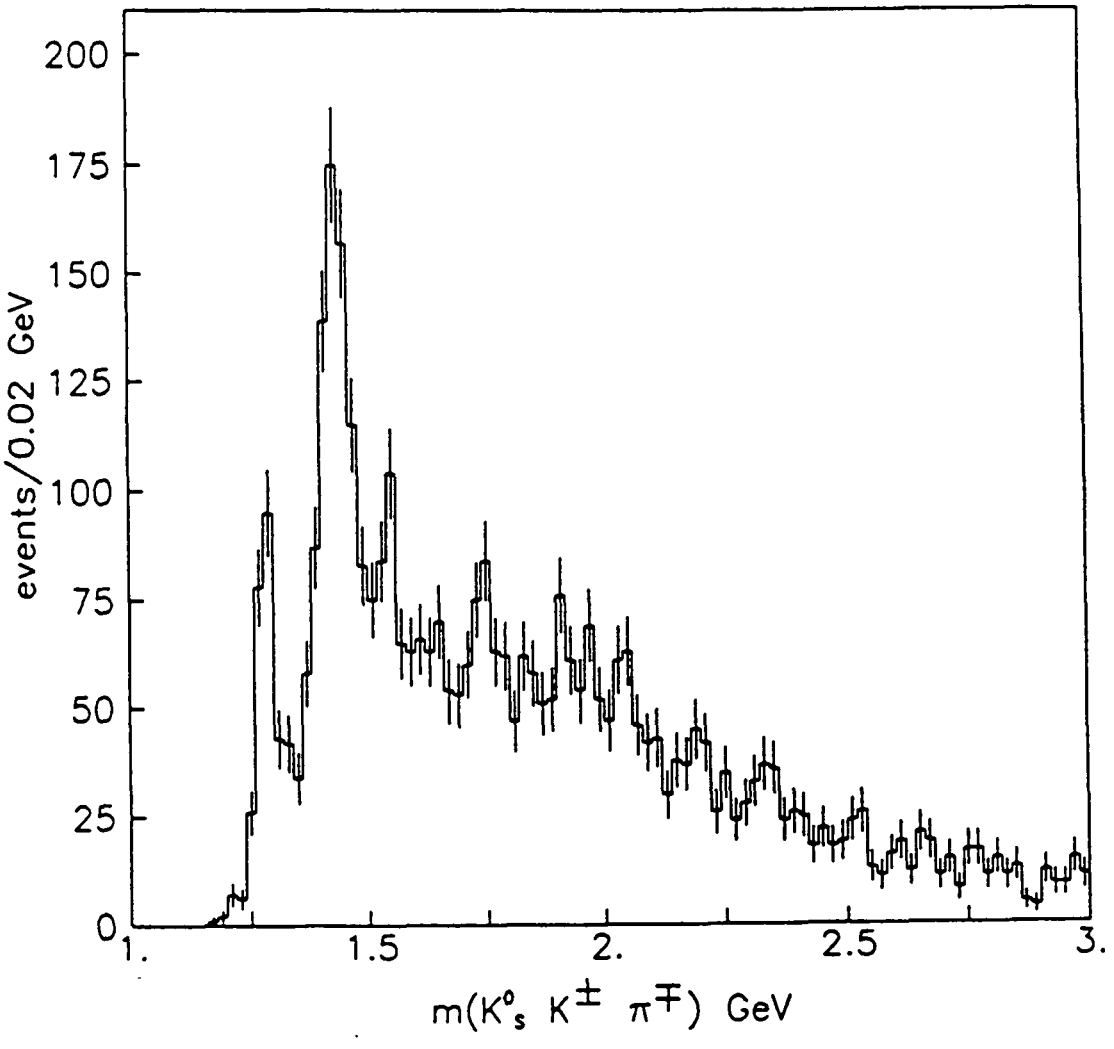

Fig. 7 $K^0_S K^{\pm}\pi^{\mp}$ effective mass spectrum at 300 GeV/c.

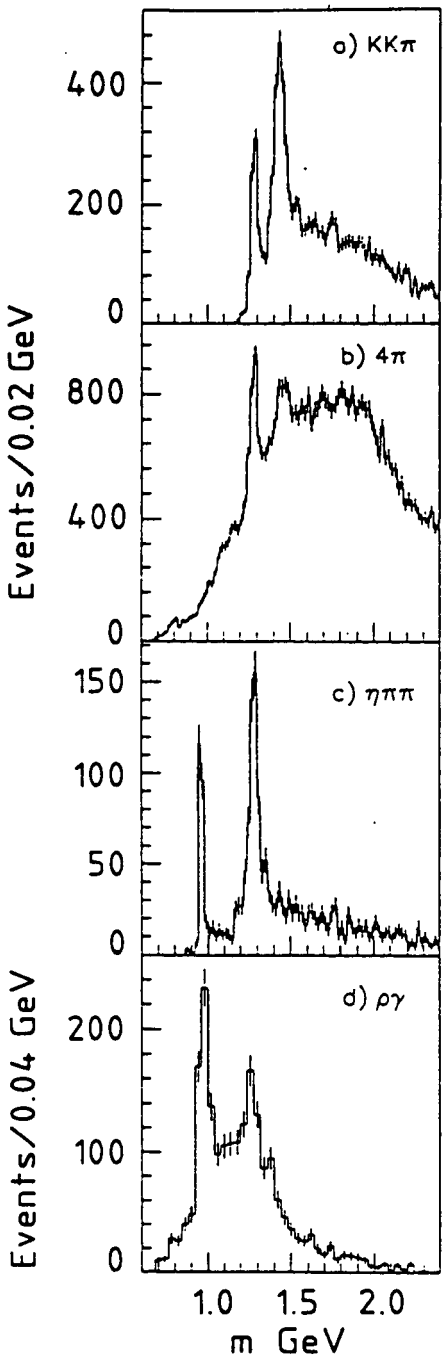

Fig. 8. Effective mass distributions for (a) $K^0_S K^{\pm}\pi^{\mp}$, (b) $\pi^+\pi^-\pi^+\pi^-$, (c) $\eta\pi^+\pi^-$ and (d) $\rho^0\gamma$ channels.

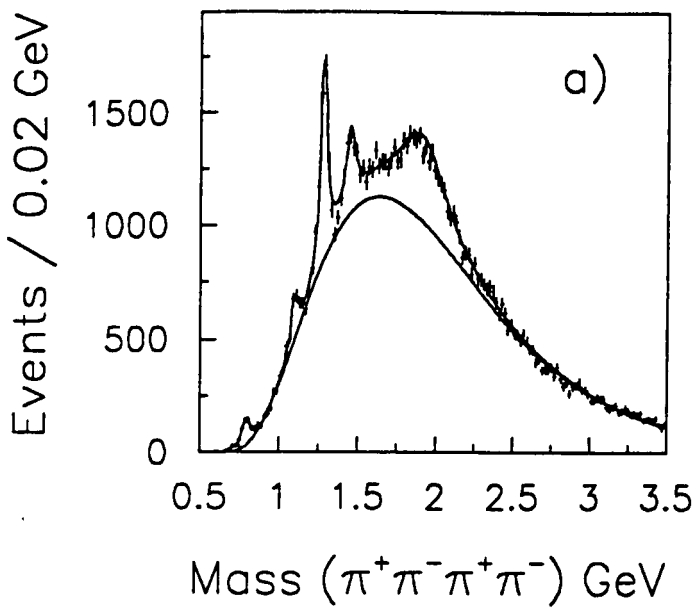

Fig. 9. $\pi^+\pi^-\pi^+\pi^-$ effective mass spectrum for 450 GeV/c data.

An exposure of the 15-foot bubble chamber filled with a Ne/H_2 mixture to a quad-triplet beam from the TEVATRON running at 800 GeV/c.

FNAL E632 Proposal 254

Berkeley - Birmingham - Brussels - CERN - Chandigarh - FNAL-
Hawaii - IHEP(Serpukhov) - Illinois - Imperial College London - ITEP (Moscow) -
Jammu - MPI Munich - Moscow State University - Oxford -
RAL - Rutgers - Saclay - Tufts

For the majority of the original groups of the experiment, data-processing finished during 1992. However, IHEP(Serpukhov), ITEP(Moscow) and Moscow State University are in the process of measuring a large unbiassed sample. A considerable increase in statistics has already been obtained, which should provide sufficient data at the highest-ever neutrino energy for many comparisons to be made with experiments at lower neutrino energies - fragmentation studies, energy dependences in strange particle production, neutral currents, etc.

Several new analyses are under way and the results should be published in the near future.

E632 (and BEBC) Publications since 1 October 1994

1. Neutral strange particle production in neutrino and antineutrino charged-current interactions on neon.

   Physical Review D50 (1994) 6691-6703

2. Spin alignment and parity violation effects in ρ^0 production in neutrino and antineutrino charged-current interactions.

   Zeitschrift für Physik C66 (1995) 583-590

SLD Collaboration at the SLC

Proposal 263

Bologna, Boston, Brunel, Caltech, Cincinnati, Colarado State, Columbia, Ferrara, Frascati, Illinois, Massachusetts, MIT, Nagoya, Northeastern, Northridge, Oregon, Padova, Perugia, Pisa, Rutgers, RAL, Santa Barbara, Santa Cruz, SLAC, Tenessee, Tohoku, Vanderbilt, Washington, Wisconsin, Yale.

Abstract

The SLD status reported here is based upon 100,000 Z^o decays (with an average beam polarization of $(77.3 \pm 0.6)\%$) collected in 1994 and 1995, in addition to 1993 data sample (50,000 Z^o with polarisation of $(63.0 \pm 1.1)\%$). The availability of the SLC polarised electron beam and the excellent 3D resolution of the SLD pixel vertex detector are exploited by these analyses, and permit the collaboration to achieve a degree of precision competitive with and complementary to that of the LEP experiments for many electroweak and heavy flavor analyses.

The SLD detector continues to run smoothly with minimal maintainance, while the SLC again achieved its goal integrated luminosity for the run. The data from the 94/95 run has initiated many new analyses, however this report is necessarily selective, and concentrates on the recent advances in topological vertexing, the consolidation of established polarised asymmetry measurements and their extension to the tau lepton to probe the weak charged current.

A small contingent of UK physicists continue to make a leading contribution to the experiment in being responsible for the CCD vertex detector, developing topological vertexing, leading the R_b analysis group, developing polarised tau analyses and taking a major role in the design and build of the upgrade vertex detector - VXD3.

The collaboration anticipates running to collect an additional 500,000 Z^0 decays over the next 2 years. This running will be with VXD3, which, at the time of writing, is being prepared for final installation in SLD.

The SLD Measurement of A_{LR}

The left-right asymmetry in Z^0 production continues to provide excellent precision with the new data sample thanks to a significant reduction in the systematic

error on the electron beam polarisation. Including all the SLD data from 1992-95 (approximately 150K Z^0 decays), SLD measures $A^0_{LR} = 0.1551 \pm 0.0040$. This corresponds to a determination of the weak mixing angle of $\sin^2\theta^{eff}_W = 0.23049 \pm 0.00050$. The determination of the beam polarization remains the only significant systematic error. The polarisation is measured precisely with a Compton polarimeter, which for the 1994-95 SLD run measured $P_e = (77.34 \pm 0.61)\%$.

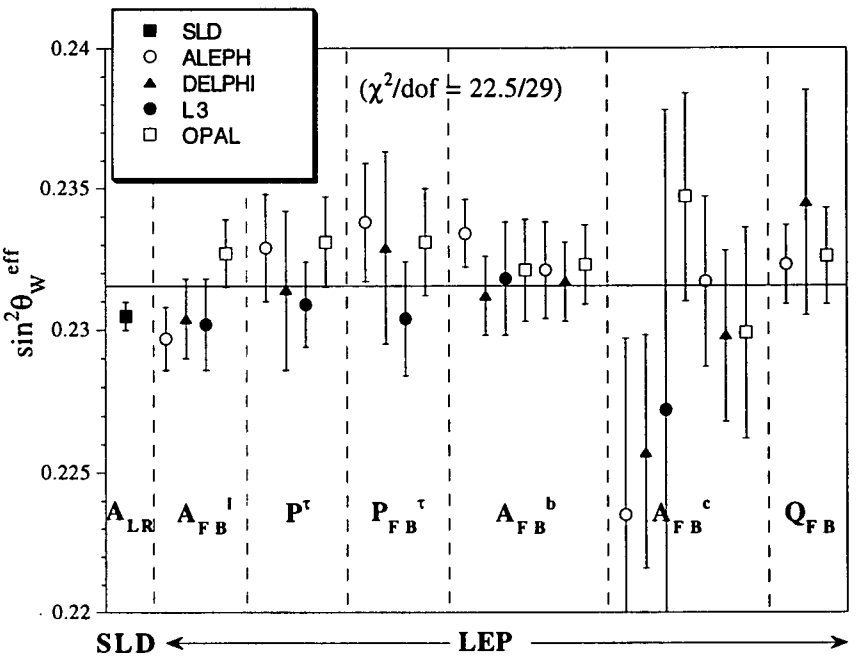

Figure 1: Weak Mixing Angle Measurements

The weak mixing angle results from the SLD, ALEPH, DELPHI, L3 and OPAL experiments (based on approximately 3.5 million Z^0 decays per LEP experiment) are shown in Figures 1 and 2 [1]. Figure 1 gives the results by individual experiment for each of seven techniques. Figure 2 summarizes the results by collaboration.

If we assume that the MSM provides a complete description of the quark and lepton couplings to the Z^0 boson, then all these results can be combined to give

$$\sin^2\theta^{eff}_W = 0.23143 \pm 0.00028$$

. If this assumption is relaxed to apply to lepton couplings only, we find

$$\sin^2\theta^{eff}_W = 0.23106 \pm 0.00035$$

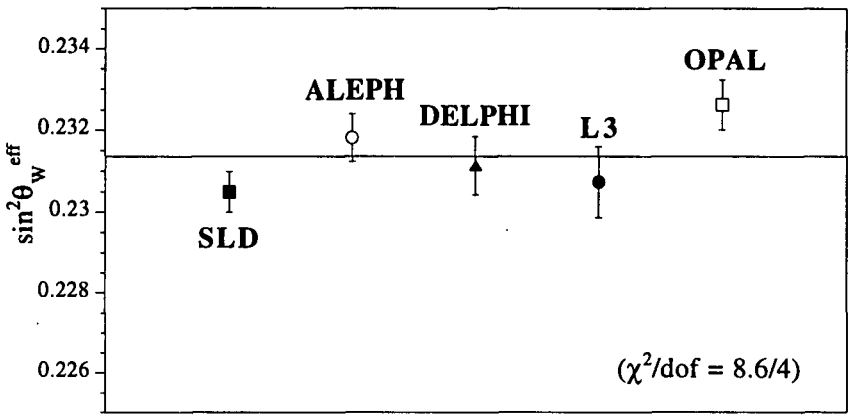

Figure 2: Weak Mixing Angle Results by Collaboration

This result is consistent with the MSM and with other precision electroweak measurements.

The LEP experiments have now completed their datataking at the Z^0 resonance with a total of about 4.5 million Z^0 decays per experiment, while the SLD experiment plans to run through 1998 and accumulate an additional 500 thousand Z^0s above the 150K Z^0s available for the current measurement. This data will provide an exceptionally precise determination of the weak mixing angle.

Charm and Beauty with a Polarized Electron Beam

Tests of the Standard Model through the measurements of Z^0 to fermion couplings at SLD benefit from an enhanced sensitivity due to the longitudinally polarized electron beams. The parity violating parameters A_b and A_c of the Zbb and Zcc couplings are, uniquely at SLD, measured *directly* from the polarised left-right forward-backward asymmetries.

The A_c measurement using reconstructed D^{*+}, D^+ [2] has been updated to include all 1993–1995 data. The preliminary result obtained is:

$$A_c = 0.64 \pm 0.11 \text{ (stat)} \pm 0.06 \text{ (syst)}.$$

The dominant systematics related to the RCBG are largely statistical in nature, so they are expected to be reduced with a larger data sample. The A_b, A_c measurements using leptons [3] has also been updated yielding preliminary results:

$$A_b = 0.87 \pm 0.07 \text{ (stat)} \pm 0.08 \text{ (syst)}$$

$$A_c = 0.44 \pm 0.11 \text{ (stat)} \pm 0.13 \text{ (syst)}.$$

The statistical correlation between the A_b and A_c results is 18%. Among the presently significant systematics, jet axis simulation and MC weighting systematics are expected to reduce with improved analysis in the future.

The A_b measurement using momentum-weighted track charge has been improved [4],[5] from the analysis on the 1993 data. This preliminary measurement using all 1993-1995 data, adopts a self-calibrated technique to measure the analyzing power (AP) from the data, resulting in a much reduced MC dependency.

The tagged-event raw signed thrust axis cosθ distributions from left-handed and right-handed electron beams are shown in Fig. 3 for the 1994-1995 data. This plot nicely shows the dual nature of the asymmetry with clearly visible forward–backward and left–right asymmetries. A maximum liklihood fit is used to extract A_b, taking into account $|Q|$-dependent AP and event flavor composition as a function of b-tag track multiplicity. The preliminary result, including all 1993-1995 data, is:

$$A_b = 0.843 \pm 0.046 \text{ (stat)} \pm 0.051 \text{ (syst)}.$$

The calibration statistical error and b-tag composition systematic will improve with more data in the future and adjustments in the b-tag procedure.

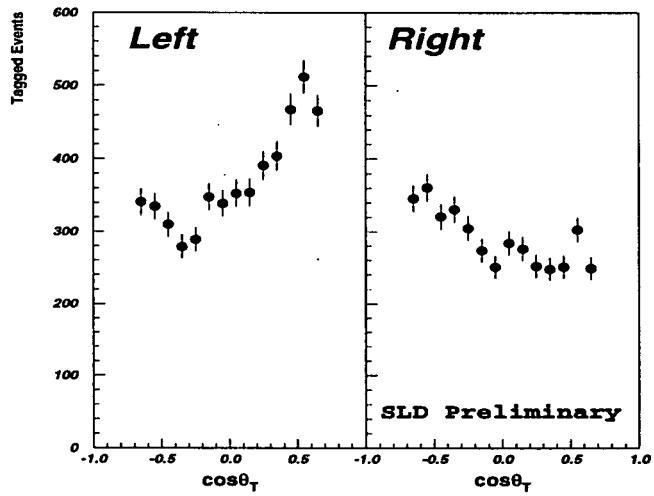

Figure 3: Distributions of raw signed thrust axis cosθ for 1994-1995 data.

The SLD Čerenkov Ring-Imaging Detector (CRID), precision vertexing and polarisation are exploited in a new A_b measurement. Exploration of the abundant

$\overline{B} \to D \to K^-$ decay signal for $B/\overline{B}$ separation has been widely promoted as a new technique for a variety of B physics measurements. In SLD, charged kaons with a momentum of 3–20 GeV are identified using the CRID gas-radiator data. This new preliminary measurement [6] is the first application of this technique for a b-asymmetry measurement.

The preliminary result from the 1994-1995 data is:

$$A_b = 0.91 \pm 0.09 \text{ (stat)} \pm 0.09 \text{ (syst)}.$$

Most of the detector and physics systematics associated with the uncertainty of b-event analyzing power can be removed with a calibration from the double hemisphere charge comparison, trading for a calibration statistical error when more data are included in the future.

The combined A_b, A_c results

These preliminary SLD measurements may be combined with a simultaneous fit to A_b and A_c, taking into account the systematic correlations between measurements. The assumed values and uncertainties of other related parameters are listed, together with the combined results in Table 1. These results can be compared with the average LEP measurements of $A_b = 0.884 \pm 0.032$ and $A_c = 0.642 \pm 0.053$, as well as with the SM prediction of $A_b = 0.935$ and $A_c = 0.666$. The LEP averages are derived from the $A_{\rm FB}^b$ and $A_{\rm FB}^c$ results [7], assuming $A_e = 0.1506 \pm 0.0028$ from a combination of the SLD $A_{\rm LR}$ and the LEP A_ℓ results.

The complementarity of the SLD direct A_b measurements is nicely illustrated in the scheme of a full Zbb coupling analysis proposed by Takeuchi *et al.* [8]. The deviations from the SM can be generally represented as a cross section like variable ξ_b and a parity violation like variable ζ_b, in addition to $\delta \sin^2\theta_W^{\rm eff}$. The ζ_b versus $\delta \sin^2\theta_W^{\rm eff}$ plot for various current experimental results is shown in Fig. 4. The SM point at (0,0) is defined by m_t=180 GeV, m_H=300 GeV, α_s=0.117 and α_{em}=1/128.96. The thin horizontal band around (0,0) corresponds to the SM m_t, m_H variations indicated in the plot. The 68% and 90% C.L. contours for the best fit to all measurements are also shown.

Topological Vertexing

Topological vertexing (TV) is a new vertexing technique developed by a Rutherford physicist and is destined to become the standard vertexing package within

Assumed parameters	
R_b	0.218 ± 0.002
R_c	0.171 ± 0.014
Br($b \to \ell$) (%)	10.80 ± 0.78
Br($b \to c \to \ell$ (%)	9.3 ± 1.6
B mixing $\overline{\chi}$	0.130 ± 0.010
Combined results	
A_b	0.858 ± 0.054
A_c	0.577 ± 0.097
A_b, A_c correlation	12.3%

Table 1: Combined SLD A_b, A_c results and assumed parameter values.

SLD. Preliminary results using this new method for the R_b and B lifetime ratio have already benefited from the ultra pure tagging it provides. With the data anticipated during the next 2 years of running, and the reduced systematics due to TV, we expect the SLD measurement of R_b will be the most precise measurement made. This is of great interest given the current anomaly in the LEP average value of R_b. With a Brunel physicist leading the analysis, the UK groups are well placed to exploit this physics.

Topological vertexing makes maximum use of the true 3D spacepoint information available from the SLD CCD vertex detector. The idea is to search for the vertices in 3D co-ordinate space. Individual track probability functions, $f_i(\mathbf{r})$, (Gaussian tubes in 3D space) are derived for each track i.

The vertex function, $V(\mathbf{r})$,

$$V(\mathbf{r}) = \sum_i f_i(\mathbf{r}) - \frac{\sum_i f_i^2(\mathbf{r})}{\sum_i f_i(\mathbf{r})} \tag{1}$$

is a smooth, continuous function defined to quantify the relative probability of the candidate vertex at $\mathbf{r}$, for which maxima may be found. The Gaussian track functions are left unnormalised so that the vertex function, $V(\mathbf{r})$, approximates to track multiplicity counting. The relative probability of there being a vertex at $\mathbf{r}$ is derived taking into account that ≥ 2 tracks must have $f_i(\mathbf{r}) > 0$ in this

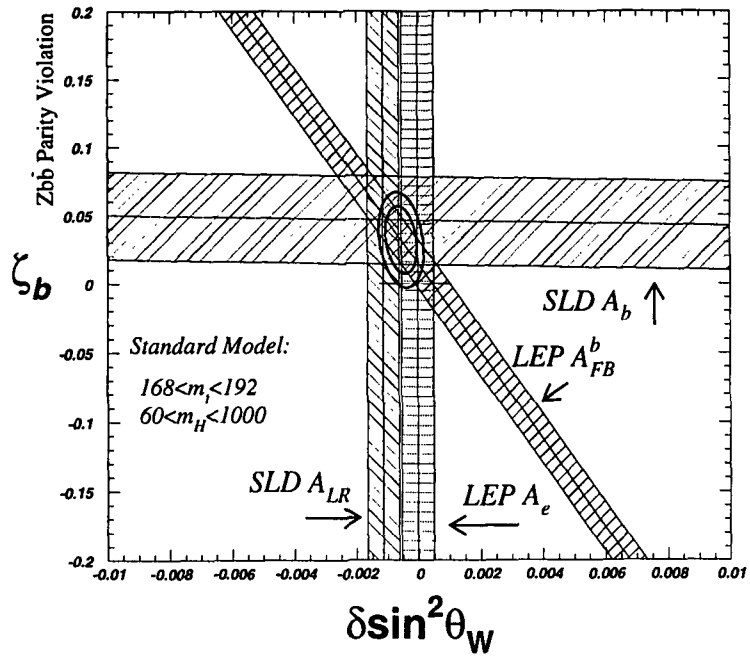

Figure 4: Zbb coupling parity violation versus $\sin^2\theta_W^{\text{eff}}$.

region.

An example of the x, y projection of $\sum_i f_i(\mathbf{r})$ and $V(\mathbf{r})$ is shown in figure 5(a) and 5(b) respectively. These plots are obtained by integrating the function over the third dimension z within the limits of ± 8 mm from the IP in the z direction.

The hemisphere of tracks chosen for this plot is taken from a Monte Carlo $Z \rightarrow b\bar{b}$ event in which the jet momentum is directed from left to right in figure 5. While the trajectories of individual tracks can be seen in figure 5(a), the regions where vertices are probable can be seen from the distribution of $V(\mathbf{r})$ in figure 5(b). In this case the algorithm resolved the hemisphere into two vertices, i.e. the primary vertex and a secondary. The peak in $V(\mathbf{r})$ produced by the primary can be seen in figure 5(b) at $X = Y = 0$, the secondary peak is displaced to the right of the IP by ~ 1.5 mm.

The 3D space is divided into 'resolved' regions which are associated with tracks to form candidate vertices. A 3D spatial point is associated with all track pairs which is the nearest local maximum in $V(\mathbf{r})$ to the point of normalised closest approach to both tracks. These spatial points are clustered into separate spatial regions, and the final set of tracks associated with each spatial region are fit

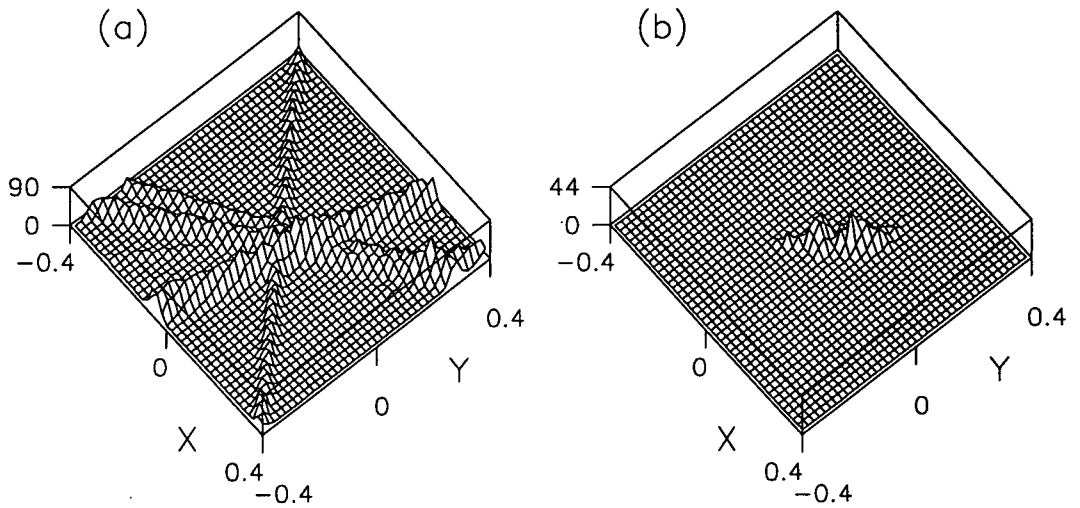

Figure 5: The track and vertex functions projected onto the x, y plane.

together to form the topological vertex structure. This structure is rich in information on the decay chain, which may be manipulated to design cuts specific to particular analyses.

Preliminary Measurements of B^0 and B^+ Lifetimes

SLD has two analyses for the lifetime ratio [11]. The first identifies semileptonic decays of B mesons with high (p, p_t) leptons and reconstructs the B vertex decay length and charge by vertexing the lepton with resultant from a reconstructed D vertex.

From the initial sample of 150K Z^o decays this analysis isolates 977 semileptonic B decays, 428 are reconstructed as B^0 decays and 549 as B^+ decays. Monte Carlo studies indicate that the neutral ($Q = 0$) sample is 98.7% pure in B hadrons. Similarly, the charged ($Q = \pm 1$) sample is 95.3% pure in B hadrons

The lifetime is extracted from the decay length distribution of the selected secondary vertices using a binned maximum likelihood technique. The distributions for the neutral and charged samples, are fitted simultaneously to determine two parameters: the lifetime ratio τ_{B^+}/τ_{B^0} and either the B^+ or the B^0 lifetime. The maximum likelihood fit yields lifetimes of

$$\langle \tau_{B^0} \rangle = 1.60^{+0.15}_{-0.14}(\text{stat}) \pm 0.10(\text{syst})\text{ps} \qquad (2)$$

$$\langle \tau_{B^+} \rangle = 1.49^{+0.11}_{-0.10}(\text{stat}) \pm 0.05(\text{syst})\text{ps} \quad (3)$$

$$\frac{\langle \tau_{B^+} \rangle}{\langle \tau_{B^0} \rangle} = 0.94^{+0.14}_{-0.12}(\text{stat}) \pm 0.07(\text{syst}) \quad (4)$$

The second analysis isolates a sample of B meson decays with a loose 2-D impact parameter tag and reconstructs the decay length and charge of the B using a topological vertex reconstruction.

This method yields a sample of 8685 reconstructed B events with 3382 reconstructing as B^0 decays and 5303 reconstructing as B^+ decays. Monte Carlo studies indicate that the resulting B^0 sample is 99.3% pure in B hadrons, similarly, the B^+ sample is 99.0% pure in B hadrons.

The resulting decay lengths for the B^0 and B^+ samples are shown in figure 6. The lifetime fit yields values of

$$\langle \tau_{B^0} \rangle = 1.55 \pm 0.07(\text{stat}) \pm 0.12(\text{syst})\text{ps} \quad (5)$$

$$\langle \tau_{B^+} \rangle = 1.67 \pm 0.06(\text{stat}) \pm 0.09(\text{syst})\text{ps} \quad (6)$$

$$\frac{\langle \tau_{B^+} \rangle}{\langle \tau_{B^0} \rangle} = 1.08^{+0.09}_{-0.08}(\text{stat}) \pm 0.10(\text{syst}) \quad (7)$$

The systematic errors for the two analyses are currently dominated by uncertaintities in the binned maximum likelihood fit procedure and are expected to decrease significantly. The lifetimes are in good agreement with the current world averages.

The R_b Measurement

The preliminary SLD R_b measurement [9] uses a lifetime double-tag technique similar to the method used by ALEPH [10]. This method allows a simultaneous measurement of R_b and the hemisphere b-tag efficiency ϵ_b to reduce systematics associated with Monte Carlo (MC) modelling of ϵ_b. The unambiguous 3D hits from the SLD CCD pixel vertex detector enable a cleaner track reconstruction such that the impact parameter distribution tails are well reproduced by the MC.

The choice of this cut is based on an optimization for a minimal total R_b error, as can be seen from Fig. 7. The efficiencies of tagging uds and c hemispheres

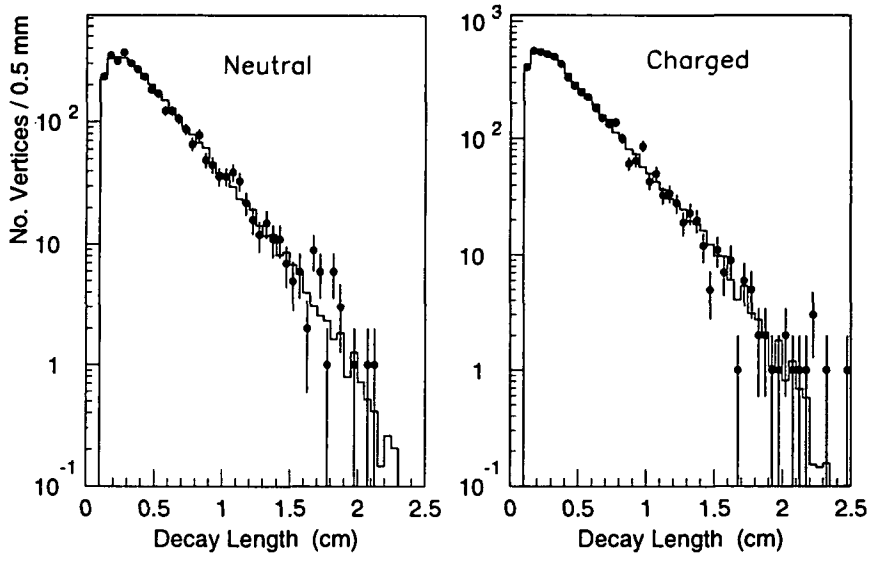

Figure 6: Decay lengths for the topological analysis

according to MC are 0.087% and 2.3% respectively at this cut. The b-hemisphere correlations also estimated from the MC are -0.2%. The measured ϵ_b from the data is 31.3 ± 0.6(stat)%, consistent with the MC prediction of 30.6%. The corresponding hemisphere b-tag purity is 94%.

Assuming a SM value of $R_c = 0.171 \pm 0.17$, the obtained preliminary result is

$$R_b = 0.2171 \pm 0.0040 \text{ (stat)} \pm 0.0037 \text{ (syst)} \pm 0.0023 \ (R_c).$$

Similar to many other R_b measurements, the b-tag purity of 94% can be improved slightly by sacrificing efficiency, but it is still difficult to contain the systematics to well below 1%. The development of an ultrahigh purity (~99%) b-tag using topological vertexing has indicated a dramatic reduction in the systematic error, and an SLD precision R_b measurement with 500K Z^0 would exceed the current precision of the LEP measurements.

Measurement of the τ Charged Weak Couplings

The weak couplings of the tau may be studied by investigating the energy spectra of various tau decay products. These spectra are determined by the spin

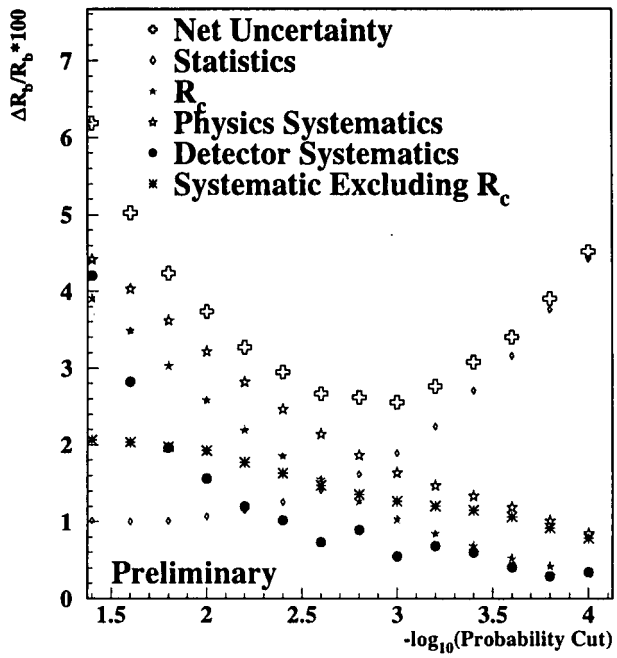

Figure 7: R_b measurement error components as a function of the hemisphere probability tag.

polarization of the taus and the nature of the decay [13]. At the Z^0, taus are produced with spin polarization due to the inherent parity violation of the Z^0 couplings. At the SLC, this is enhanced due to the electron beam polarization, the tau polarizations are much higher than at LEP, especially at high $|\cos\theta|$ (see Fig. 8). The polarization of the tau is largely determined by the beam polarization and the production angle, and is relatively unaffected by the Z^0 parity violation.

This new analysis [12] uses the 1993-1995 SLD data sample of 4552 τ-pair events to measure the tau neutrino helicity, h_{ν_τ}, and the Michel parameters, ξ and δ by analyzing the τ decays $\tau \to \pi(K)\nu_\tau$, $\tau \to e\bar{\nu}_e\nu_\tau$ and $\tau \to \mu\bar{\nu}_\mu\nu_\tau$ in $e^+e^- \to Z^0 \to \tau^+\tau^-$. The h_{ν_τ} analysis is the responsibility of Brunel physicists, and is unique in that it does not rely on spin correlations, and so is also sensitive to the *sign* of the neutrino helicity. Recent LEP measurements gain sensitivity to the sign from an analysis of a_1 decays, and consequently have large systematic errors due to the model uncertainity in the a_1 decay hadronic currents.

The decay spectrum may be parameterised in two parts, a constant part that is

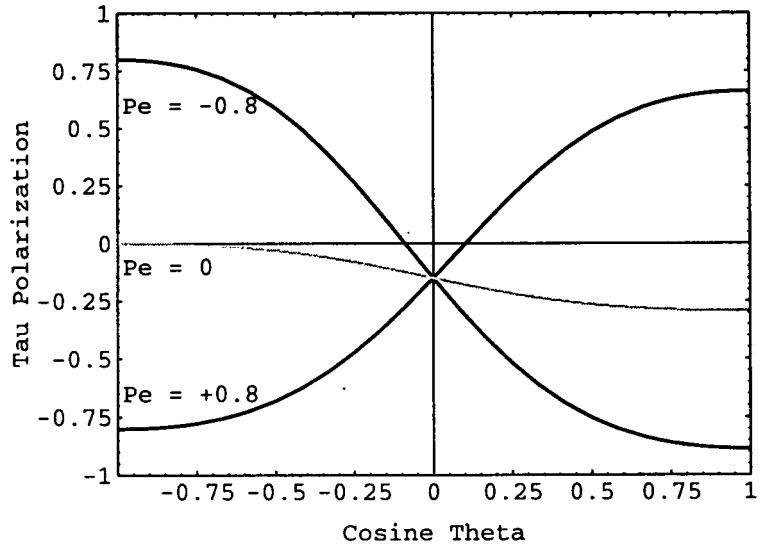

Figure 8: Tau polarization vs production angle with and without beam polarization.

unaffected by the handedness of the tau, and a polarization dependent part that changes sign depending on the handedness of the tau:

$$\begin{aligned} \frac{1}{\Gamma}\frac{d\Gamma_L}{dx} &= f(x) + g(x), \\ \frac{1}{\Gamma}\frac{d\Gamma_R}{dx} &= f(x) - g(x). \end{aligned} \tag{8}$$

In the case of the pion (kaon), we can describe this with one parameter, h_{ν_τ}, which characterizes the polarization dependent term. We get the following decay spectrum for $\tau \rightarrow \pi(\mathrm{K})\nu_\tau$:

$$\begin{aligned} f(x) &= 1, \\ g(x) &= \mathrm{h}_{\nu_\tau}\frac{2x - 1 - m_h^2/m_\tau^2}{1 - m_h^2/m_\tau^2}, \end{aligned} \tag{9}$$

where m_τ^2 and m_h^2 are the masses of the τ and the hadron respectively, and x is the hadron energy scaled by the τ energy ($x = \frac{E_\pi}{E_\tau}$).

In the case of the leptons, neglecting mass differences, we can describe the energy spectrum with the three Michel parameters ρ, ξ and δ. Here the parameter ρ

describes the non-polarization-dependent term, and ξ and δ describe the polarization dependent terms. We get the following spectrum for $\tau \to \ell \bar{\nu}_\ell \nu_\tau$:

$$\begin{aligned} f(x) &= f_1 + \rho \cdot f_2, \\ g(x) &= \xi(g_1 + \delta \cdot g_2), \end{aligned} \tag{10}$$

where $x = \frac{E_\ell}{E_\tau}$.

These decay spectra are combined with the production cross sections to get theoretical decay distributions:

$$\frac{1}{\sigma}\frac{d^2\sigma(x,z,P_e)}{dxdz} = f(x) - P_\tau(z,P_e) \cdot g(x), \tag{11}$$

which illustrates the importance of high tau polarization for measuring the polarization dependent terms.

In the SLD data, one can clearly see the differences in the decay particle energy spectra due to different regions of z and P_e. Fig. 9 shows the energy spectrum of $\tau \to \pi(\mathrm{K})\nu_\tau$ decays for both data and Monte Carlo, plotted separately for two regions of (z,P_e). The difference is expected to be less obvious in the three-body decays $\tau \to \ell \bar{\nu}_\ell \nu_\tau$, but is still quite visible as shown in Fig. 10.

The tau neutrino helicity, h_{ν_τ}, and the Michel parameters ξ and $\xi\delta$ are determined using an unbinned maximum likelihood fit to the energy spectra of the decay channels $\tau \to \pi(\mathrm{K})\nu_\tau$ and $\tau \to \ell \bar{\nu}_\ell \nu_\tau$. The fit function is the theoretical differential cross section (Eq. 11) corrected for radiative and detector effects.

Fitting the $\tau \to \pi(\mathrm{K})\nu_\tau$ sample yields $h_{\nu_\tau} = -0.89 \pm 0.21(\mathrm{stat})$, which can be interpreted as twice the helicity of the tau neutrino. The fit to the $\tau \to \ell \bar{\nu}_\ell \nu_\tau$ channels gives $\xi = 1.17 \pm 0.35(\mathrm{stat})$ and $\xi\delta = 0.49 \pm 0.24(\mathrm{stat})$.

Including systematic errors the SLD preliminary values for h_{ν_τ} and the Michel parameters ξ and $\xi\delta$ are

$$\begin{aligned} h_\nu &= -0.89 \pm 0.21(\mathrm{stat}) \pm 0.07(\mathrm{syst}), \\ \xi &= 1.17 \pm 0.35(\mathrm{stat}) \pm 0.21(\mathrm{syst}), \\ \xi\delta &= 0.49 \pm 0.24(\mathrm{stat}) \pm 0.13(\mathrm{syst}). \end{aligned}$$

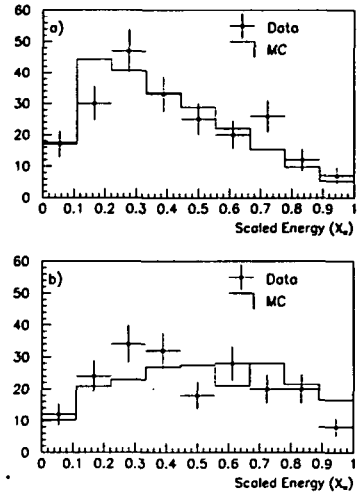

Figure 9: $\tau \rightarrow \pi(\mathrm{K})\nu_\tau$ decay energy spectra: (a) The sum of the spectra for pions in the forward direction with beam polarization $P_e < 0$ and in the backward direction with $P_e > 0$; (b) The sum of the spectra for pions in the backward direction with $P_e < 0$ and in the forward direction with $P_e > 0$. In each case the error bars are data and the histogram is from Monte Carlo.

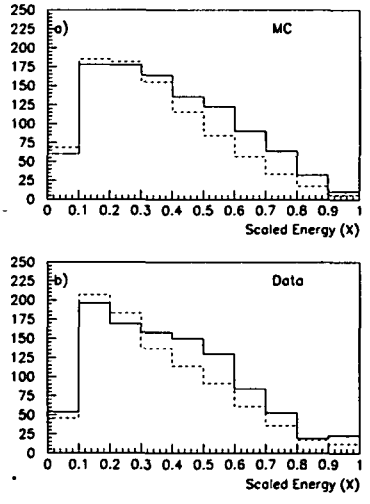

Figure 10: $\tau \rightarrow \ell\bar{\nu}_\ell\nu_\tau$ decay energy spectra from (a) Monte Carlo, and (b) the SLD data. For both histograms, the solid line is the sum of the spectra for leptons in the forward direction with beam polarization $P_e < 0$ and in the backward direction with $P_e > 0$, and the dashed line is the sum of the spectra for leptons in the backward direction with $P_e < 0$ and in the forward direction with $P_e > 0$.

The results are consistent with the Standard Model V-A predictions of -1, 1, $\frac{3}{4}$. These measurements provide an interesting cross check with other experimental results [15], [16], [17] since this analysis does not rely on spin correlations and is the first measurement to be performed with polarized beams. These first results demonstrate the power of polarized beams for probing deviations from the Standard Model in the weak couplings. Work is in progress at Brunel to extend the helicity analysis to the ρ channel, with the prospect of a 3% measurement with 500,000 Z^0.

1 References

References

[1] LEP Electroweak Working Group, *A combination of preliminary LEP electroweak results for the 1995 summer conferences,* LEPEWWG-95-02, 1995. LEP Heavy Flavor Group and SLD Heavy Flavor Group, *Combined LEP and SLD Electroweak Heavy Flavour Results for Summer 1995 Conferences,* LEPHF-95-02, SLD Physics Note 39, 1995.

[2] K. Abe *et al.*, SLAC–PUB–6681, submitted to *Phys. Rev. Lett.*

[3] K. Abe *et al.*, *Phys. Rev. Lett*, **74**, 2895 (1995).

[4] K. Abe *et al.*, contribution (EPS0250) to the International Euro-Physics Conference on High Energy Physics, Brussels, July 95.

[5] K. Abe *et al.*, *Phys. Rev. Lett.* **74** , 2890 (1995).

[6] K. Abe *et al.*, contribution (EPS0251) to the International Euro-Physics Conference on High Energy Physics, Brussels, July 95.

[7] A. Olchevski, talk presented at the International Euro-Physics Conference on High Energy Physics, Brussels, July 95.

[8] T. Takeuchi, A. Grant, J. Rosner, FermiLab–Conf–94/279–T, talk presented at the DPF'94 Meeting, Albuquerque, NM, August 94.

[9] K. Abe *et al.*, contribution (EPS0222) to the International Euro-Physics Conference on High Energy Physics, Brussels, July 5.

[10] ALEPH Collaboration, D. Buskulic *et al*, *Phys. Lett.* **B313**, 535 (1993).

[11] K. Abe et al., "Measurement of B^0 and B^+ Lifetimes at SLD", SLAC-PUB-6972, August 1995, submitted to the 1995 International Symposium on Lepton and Photon Interactions at High Energies, Beijing, China.

[12] K. Abe et al., "Measurement of the τ Charged Weak Couplings with SLC Polarized Beams", SLAC-PUB-6971, October 1995, submitted to the 1995 International Symposium on Lepton and Photon Interactions at High Energies, Beijing, China.

[13] Y.S. Tsai, *Phys. Rev.* **D4**, 2821 (1971).

[14] K.Mursula, M. Roos, F. Scheck, *Nucl. Phys.* **B219**, 321 (1989).
W. Fetscher H.J. Gerber, K.F. Johnson, *Phys Lett.* **B173**, 102 (1986).

[15] ARGUS Collaboration, H. Albrecht *et al., Phys. Lett.* **B337**, 383 (1994); *Phys.Lett.* **B349**, 576 (1995).

[16] ALEPH Collaboration, D. Buskulic *et al., Phys. Lett.* **B346**, 379 (1995).

[17] CLEO Collaboration, J. Bartelt *et al.*, "$\pi^-\pi^+$ Energy Correlation in τ Pair Events", Proceedings of the 27th Int. Conf. on High Energy Physics, Glasgow, Scotland, July 1994.

Publications since last year's report

1) RECENT RESULTS FROM THE SLD USING A HIGHLY POLARIZED ELECTRON BEAM. By SLD collaboration (Tracy Usher for the collaboration). SLAC-PUB-95-6963, Oct 1995. 11pp. Presented at 9th Les Rencontres de Physique de la Vallee d'Aoste: Results and Perspectives in Particle Physics, La Thuile, Italy, 5-11 Mar 1995.

2) PRODUCTION OF CHARM AND BEAUTY IN E+ E- WITH POLARIZED ELECTRON BEAM. By SLD Collaboration (D. Su et al.). SLAC-PUB-95-7000, Sep 1995. 9pp. Presented at Int. Symp. on Heavy Flavor Physics, Pisa, Italy, Jun 6-10, 1995.

3) MEASUREMENT OF THE AVERAGE B HADRON LIFETIME IN Z0 DECAYS USING RECONSTRUCTED VERTICES. By SLD Collaboration (K. Abe et al.). SLAC-PUB-95-6976, Sep 1995. 9pp. Published in Phys.Rev.Lett.75:3624-3628,1995. e-Print Archive: hep-ex/9511005

4) FIRST MEASUREMENT OF THE T ODD CORRELATION BETWEEN THE Z0 SPIN AND THE THREE JET PLANE ORIENTATION IN POLARIZED Z0 DECAYS TO THREE JETS. By SLD Collaboration (K. Abe et al.). SLAC-PUB-95-6969, Oct 1995. 15pp. Published in Phys.Rev.Lett.75:4173-4177,1995. e-Print Archive: hep-ex/9510005

5) THE LIFETIME PROBABILITY TAG MEASUREMENT OF R(B) USING THE SLD. By SLD Collaboration. SLAC-PUB-95-7004, Aug 1995. 22pp. Contributed to International Europhysics Conference on High Energy Physics (HEP 95), Brussels, Belgium, 27 Jul - 2 Aug 1995.

6) MEASUREMENT OF THE POLARIZED FORWARD - BACKWARD ASYMMETRY OF Z0 — B ANTI-B USING A LIFETIME TAG AND MOMENTUM WEIGHTED TRACK CHARGE. By SLD Collaboration (K. Abe et al.). SLAC-PUB-95-6979, Aug 1995. 13pp. Submitted to Int. Europhysics Conf. on High Energy Physics, Brussels, Belgium, Jul 27-Aug 1, 1995.

7) HIGHLIGHTS OF SLD PHYSICS. By SLD Collaboration (Geordie Zapalac for the collaboration). SLAC-PUB-95-6974, Aug 1995. 6pp. Presented at International Symposium on Particle Theory and Phenomenology, Ames, Iowa, 22-24 May 1995.

8) VXD3: THE SLD VERTEX DETECTOR UPGRADE BASED ON A 307 MPIXEL CCD SYSTEM. By SLD Collaboration (S. Hedges et al.). SLAC-PUB-95-6950, Jul 1995. 15pp. Contributed to International Europhysics Conference on High Energy

Physics (HEP 95), Brussels, Belgium, 27 Jul - 2 Aug 1995.

9) THE PRODUCTION OF PI+-, K+-, P, K0 AND LAMBDA0 IN HADRONIC Z0 DECAYS. By SLD Collaboration (Kenneth Baird et al.). SLAC-PUB-95-6933, Aug 1995. 10pp. Presented at Rencontres de Moriond on QCD and High-Energy Interactions, Les Arcs, France, Mar 19-26, 1995.

10) MEASUREMENT OF ALPHA-S FROM HADRONIC EVENT OBSERVABLES AT THE Z0 RESONANCE. By SLD Collaboration (Kenneth Baird et al.). SLAC-PUB-95-6932, Aug 1995. 8pp. Presented at Rencontres de Moriond on QCD and High-Energy Interactions, Les Arcs, France, Mar 19-26, 1995.

11) MEASUREMENT OF THE TAU LIFETIME AT SLD. By SLD Collaboration (K. Abe et al.). SLAC-PUB-95-6767, Apr 1995. 20pp. Published in Phys.Rev.D52:4828-4837,1995. e-Print Archive: hep-ex/9506004

12) MEASUREMENTS OF R(B) WITH IMPACT PARAMETERS AND DISPLACED VERTICES. By SLD Collaboration (K. Abe et al.). SLAC-PUB-95-6569, May 1995. 36pp. Submitted to Phys.Rev.D

13) THE ENDCAP CERENKOV RING IMAGING DETECTOR AT SLD. By K. Abe et al. SLAC-PUB-95-6693, Oct 1994. 6pp. Presented at Nucl. Sci. Symp., Norfolk, VA, Oct 30 - Nov 1, 1994.

14) PRECISE MEASUREMENT OF THE LEFT-RIGHT CROSS-SECTION ASYMMETRY IN Z BOSON PRODUCTION BY E+ E- COLLISIONS. By SLD Collaboration (Amitabh Lath for the collaboration). SLAC-PUB-6667, Sep 1994. 8pp. Presented at 1994 Meeting of the American Physical Society, Division of Particles and Fields (DPF 94), Albuquerque, NM, 2-6 Aug 1994.

15) A PRECISE MEASUREMENT OF THE LEFT-RIGHT ASYMMETRY OF Z BOSON PRODUCTION AT THE SLAC LINEAR COLLIDER. By SLD Collaboration (R.C. King for the collaboration). SLAC-PUB-95-6766, Apr 1994. 31pp. Presented at the Zeuthen Workshop on Elementary Particle Theory: Physics at LEP200 and Beyond, Teupitz, Germany, April 10-15, 1994. Published in Nucl.Phy

16) PRECISION ELECTROWEAK PHYSICS WITH THE SLD / SLC: THE LEFT-RIGHT POLARIZATION ASYMMETRY. By SLD Collaboration (P.C. Rowson for the collaboration). SLAC-PUB-6700, Dec 1994. 21pp. Talk given at Tennessee International Symposium on Radiative Corrections: Status and Outlook, Gatlinburg, TN, 27 Jun - 1 Jul 1994.

17) A TEST OF THE FLAVOR INDEPENDENCE OF STRONG INTERACTIONS.

By SLD Collaboration (K. Abe et al.). SLAC-PUB-6687, Dec 1994. 12pp. Submitted to Phys.Rev.Lett. e-Print Archive: hep-ex/9501005

18) A MEASUREMENT OF THE LEFT-RIGHT, FORWARD - BACKWARD ASYMMETRY FOR CHARM QUARKS USING D*+ AND D+ MESONS. By SLD Collaboration (M.E. King et al.). SLAC-PUB-6653, Sep 1994. 7pp. Presented at DPF Meeting, Albuquerque, N. Mex., Aug 2-6, 1994. Published in Phys.Rev.Lett.75:3609-3613,1995.

19) OBSERVATION OF TARGET ELECTRON MOMENTUM EFFECTS IN SINGLE ARM MOLLER POLARIMETRY. By M. Swartz (SLAC) et al. SLAC-PUB-6467, Dec 1994. 29pp. Published in Nucl.Instrum.Meth.A363:526-537,1995. e-Print Archive: hep-ex/9412006

20) PERFORMANCE OF THE SLD CENTRAL DRIFT CHAMBER. By M.D. Hildreth et al.SLAC-PUB-6656, Sep 1994. 8pp. Contributed to IEEE 1994 Nuclear Science Symposium and Medical Imaging Conference, Norfolk, VA, 30 Oct - 5 Nov 1994.

21) A STUDY OF K(S), LAMBDA AND ANTI-LAMBDA PRODUCTION IN HADRONIC Z0 DECAYS. By SLD Collaboration (K.G. Baird et al.). SLAC-PUB-6601, Aug 1994. 7pp. Presented at DPF Meeting, Albuquerque, N. Mex., Aug 2-6, 1994.

22) MEASURING THE LEFT-RIGHT CROSS-SECTION ASYMMETRY IN Z BOSON PRODUCTION BY E+ E- COLLISIONS AT THE SLC. By SLD Collaboration (Michael J. Fero for the collaboration). SLAC-PUB-6679, Oct 1994. 4pp. Presented at 27th International Conference on High Energy Physics (ICHEP), Glasgow, Scotland, 20-27 Jul 1994. In *Glasgow 1994, Proceedings, High energy physics, vol. 2* 399-402, and SLAC Stanford - SLAC-PUB-6679 (94/10,rec.Feb.95) 4 p.

23) HEAVY QUARK PHYSICS AT SLD (PRELIMINARY RESULTS). By SLD Collaboration (E. Vella et al.). SLAC-PUB-6711, Aug 1994. 19pp. Presented at SLAC Summer Inst., Stanford, CA, Aug 8-19, 1994.

24) PRECISION STANDARD MODEL TESTS WITH POLARIZED E+ E- BEAMS. By SLD Collaboration (Michael J. Fero et al.). SLAC-PUB-6678, Oct 1994. 19pp. Invited talk at Int. Conf. on Physics in Collision, Tallahassee, FL, Jun 15017, 1994.

25) ELECTROWEAK COUPLING MEASUREMENTS FROM POLARIZED BHABHA SCATTERING AT SLD. By SLD Collaboration (Kevin T. Pitts et al.). SLAC-PUB-6699, Sep 1994. 10pp. Presented at Int. symp. on High Energy Spin Physics, Bloomington, IN, Sep 15-22, 1994.

26) A PRELIMINARY MEASUREMENT OF THE AVERAGE B HADRON LIFETIME. By SLD Collaboration (Steven L. Manly et al.). SLAC-PUB-6668, Sep 1994. 10pp. Presented at Int. Conf. on High Energy Physics, Glasgow, Scotland, Jul 20-27, 1994. In *Glasgow 1994, Proceedings, High energy physics, vol. 2* 447-449, and SLAC Stanford - SLAC-PUB-6668 (94/09,rec.Jan.95) 10 p.

27) THE JET CONE ENERGY FRACTION IN E+ E- ANNIHILATION. By Y. Ohnishi (Nagoya U.), H. Masuda (SLAC). SLAC-PUB-6560, Oct 1994. 18pp. Submitted to Phys.Rev.D

28) PERFORMANCE OF THE SLD CCD PIXEL VERTEX DETECTOR AND DESIGN OF AN UPGRADE. By SLD Collaboration (M.G. Strauss for the collaboration). SLAC-PUB-6686, Oct 1994. 7pp. Presented at 27th International Conference on High Energy Physics (ICHEP), Glasgow, Scotland, 20-27 Jul 1994. In *Glasgow 1994, Proceedings, High energy physics, vol. 2* 1179-1181, and SLAC Stanford - SLAC-PUB-6686 (94/10,rec.Dec.) 7 p.

29) THE LEFT-RIGHT FORWARD - BACKWARD ASYMMETRY OF HEAVY QUARKS MEASURED WITH JET CHARGE AND WITH LEPTONS AT THE SLD. By SLD Collaboration (David C. Williams for the collaboration). SLAC-PUB-6648, Oct 1994. 6pp. Presented at 1994 Meeting of the American Physical Society, Division of Particles and Fields (DPF 94), Albuquerque, NM, 2-6 Aug 1994.

30) MEASUREMENT OF ALPHA-S (M(Z)**2) FROM HADRONIC EVENT OBSERVABLES AT THE Z0 RESONANCE. By SLD Collaboration (K. Abe et al.). SLAC-PUB-6641, Sep 1994. 85pp. Published in Phys.Rev.D51:962-984,1995. e-Print Archive: hep-ex/9501003

31) A SEARCH FOR JET HANDEDNESS IN HADRONIC Z0 DECAYS. By SLD Collaboration (Hiroaki Masuda for the collaboration). SLAC-PUB-6645, Sep 1994. 5pp. Contributed to 27th International Conference on High Energy Physics (ICHEP), Glasgow, Scotland, 20-27 Jul 1994.

32) MEASUREMENT OF A(B) FROM THE LEFT-RIGHT FORWARD - BACKWARD ASYMMETRY OF B QUARK PRODUCTION IN Z0 DECAYS USING A MOMENTUM WEIGHTED TRACK CHARGE TECHNIQUE. By SLD Collaboration (K. Abe et al.). SLAC-PUB-6644, Sep 1994. 20pp. Published in Phys.Rev.Lett.74:2890-2894,1995.

33) A SEARCH FOR JET HANDEDNESS IN HADRONIC Z0 DECAYS. By SLD Collaboration (K. Abe et al.). SLAC-PUB-6643, Aug 1994. 17pp. Published in Phys.Rev.Lett.74:1512-1516,1995. e-Print Archive: hep-ex/9501006

34) MEASUREMENT OF A(B) AND A(C) FROM THE LEFT-RIGHT FORWARD - BACKWARD ASYMMETRY OF LEPTONS IN HADRONIC EVENTS AT THE Z0 RESONANCE. By SLD Collaboration (K. Abe et al.). SLAC-PUB-6607, Jul 1994. 15pp. Published in Phys.Rev.Lett.74:2895-2899,1995.

THE STUDY OF CP VIOLATION IN THE NEUTRAL KAON SYSTEM AT LEAR

PS195 **PROPOSAL 265**

Athens, Basel, Boston, CERN, Coimbra, ETH Zurich, Fribourg, Ioannina, Liverpool, Lubljana, Marseille, Orsay, PSI, Saclay, Stockholm, Thessaloniki

Introduction

The CPLEAR experiment investigates CP, T and CPT symmetries in the decay of neutral kaons produced at LEAR. Unlike other experiments which use beams of K^0_L and/or K^0_S, this experiment measures the difference between the decays of initially pure K^0 and $\bar{K}^0$ to a variety of final states $\pi^+\pi^-$, $\pi e \upsilon$, $\pi^+\pi^-\pi^0$ and $\pi^0\pi^0$.

The principle of the method is to compare the process of the initial K^0 decaying into a well defined eigenstate at a well defined eigentime t with that of $\bar{K}^0$ into the "same" state. Any difference is a sign of CP violation. This difference arises mainly through the K^0_L - K^0_S interference term. The relevant parameters are then extracted from time dependent decay rate asymmetries of the form

$$A_f(t) = \frac{R(t, \bar{K}^0 \to \bar{f}) - R(t, K^0 \to f)}{R(t, \bar{K}^0 \to \bar{f}) + R(t, K^0 \to f)}$$

The use of such asymmetries has the advantage that all acceptances which are common to K^0 and $\bar{K}^0$ cancel, thus considerably reducing the systematic uncertainties. In addition, it is possible to make detailed comparisons between the different rates to provide a better knowledge of the detector performance.

The present understanding of CP violation is not clear. It can be incorporated into the Standard Model by introducing a complex phase into the CKM matrix which should show up as an effect in the decay amplitudes. However, the recent discovery of the top mass at a value of around 180 GeV means that direct CP violation will be very difficult to determine. It is therefore essential to rule out other possible sources such as CPT violation or anomalies in T violation.

The experiment has recently completed its data taking phase for 1995 and will use the running period of 1996 to reduce the largest source of systematic error due to regeneration effects ($K^0 \to \bar{K}^0$). Already from the analysed data, world class measurements are available on the CP violation parameters, a first direct determination of T violation and limits on a possible CPT violation in a region where quantum gravity effects could modify conventional quantum field theory.

The CPLEAR experiment

The CPLEAR experiment uses an intense 200 MeV/c antiproton beam (~$10^6\bar{p}$/s) from the Low Energy Antiproton Ring (LEAR) at CERN. The K° and $\bar{K}^\circ$ mesons are symmetrically produced in proton-antiproton annihilations at rest through the reactions

$$p\bar{p} \rightarrow K^-\pi^+K^\circ, \qquad Br = 2 \times 10^{-3}$$
$$p\bar{p} \rightarrow K^+\pi^-\bar{K}^\circ, \qquad Br = 2 \times 10^{-3}$$

The strangeness of the neutral kaon is tagged by observing the sign of the charged kaon. The symmetrical production of K° and $\bar{K}^\circ$ together with a symmetrical detection of their decay states has the advantage of minimising the systematic effects.

The detector, shown in figure 1, has a cylindrical geometry and is mounted inside a solenoid of 3.6m length and 1m radius, which produces a magnetic field of 0.44 T parallel to the antiproton beam. The antiprotons are stopped and annihilate inside a spherical target filled with gaseous hydrogen at 15 atmospheres pressure. The charged particle tracking is performed with two multiwire Proportional Chambers, six layers of Drift Chambers and two layers of Streamer Tubes. These streamer tubes are the responsibility of the Liverpool Group and operated successfully at high rates up to 50 KHz/wire. They provide a fast 'Z' coordinate using end-to-end timing to determine the on-line momenta of charged tracks for triggering, when used in conjunction with other tracking devices. The charged kaons and pions are identified using the Particle Identification Detector (PID), consisting of Scintillator-Cerenkov-Scintillator sandwich (SCS). The threshold for producing light in the Cerenkov counter is 300 MeV/c for pions and 700 MeV/c for kaons. Therefore $K^\pm$ mesons produced in the annihilation process with momenta less than 700 MeV/c are required to have a *SCS* pattern in the PID. Finally, there is an 18-layer gas sampling electromagnetic calorimeter (6.2 radiation lengths) with a high spatial resolution of the order of 5mm.

Because of the small branching ratio of the desired channels, the experiment requires a high annihilation rate. In order to provide an efficient online event selection and background rejection, a sophisticated multi-level trigger has been developed. The maximum trigger decision time is around 34μs and the trigger rejection factor is about 1000. The data acquisition system writes about 450 events per second on tape at a beam intensity of 1 MHz.

Following an extensive period of development, the spherical target was replaced by a cigar shaped H_2 target operating at 30 atmospheres, surrounded by a small 4 cm diameter proportional chamber consisting of 100 wires which was successfully tested in September 1994. The new chamber/target combination operated for the full 1995 running period. The chamber was installed in the on-line trigger, which improved the quality of selected events, removed data at short lifetime (<1 τ_S) and reduced the dead times of the overall trigger and DAQ. The number of $\pi\pi$ events is shown in the table below.

CPLEAR data sets for 1993-95 running

Year	Average beam rate kp̄/sec	Number of antiprotons $x10^{12}$	Number of events on tape $x10^{9}$	$\pi^+\pi^-(>1\tau_s)$ final sample $x10^{6}$	$\pi^0\pi^0$ final sample $x10^{6}$
93	580	2.0	1.1	12	0.5
94	540	1.6	1.0	9	0.6
95	750/950	4.1	1.6	30	1.5

Status of the Physics Analysis

The last 1995 data taking period has recently finished. All the 1994 data has been produced and the first stage of production has been started for the 1995 data. All the results presented here use data recorded between 1990 and mid-1994.

(i) $\pi^+\pi^-$ channel

The asymmetry

$$A_{+-}(t) = \frac{R(\bar{K}^0 \to \pi^+\pi^-) - R(K^0 \to \pi^+\pi^-)}{R(\bar{K}^0 \to \pi^+\pi^-) + R(K^0 \to \pi^+\pi^-)}$$

is shown in figure 2. A fit to this asymmetry for the magnitude and phase of η+-, using the CPLEAR value of Δm measured from the semileptonic decays, yields:

$$|\eta_{+-}| = [2.312 \pm 0.043_{stat} \pm 0.030_{syst} \pm 0.011_{\tau_s}] \times 10^{-3}$$

$$\phi_{+-} = 42.7^\circ \pm 0.9^\circ_{stat} \pm 0.6^\circ_{syst} \pm 0.9^\circ_{\Delta m}$$

where the additional uncertainty of 0.011 x 10^{-3} on $|\eta_{+-}|$ is due to the uncertainty of τ_s and 0.9° on ϕ_{+-} is due to the uncertainty on the present value of $\Delta m = m_L - m_S$

(ii) $\pi^0\pi^0$channel

A new technique to reconstruct the kaon decay vertex has been introduced to improve the vertex resolution. This has improved the lifetime resolution to $1\tau_S$. A fit to the asymmetry A_{00}, shown in figure 3, yields:

$$|\eta_{00}| = [2.49 \pm 0.40_{stat}] \times 10^{-3}$$

$$\phi_{00} = 50.8^{\circ} \pm 7.1^{\circ}{}_{stat}$$

This measurement is presently dominated by statistical uncertainty, but clearly shows directly CP violation in the $\pi^{\circ}\pi^{\circ}$ channel.

(iii) $\pi e \nu$ channel

The semileptonic decay channel enables a measurement of Δm, and the parameter x, a measure of any violation of $\Delta S = \Delta Q$ rule. Figure 4 shows the asymmetry $A_{\Delta m}$. A fit to this asymmetry yields.

$$\Delta m = [0.5274 \pm 0.0029_{stat} \pm 0.0005_{syst}] \times 10^{10} \hbar s^{-1}$$

$$\Re e(x) = [12.4 \pm 11.9_{stat} \pm 6.9_{syst}] \; 10^{-3}$$

A first direct measurement of T violation and CPT violation has been made by the construction of the asymmetries A_T and A_{CPT} shown in figures 5 and 6 respectively. Fits to the asymmetries yields:

$$A_T = [6.3 \pm 2.1_{stat} \pm 1.8_{syst}] \times 10^{-3}$$

$$\Re e(\delta_{CPT}) = [0.07 \pm 0.53_{stat} \pm 0.45_{syst}] \times 10^{-3}$$

The value of A_T is 2.3σ from zero and provides first direct experimental evidence of T violation in the K° system.

(vi) $\pi^{+}\pi^{-}\pi^{\circ}$ channel

The decays of neutral kaons to $\pi^{+}\pi^{-}\pi^{\circ}$ is complicated due to the angular momentum dependence of the CP value of the final state. Hence there are three decay modes.

$$K_L \to \pi^+\pi^-\pi^\circ\,(I = 0)\;CP\ allowed$$

$$K_S \to \pi^+\pi^-\pi^\circ\,(I = 0)\;CP\ violating$$

$$K_S \to \pi^+\pi^-\pi^\circ\,(I = 1)\;CP\ allowed,\ angular\ mom.\ suppressed$$

A Dalitz plot analysis enables the quantity of each mode to be determined since the CP conserving K_S decays are distributed antisymmetrically across the Dalitz plot whereas the CP violating K_S and K_L decays are distributed symmetrically.

The construction of asymmetries from different regions of the Dalitz plot enables the extraction of the parameters λ, the ratio of CP allowed decay widths $\Gamma(K_S \to \pi^+\pi^-\pi^\circ)/\Gamma(K_L \to \pi^+\pi^-\pi^\circ)$, and η_{+-o}.

The CP conserving asymmetry is shown in figure 7 and a fit yields:

$$\lambda = \frac{\Gamma(K_S \to \pi^+\pi^-\pi^\circ)\ CP{=}+1}{\Gamma(K_L \to \pi^+\pi^-\pi^\circ)\ CP{=}-1} = [34 \pm 10_{stat}] \times 10^{-3}$$

providing the first measurement of $K_s \to \pi^+\pi^-\pi^\circ$ CP allowed transition
B.R. $[K_s \to \pi^+\pi^-\pi^\circ]$
The CP violating asymmetry is shown in figure 8 and a fit yields:

$$\Re e(\eta_{+-o}) = [6 \pm 14_{stat} \pm 2_{syst}] \times 10^{-3}$$

$$\Im m(\eta_{+-o}) = [-2 \pm 19_{stat} \pm 4_{syst}] \times 10^{-3}$$

A comparison with previous experiments is shown in figure 9.

(v) Combined results

The combination of the above measurements can provide a sensitive test of discrete symmetries and quantum mechanics.

A comparison of ϕ_{+-} with superweak phase $\phi_{SW} = 43.3^\circ \pm 0.16^\circ$ yields a direct test of CPT invariance resulting in a limit of the K° - $\bar{K}^\circ$ mass difference of

$$\left|\frac{m_{\bar{K}^0} - m_{K^0}}{m_{K^0}}\right| < 2.1 \times 10^{-18} \text{ (90\% c.l.)}$$

Furthermore some approaches to quantum gravity can produce a violation of CPT and alter the asymmetries A_{+-} and $A_{\Delta m}$. A combined fit to these asymmetries results in an upper limit for CPT violation described by the three parameters α,β and γ.

$$\alpha < 4.0 \times 10^{-17} GeV, \quad |\beta| < 2.3 \times 10^{-19} GeV, \quad \gamma < 3.7 \times 10^{-21} GeV$$

These upper limits enter the range **O** (m^2_K/M_{Pl})

Future prospects and conclusions

The largest systematic uncertainty on the measurement of η_{+-} is that caused by the lack of knowledge of the forward scattering amplitudes of K^0 and $\bar{K}^0$ in matter. This regeneration error is responsible for a 0.6° systematic error on ϕ_{+-} and a 0.02 x 10^{-3} systematic error on $|\eta_{+-}|$.

In 1996 CPLEAR will measure the difference of the forward scattering amplitudes of K^0 and $\bar{K}^0$ at low energies. This will be performed by the insertion of a cylindrical absorber (120° arc) made of 2cm thick carbon at a radius of 7cm (between PC0 and PC1). 90% of the original K_Ss have decayed before reaching the absorber. The interference between the remaining K_S and the K_S regenerated from the K_L within the absorber will enable the measurement to be made. CPLEAR has been approved for 70 days of data-taking which will reduce the systematic error due to regeneration to 0.1° on ϕ_{+-}.

Publications

1. Bose-Einstein correlations in $\bar{p}p$ annihlations at rest

   R. Adler et al for the CPLEAR Collaboration
   CERN-PPE/94-64
   Zeitschrift für Physik C 63, [1994] p. 541-547

2. Inclusive measurement of $\bar{p}$ annihilation in gaseous hydrogen to final states containing ϱ and f_2

   The CPLEAR Collaboration
   CERN-PPE/94-95
   Zeitschrift für Physik C 65, Vol. 2 [1995] p. 199-205

3. Measurement of K_L - K_S mass difference using semileptonic decays of tagged neutral kaons

   The CPLEAR Collaboration
   CERN-PPE/95-103
   Physics Letters B 363 [1995] p. 237-242

4. Measurement of the CPLEAR violation parameter η_{+-} using tagged K° and $\bar{K}^\circ$

   The CPLEAR Collaboration
   CERN-PPE/95-107
   Physics Letters B 363 [1995] p. 243-248

5. A new determination of the K_L-K_S mass difference and the phase of the CP violation parameter η_{+-} from an evaluation of experimental data

   The CPLEAR Collaboration
   CERN-PPE/95-112
   Submitted to Zeitschrift für Physik C

6. First observation of a particle-antiparticle asymmetry in the decay of neutral kaons into $\pi^\circ\pi^\circ$

   The CPLEAR Collaboration
   Submitted to Zeitschrift für Physik C

7. Tests of CPT symmetry and quantum mechanics with experimental data from CPLEAR

   Submitted to Physics Letters B

Figure Captions

1. The CPLEAR Detector

2. The $\pi^+\pi^-$ asymmetry $A_{+-}[t]$. The solid curve is the result of our fit

3. The $\pi^\circ\pi^\circ$ asymmetry $A_{oo}(t)$. The solid curve is the result of our fit

4. The semileptonic asymmetry $A_{\Delta m}(t)$. The solid curve is the result of our fit for Δm

5. The semileptonic asymmetry $A_{CPT}[t]$. The dotted line is the result of our fit

6. The semileptonic decay, the asymmetry A_2 as a function of the decay time

7. $\pi^+\pi^-\pi^\circ$ CP conserving asymmetries $A^{+-0}[t]$. The solid curves are the result of our fit for λ

8. $\pi^+\pi^-\pi^\circ$ CP violating asymmetry $A^{+-0}[t]$. The solid curve is the result of our fit for η_{+-0}. The dotted curve is the result of our fit where $\Re e[\eta_{+-0}] = \Re e[\eta_{+-}]$ is fixed

9. An argand diagram comparing the CPLEAR result for η_{+-0} with those from previous experiments

The CPLEAR Detector

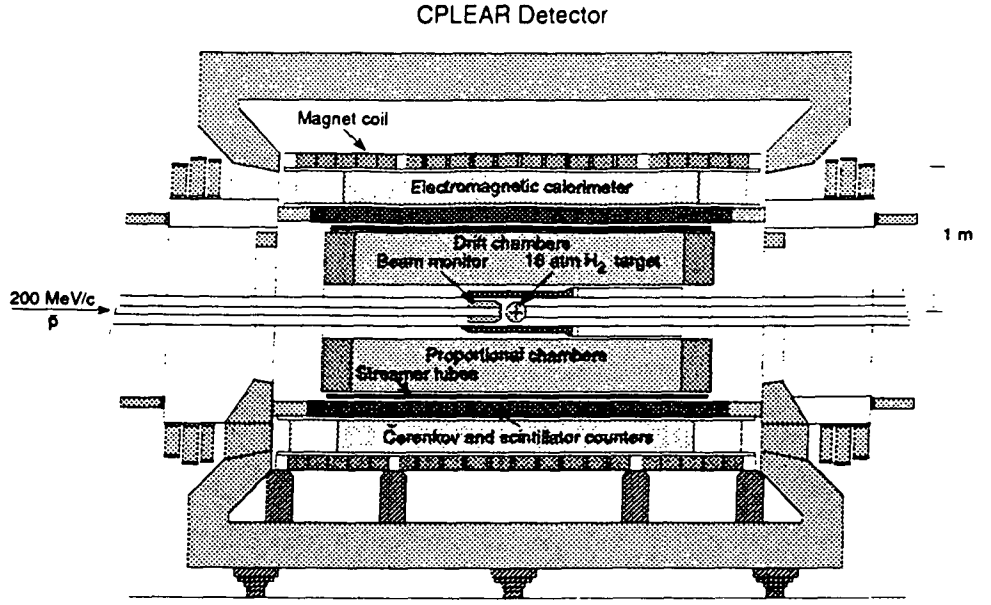

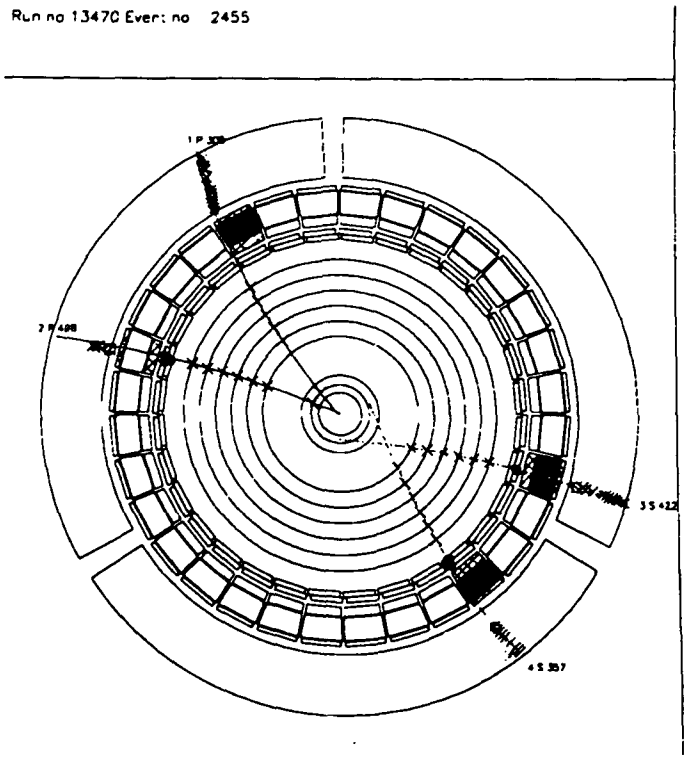

H_2 target (16 bar)

Proportional chambers

Drift chambers

Streamer tubes

Scintillation counters

Čerenkov Counter

Calorimeter

Figure 1.

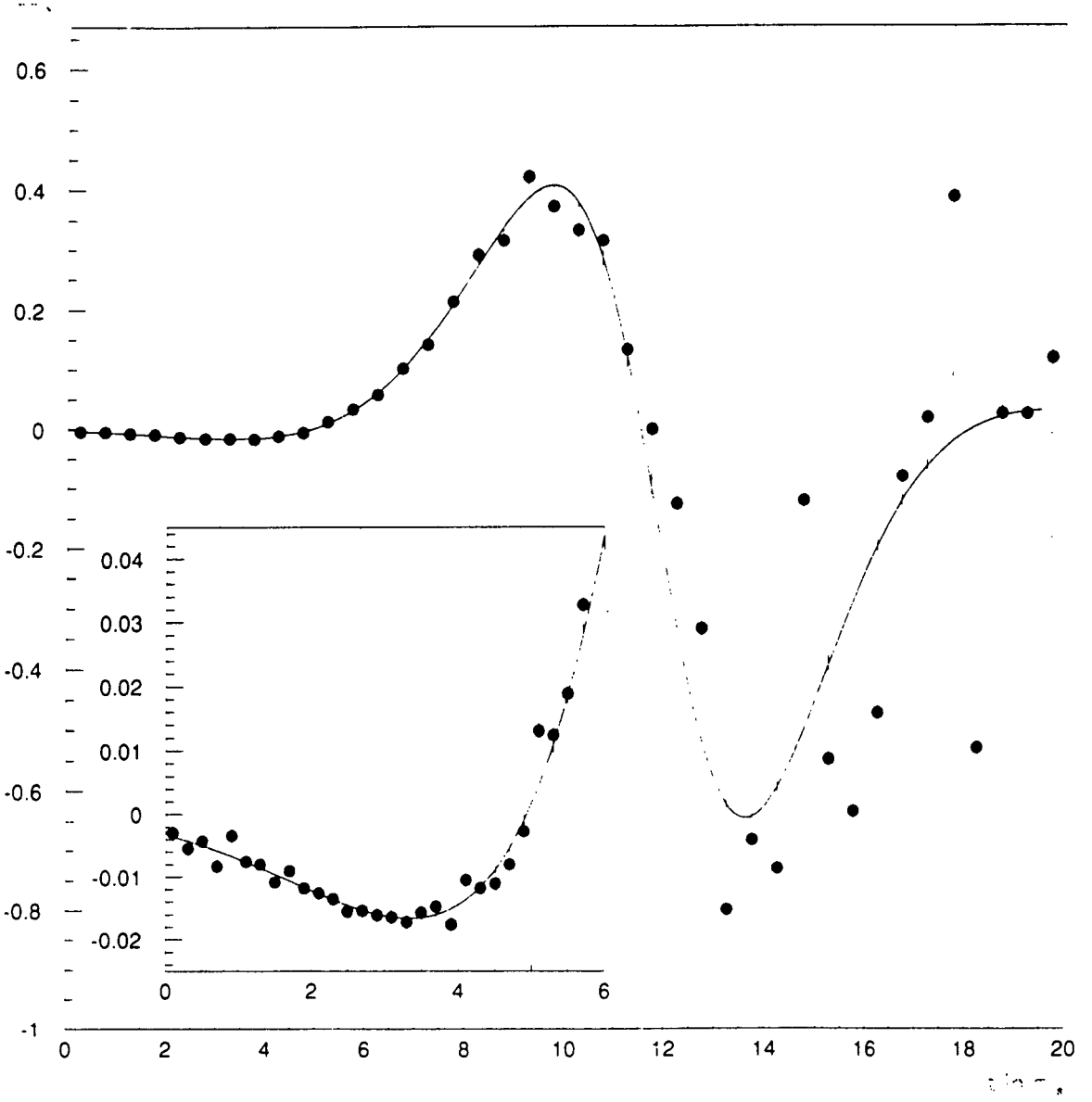

Figure 2.

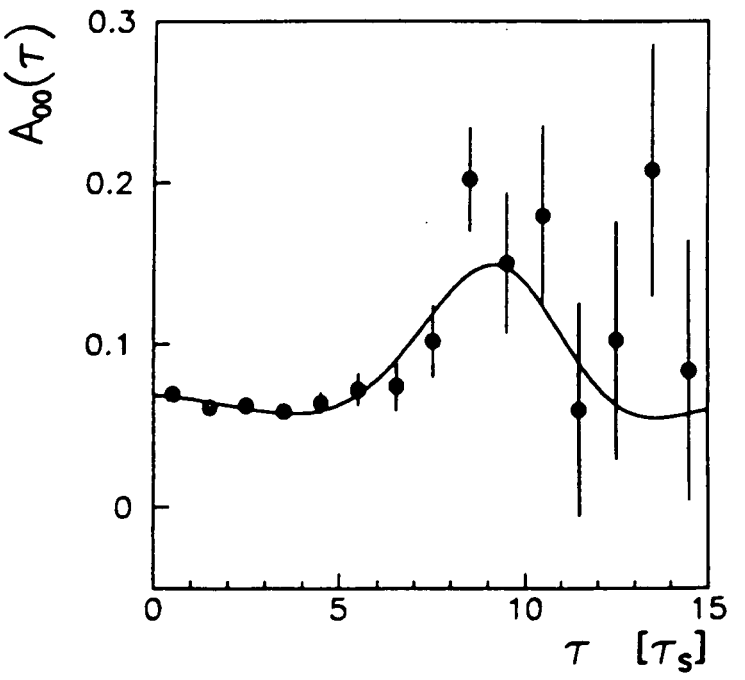

Figure 3.

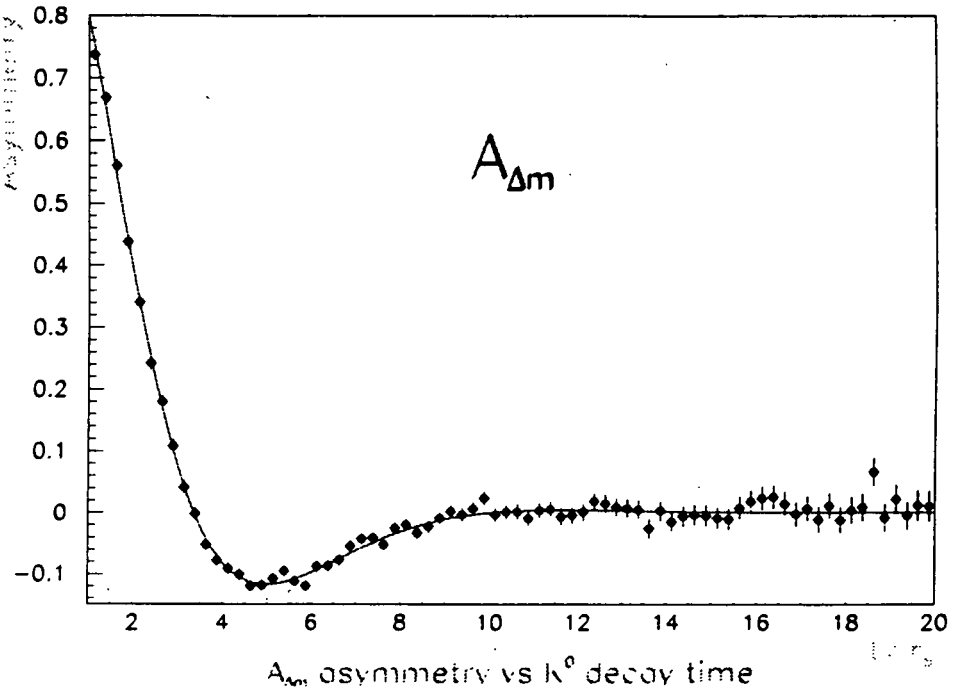

$A_{\Delta m}$ asymmetry vs K^0 decay time

Figure 4.

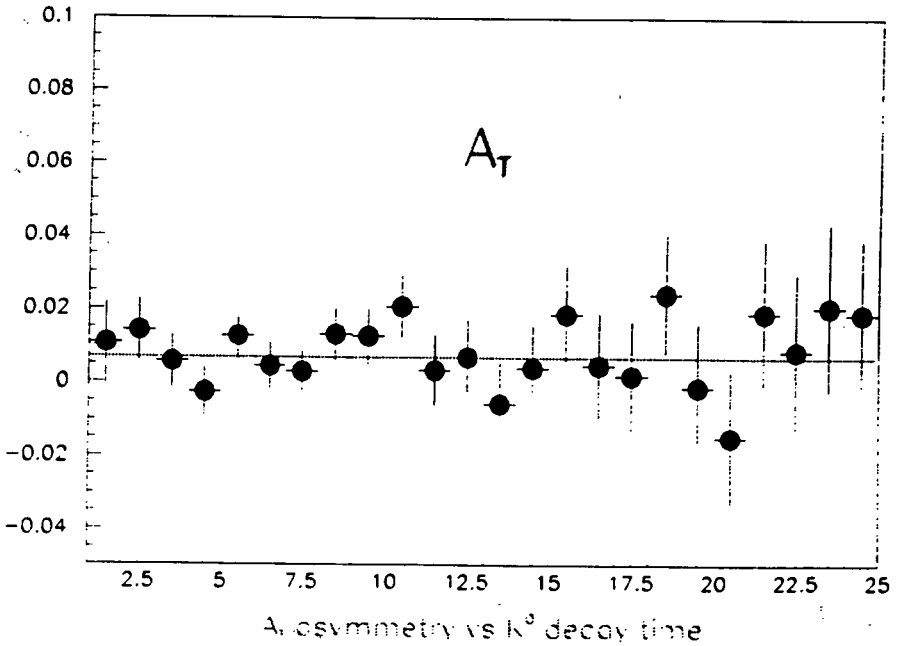

A_T asymmetry vs K^0 decay time

Figure 5.

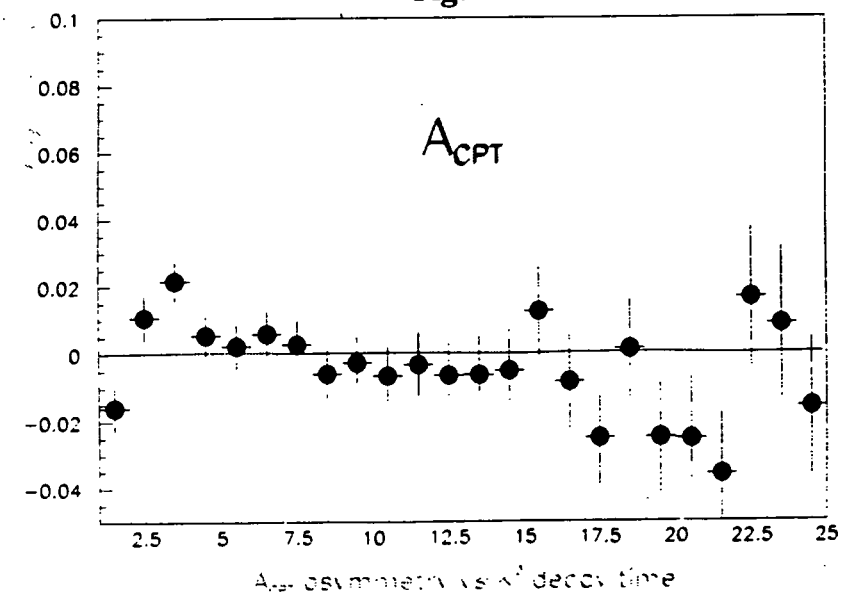

A_{CPT} asymmetry vs K^0 decay time

Figure 6.

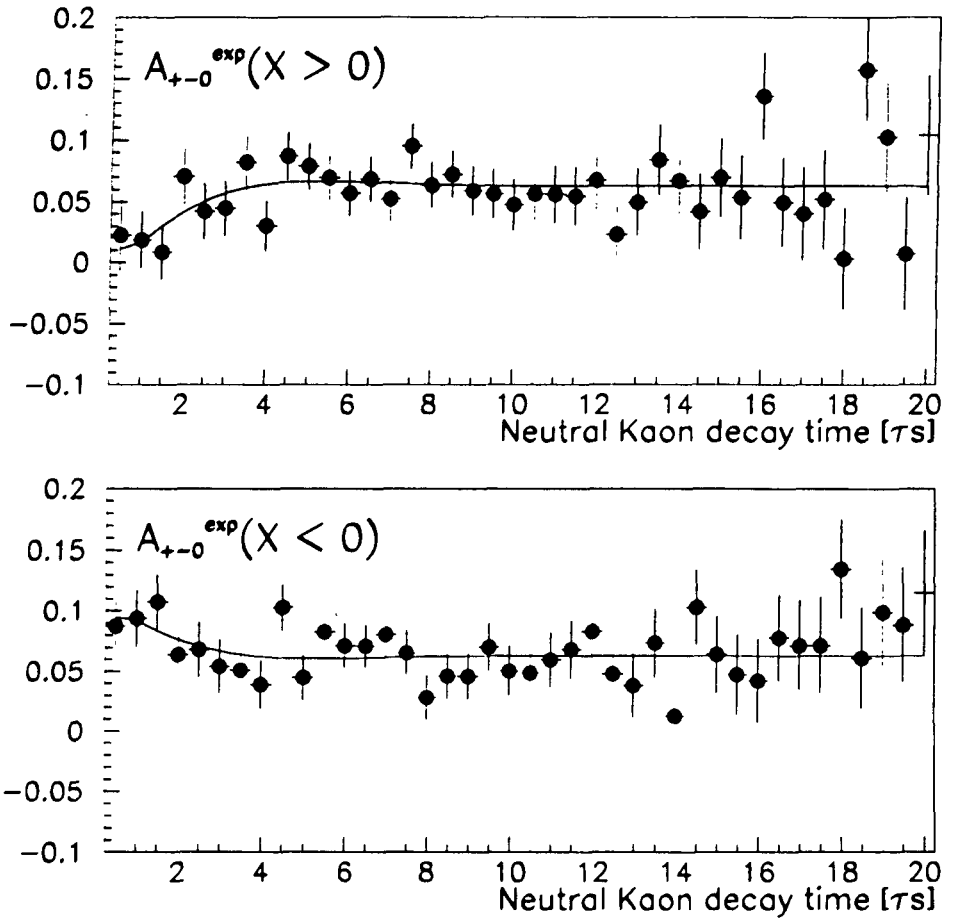
$A_{+-0}^{exp}(X > 0)$
$A_{+-0}^{exp}(X < 0)$
0.2
0.15
0.1
0.05
0
−0.05
−0.1
2
4
6
8
10
12
14
16
18
20
Neutral Kaon decay time [τs]

Figure 7.

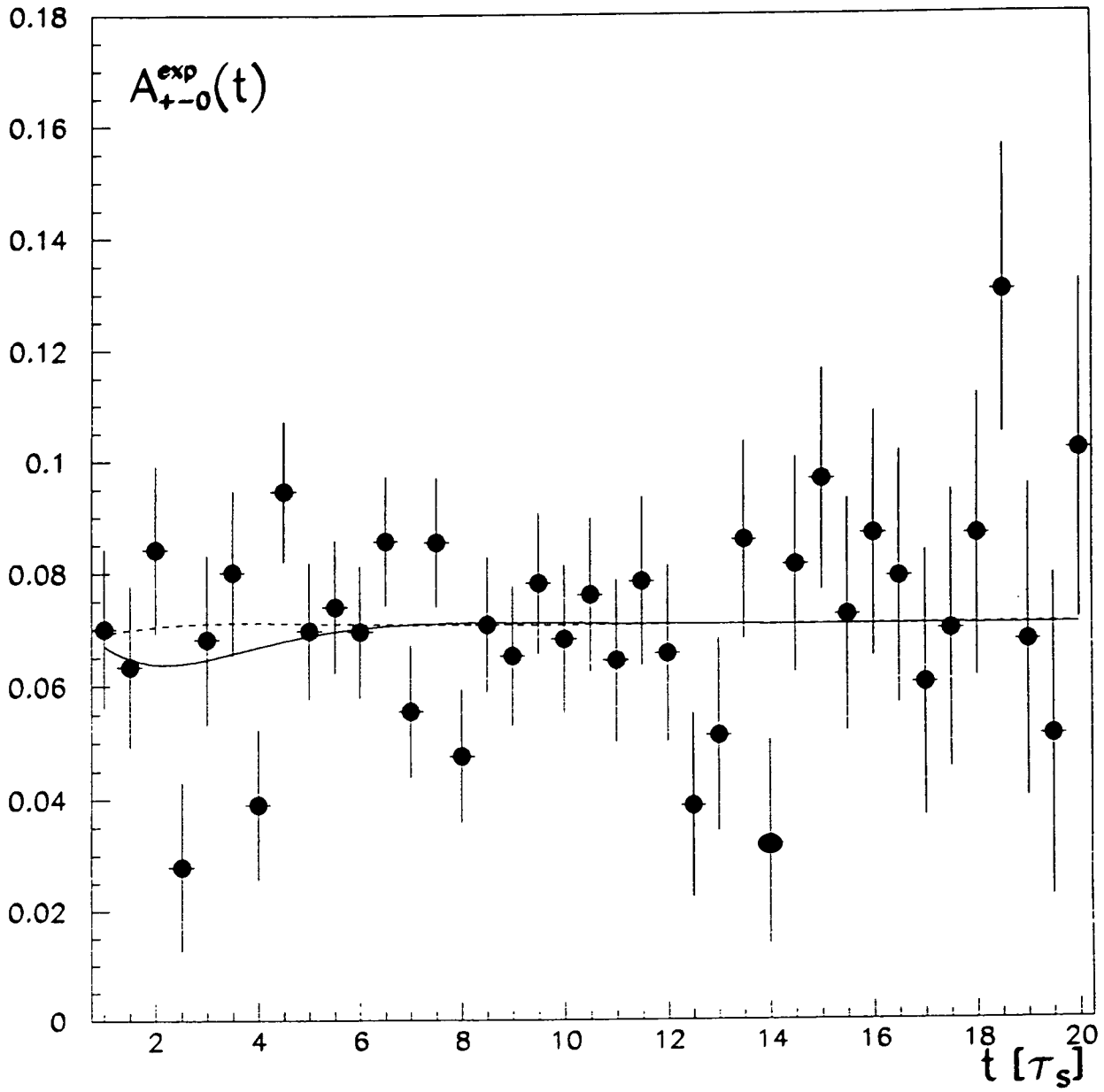
$A^{exp}_{+-0}(t)$
0.18
0.16
0.14
0.12
0.1
0.08
0.06
0.04
0.02
0
2
4
6
8
10
12
14
16
18
20
t [τ_S]

Figure 8.

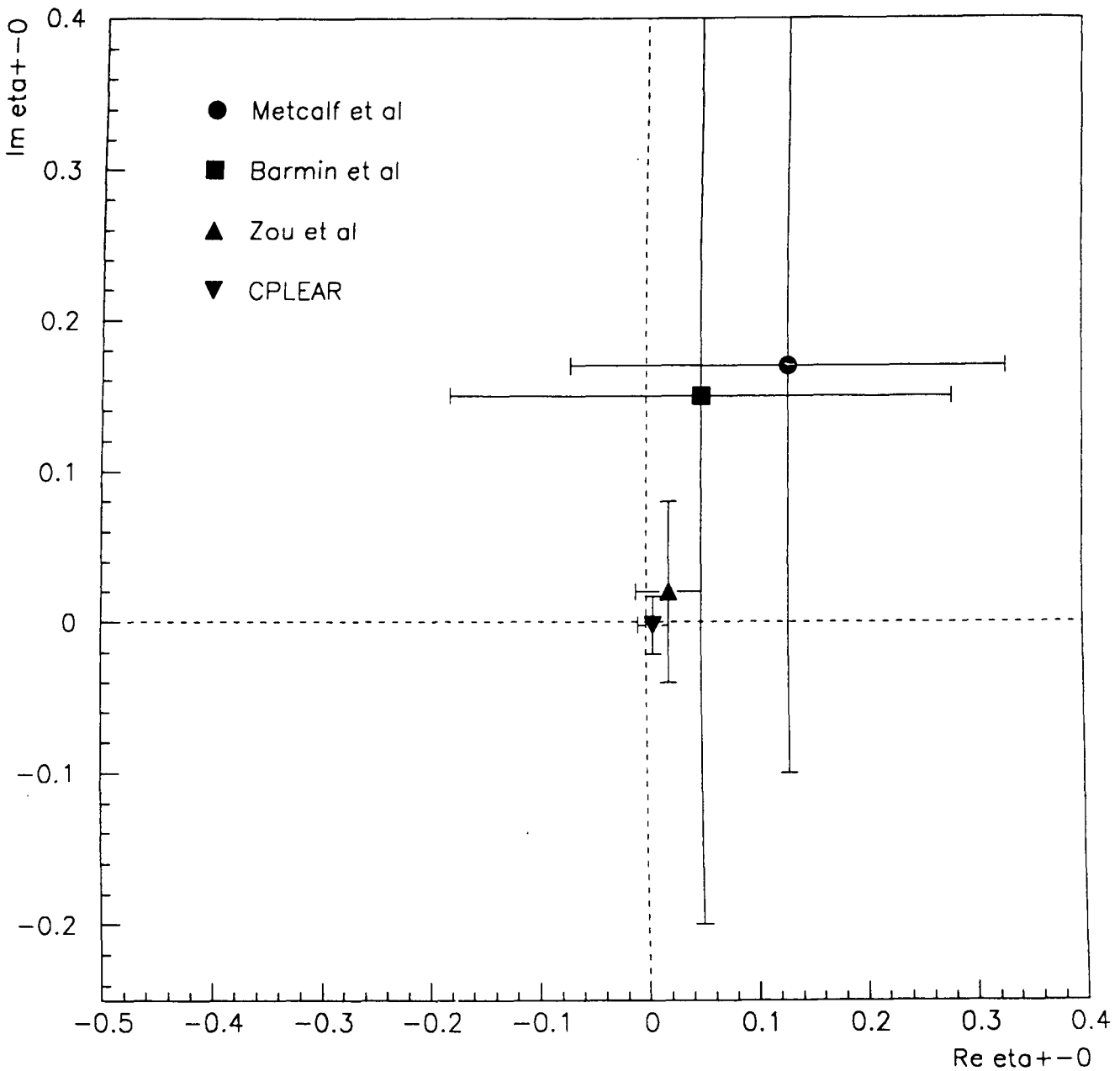
Im eta+−0
Re eta+−0
Metcalf et al
Barmin et al
Zou et al
CPLEAR
0.4
0.3
0.2
0.1
0
−0.1
−0.2
−0.5
−0.4
−0.3
−0.2
−0.1
0
0.1
0.2
0.3
0.4

Figure 9.

CRYSTAL BARREL EXPERIMENT

PS197 **PROPOSAL 268**

Queen Mary & Westfield College, London; Rutherford Appleton Laboratory; Lawrence Berkeley Laboratory; UCLA; University of Bochum; University of Bonn; University of Budapest; CERN; University of Hamburg; University of Karlsruhe; University of Mainz; University of Munich; Carnegie Mellon, Pittsburgh; CRN Strasbourg; University of Zurich.

The Crystal Barrel is a 4π spectrometer designed to provide complete and precise information on almost all final states produced in $\bar{p}p$ and $\bar{p}d$ annihilations at low energy. The physics goal is to identify all light mesons in the mass range from 0.14 to 2.3 GeV/c^2, to determine their quantum numbers and decay properties and to study the annihilation dynamics. The main interest is to find and identify the glueballs and hybrid mesons predicted by QCD.

The experiment uses antiproton beams from the LEAR facility at CERN over the momentum range 0.1 to 2.0 GeV/c. The apparatus has "4π" geometry and is mounted inside a solenoidal magnetic field of 1.5 T. The $\bar{p}p$ (or $\bar{p}d$) interactions take place in a hydrogen target; usually liquid hydrogen is used but two runs have been made during the past year using a H_2 gas target operating at 12 atm pressure to enhance the rate of P-state annihilations for antiprotons interacting at rest. Also during the past year a new silicon strip detector has been installed surrounding the target, replacing the two cylindrical multiwire proportional chambers previously used. As well as giving improved vertex measurements it also significantly increases the efficiency for detecting neutral kaons decaying to charged pions. A cylindrical jet drift chamber (JDC) is used to measure the momenta of charged particles and ionization sampling gives discrimination between π's and K's for momenta below 500 MeV/c. Nearly all neutrals and charged particles are detected in a 1380 element barrel shaped CsI detector covering 97% x 4π solid angle.

The RAL group has been heavily involved in the design of the H_2 gas targets. It is also responsible for the ADC and discriminator systems associated with the CsI detector and for the beam defining and veto counters. The special hardware constructed to give a fast trigger on the total energy deposited in the CsI crystals has been frequently used during the past year. The RAL group is also responsible for the maintenance of the software used in both the crystal readout and online data monitoring.

S- and P- state annihilation in $\bar{p}p$ interactions at rest

It is of some importance to know the fractions of S- and P-state annihilations in $\bar{p}p$ interactions at rest. As a result of the effects of Stark mixing, these quantities depend on the H_2 target density. Two body branching fractions have been used to derive the fraction of P-state annihilation as a function of target density. Due to the Stark mixing it is necessary to take into account an enhancement of annihilations from fine structure states over that expected from a statistical population. The enhancement factors were obtained from an atomic cascade calculation which fits available $\bar{p}p$ atom X-ray measurements. The P-state fraction in liquid hydrogen is found to be $f_P = 0.13 \pm 0.04$ and in gas at 12 atm pressure $f_P = 0.50 \pm 0.05$. These values are significantly different from, but more reliable than, those obtained in previous evaluations.

$\bar{p}p \rightarrow \eta\,\pi^0\,\pi^0\,\pi^0$ in flight

Data on this reaction at 1940 MeV/c have been finalised for publication. The main development since last year's report concerns presentation: plots have been found which display the two 2^{-+} resonances at 1645 and 1850 MeV. The former decays to $a_2(1320)\pi$. Fig. 1(a) shows this channel by selecting a_2 events within a window of $\pm$ 50 MeV in $\eta\pi$ mass,

but rejecting events where a $\pi\pi$ mass combination is compatible with f_0 (975) or f_2 (1270). Fig. 1(b) does the converse selection, identifying $\pi\pi$ pairs in the mass range 1150 - 1350 MeV compatible with f_2 (1270), but rejecting events where the $\eta\pi$ pair lies within ± 120 MeV of a_2 (1320). This selection enhances the η_2 (1850) → f_2 (1270) η signal. On the figures, the dashed curves show Monte Carlo simulations of phase space after these cuts; the full curves show the fit.

The η_2 (1645) makes a natural candidate for the 2^{-+} $q\bar{q}$ state expected at about this mass as partner to π_2 (1670). The second resonance η_2 (1850) is a natural candidate for a glueball or hybrid. Its strong decay to f_2 (1270) η compared to a_2 (1320) π makes it unlikely to be a $q\bar{q}$ state (or the high mass tail of η_2 (1645)). We are now actively searching for an I = 1 hybrid partner in the mass range 1800 - 1900 MeV, decaying to 3π.

$\bar{p}p \rightarrow 5\pi^0$ at rest

The 4π mass spectrum for this reaction, Fig. 2, differs significantly from phase space. We are able to fit this spectrum well, using as ingredients f_0 (1335), f_0 (1505) and f_0 (1750) which we have discovered in analyses of other reactions. The histograms show data (full histograms) and phase-space (dashed) for 4π, 3π and 2π. The 2π mass spectrum strongly rules out the narrow f_0 (750) resonance claimed by Svec, which predicts the full histogram on Fig. 2(d).

There is some hint in the data of f_0 (1500) → $\pi\pi$ (1300). At the moment, the evidence is not conclusive. If confirmed, it would be strong evidence against f_0 (1500) being a conventional ground state $q\bar{q}$ meson. It would be explained naturally by f_0 (1500) being a gg state of small radius; r = 0.3 fm is predicted by lattice QCD calculations, compared with 0.8 - 0.9 fm for $q\bar{q}$ states.

Further analysis of $\pi\pi$ data

In earlier work, we have presented evidence for new 0^+ resonances f_0 (1335), f_0 (1505) and f_0 (1750). These escaped detection in earlier analyses of $\pi\pi$ elastic scattering and $\pi\pi \rightarrow K_s^0K_s^0$. In collaboration with A Sarantsev and V Anisovich, we have undertaken a re-analysis of these data using parameters consistent with those fitting $\bar{p}p \rightarrow 3\pi^0$ at rest and also $\bar{p}p \rightarrow \eta\eta\pi$ and $\bar{p}p \rightarrow \eta\pi^0\pi^0$.

The f_0 (1505) shows up very clearly in CERN-Munich data on $\pi^+\pi^- \rightarrow \pi^+\pi^-$ and we fit a decay width $\Gamma_{2\pi} = 60 \pm 12$ MeV. Since annihilation data determined the relative branching ratios of f_0 (1500) to $\pi\pi$, $\eta\eta$ and $\eta\eta'$, this result is important because it provides an absolute normalisation of all decay modes.

The f_0 (1335) appears weakly in CERN-Munich data, which require a very small coupling to 2π, $\Gamma_{2\pi} \leq 40$ MeV. The data on $\pi^+\pi^- \rightarrow K_s^0K_s^0$ show a definite peak at 1300 - 1335 MeV, presumably due to f_0 (1335). This strong $K\bar{K}$ coupling is surprising; it has proved difficult to achieve simultaneous fits of this resonance to all data with consistent parameters. Work continues on this, and also on fits to Crystal Barrel data on $\bar{p}p \rightarrow K_sK_s^0\pi^0$, $K_L^0K_L^0\pi$ and $K^+K^-\pi^0$.

$\bar{p}p \rightarrow \eta\pi^0\pi^0\pi^0$ at rest

A search for resonances below 1750 MeV decaying to $\eta\pi^0\pi^0$ has been made. Neglecting the production of 2^{++} mesons with mass below 1.75 GeV which are not expected to decay to $\eta\pi^0\pi^0$, all other accessible states (0^{-+}, 1^{++} and 2^{-+}) are produced via P-wave annihilation at rest. The data presently under discussion were obtained using a liquid hydrogen target where the P-wave fraction is expected to be approximately 10%. New data from a run with a gas target are presently being analysed.

The data are illustrated by Fig. 3 where the large combinatorial background is evident. Using the convenient shorthand $\sigma \equiv (\pi\pi)$ s-wave, the data were fitted using the unbinned maximum likelihood method with contributions from $a_0(980)\sigma$, $a_2(1320)\sigma$, $f_1(1285)\pi^0$, $\eta(1400)\pi^0$, $f_1(1510)\pi^0$ and $\eta_2(1645)\pi^0$ plus incoherent background distributed as phase space. Fig. 3 illustrates the current status of the fits which are still continuing and are therefore preliminary. One defect appears in the description of the $\eta\pi^0\pi^0$ region 1520-1590 MeV when filtered events contain an $\eta\pi$ combination consistent with an $a_2(1320)$, Fig. 3(d). There was no requirement for an additional component from $\eta(1295)$ decaying to $a_0(980)\pi^0$ or from $f_1(1420)$. There is a structure evident when events are filtered to contain an $a_2(1320)$, which is the $\eta_2(1645)$ with width 160 MeV which is also seen in the in flight data (see above). A possible weak 0^{-+} signal was evident at 1650 MeV when events were filtered to contain an $a_0(980)$ and not an $a_2(1320)$ which could not be distinguished from $\eta_2(1645) \rightarrow (a_0(980)\pi^0)_{L=2}$.

$\bar{p}p \rightarrow \omega\omega\pi^0$

There is speculation that the $f_2(1640)$ seen decaying to $\omega\omega$ may just be a threshold effect echoing the high mass tail of the $f_2(1520)$ (the "AX" J = 2 resonance, not the predominantly $s\bar{s}$ $f_2'(1525)$). It is important that the $f_2(1520)$ is seen distinct from the $f_0(1500)$ (from differing decay modes), and confirmation of the quantum numbers of the object at 1640 MeV decaying to $\omega\omega$ is needed. To this end, data from 8.24×10^6 all-neutral triggers has been utilised to extract the $\omega\omega\pi^0$ final state (where $\omega \rightarrow \pi^0\gamma$ for both ω's) resulting in 715 events relatively free from background. As shown in Fig. 4, there appears to be a threshold enhancement in the $\omega\omega$ system, and a partial wave analysis is in progress to determine whether the quantum numbers of this enhancement are $J^{PC} = 0^{++}$ or 2^{++}.

$\bar{p}p \rightarrow \pi^+\pi^-\eta\eta\pi^0$ at 1.94 GeV/c

The only resonance observed to date with exotic quantum numbers (i.e., quantum numbers not accessible to $q\bar{q}$) is a $J^{PC} = 1^{-+}$ state at 1910 MeV which was observed to decay to $f_1(1285)\pi^0$. Crystal Barrel data have been searched to try to find this resonance decaying to $f_1(1285)\eta$. Approximately 2×10^6 two-prong triggered events result in 1302 events corresponding to the $\pi^+\pi^-\eta\eta\pi^0$ final state. After selecting events possessing an $\pi^+\pi^-\eta$ combination falling within a window placed around the $f_1(1285)$ mass, the mass distribution shown in Fig. 5 is obtained. Analysis of the $\pi^+\pi^-\pi^0\pi^0\eta$ final state to search for the same resonance decaying to $f_1(1285)\pi$ is in progress.

PUBLICATIONS

1 High-statistics study of $f_0(1500)$ decay into $\pi^0\pi^0$
Crystal Barrel Collaboration
Physics Letters **B342**, 433 (1995).

2 η-decays into three pions
Crystal Barrel Collaboration
Physics Letters **B346**, 203 (1995).

3 Observation of radiative $\bar{p}p$ annihilation into a ϕ meson
Crystal Barrel Collaboration
Physics Letters **B346**, 363 (1995).

4 First observation of Pontecorvo reactions with a recoiling neutron
Crystal Barrel Collaboration
Zeit. Phys. **A351**, 325 (1995).

5 First observation of the production of nucleon resonances in antiproton annihilation in liquid deuterium
Crystal Barrel Collaboration
Phys. Lett. **B352**, 187 (1995).

6 High statistics study of f_0 (1500) decay into $\eta\eta$
Crystal Barrel Collaboration
Phys. Lett. **B353**, 571 (1995).

7 Coupled channels analysis of $\bar{p}p$ annihilation into $\pi^0\pi^0\pi^0$, $\pi^0\eta\eta$ and $\pi^0\pi^0\eta$
Crystal Barrel Collaboration
Phys. Lett. **B355**, 425 (1995).

8 E decays to $\eta\pi\pi$ in $\bar{p}p$ annihilation at rest
Crystal Barrel Collaboration
Phys. Lett. **B358**, 389 (1995).

Internal Report

Total energy trigger module
C A Baker
CB Note 284

Ph.D. Thesis

Analysis of $\bar{p}p \rightarrow \pi\pi\pi\eta$
A R Cooper
Queen Mary and Westfield College, London (October 1994)

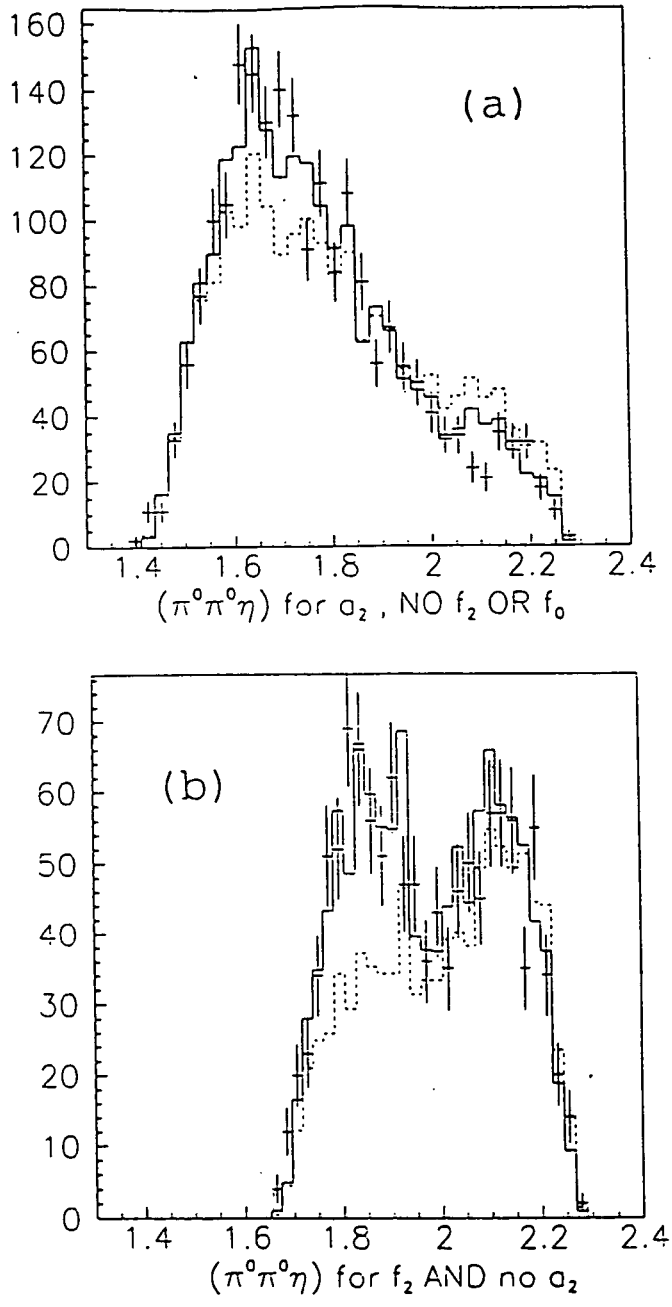

Fig. 1 Mass spectrum for $\pi^0\pi^0\eta$ showing resonances decaying to (a) $a_2(1320)\pi$ and (b) $f_2(1270)\eta$. (See text)

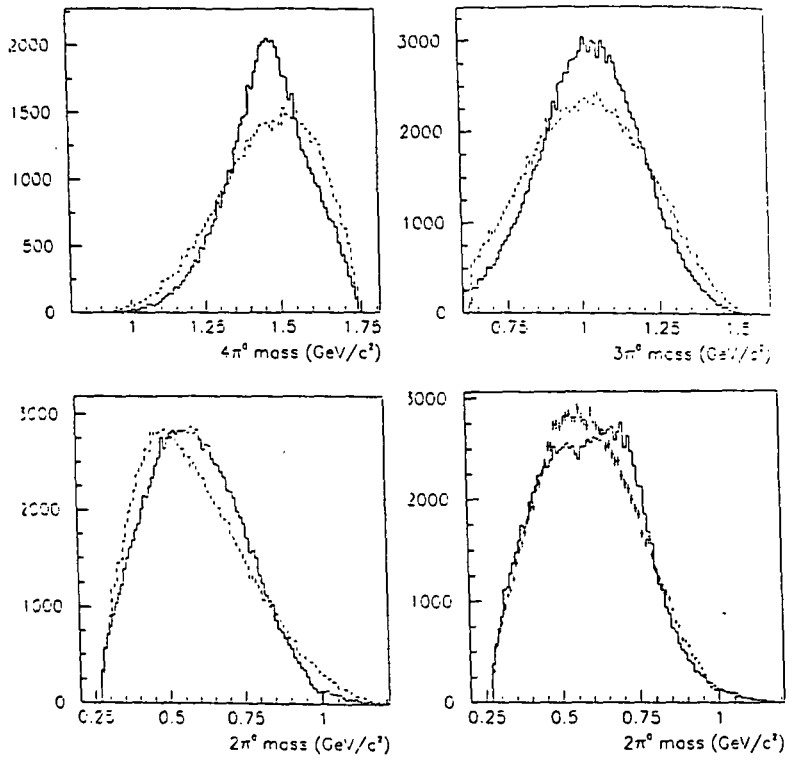

Fig. 2 Mass spectra (full histograms) from Crystal Barrel data on $\bar{p}p \rightarrow 5\pi^0$; (a) $4\pi^0$, (b) $3\pi^0$ and (c) $2\pi^0$, compared with 5π phase space (dashed); (d) the data (with error bars) fitted with Svec's narrow $f_0(750)$ (histogram).

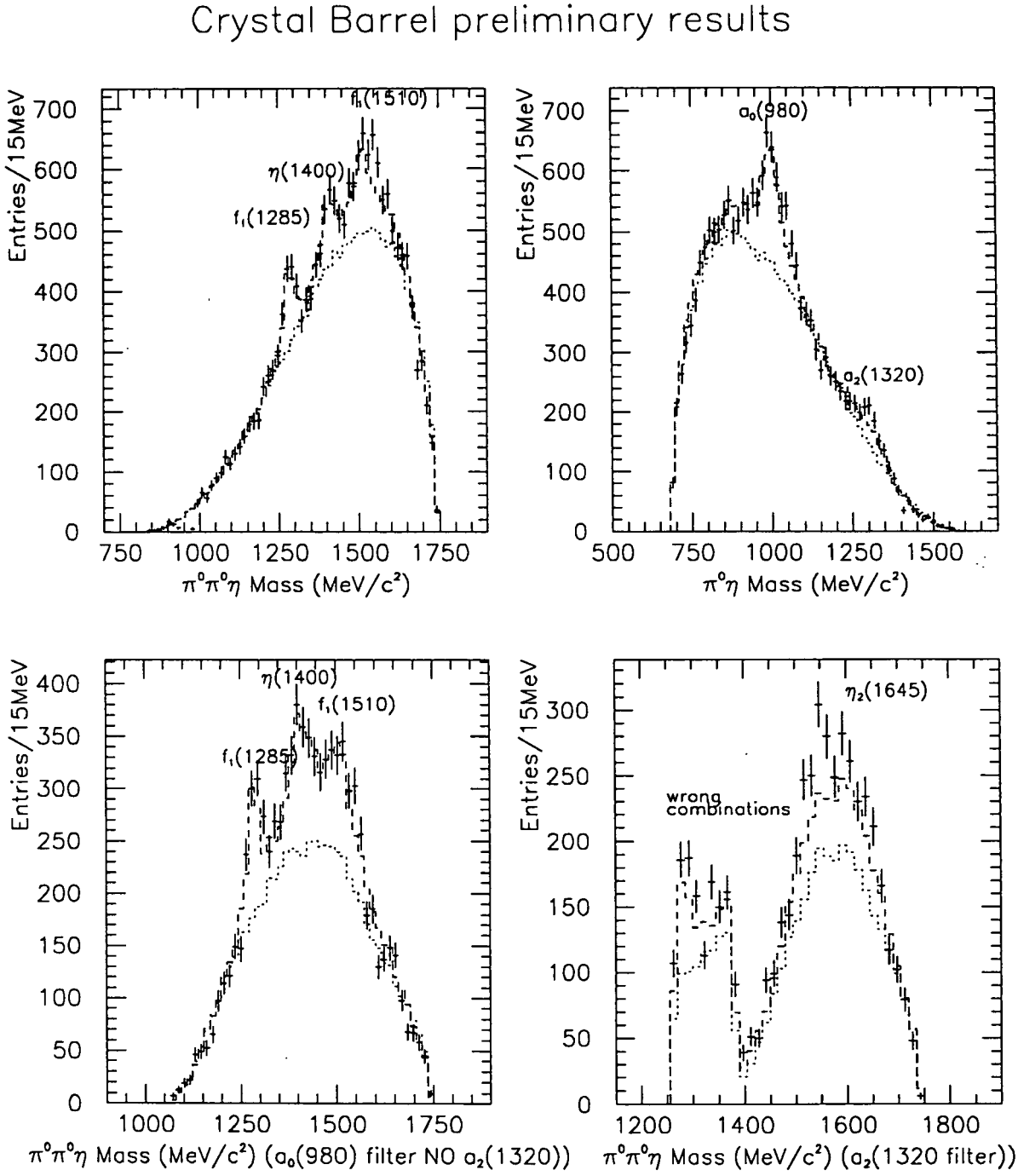

Fig. 3 Results from $\bar{p}p$ annihilation at rest into $\eta\pi^0\pi^0\pi^0$. The present partial wave fit is shown as the dashed histogram. The dotted histogram shows the acceptance corrected phase space. (a) Top left: The $\eta\pi^0\pi^0$ distribution shows peaks consistent with $f_1(1285)$, $\eta(1400)$ and $f_1(1510)$. (b) Top right: Enhancements due to $a_0(980)$ and $a_2(1320)$ are present. (c) Bottom left: Events filtered to contain an $\eta\pi^0$ combination forming an $a_0(980)$ and not an $a_2(1320)$. There may be an additional weak 0^{-+} signal at 1650 MeV from a resonance decaying to $a_0(980)\pi^0$. (d) Bottom right: Events filtered to contain an $\eta\pi^0$ combination forming an $a_2(1320)$ showing the enhancement due to $\eta_2(1645)$. The events below threshold are due to wrong combinations.

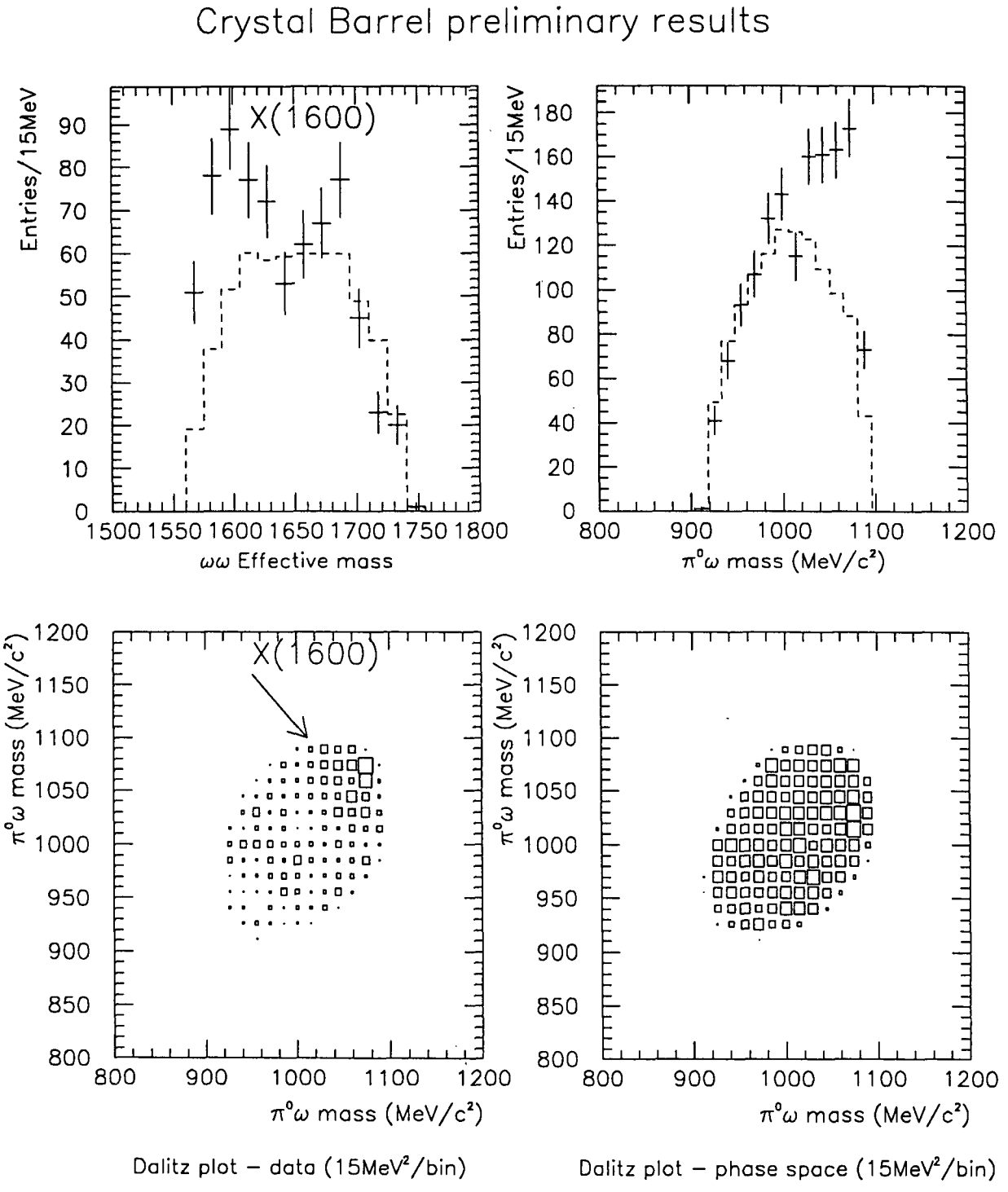

Fig. 4 Results from $\bar{p}p$ annihilation at rest into $\omega\omega\pi^0$. The dashed histogram shows the acceptance corrected phase space. (a) Top left: There is a threshold enhancement, possibly from a resonance X(1600) decaying to $\omega\omega$. (b) Top right: A reflection of the threshold enhancement. (c) Bottom left: The Dalitz plot showing a band at $\omega\omega$ threshold. (d) Bottom right: The Dalitz plot for the acceptance corrected phase space.

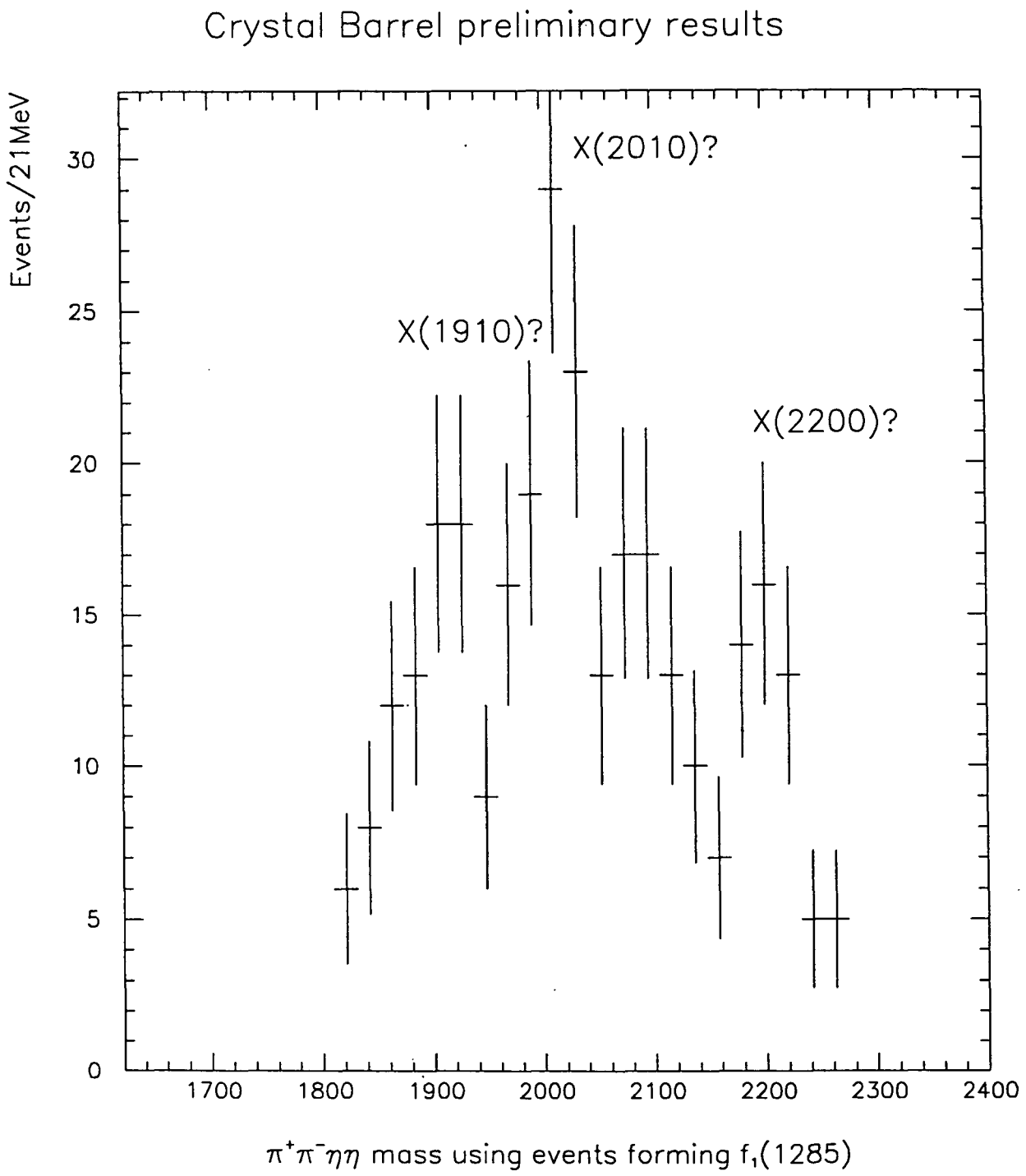

Fig. 5 Results from $\bar{p}p$ annihilation at 1.94 GeV/c into $\pi^+\pi^-\eta\eta\pi^0$. Events have been selected to contain $\pi^+\pi^-\eta$ combinations that lie within a window placed around $f_1(1285)$ to give indications of the presence of resonances decaying to $f_1(1285)\eta$. Detailed analysis is in progress so only speculative enhancements are indicated.

DARK MATTER EXPERIMENTS

Proposal 270

Particle Physics/Astrophysics collaboration
Imperial College London (Astrophysics)
Imperial College London (Particle Physics)
University of Sheffield (Particle Physics)
Birkbeck College London (Cosmic Ray Physics)
University of Nottingham (Cosmic Ray Physics)
RAL (Particle Physics, Astronomy, Technology)

A major unresolved problem at the interface of particle physics and cosmology is the identity of the non-luminous matter which is known to comprise 90% of the mass of our own Galaxy and up to 99% of the universe as a whole. There is also evidence that much of the dark matter may be non-baryonic, and could thus consist of relic stable elementary particles. Candidate particles include low-mass neutrinos, axions or weakly interacting massive particles such as the neutralino.

An experimental programme to search for WIMPS was funded jointly from particle physics and astronomy budgets, initially for the period 1991-95. These experiments search for nuclear recoil events from the interaction of dark matter particles. The UK programme is based on scintillating targets, in particular NaI and liquid Xe, but with the addition of new techniques to discriminate nuclear recoil from background. The experiments are carried out in an underground facility established in the Boulby salt mine (near Whitby UK).

During the past year, analysis of 6 months of data from a low background 6kg NaI detector has enabled new dark matter limits to be set which are currently world-best. Using pulse shape analysis, the majority of the background events can be shown to be due to electron recoils from gammas or beta decay in the material (Fig 1). More detailed analysis sets a 90% confidence limit on the proportion of nuclear recoil events, which varies from 1/10 of background at 5 keV to 1/40 of background at 20 keV (Fig 2). Full statistical analysis for the low energy spectrum between 4 and 25 keV yields new limits for dark matter interactions which are a factor 50 lower than those set by underground Ge detectors in the case of spin dependent interactions. Limits for coherent interactions are now also slightly lower than the Ge detector limits, with continuous improvements now to come from longer running and larger target masses.

Other improvements being studied include higher purity target material, improved light collection with larger photomultipliers, and the use of avalanche photodiodes for higher light collection efficiency.

Studies have also been made of a new type of liquid xenon detector based on proportional scintillation in an electric-field-defined fiducial region, with an outer self-shielding zone. This is named the 'ZEPLIN' configuration. Work on liquid xenon was suspended during 1994, in order to bring the UVIS detector into operation, but it is hoped to restart this in collaboration with the UCLA particle physics group. Collaboration on directional TPC detectors developed by UCSD has also been discussed.

Early in 1995 a major funding setback occurred when the new 4-year proposal was strongly endorsed by particle physics and astronomy referees but the 50% astronomy contribution could not be renewed. The programme has continued with predominantly particle physics funding, but equipment and support staff are currently reduced to 50% of the previous level. To maintain our competitive world position, proposals will be submitted to restore at least part of the lost funding

Recent publications

Strategies for the detection of particle dark amtter
P F Smith, Proc Conf on Sources of dark Matter (UCLA 1994) 221

Results from stage 1 of a Galactic dark matter search using low background sodium iodide detectors
J J Quenby et al., Phys. Lett B 351 (1995) 70

New dark matter limits from NaI detectors
G J Davies, HEP 95 (Brussels, 1995) to be published

Dark Matter Limits from NaI detectors
N J C Spooner, TAUP 95 to be published

Data analysis for nal dark matter experiments
N J T Smith, TAUP 95 to be published

Dark Matter Limits from NaI detectors
N J C Spooner, Proc Conference Dark Matter (Rome 1995) to be published

New dark matter limits from pulse shape discrimination in a 6kg NaI crystal
P F Smith et al., Physics Letters (to be published)

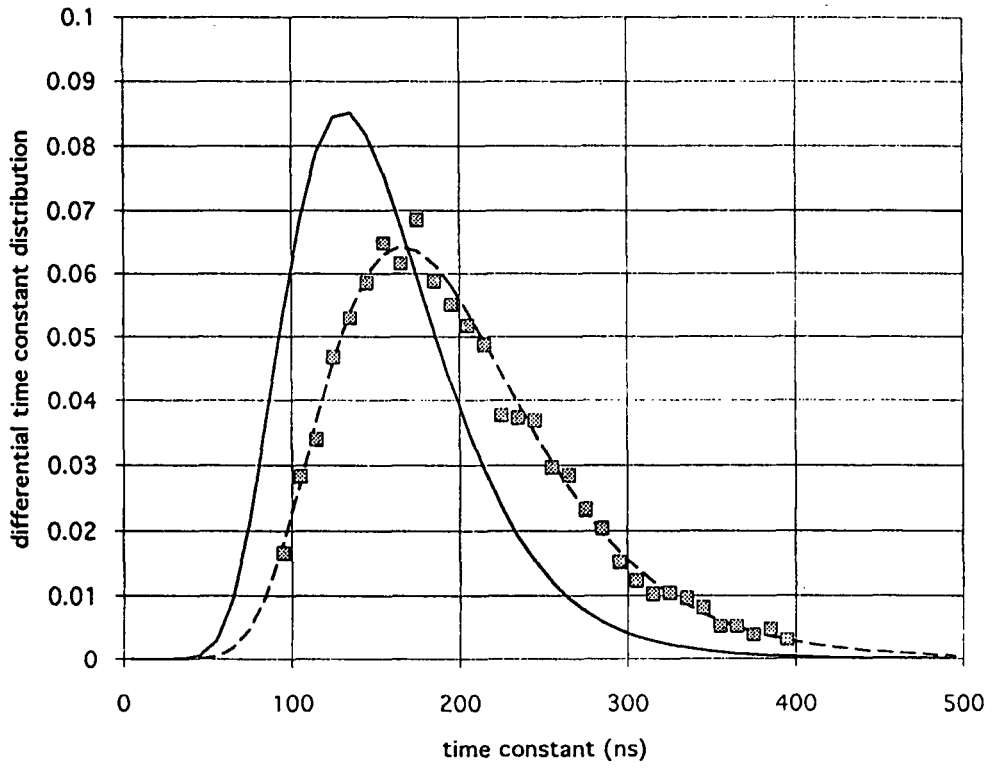

Fig 1 Distribution of pulse time constants for 7-10keV pulses in a low background 6kg NaI detector, showing consistency with gamma events rather than nuclear recoil events.

dashed line: distribution of time constants for gamma calibration
full line: distribution for nuclear recoils from neutron scattering
points: distribution for 6 months background events

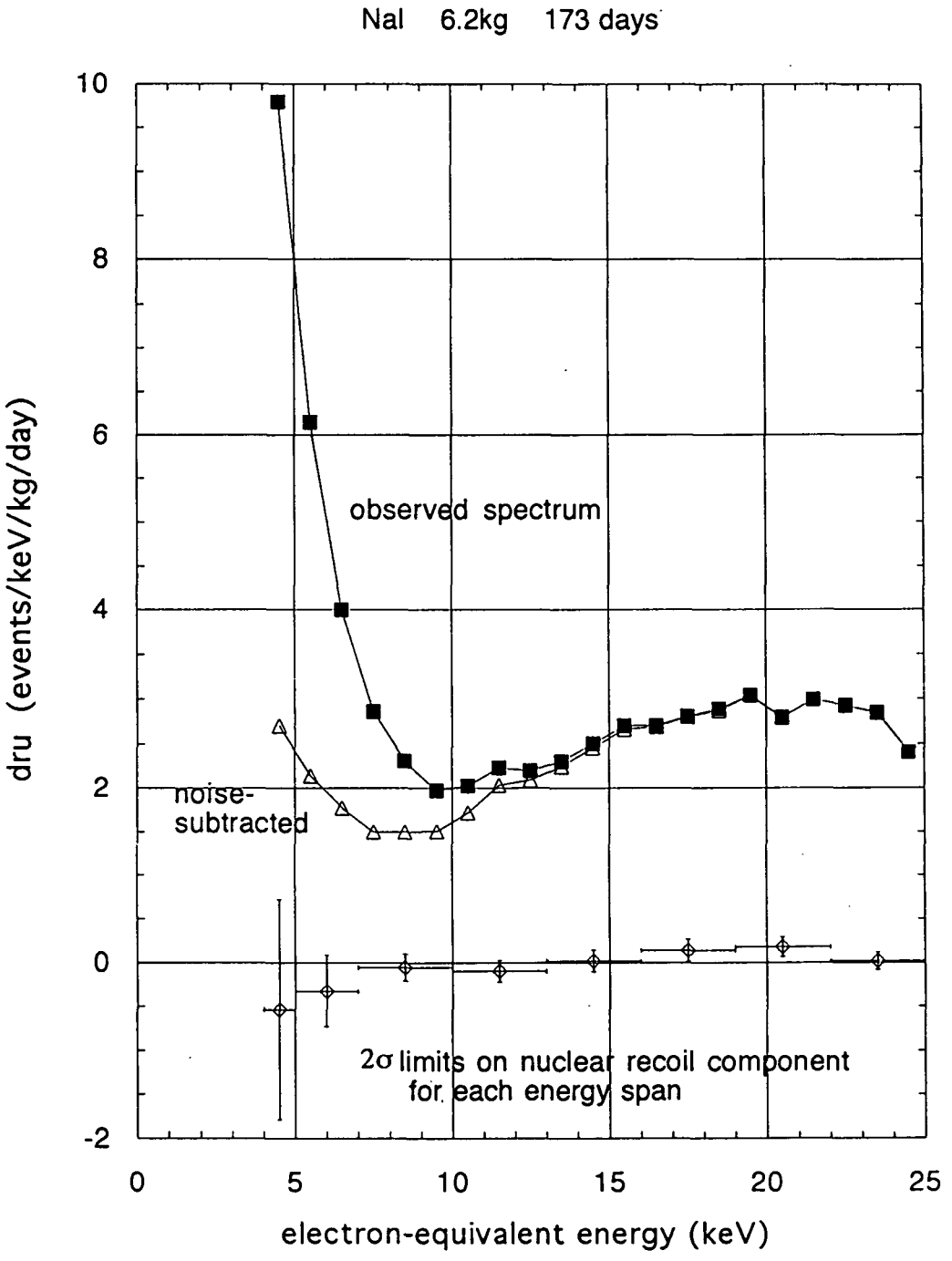

Fig 2 Background spectrum before and after pulse shape discrimination:

filled points: observed differential count rate
open points: after removal of fast noise pulses
lower points: 90% confidence limits on nuclear recoil events
(horizontal bars show energy span for each vertical limit)

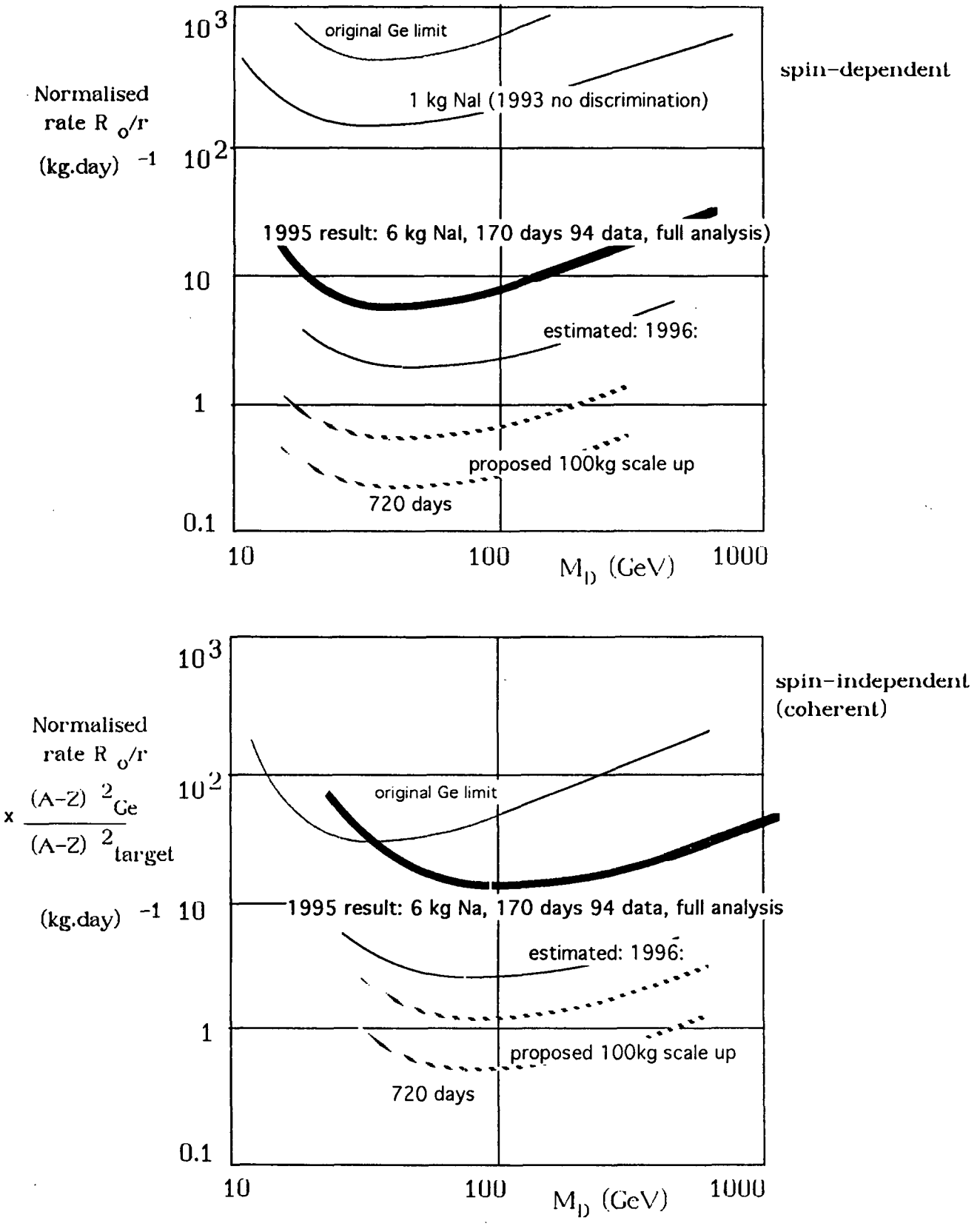

Fig 3 Summary of improvements in UK dark matter limits with time
Upper curves show original limits from Ge background
Thick curves show achieved final results from 1994 data (current world best).
1996 curves are forecast improvements by the end of 1996
Dashed curves are for proposed scale up to the 100kg level with further improvements in background and light collection

Studies of Heavy Ion Collisions

NA34/P213/EMU 09 **Proposals 273, 278**

Aichi College - Aichi University - Bari - CERN - University College, Dublin - Gifu - University College London - Nagoya University - Nagoya Institute - Roma - Salerno - Toho - Torino - Utsonomiya - Yokohama.

Data retrieval and analysis have effectively finished, A paper on charmed particle production by ion collisions has been published whereas reports on correlation studies and isotope separation in electromagnetic dissociation events are under consideration.

Publications

1. A hybrid set-up to study charmed particle production in ^{32}S nucleus central interactions.
   N.Armenise et al,

   Nucl. Instrum and Methods in Physics research A361 (1995) 497

2. Charged particle multiplicity and transverse energy measured in ^{32}S central interactions at 200GeV per nucleon
   S.Aoki et al,
   Nuovo Cim 108A (1995) 1125

RELATIVISTIC HEAVY ION INTERACTIONS

WA85/WA94 Proposal 275

Athens; Bari; Bergen; Birmingham; CERN; Collège de France; Košice;
Legnaro; Madrid; Padova; Serpukhov.

The study of strange baryon spectra in heavy ion collisions is a useful probe of the dynamics of hadronic matter under extreme conditions. The relative abundances for different baryon and antibaryon species allow the degree and nature of flavour equilibration to be studied, while the transverse mass (m_T) spectra provide independent information on the temperatures achieved in the collision [1]. The onset of a Quark-Gluon Plasma (QGP) phase during the collisions is expected to enhance strangeness production and, in particular, the antihyperon yield with respect to normal hadronic interactions and to give rise to a large $\overline{\Xi^-}/\overline{\Lambda}$ ratio [2]. The WA85 experiment has high statistics data on strange baryon and antibaryon spectra ($\Lambda, \overline{\Lambda}, \Xi^-, \overline{\Xi^-}, \Omega^-, \overline{\Omega^-}$), and is the only experiment to have obtained results on Ω^- production in heavy ion interactions.

The WA85 experiment [3] is a dedicated experiment aimed at studying strange particle production at $p_T > 1$ GeV/c and central rapidity. It was performed using the CERN Omega Spectrometer with a ^{32}S beam at 200 GeV/c per nucleon incident on a tungsten target. The Omega Multi Wire Proportional Chambers (MWPCs) were modified to select only high p_T tracks so that only a few tracks are recorded out of the several hundred produced in a central collision, making reconstruction of both strange and multi-strange baryons possible. The apparatus and trigger, designed to select central collisions, have been discussed previously [4].

The methods for reconstructing Λ [4] and Ξ^- [5] decays have already been described. Figure 1 shows a fully reconstructed $\overline{\Xi^-}$ candidate. Results from our earlier data (10 million triggers) have already been presented [4,5,6,7,8]. In this report we concentrate on our later high statistics results based on 60 million triggers. Preliminary results were presented at the Quark Matter '93 Conference in Borlänge, Sweden [9]. Since then the data have been re-analysed and in particular the corrections and systematics calculated in more detail [10]. We have also analysed our reference proton-tungsten data [11] for comparison with the sulphur data. We have successfully reconstructed K^+ and K^- mesons in sulphur-tungsten interactions from their tau decay $K^+ \rightarrow \pi^+\pi^+\pi^-$ [12]. Figure 2 shows the effect mass distributions for K^+ and K^- candidates.

The number of reconstructed K^+, K^-, K^0, Λ, $\overline{\Lambda}$, Ξ^- and $\overline{\Xi^-}$ candidates are given in Table 1. The m_T distributions of the various particle species have been fitted using the expression

$$\left(\frac{1}{m_T}\right)^{\frac{3}{2}} \frac{dN}{dm_T} = A \exp(-\beta m_T).$$

The strange baryons were fitted in the rapidity interval $2.3 < y_{lab} < 2.8$ whereas the charged kaons were fitted in the interval $2.3 < y_{lab} < 3.0$ and the K^0s in the interval

$2.5 < y_{lab} < 3.0$. The inverse slopes ($1/\beta$) are given in Table 2, where the errors are statistical only. The systematic error has been estimated, by simulation, to be about $\pm$ 10 MeV.

The relative production rates for hyperons have also been calculated in sulphur-tungsten and proton-tungsten interactions and are summarised in table 2. The Ξ^-/Λ and $\overline{\Xi^-}/\overline{\Lambda}$ ratios are shown for pp, pW, SW, and SS interactions in figure 3. The ratios Ξ^-/Λ and $\overline{\Xi^-}/\overline{\Lambda}$ increase by about 30% from p-W to S-W interactions and the ratio $\overline{\Xi^-}/\overline{\Lambda}$ in S-W interactions is over three times greater than that observed in pp interactions [10,13], a four standard deviation effect.

Ω^- and $\overline{\Omega^-}$ hyperons have been observed for the first time in heavy ion interactions [14]. In order to isolate the small number of Ω^- candidates from background, more stringent selections are required than for Ξ^-s [15]. Figure 4(a) shows the final ΛK^- (and c.c.) effective mass spectrum for events unambiguous with Ξ^-. The dotted lines show background generated by mixing V^0s with non-V^0 tracks from different events. We obtain an uncorrected $\overline{\Omega^-}/\Omega^-$ ratio of 0.57 ± 0.41 in the phase space region $2.5 < y_{lab} < 3.0$ and $p_T > 1.6$ GeV/c [15]. More recently[16], the fully corrected $\Omega^- + \overline{\Omega^-}$ yields have been caluculated, allowing the production ratio $R_{\Omega\Xi} = (\Omega^- + \overline{\Omega^-})/(\Xi^- + \overline{\Xi^-})$ to be calculated in the region $2.5 < y_{lab} < 3.0$ and $p_T > 1.6$ GeV/c; we obtain 0.8 ± 0.4, or $R_{\Omega\Xi} > 0.79$ at 95% confidence level. The value obtained for the $(\Omega^- + \overline{\Omega^-})/(\Xi^- + \overline{\Xi^-})$ ratio is compared with the upper limit of the ratio $\overline{\Omega^-}/\overline{\Xi^-}$ obtained in pp interactions by the AFS collaboration in figure 4(b). The kinematic region for the AFS result is similar to that used for the WA85 result. As can be seen from figures 3 and 4 both the $\overline{\Xi^-}/\overline{\Lambda}$ and the $(\Omega^- + \overline{\Omega^-})/(\Xi^- + \overline{\Xi^-})$ ratios show a clear enhancement in multistrange production ratios with respect to pp collisions.

The WA94 experiment [17] is a successor to WA85, in which a sulphur target is used. In the first phase of the experiment the Omega MWPCs were used to measure hyperon decays in SS interactions. 100 million triggers were obtained in November 1991. The Ξ^-, $\overline{\Xi^-}$, Λ and $\overline{\Lambda}$ spectra have been fully corrected for acceptance, reconstruction efficiency and feed-down, allowing the m_T spectra and the relative production ratios to be determined [18]. Charged kaons have also been identified in SS interactions [19]. Figure 5 shows the m_T spectra for Ξ^-, $\overline{\Xi^-}$, Λ and $\overline{\Lambda}$ in the rapidity interval $2.5 < y_{lab} < 3.0$. The distributions have been fitted using expression (1). The values obtained for the inverse slope are shown in Table 2. In general, the values obtained are some 15 MeV lower than those obtained in SW interactions in an equivalent centre-of-mass rapidity interval. The particle production ratios are given in Table 3. As can be seen, the ratios are very similar to those obtained by WA85, and therefore again the $\overline{\Xi^-}/\overline{\Lambda}$ ratio is considerably higher than the pp value[10,13].

A second period of data taking took place in April 1992, using the Omega RICH in conjunction with a silicon telescope built from the existing WA82 charm decay detector, an array of silicon microstrips. The aim of this phase of the experiment is to use the Omega RICH to obtain identified proton spectra to compare with the hyperon spectra already obtained. The operation of the silicon telescope also provided valuable experience for the purpose-built silicon telescope used in the WA97 experiment [20]. New reconstruction code was required to find tracks in the telescope in a high track density environment. Analysis of these data is now near completion and figure 6 shows a RICH event with a ring of photon impacts consistent with a pion track.

Reference data using the Omega MWPCs was obtained from an incident proton beam at 200 GeV/c in October and November 1993. 60 million triggers were recorded. The event reconstruction was completed in 1994 using the RAL IBM system and the analysis of these data is now underway.

REFERENCES

[1] J. Rafelski and B. Müller, Phys. Rev. Lett **48** (1982) 1066;
Phys. Rev. Lett **56** (1986) 2334.
P. Koch, B. Müller and J. Rafelski, Phys. Rep. **142** (1986) 167.
J. Ellis and U. Heinz, Phys. Lett. **262B** (1991) 223.

[2] J. Rafelski, Phys. Lett. **262B** (1991) 333.

[3] WA85 Proposal, A. Apostolakis et al., CERN/SPSC 84-76, SPSC/P206 and CERN/SPSC 87-18,SPSC/P206 Add. 1 (1987).

[4] The WA85 Coll., (S. Abatzis *et al.*), Phys. Lett. **244B** (1990) 130.

[5] The WA85 Coll., (S. Abatzis *et al.*), Phys. Lett. **259B** (1991) 508.

[6] The WA85 Coll., (S. Abatzis *et al.*), Phys. Lett. **270B** (1991) 123.

[7] The WA85 Coll., (B. Ghidini *et al.*), Proc. Int. Europhysics Conf. on High Energy Physics, Geneva, 1991, p. 466.

[8] The WA85 Coll., (D. Evans *et al.*), Proc. Hadron Structure '92, Stará Lesná, Czechoslovakia, 1992, p. 257.

[9] The WA85 Coll., (D. Evans *et al.*), Nucl Phys. **A566** (1994) 225c.

[10] The WA85 Coll., (S. Abatzis *et al.*), Phys. Lett. **B359** (1995) 382-386.

[11] The WA85 Coll., (J.P. Davies *et al.*), AIP Conference Proceedings 340 (1995) pp. 223-233.

[12] The WA85 Coll., (S. Abatzis *et al.*), Phys. Lett. **B355** (1995) 401-405.

[13] AFS Coll., T. Åkesson et al., Nucl. Phys. **B246** (1984) 1.

[14] The WA85 Coll., (F. Antinori *et al.*, Nucl. Phys. **A566** (1994) 491c.

[15] The WA85 Coll., (S. Abatzis *et al.*), Phys. Lett. **B316** (1993) 615.

[16] The WA85 Coll., (S. Abatzis *et al.*), Phys. Lett. **B347** (1995) 158-160.

[17] WA94 Proposal. S. Abatzis et al., CERN/SPSLC 91-5 SPSLC/P257.

[18] The WA94 Coll., (S. Abatzis *et al.*), Phys. Lett. **B354** (1995) 178-182.

[19] The WA94 Coll., (O. Villalobos Baillie *et al.*), AIP Conference Proceedings 340 (1995) pp. 259-272.
The WA94 Coll., (J.B. Kinson *et al.*), Nucl. Phys. **A590** (1995) 317-332.

[20] WA97 Proposal. N. Armenise et al., CERN/SPSLC 91-29, SPSLC/P263.

PUBLICATIONS (From October 1994 until October 1995)

1. Measurement of the Omega/Xi Production Ratio in Central S-W Interactions at 200 A GeV/c.
   Athens, Bari, Bergen, Birmingham, CERN, Collège de France and Trieste.
   NATO Advanced Science Institutes Series, Series B, Physics, 1995, Vol. 346, Ch. 62, pp 457-460.

2. Strange Baryon Production in Sulphur-Sulphur Interactions at 200 GeV/c per Nucleon.
   Athens, Bari, Bergen, Birmingham, CERN, Collège de France, Košice, Legnaro, Madrid, Padua, Protvino, Strasbourg, and Trieste.
   Proc. Hadron Structure '94, Košice (september 1994).

3. Results on K^0, Λ, Ξ^- and Ω^- Production in SW Collisions at 200 GeV/c.
   Athens, Bari, Bergen, Birmingham, CERN, Collège de France, and Madrid.
   Proc. Int. Conf. on High Energy Physics (ICHEP'94), Glasgow (July 1994). (published 1995) pp. 521-523.

4. Strange Particle Production in Sulphur-Sulphur Interactions at 200 GeV/c per Nucleon.
   Athens, Bari, Bergen, Birmingham, CERN, Collège de France, Košice, Legnaro, Madrid, Padua, Protvino, Strasbourg, and Trieste.
   Proc. Int. Conf. on High Energy Physics (ICHEP'94), Glasgow (July 1994). (published 1995) pp. 525-527.

5. Baryon and Antibaryon Production with 1, 2, and 3 units of Strangeness in SW Interactions at 200 GeV/c per Nucleon.
   Athens, Bari, Bergen, Birmingham, CERN, Collège de France, and Madrid.
   Proc. Int. Conf. on Strangeness and Quark Matter, Crete, (September 1994). World Scientific, Editors: G. Vassiliadis, A.D. Panagiotou, S. Kumar, and J. Madsen, pp 91-100.

6. Strange Baryon and Antibaryon Production in Sulphur-Sulphur Interactions at 200 GeV/c per Nucleon.
   Athens, Bari, Bergen, Birmingham, CERN, Collège de France, Košice, Legnaro, Madrid, Padua, Protvino, Strasbourg, and Trieste.
   Proc. Int. Conf. on Strangeness and Quark Matter, Crete, (September 1994). World Scientific, Editors: G. Vassiliadis, A.D. Panagiotou, S. Kumar, and J. Madsen, pp 101-109.

7. On Enhancing Strangeness in Proton-Tungsten and Proton-Sulphur Data at 200 GeV/c
Athens, Bari, Bergen, Birmingham, CERN, Collège de France, and Madrid.
Proc. Int. Conf. on Strangeness and Quark Matter, Crete, (September 1994). World Scientific, Editors: G. Vassiliadis, A.D. Panagiotou, S. Kumar, and J. Madsen, pp 179-184.

8. Measurement of the Ω/Ξ production ratio in central S-W interactions at 200 A GeV/c.
Athens, Bari, Bergen, Birmingham, CERN, Collège de France, Madrid and Triest.
Phys. Lett. **B347**, (1995), 158-160.

9. Λ and Ξ^- Production in Proton-Tungsten Interactions at 200 GeV per Nucleon.
Athens, Bari, Bergen, Birmingham, CERN, Collège de France, and Madrid.
Strangeness in Hadronic Matter, Tucson, USA (1995) AIP Conference Proceedings 340, (1995), pp 223-233.

10. Review of Strange Particle Production from the WA85 Collaboration.
Athens, Bari, Bergen, Birmingham, CERN, Collège de France, and Madrid.
Strangeness in Hadronic Matter, Tucson, USA (1995) AIP Conference Proceedings 340, (1995), pp 235-246.

11. Charged Kaon Spectra in SW Interactions at 200 GeV/c per nucleon.
Athens, Bari, Bergen, Birmingham, CERN, Collège de France, and Madrid.
Strangeness in Hadronic Matter, Tucson, USA (1995) AIP Conference Proceedings 340, (1995), pp 247-253.

12. Ω/Ξ production ratio in S-W.
Athens, Bari, Bergen, Birmingham, CERN, Collège de France, and Madrid.
Strangeness in Hadronic Matter, Tucson, USA (1995) AIP Conference Proceedings 340, (1995), pp 254-258.

13. New Results on Strange and Multistrange Baryon Production and Charged Kaon Production in Sulphur Sulphur Interactions at 200 GeV/c per Nucleon.
Athens, Bari, Bergen, Birmingham, CERN, Collège de France, Košice, Legnaro, Madrid, Padua, and Protvino.
Strangeness in Hadronic Matter, Tucson, USA (1995) AIP Conference Proceedings 340, (1995), pp 259-272.

14. Results on the Production of Baryons with $|S| = 1, 2, 3$ and Strange Mesons in S-W Collisions at 200 GeV/c per Nucleon.
Athens, Bari, Bergen, Birmingham, CERN, Collège de France, and Madrid.
Nucl. Phys. **A590** (1995) 307-316.

15. Strange Particle Production in Sulphur-Sulphur Interactions at 200 GeV/c per Nucleon.
Athens, Bari, Bergen, Birmingham, CERN, Collège de France, Košice, Legnaro, Madrid, Padua, and Protvino.
Nucl. Phys. **A590** (1995) 317-332.

16. A study of cascade and strange baryon production in sulphur-sulphur interactions at 200 GeV/c per nucleon.
Athens, Bari, Bergen, Birmingham, CERN, Collège de France, Košice, Legnaro, Madrid, Padua, and Protvino.
Phys. Lett. **B354** (1995) 178-182.

17. Charged Kaon Production in S-W Collisions at 200 GeV/c per nucleon.
Athens, Bari, Bergen, Birmingham, CERN, Collège de France, and Madrid.
Phys. Lett. **B355** (1995) 401-405.

18. Study of charged particle production using Omega RICH in WA94 experiment.
Athens, Bari, Bergen, Birmingham, CERN, Collège de France, Košice, Legnaro, Madrid, Padua, and Protvino.
2nd Int. Workshop on RICH Detectors (RICH'95), Uppsala, Sweden, June 1995.

19. Production of Strange and Multistrange Hyperons and Antihyperons in S-W Interactions at 200 GeV/c per nucleon.
Athens, Bari, Bergen, Birmingham, CERN, Collège de France, and Madrid.
Phys. Lett. **B359** (1995) 382-386.

THESES (Ph.D)

1. A.C. Bayes, Strange Particle Production in Sulphur-Sulphur Interactions at 200 GeV/c per Nucleon.
University of Birmingham, June 1995 (RAL-TH-95-008)

Table 1: Particle yields from pW, SW, and SS data.

Candidate	Number of Events		
	WA85 pW	WA85 SW	WA94 SS
K^+	—	603	—
K^-	—	385	—
K^0	11,549	10,400	—
Λ	31,114	61,071	56,140
$\overline{\Lambda}$	8,715	15,765	18,014
Ξ^-	294	610	547
$\overline{\Xi^-}$	136	253	278

Table 2: Particle inverse slopes in pW, SW, and SS interactions.

Particle	pW Data	SW Data	SS Data
K^+	—	211 ± 12	$172 \pm 20^*$
K^-	—	198 ± 13	$152 \pm 25^*$
K^0	224 ± 3	219 ± 5	—
Λ	197 ± 2	233 ± 3	213 ± 2
$\overline{\Lambda}$	185 ± 5	232 ± 7	204 ± 5
Ξ^-	211 ± 14	244 ± 12	222 ± 10
$\overline{\Xi^-}$	216 ± 16	238 ± 16	208 ± 25
* Preliminary results			

Table 3: Relative production rates in pW, SW, and SW interactions.

Ratio	WA85 pW $2.3 < y_{lab} < 3.0$	WA85 SW $2.3 < y_{lab} < 3.0$	WA94 SS $2.5 < y_{lab} < 3.0$
K^+/K^-	—	$1.67 \pm 0.15^\dagger$	$1.91 \pm 0.37^*$
$\overline{\Lambda}/\Lambda$	0.20 ± 0.02	0.196 ± 0.011	0.23 ± 0.01
$\overline{\Xi^-}/\Xi^-$	0.47 ± 0.07	0.47 ± 0.06	0.55 ± 0.07
Ξ^-/Λ	0.070 ± 0.006	0.097 ± 0.006	0.09 ± 0.01
$\overline{\Xi^-}/\overline{\Lambda}$	0.16 ± 0.02	0.23 ± 0.02	0.21 ± 0.02
† $2.3 < y_{lab} < 3.0$, $p_T > 0.9$ GeV/c.			
* Preliminary result ($2.7 < y_{lab} < 3.2$, $1 < p_T < 2$ GeV/c.)			

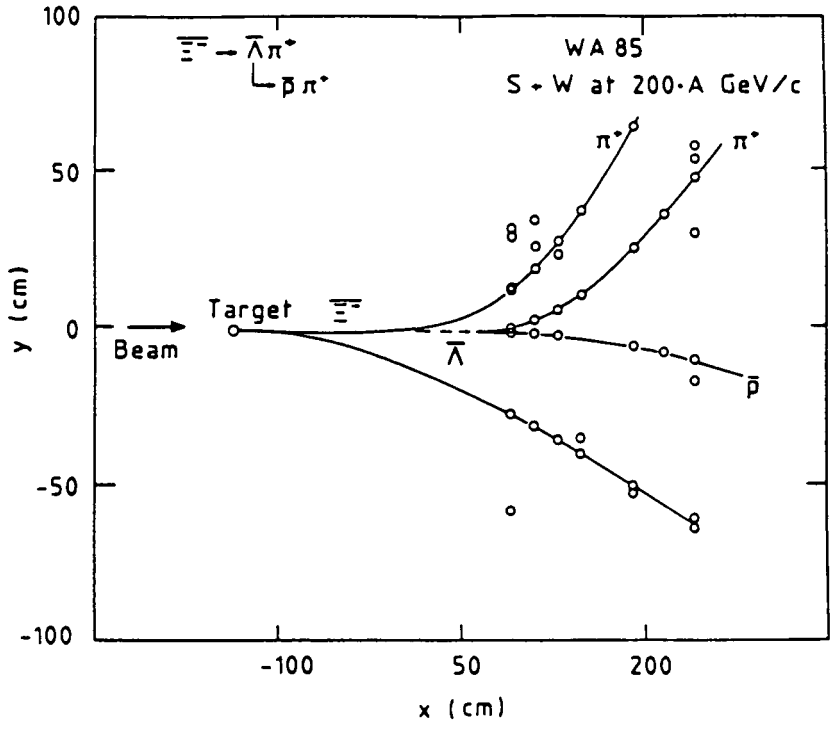

Figure 1: Fully reconstructed $\bar{\Xi}^-$ candidate.

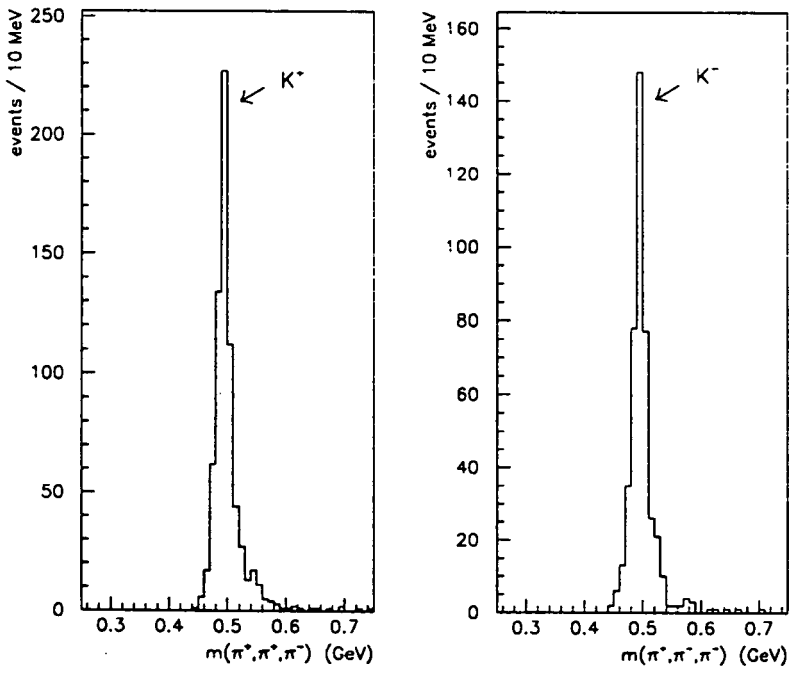

Figure 2: Effective mass plot of K^+ and K^- mesons.

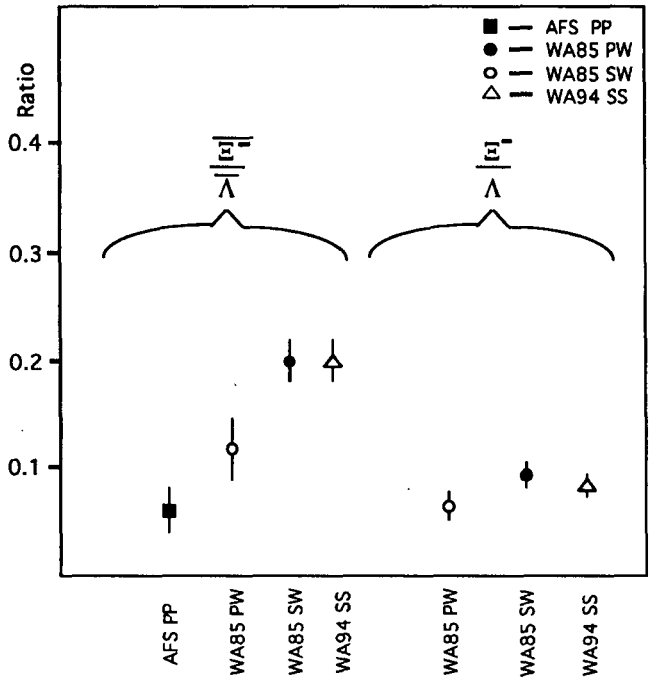

Figure 3: The ratios Ξ^-/Λ and $\overline{\Xi^-}/\overline{\Lambda}$ from different interactions.

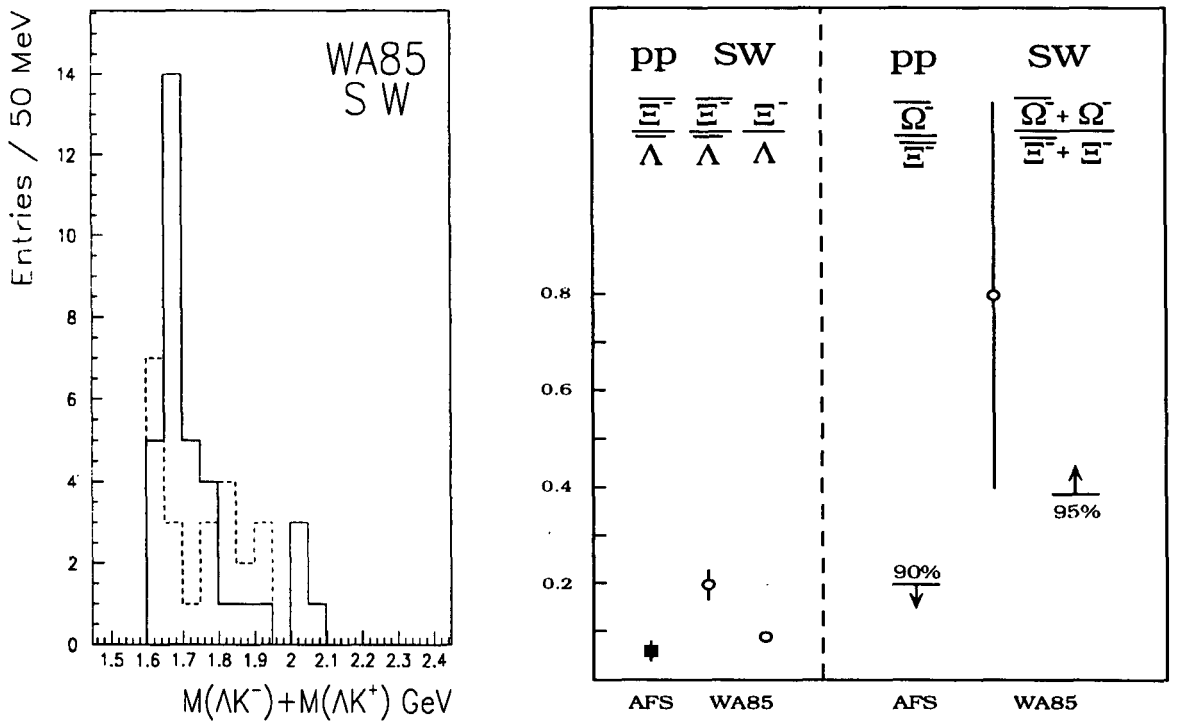

Figure 4: (a) $(\Lambda\ K^- + \overline{\Lambda}\ K^+)$ mass spectrum with the combinatorial background shown as a dashed line and (b) comparison of ratios in pp and central SW interactions.

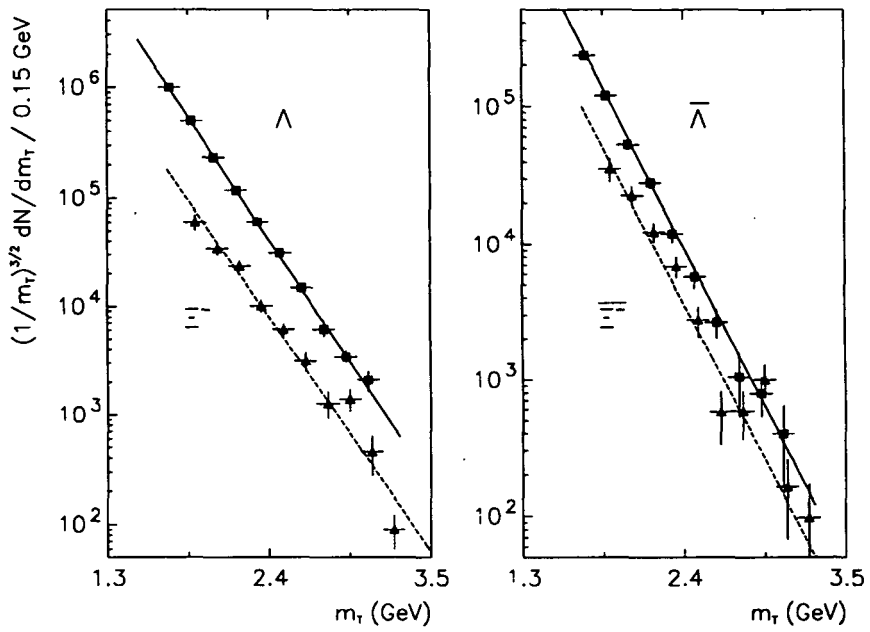

Figure 5: Transverse mass distributions for Λ, $\overline{\Lambda}$, Ξ^-, and $\overline{\Xi^-}$ from the WA94 SS data.

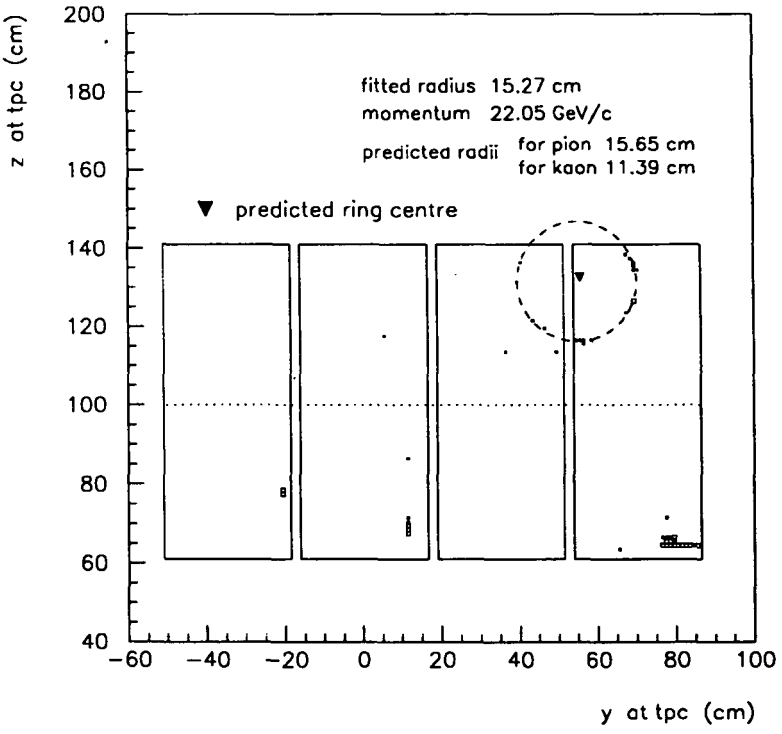

Figure 6: Reconstructed event showing boundaries of RICH TPC modules and photon impacts. The circle shows the prediction for a pion candidate.

The Sudbury Neutrino Observatory (SNO)

The Sudbury Neutrino Observatory (SNO) is a joint Canadian, US and UK venture designed to study neutrinos from the sun and other astrophysical sources using a 1000 ton heavy water (D_2O) Cerenkov detector (see Fig.1). All four existing solar neutrino experiments, Homestake, Kamioka, Sage and Gallex, report a deficiency of electron neutrinos relative to the standard solar model. A non-zero neutrino mass and neutrino oscillations could explain the observations but that is only a speculation without the positive evidence that SNO will be able to provide.

The unique advantage of the SNO detector is that the use of D_2O as a detecting medium enables not only the flux and energy spectrum of electron neutrinos but also the total flux of **all** neutrino types above an energy of 2.23 MeV to be measured. With these two measurements it will be possible to show clearly whether neutrino oscillations are occurring and independently test solar models by determining the production rate of ^8B electron neutrinos in the solar core. The ν reactions are $\nu_e d \rightarrow ppe^-$ (charged current), and $\nu d \rightarrow np\nu$, (neutral current), for which the signal is a free neutron.

The planned SNO detector consists of an acrylic vessel containing 1000 tons of D_2O immersed in 7000 tons of high purity light water. Surrounding the acrylic vessel are some 9600 photomultiplier tubes (PMTs) and the whole detector is located 2000m underground. In order to improve the light collection, and hence the signal to noise of the detector, the Oxford group has developed non-imaging concentrators to mount around the PMTs. They have the twin virtues of increasing by 65% the detection of photons from the D_2O, (but not the H_2O), thus increasing the signal while simultaneously preventing a PMT from detecting photons from the adjacent PMTs. This greatly reduces the probability of a radio-active decay near one of the PMTs being misidentified as an event in the D_2O, which could have been a major source of background at low energies. These advantages have made the concentrators central to the design of the detector.

Besides the design and manufacture of the concentrators, Oxford is also involved in developing techniques for purifying water to mass concentrations of 10^{-15} ^{232}Th and 10^{-14} ^{238}U whose decay photons can photodissociate deuterium and so mimic the neutral current neutrino induced reactions which also releases a neutron. The neutrons are detected in the Cerenkov counter via radiative capture on chlorine provided by a 0.2% $MgCl_2$ concentration in the D_2O. It is this solution which must be purified and the technique of seeded ultrafiltration using hydrous titanium, HTiO has been adapted to absorb and assay the undesirable radio-active species of thorium, radium, and lead. The primary absorption process is illustrated schematically in Fig.2. There are also secondary processes involving HTiO and solvent extraction for which the end product (starting from some hundreds of tons) is 12ml which can be counted via beta-alpha coincidences in liquid scintillator. It is also desirable to remove the (radio-active) potassium which occurs as a 5ppm impurity in the $MgCl_2$. A

technique is being developed to remove the potassium from concentrated $MgCl_2$ solution using sodium tetraphenyl boron. The same technique will be used for purifying the ^6Li which will be added to the D_2O, without the $MgCl_2$, as a non-radiative neutron absorber so that a clean measurement of charged current events can be made.

Fig.3 indicates the energy spectra expected from the Cerenkov detector under various operating conditions:

(i) H_2O in the acrylic vessel, radio-activity background and a few neutrino-electron scattering events,

(ii) D_2O + ^6Li, charged current (c.c.) events with a spectrum identical to ^8B β-decay superimposed on background.

(iii) D_2O + $MgCl_2$, neutral current (n.c.) events with the γ-ray spectrum from neutron radiative capture, superimposed on charged current events and background.

The rates for c.c. and n.c. events can be separated by subtraction.

The SNO group at Oxford plays the leading rôle in the development of software for the optimisation of the running of the experiment and for the analysis of data via the programme SNOMAN: **S**udbury **N**eutrino **O**bservatory **M**onte Carlo **AN**alysis code. The core of the programme has been written and documented and is now being implemented throughout the collaboration. One of the most interesting developments which have emerged from the Oxford work has been the application of neural network techniques for the separation of charged current and neutral current events. Three examples of different network outputs are shown in Fig.4 where it is apparent that the separation of c.c. and n.c. events is a great improvement on the simple energy spectrum of Fig.3. For Fig.4 an energy cut has been imposed to exclude the radio-activity background.

Status Report

The detector cavity of Fig.1 together with the ancillary rooms of the underground laboratory have been sealed off from the rest of the mine and clean for the past year.

The upper half of the geodesic support structure (Fig.1) has been assembled and the panels carrying photomultipliers and concentrators fitted to the structure. Cabling of these photomultipliers is now in progress. All of the Oxford concentrators have now been manufactured and the half not yet installed are stored in Sudbury.

The seeded ultra-filtration (SUF) plant for the purification/assay of 200l/min of D_2O, shown schematically in Fig.2, has reached the manufacturing stage. The elution system for the filters has been separated from the main D_2O and is being built as a free-standing automated system.

The development work on the removal of potassium from $MgCl_2$ solution and the concentration of lead and thorium by solvent extraction is well advanced but not yet complete.

The jigs for assembling the top half of the acrylic vessel in the detector cavity have been installed with a major contribution from the technical staff in Oxford. Work has started on the alignment and bonding of the acrylic panel which make up the vessel. This will be a long slow job which it is expected will take a full year for the two halves of the sphere.

N.W. Tanner October 1995

SNO COLLABORATION

Queen's University, Kingston, Ontario

CRPP, Carleton University, Ottawa

Chalk River National Laboratories

University of Guelph, Ontario

Laurentian University, Sudbury, Ontario

U.B.C., Vancouver

Princeton University

University of Pennsylvania

Los Alamos National Laboratory

University of Washington, Seattle

Lawrence Berkeley Laboratory

University of Oxford

M. Bowler, S. Brice, G. Doucas, H. Heron, N.A. Jelley, A.B. Knox, M.D. Lay, (W. Locke), J. Lyon, N.W. Tanner, R.K. Taplin, M. Thorman, D.L. Wark.

J.C. Barton, P.T. Trent (Birkbeck College)

E.W. Hooper (AEA Technology)

Publications

G.D. Doucas *et al* "Light Concentrators for the Sudbury Neutrino Observatory" (accepted by Nucl. Instr. & Meth.).

M.E. Moorhead *et al* "Design Criteria for Purification and Assay of Heavy Water by Seeded Ultrafiltration" (internal technical review document).

R.J. Boardman *et al* "A Cerenkov Radiation Source for Photomultiplier Calibration" Nucl. Inst. & Meth. **A345**, 356 1994.

D.L. Wark "The Search for Solar Neutrinos", Endeavour 17, No 3 104 1993.

N.W. Tanner "Solar Neutrino Counters" Phil. Trans. R. Soc. London A (1194) **346** 23.

M.E. Moorhead and N.W. Tanner "Light Reflecting Concentrators for Photomultipliers with Curve Photocathodes" submitted to Applied Optics.

M.E. Moorhead and N.W. Tanner "Optical Properties of K_2CsSb Bialkali Photocathodes" submitted to Nucl. Inst. & Meth.

Theses of: A.P. Ferraris, R.J. Boardman, M.D. Lay, K. Howard, M.E. Moorhead, R.K. Taplin.

5.10.95

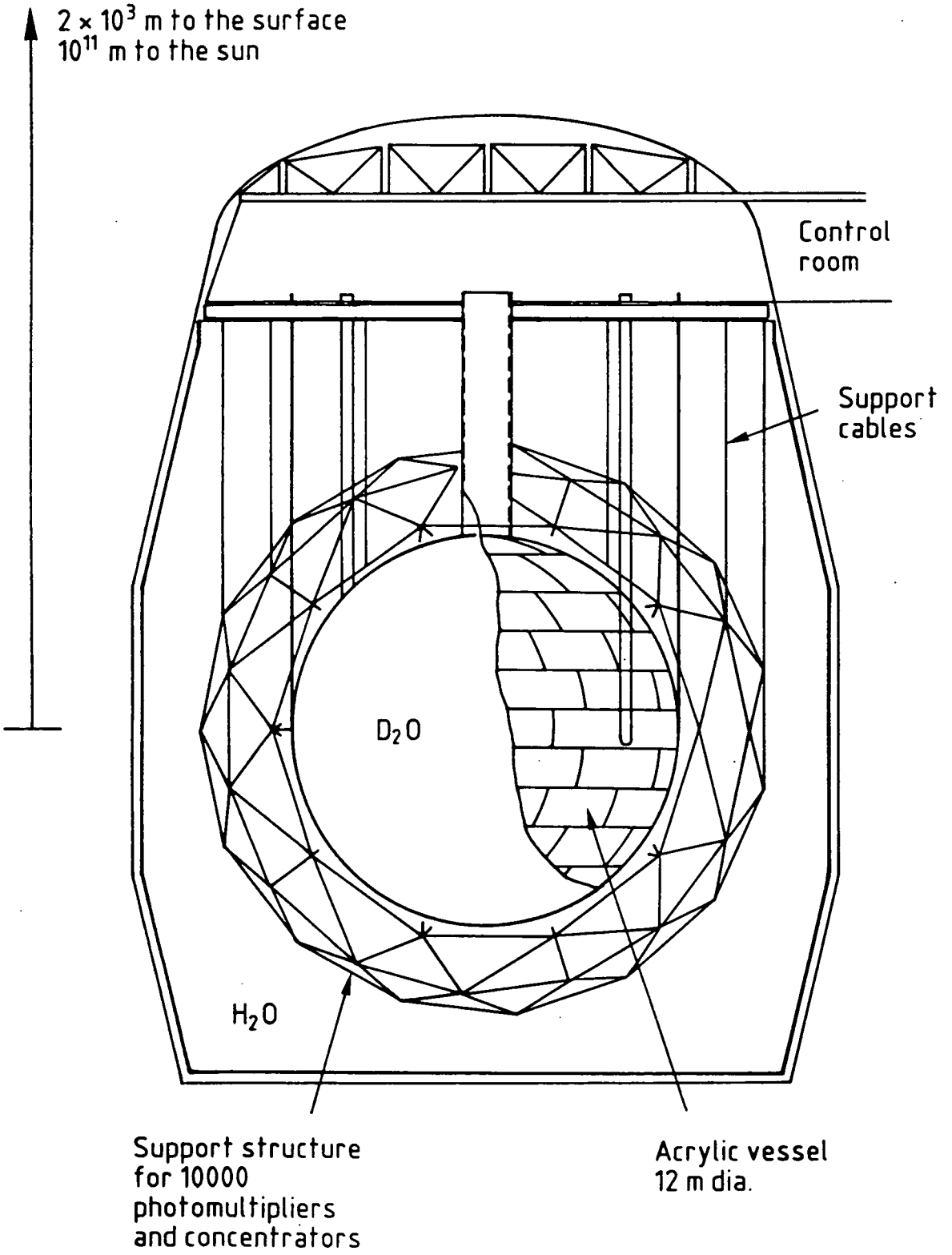

Figure 1. A drawing of the SNO Cerenkov counter showing the cavity 22m diameter by 30m deep, 2000m below the surface, the support structure 17.5m diameter for 10000 photomultipliers, and the acrylic vessel for D_2O, 12m diameter.

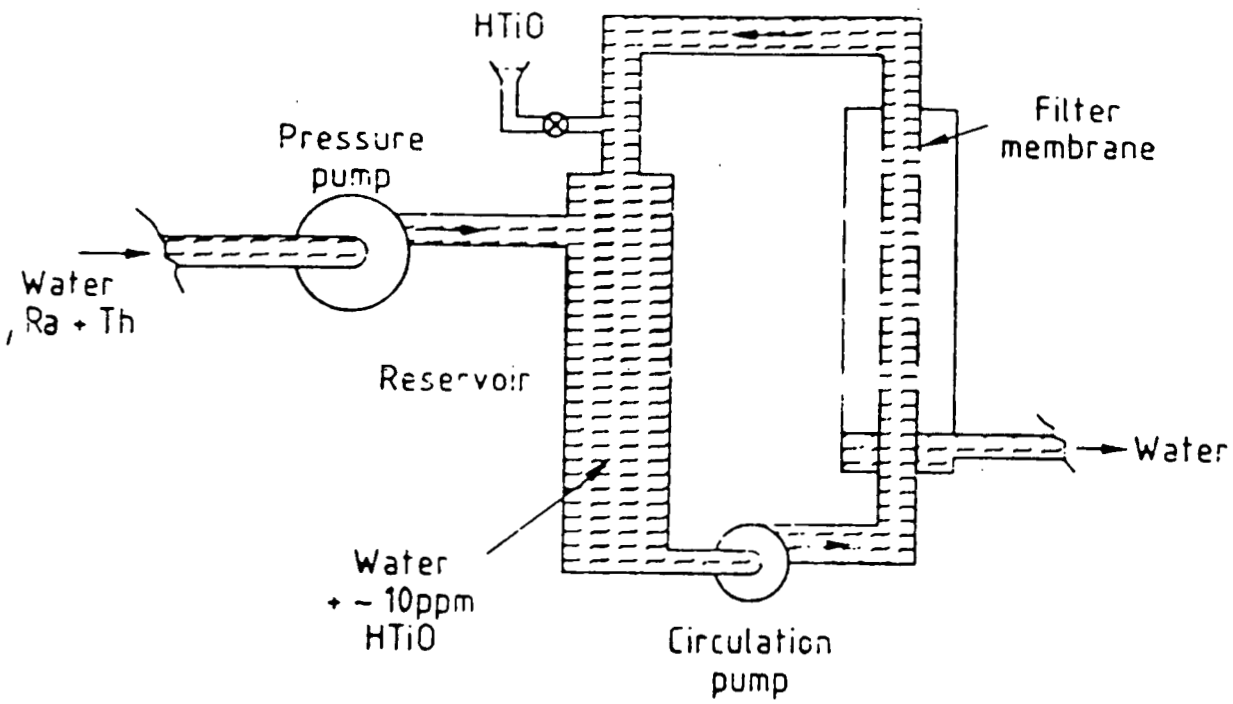

Figure 2. Schematic diagram of the system for seeded ultrafiltration using *ca.* 10 p.p.m. of finely divided hydrous titanium oxide (abbreviated HTiO) to absorb Ra and Th in water and extract via a filter of pore size *ca.* 10nm.

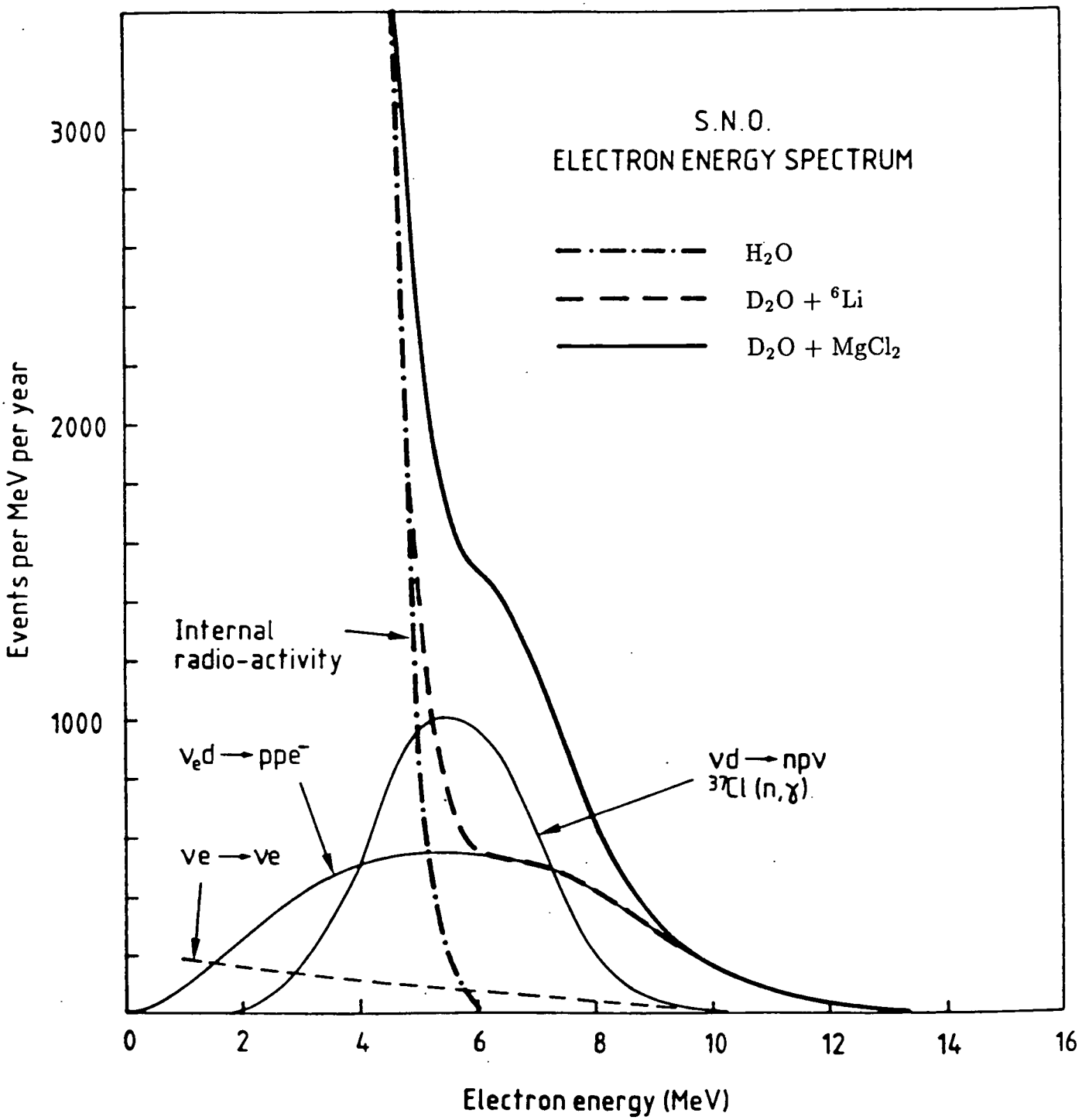

Figure 3. Simulated energy spectra expected from the Cerenkov detector for various fillings of the acrylic vessel (see Fig.1).

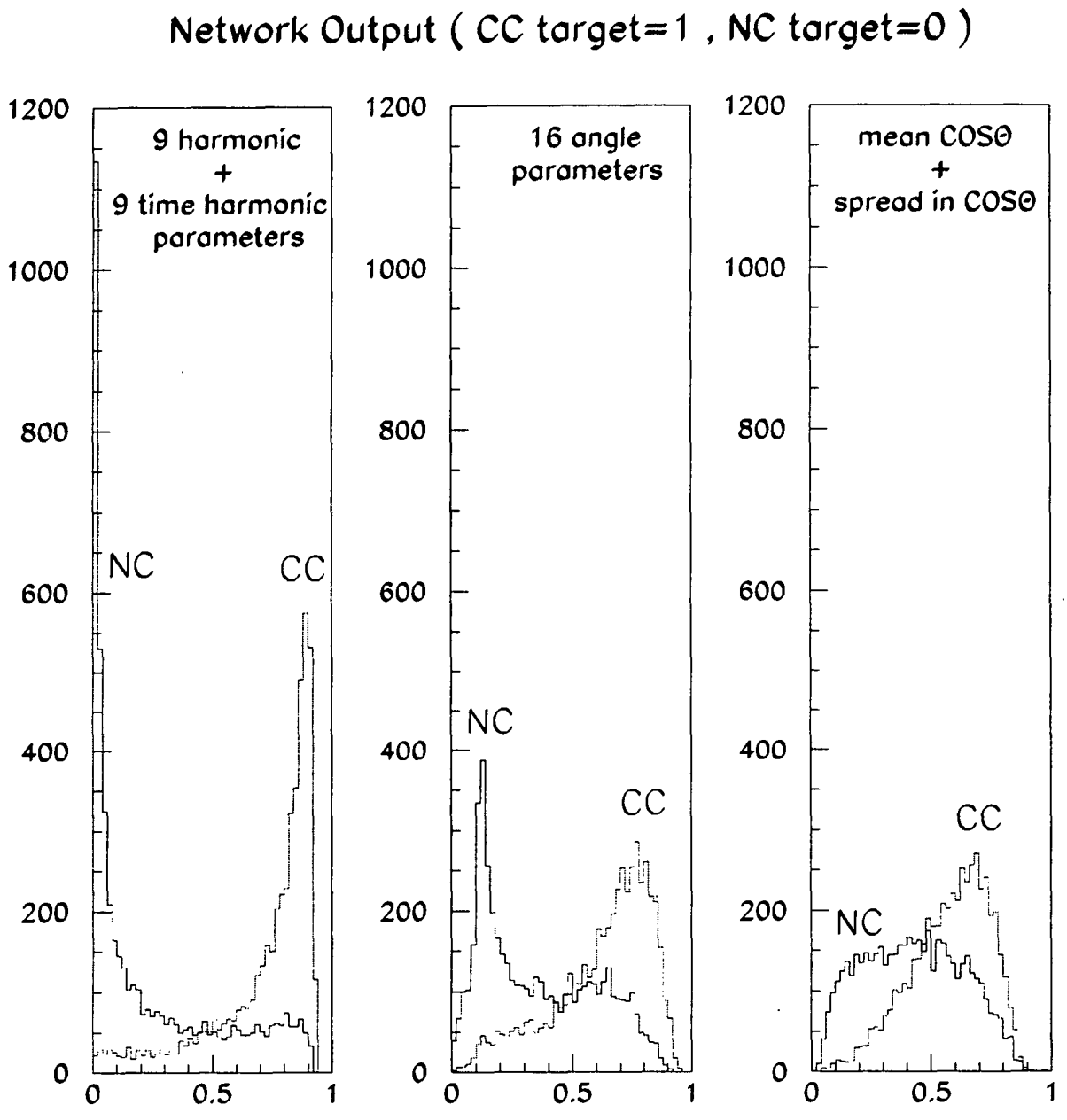

Figure 4. Outputs from neural network analyses of the mix of charged current and neutral current events above the radio-active background with the aim of separating these two kinds of events without incurring the statistical penalty of a subtraction.

A search for the H-particle and other strange matter

Birmingham University, Brookhaven, Carnegie-Mellon, Freiburg, Kyoto,
Kyoto-Sangyo, Los Alamos, Manitoba, New Mexico,
Triumf, Vassar College

This project comprises several related experiments on systems with multiple strangeness. Two of these (E813, E836) are searches for the S=-2, B=2 H-particle[1]. The third, E886, is a search for other forms of strange matter.

A. E813 - A search for the H-particle in $\Xi^- d$ interactions

Brookhaven E813 is a search for the H-particle, a strangeness-2 dibaryon, by Ξ^- interactions at rest in deuterium. In E813, K^- at 1.8 GeV/c enter a liquid hydrogen target, producing Ξ^- by the reaction

$$K^- p \rightarrow K^+ \Xi^-.$$

The K^+ are detected in a magnetic spectrometer. The Ξ^- pass through a tungsten degrader and a Si surface-barrier detector, and stop in a liquid D_2 target, where they form $\Xi^- d$ atoms which produce H-particles via the process

$$\Xi^- d \rightarrow H n.$$

Thus the signal of H-particle production is a K^+ in the magnetic spectrometer, a signal from a slow Ξ^- in the Si detector, and a monoenergetic neutron in the neutron TOF spectrum. A schematic diagram of the layout of the apparatus is given in fig. 1.

During 1995, analysis has been almost completed for all data taken during the main data-taking runs in 1991-3. Cuts were applied on all detector pulse heights, in particular the Si detectors tagging the Ξ^-, and also on the vertex position relative to the hit in the bank of Si detectors. The data are summarised in a plot of the neutron time-of-flight spectrum. Two such plots are shown in fig. 2, in the form of spectra of β^{-1}. The background spectrum is taken from a scaled, non-Si-tagged spectrum. The production of a bound H-particle would result in a peak in this spectrum. No clear peak is visible, other than the γ peak at $\beta^{-1} = 1$. The largest candidate peak is at $\beta^{-1} = 3.04$, which would correspond to an H-particle binding energy of 56 MeV. The statistical significance of this peak is about at the 3-σ level[2]. While suggestive, this peak does not, of course, establish the existence of a bound H-particle. An independent confirmation is required.

Because of this, another data-taking run was carried out in 1995. After initial problems with target leaks, the run went well and the total data sample was doubled. Analysis of the 1995 data is in progress.

As a part of the analysis, calculations have been made on the decays of the $\Xi^- d$ atom. The calculation of the sensitivity of the experiment relies on an understanding of the processes in this atom. These calculations, which have been carried out for

us by Dr. C.J. Batty, have recently been extended to use an improved model which gives a substantially better fit to $\bar{p}p$ atom data. The implications of this model for the $\Xi^- d$ atom are being studied.

B. E836 - A search for the H-particle in $K^-\ ^3He$ interactions

This experiment searches for H-particle production in the process

$$K^-\ ^3He \rightarrow HK^+n.$$

Only one target is involved, a liquid ^3He target, and there is no slow Ξ to tag in Si detectors. Apart from these differences, the experimental apparatus is very similar to that for the H_2/D_2 version, E813. The ^3He-target experiment is sensitive to a wider range of H-particle binding energies than is E813.

No further data taking took place during 1995. The first stage of analysis of the data taken during the 1994 run is now complete. The results take the form of a plot of missing mass, calculated assuming a neutron spectator. This is shown in fig. 3. There is a broad distribution from quasi-free Ξ production. A bound H-particle would give rise to an additional peak in the spectrum. If the H-particle binding energy is less than about 30 MeV, the corresponding peak would be lost in the quasi-free distribution. However, the region of the spectrum corresponding to binding energies between 30 and 500 MeV shows no peaks and very little background. Also shown in fig. 3 is the peak height expected from the calculations of Aerts and Dover[3]. It seems that either these calculations overestimate the yield by at least an order of magnitude, or that no bound H-particle exists in this mass region.

The analysis so far has not used the neutron detector information. If an H is produced, there is a significant chance that the associated neutron will be detected. Analysis of the neutron spectra is now under way.

C. E886 - A search for new strange particles in nucleus-nucleus collisions

Experiment E886 is a search for strangelets and other exotic forms of matter in relativistic heavy ion collisions. Such objects are expected to have anomalously large mass-to-charge ratios (M/Z). Any object with $M/Z \geq 4GeV/c^2$ cannot be a known nucleus and is potentially a strangelet. After a test run in 1992, (which produced results which were published in 1993 and 94), the main data run took place during 1993.

The apparatus was again similar to that for experiments E813 and 836, but the H-particle production target was removed and replaced by 4 scintillation counters [4,5,6]. The AGS D6 beamline was used as a focusing spectrometer, producing a M/Z measurement, which was repeated in the associated open geometry spectrometer. The charge (Z) of the particles was deduced from pulse height measurements in four plastic scintillators placed in the region between the beamline and the open

spectrometer. Requiring agreement between the two M/Z measurements resulted in very clean spectra and good particle identification capabilities, see fig. 4.

Analysis of this experiment is now complete. In previous years we have published cross sections for the production of π, K, p, d and other nuclear fragments, the first such cross sections to be published for a Au beam and AGS energies. The final stage of analysis, which has been completed this year, was to set limits on the production of strangelets and also of H-nuclear bound systems (i.e. H-hypernuclei). No such systems were seen. For H-hypernuclei, we set a limit on the production cross cross section of about $10^{-5} mb/(GeV)^2$, at $y = 0.6$ and $p/Z = 0.18 GeV/c$, for lifetimes above about 30 ns. This appears to be in disagreement with a calculation[7] of the yield; if so, this sets an upper limit on the lifetimes of H-nuclear systems. The data have been published in Phys. Rev.[8].

For strangelet production, we obtained limits for both Si + Pt and Au + Pt collisions. The limits for Au + Pt collisions are shown in fig. 5, both as invariant cross section and as probability per central collision. Several predictions have been published of strangelet production probabilities. In general, those based on a coalescence model alone predict probabilities well below the sensitivity of our experiment. Calculations involving the formation of a quark-gluon plasma predict yields comparable with our sensitivity. Predictions of three such calculations[7,9,10] are superimposed on our data in fig. 5. Two of these are ruled out by our data and the third is comparable with our limits. If these calculations are correct, we can exclude either the formation of a quark-gluon plasma in these Au + Pt collisions or the stability (or meta-stability) of strangelets in this region of M/Z. The data have been submitted for publication in Phys. Rev. Letters.

References

[1] R.L. Jaffe, Phys. Rev. Lett. **38**, 195 (1977).
[2] F. Merrill, Ph.D. thesis, Carnegie-Mellon University, 1995.
[3] A.T.M. Aerts and C.B. Dover, Phys. Rev. D**28**, 450 (1983).
[4] G.E. Diebold *et al.*, Phys. Rev. C**48**, 2984 (1993).
[5] N. Saito *et al.*, Phys. Rev. C**49**, 3211 (1994).
[6] A. Rusek, Ph.D. thesis, University of New Mexico, 1995.
[7] A.J. Baltz *et al.*, Phys. Lett. B **325**, 7 (1994).
[8] A. Rusek *et al.*, Phys. Rev. C**52**, 1580 (1995).
[9] H.J. Crawford *et al.*, Phys. Rev. D**45**, 857 (1992).
[10] Z. Arvay *et al.*, Z. Phys. A**348**, 201 (1994).

Publications, Conference Contributions and theses

Search for H-dibaryon-nucleus bound states in relativistic Au + Pt collisions, A. Rusek, B. Bassalleck, A. Berdoz, T. Bürger, M. Burger, R.E. Chrien, G.E. Diebold, H. En'yo, H. Fischer, G.B. Franklin, J, Franz, T. Iijima, K. Imai, J. Lowe, R. Magahiz, A. Masaike, C. Mayer, F. Merrill, S. Mihara, J.M. Nelson, K. Okada, P. Pile, B.P. Quinn, E. Rössle, N. Saito, R. Sawafta, H. Schmitt, R.A. Schumacher, R.L. Stearns, R. Stotzer, I.R. Sukaton, R. Sutter, F. Takeuchi, D.M. Wolfe, K. Yamamoto, S. Yamashita, S. Yokkaichi, V. Zeps, R. Zybert, Phys. Rev. **C52**, 1580 (1995).

Search for strangelets in relativistic Si + Pt and Au + Pt collisions, A. Rusek, B. Bassalleck, A. Berdoz, T. Bürger, M. Burger, R.E. Chrien, G.E. Diebold, H. En'yo, H. Fischer, G.B. Franklin, J, Franz, T. Iijima, K. Imai, J. Lowe, R. Magahiz, A. Masaike, C.A. Meyer, R. McCrady, F. Merrill, S. Mihara, J.M. Nelson, K. Okada, P. Pile, B.P. Quinn, E. Rössle, N. Saito, R. Sawafta, H. Schmitt, R.A. Schumacher, R.L. Stearns, R. Stotzer, I.R. Sukaton, R. Sutter, F. Takeuchi, D.M. Wolfe, K. Yamamoto, S. Yamashita, S. Yokkaichi, V. Zeps, R. Zybert, Phys. Rev. Letters, submitted.

A multi-cell target for $\Lambda - \Lambda$ hypernuclei searches, B. Bassalleck, A. Berdoz, J. Birchall, T. Bürger, M. Burger, R.E. Chrien, C.A. Davis, G.E. Diebold, J. Dornboos, M. Eggers, H. Fischer, G.B. Franklin, J, Franz, L. Gan, T. Iijima, K. Imai, M. Landry, L. Lee, J. Lowe, R. Magahiz, C. Maher, A. Masaike, M. May, R. McCrady, F. Merrill, K. Okada, S.A. Page, P.H. Pile, B.P. Quinn, W.D. Ramsay, E. Rössle, A. Rusek, R. Sawafta, H. Schmitt, R.A. Schumacher, R.L. Stearns, R. Stotzer, I.R. Sukaton, R. Sutter, F. Takeuchi, W.T.H. van Oers, D.M. Wolfe, K. Yamamoto, M. Yosoi, V. Zeps and R. Zybert, International Conference on Hypernuclear and Strange-Particle Physics, Vancouver, July 4 - 8. 1994, Nucl. Phys. **A585**, 339c (1995).

A. Rusek, A search for strangelets and other rare objects in relativistid Au + Pt collisions, Ph.D. thesis, University of New Mexico, 1995.

I.R. Sukaton, H-particle search through direct production from carbon targets using (K^-, K^+) interactions, Ph.D. thesis, Carnegie Mellon University, 1995.

F. Merrill, H dibaryon search through Ξ^- capture on the deuteron, Ph.D. thesis, Carnegie Mellon University, 1995.

T. Iijima, Search for the H dibaryon by Ξ^- capture on the deuteron, Ph.D. thesis, Kyoto University, 1995.

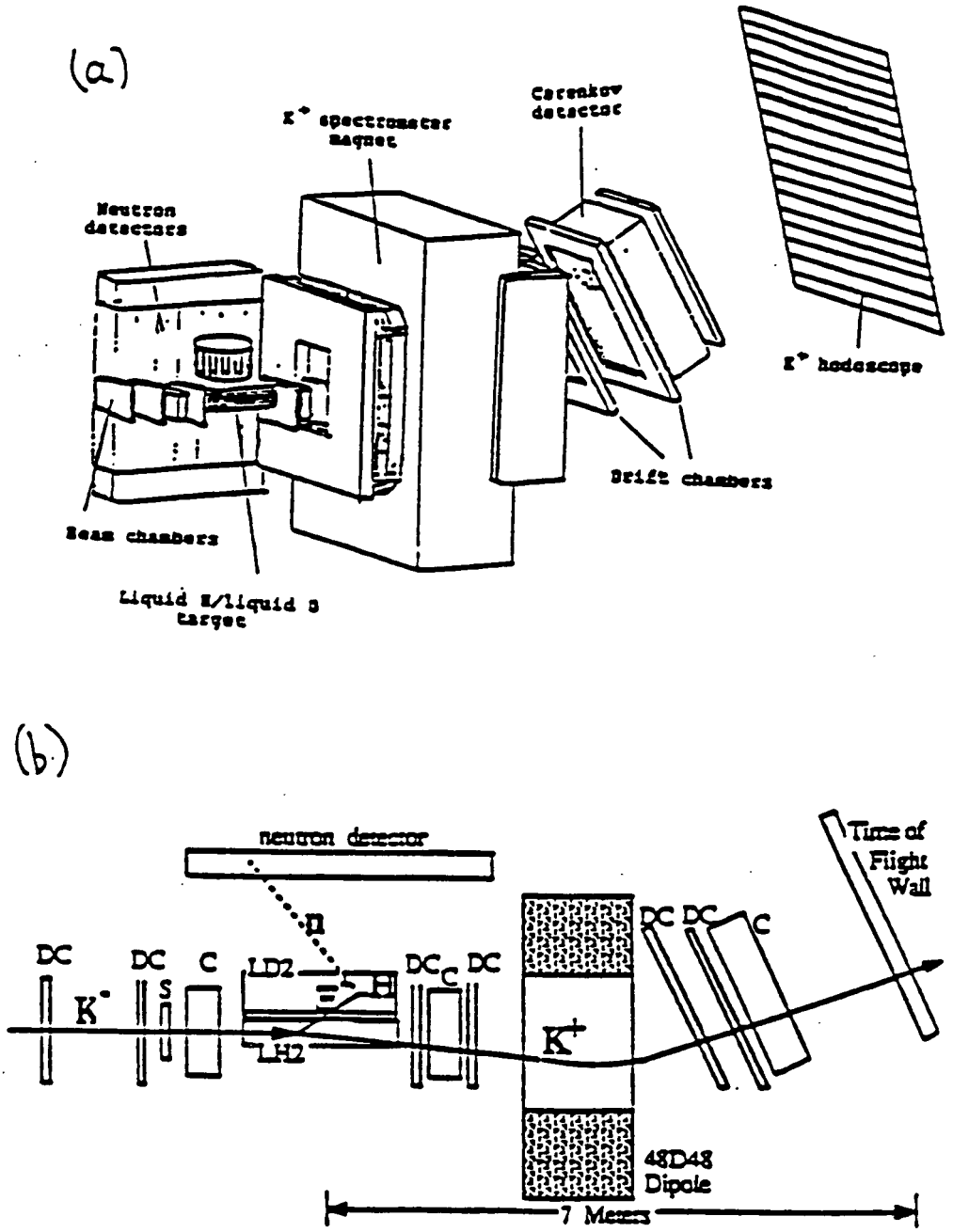

Fig. 1. Layout of the main components of the apparatus for E813/836. The perspective view, (a), shows the general layout, while the side view, (b), shows more detail. The neutron counters, some of which are not shown for clarity, surround the target on both sides. Several Cerenkov and scintillation counters are also omitted from this drawing. For the strangelet search, E886, the apparatus is essentially the same except that the liquid H_2/liquid D_2 target is replaced by 4 scintillation counters.

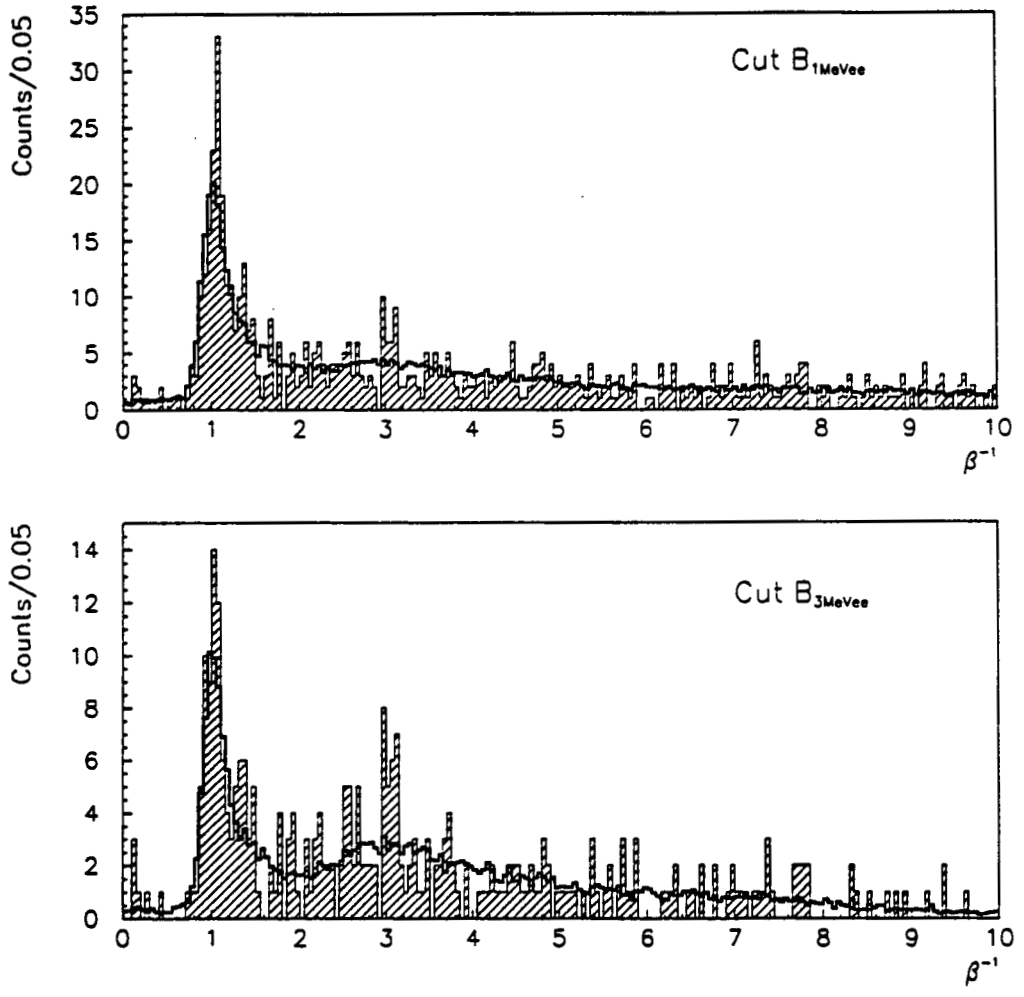

Fig. 2. Neutron time-of-flight spectra from the $\Xi - d$ atom H-particle search, for two different neutron detector thresholds. The peak at $\beta^{-1} = 1$ results from γ rays.

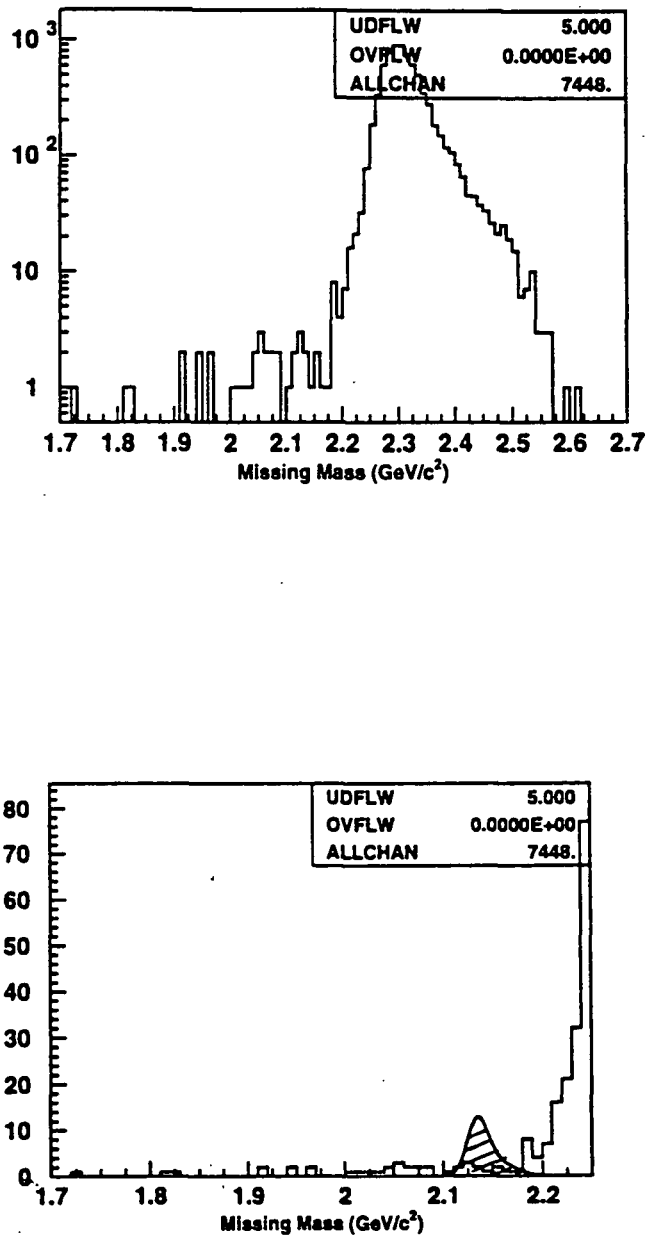

Fig. 3. Missing mass spectrum from the $K^- {}^3He \rightarrow HK^+n$ reaction. The lower plot shows the spectrum away from the quasi-free distribution, on a linear scale. The shaded peak in the lower plot shows the yield predicted by Aerts and Dover[3] for an H-particle mass of 2180 MeV.

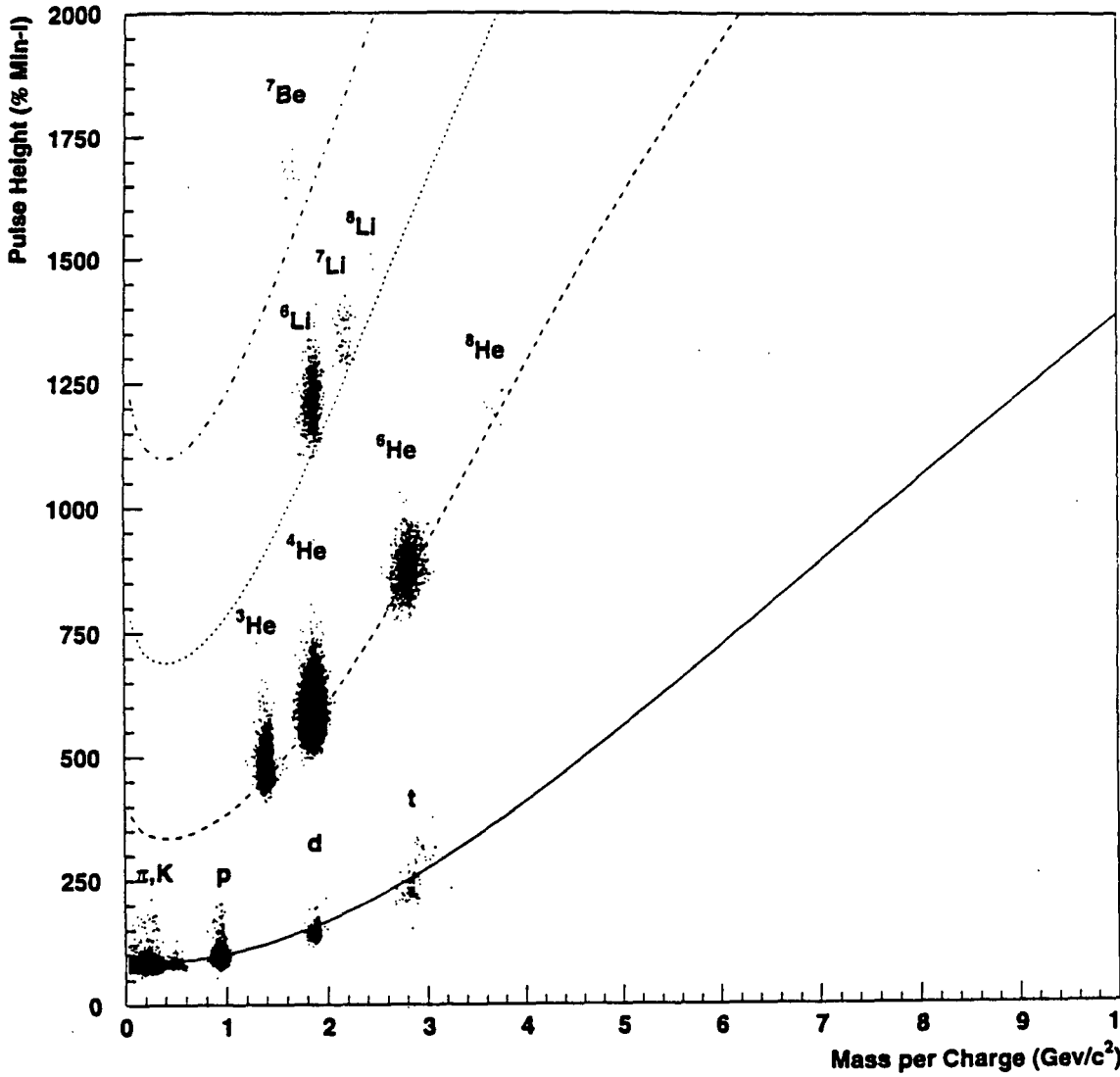

Fig. 4. Pulse height vs. M/Z for particles from Au + Pt interactions at 10.8A GeV/c. All cuts have been applied to the data, including the requirement of agreement between front and back spectrometers. The lines indicate the most probable pulse height, from Vavilov distributions corrected for scintillator non-linearities.

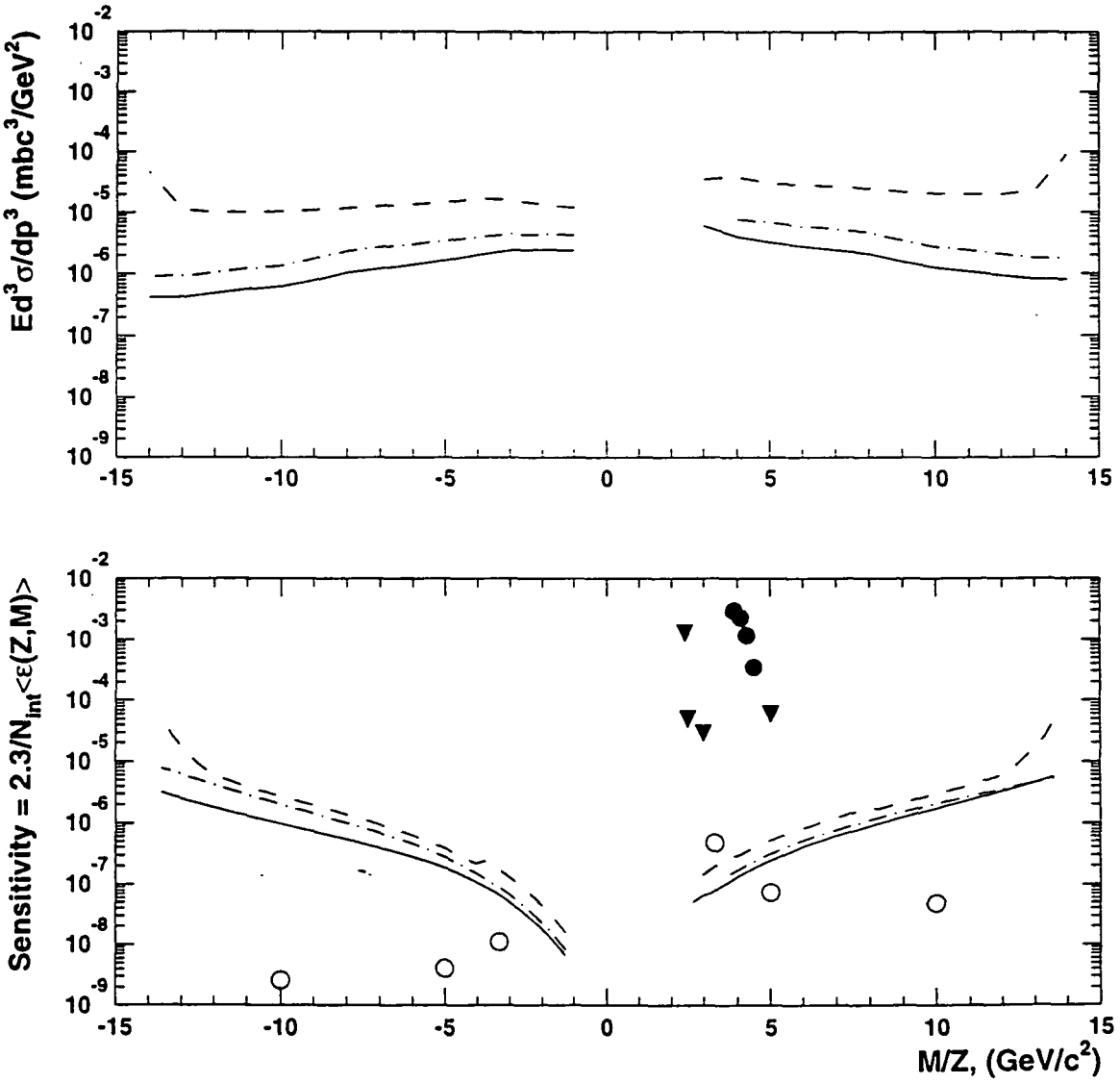

Fig. 5. Limits on strangelet production at 90% CL in Au + Pt collisions, as a function of M/Z and Z. The upper plot shows the invariant cross section and the lower plot shows the probability per central collision. The points represent predicted strangelet production probabilities: triangles, ref. [7], open circles, ref. [9], solid circles, ref. [10].

Measurement of Beauty Particle Lifetimes and Hadroproduction Cross-section

WA92 — Proposal 280

Bologna; CERN; Genoa; Imperial College; Moscow; Pisa; Rome; Southampton

This experiment uses a 350 GeV negative pion beam incident on tungsten and copper targets at the CERN Omega Spectrometer. Its aim is to identify a sample of B mesons, large enough to address several important physics issues, including measurements of the lifetimes of charged and neutral B mesons and the B hadroproduction cross-section.

Heavy nuclear targets are used to exploit the A^1 mass number dependence of the $b\bar{b}$ cross-section. But, even so, the B-signal to noise ratio is only 10^{-6}. Methods used successfully to isolate charm signals from fixed target experiments will not work with beauty. Fully reconstructible channels account for about 10% of charm decay vertices compared with 10^{-3} for beauty. It is hopeless to rely on reconstructing the invariant mass of B-decays. Instead, the identification uses the cascade decay topology, the identification of the daughter charm decay and the high-p_T of leptons emerging from the B-decay.

The experimental triggers emphasize characteristic features of B-decay: impact parameter, to select secondary vertices; lepton triggers, to exploit the large semileptonic branching fraction; high p_T, to select high mass decays. The detector is based around the Omega spectrometer, with muon and electron identification and a dense array of high precision ($\sigma < 3\,\mu$m) silicon microstrip detectors, acting as an electronic emulsion stack in which the cascade $b \rightarrow c$ decay chain can be observed.

During 1992-93, 150M triggers were recorded. The trigger algorithm enriches, by a factor ~ 20, the Beauty fraction of the data while maintaining a high ($\sim 50\%$) acceptance. On reasonable assumptions for the B cross-section we estimate that more than 1000 B's are on tape, from which we expect that a few hundred will be identifiable. Analysis of 20% of the triggers has so far yielded about 20 Beauty candidates with small backgrounds. Using this sample a cross-section of $\sigma(b\bar{b}) = 7 \pm 2\,$nb/nucleon has been obtained. From the full data sample we expect to measure the charged to neutral B-lifetime ratio and the $b\bar{b}$ cross-section to a precision of $\sim 10\%$.

The discriminating power of the silicon vertex detectors has allowed measurements of charm physics with very low backgrounds. An analysis of kinematic correlations in $D\overline{D}$ production and a new upper limit on the FCNC process $D \rightarrow \mu^+\mu^-$ have been published during 1995.

WA92 - Publications in refereed journals: 1994 - 95

"The use of a decay detector in the search for beauty decays in the WA92 experiment."
Nucl. Instr. & Methods A351 (1994) 222 - 224.

"A secondary-vertex trigger for a beauty search: results from the WA92 experiment."
Nucl. Instr. & Methods A351 (1994) 225 - 228.

"Study of charm correlations in π^--nucleon interactions at 26 GeV centre of mass energy."
Phys.Lett B348 (1995) 256-262.

"Search for the decay $D^0 \rightarrow \mu^+\mu^-$."
Phys.Lett B353 (1995) 563-570.

Proposal 282

A Measurement of the Beta Spectrum of ^{63}Ni using a New Type of Cryogenic Detector

Oxford University

A precision measurement of the beta spectrum of ^{63}Ni has been performed using a new type of cryogenic particle detector. This is the first nuclear physics experiment using this technique, and we discuss the principles of the method, its advantages and its shortcomings. Careful studies of detector stability, calibration, pulse pile-up and systematics have made it possible to collect large numbers of events (~10^8) over long periods (~28 days). The measurement is consistent with no 17 keV/c^2 neutrino admixture, giving a preferred value of (-0.05 ± 0.31) %.

1. Introduction

The original motivation for this work was to investigate the 17 keV/c^2 neutrino question using a new type of cryogenic detector being developed in Oxford. Although the evidence for this neutrino [1] has now disappeared, and has been shown to be due to instrumental effects [2, 3], it has stimulated substantial improvements in beta-spectrum measurement techniques with magnetic spectrometers and with semiconductor detectors [4-6]. We report here the highlights of a measurement based on a wholly new technique where the source is fully enclosed within the detector and there are no dead layers. This arrangement avoids the distortions in the measured beta spectrum which result from electron backscattering, final-state atomic effects which generate secondary electrons and x-rays, and the generation of fluorescence x-rays within the detector, thus permitting a calorimetric measurement of each beta-decay event. Also, a high counting rate is obtained with a very thin (less than a monolayer) source, thus avoiding non-uniform energy losses in the source which have plagued many beta-decay experiments.

2. Principles of the detector

For ionising particles incident on semiconductor detectors only a small fraction of the kinetic energy goes into the production of electron/hole pairs (30% for Si and 10% for InSb) [7]. The remainder goes into the production of phonons, the quanta of lattice vibrations. These phonons can be detected if one works at a low temperature, ≤100 mK, where the background of thermally generated phonons is small. We choose the direct-gap semiconductor InSb as the absorber because the charge carrier lifetimes are short and the recombination processes lead to the production of more phonons. The charge signal is not directly detected.

An excellent phonon sensor is the superconducting tunnel junction (STJ). Phonons which have energy $\Omega \geq 2\Delta$, where 2Δ is the Cooper pair binding energy, readily break Cooper pairs in the films comprising the STJ creating electronic excitations (quasiparticles) which are detected as an increase in the tunnel current [8]. During the subsequent thermalization and decay of high energy phonons into ones of lower energy, phonons with energy $\Omega < 2\Delta$ are not directly detected, and so the pulses have a short decay time compared to a thermal detector. To fabricate the STJs we use Al films which have $2\Delta \approx 400$ μeV. This is small compared with the maximum phonon energy in InSb of about 17 meV and large compared to the thermal energy at 100 mK of about 24 μeV. Each phonon sensor consists of a series-connected array of 200 STJs covering an area of 20 mm^2 on one surface of each crystal, yielding a position independent response to electrons from the source.

This cryogenic detector scheme is significantly different from that of the low temperature thermal detector [9]. In the thermal detector, the phonons thermalize to a slightly higher temperature on a time scale of a few 100's of μs, when the temperature rise is sensed, and there is a long thermal decay (~10's of ms) during which the detector returns to its starting temperature. Low statistics measurements of the beta-decay spectrum of ^{187}Re [10, 11] have been made by this method. However this mode of operation is too slow for a high-rate experiment, and in our scheme the phonons are detected before they thermalize.

3. Experimental arrangement

A schematic of the experimental arrangement is shown in Fig. 1. Each of two detectors consists of a single crystal of InSb in which the particle energy is absorbed. The two

crystals (each of dimensions 12×12×2 mm^3) enclose the thin ($2x10^{-4}$ μg cm^{-2}) ^{63}Ni beta source of 1-mm diameter which was electroplated onto the face of one of the crystals from a 10-μl drop of dilute buffered $^{63}NiCl_2$ solution [12]. The maximum beta electron energy is ~67 keV which corresponds to an electron range in InSb of about 10 μm, much less than the crystal thickness. The Al films comprising the STJ arrays are 115 nm thick and were deposited in a high-vacuum thermal evaporator using shadow masks and an intermediate oxidation step to form the tunnel barriers. The thin SiO layers provide electrical isolation from the crystals which are conducting at the temperature of operation. The detectors are mechanically and thermally clamped and mounted in a conventional dilution refrigerator where they can be operated at a constant temperature, typically 30 to 100 mK.

4. Detector operation and data acquisition

The kinetic energy of electrons from the source is converted into non–equilibrium phonons which propagate from the interaction site, becoming isotropically distributed by decay and scattering processes within the crystal in a few μs. The electronic signals from the STJ arrays can be read out over short time scales (< 1 ms), determined by the characteristic time for the non–equilibrium phonons to decay to energies below the superconducting gap 2Δ. Counting rates of up to 100 Hz were possible in these detectors with pulse pile-up below the 5 % level.

The pulse height in each channel, measured with charge-sensitive preamplifiers, is used to determine the amount of energy deposited within each InSb crystal. The kinetic energy of a beta electron emitted from the enclosed source may be completely absorbed in one of the two crystals, or shared between them, for example, due to back-scattering of the electron from one crystal into the other, or by the emission of a fluorescent x-ray.

Pulses arriving at an average rate of 80 Hz are read out from the arrays using an integration time ~200 μs. Individual pulse shapes were sampled at a rate of 1 MHz using 12-bit waveform digitisers over a period of ~1.3 ms (including 0.5 ms pre-pulse information) [13]. At five minute intervals, the devices were checked for stability using 200 constant energy pulses from a variable energy precision infrared LED which were directed on to one edge of the detectors by an optical fibre. Every 3 hours, variable energy LED pulses were used to measure the device linearities over the range 0-100 keV, and to measure the pile-up spectrum, taking care that the data acquisition was triggered in a manner identical to that for beta events. The differential non-linearities of the waveform

digitisers were measured separately using a slowly varying ramp signal. An external ^{57}Co γ source (with γ energies 122 & 136 keV) was used approximately every 60 hours to validate the stability of the LED calibration against an absolute energy calibration. Corrections based on the LED calibration data were made for drifts and linearity. Two forms of cross-talk between the 2 channels were identified at the ~1% level, phonon cross-talk and electronic capacitive cross-talk, and were corrected for.

The ^{63}Ni beta spectrum data was acquired over a period of 4 weeks in two independent runs carried out with slightly different conditions. The devices remained relatively stable over this period with slow drifts in the electronic signal for a fixed energy deposition of less than $\pm$ 5 %. A total of 6.1×10^7 ^{63}Ni events and 6×10^6 LED calibration pulses were recorded during the first two week run and the results are reported here. Further experimental details and a full analysis will be published in due course.

5. Data Analysis

The detector response function, including the effect of pulse pile-up, as measured with the LED pulser is shown in Fig. 2. The result obtained is independent of the amplitude of the LED pulses. The pile-up spectrum makes a significant contribution to the measured beta spectrum only immediately above the end-point. The error associated with convoluting a theoretical beta spectrum with this response function has a maximum at the end-point and is equal to ~ 0.1 % of dN /dE which is an order of magnitude smaller than the statistical uncertainty associated with the ^{63}Ni counts. For energies below 60 keV the convolution error is negligible.

The full spectrum including pulse pile-up and background is shown as curve (1) in Fig. 3(a). Curve (2) results from deconvoluting the pile-up response function of Fig. 3. Also shown is the estimated ^{115}In beta spectrum [14] from the InSb absorbers which is the dominant background only between 300 and 400 keV. One problem with this detection scheme is that it is not possible to easily remove the beta source in order to measure the background or replace it with a calibration source. Backgrounds were measured with similar InSb devices, and with Si and Ge semiconductor detectors in the same room. For energies less than 60 keV the background is less than 1%, and is 10% of the pulse pile-up rate at the end-point.

In our fitting of the ^{63}Ni spectrum we assume a theoretical end-point of 66.85 keV, a theoretical spectrum (see ref.[1]), and let the energy scale of the ^{63}Ni data vary as a free

parameter. Convoluting the theoretical spectrum with the measured response function reproduces the observed pile-up spectrum above the ^{63}Ni end-point. Figure 3(b) shows the residuals from a fit over the range 30-60 keV, where the relative background rate, radiative and exchange theoretical corrections and convolution error are negligible. A fit including an admixture of a neutrino of mass 17 keV/c^2 gives the result (-0.05 ± 0.31) %. We are currently investigating the presence of radiative corrections and exchange corrections to the nuclear beta transition matrix element, which are important at low energies (< 10 keV) and close to the end-point.

6. Conclusions

This experiment demonstrates the power of the calorimetric properties of a cryogenic detector scheme based on the detection of the non-equilibrium phonons produced by nuclear particles, and the feasibility of long term, high counting rate acquisition with STJ detector technology. The calorimetric measurement of the ^{63}Ni beta spectrum is consistent with no 17 keV/c^2 neutrino admixture.

Acknowledgments

This work is supported in part by PPARC grant GR/J60896 and EC Network contract ERB CHRX CT93 0341.

References

1. A. Hime and N. A. Jelley, Phys. Lett. B 257 (1991) 441.
2. A. Hime, Phys. Lett. B 299 (1993) 165.
3. M. G. Bowler and N. A. Jelley, Phys. Lett. B 331 (1994) 193.
4. F. Boehm, Nucl. Phys. B(Proc. Suppl.)31 (1993) 57.
5. G. E. Berman et al., Phys. Rev. C48 (1993) R1.
6. H. Abele et al., Phys. Lett. B316 (1993) 26.
7. C. A. Klein, IEEE Trans. Nuc. Sci. (1968) 214.
8. W. Eisenmenger, in: Physical Acoustics, eds. W. P. Mason and R. N. Thurston, (Academic Press, London, 1976) vol. XII, p. 79.
9. S. H. Moseley et al., J. Appl. Phys. 56 (1984) 1257.
10. E. Cosulich et al., Phys. Lett. B295 (1992) 143.
11. E. Cosulich et al., Nuclear Physics A to be published (1995) .
12. A. M. Swift, D.Phil. thesis, Oxford (1994).
13. A. D. Hahn, D.Phil. thesis, Oxford (1994).
14. L. Pfeiffer et al., Phys. Rev. C 19 (1979) 1035.

Figures

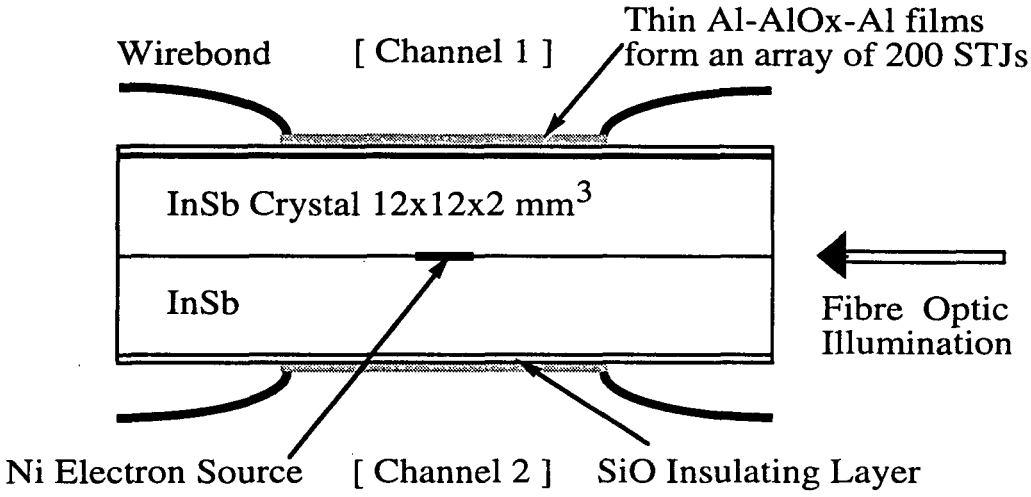

Fig. 1. Schematic arrangement of beta-source and detectors.

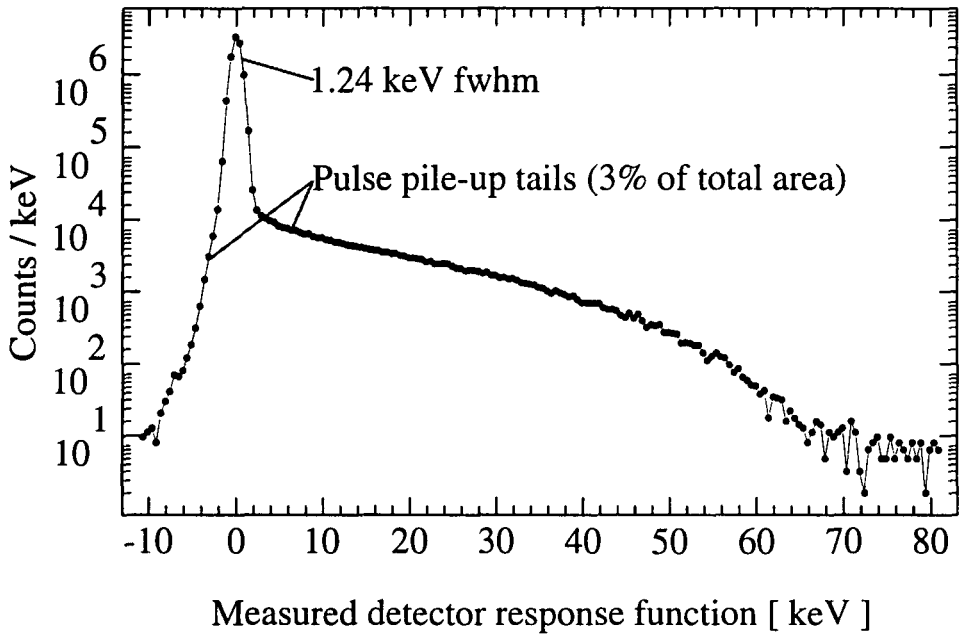

Fig. 2. Response function of the calorimetric spectrometer measured using LED calibration pulses. The response function has two parts: the Gaussian-shaped resolution of the detector system, and pulse pile-up.

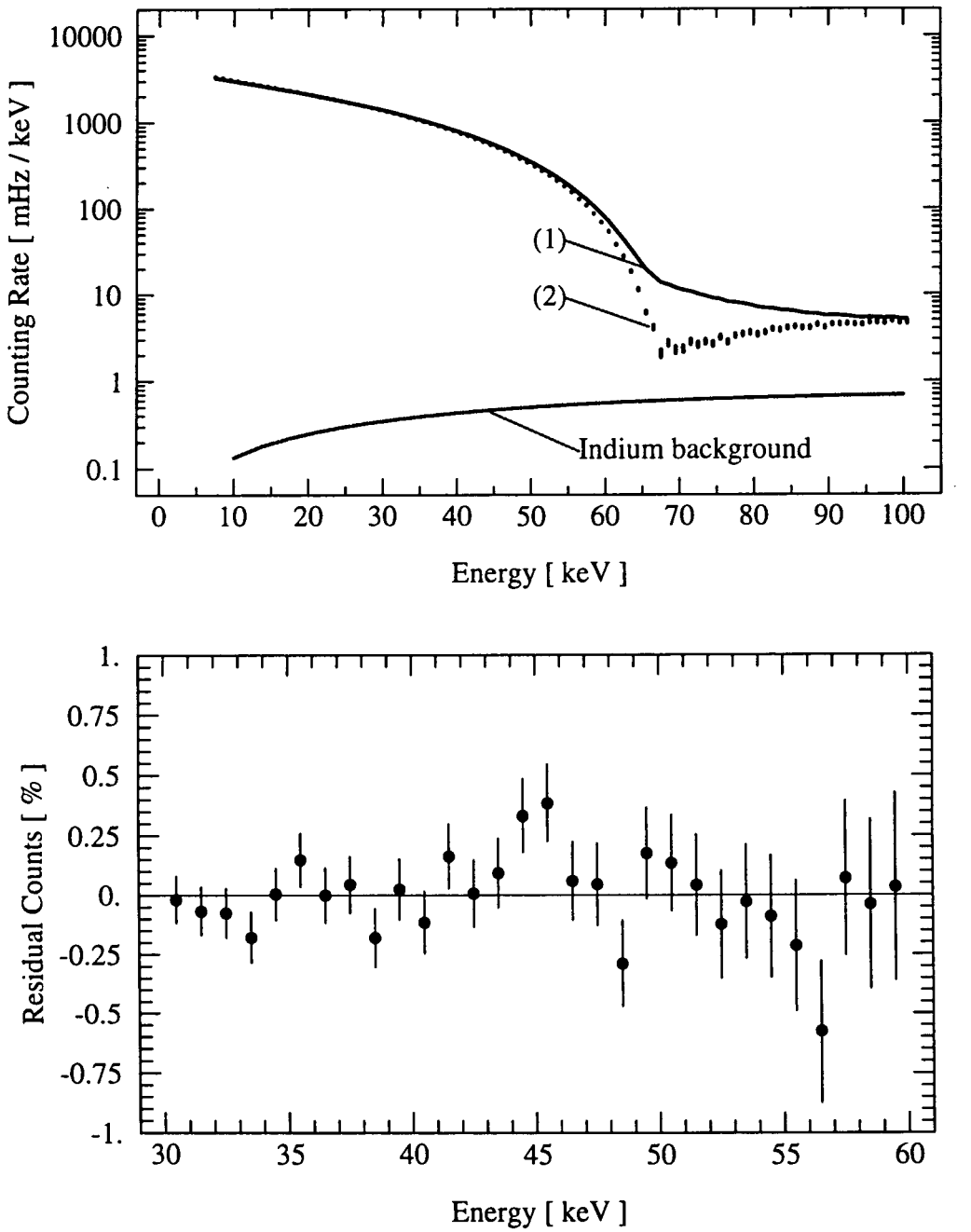

Fig. 3. (a) Beta-decay spectrum of ^{63}Ni. Curve (1) is the spectrum including pulse pile-up and background. Curve (2) results from deconvoluting the pile-up response function shown in Fig. 2. The calculated background due to the beta-decay of ^{115}In is also shown. (b) Residuals from a fit to the data in the interval 30-60 keV of the theoretical spectrum convoluted with the pile-up response function.

NA48 Proposal 283

A Precision Measurement of ϵ'/ϵ in CP Violating $K^0 \to 2\pi$ Decays

Cagliari, Cambridge, CERN, Dubna, Edinburgh, Ferrara, Florence, Mainz, Perugia, Pisa, Saclay, Siegen, Torino, Vienna, Warsaw Collaboration

This experiment, approved in 1991, aims to measure precisely the strength of CP-violation in the decay amplitude relative to the dominant CP-violation in the K^0 mass matrix, by comparing the ratio of decays into two charged and two neutral pions for K_S and K_L. The technique, while similar in some respects to that of the NA31 experiment, is very different to that of previous experiments. The $\pi^+\pi^-$ decays will be detected and measured in a classical magnetic spectrometer while the $2\pi^0$ decays will be detected and measured in a novel electromagnetic calorimeter using liquid krypton as the ionizing medium. The liquid krypton technique has been shown to work in a small test calorimeter, and achieves the required precision in energy, position and timing. The calorimeter consruction has progressed well, and the cryostat and electrode structure are at CERN; prototype electronics have been tested in a beam and the final layout is in progress. There was a test run in August and September with all detectors except the liquid krypton calorimeter and one of the four drift chambers; most detectors were equipped with prototype readout, and the hadron calorimeter and muon chambers were read out with alternative electronics. Prototypes of the advanced triggering and readout systems were used, and about 0.55 TBytes of data were obtained in about 3 weeks of data taking, mostly minimum bias running. The mass distribution for K_S decays is shown in Figure 1.

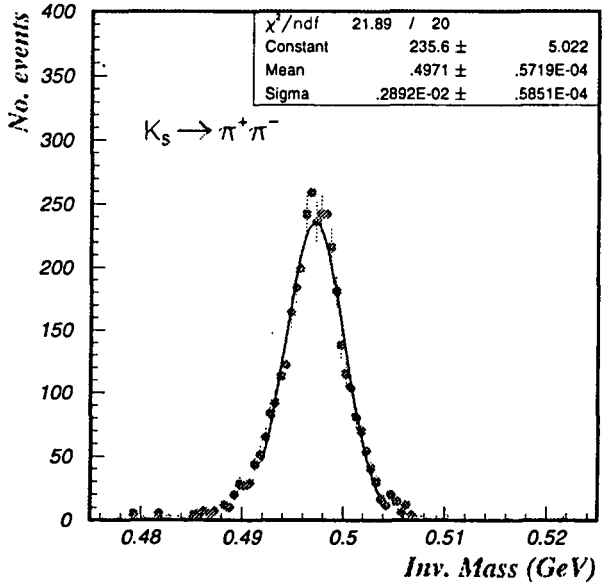

Figure 1: *The K_S mass distribution for selected events using the charged particle spectrometer.*

All of the data were recorded remotely on the Meiko CS2 installed in the CERN computer centre; a standby system in the control room was not tested.

In a related development, a study was made of an alternative to lead as a converter of photons in the anti-K_S counter (AKS) situated at the exit of the K_S collimator, its purpose being to veto

all K_S decays before it and so define the fiducial region. The counter consists of scintillators attached to photomultipliers and so to detect the neutral decays 11 mm (2 X_0) of lead is placed in the beam to convert at least one of the photons. Unfortunately this converter also scatters the K_S beam and so can produce a different acceptance between K_L and K_S decays. To help reduce this problem studies were performed on a tungsten crystal in a photon beam. Theoretical predictions indicated that the radiation length of a crystal is dramatically reduced near its axes and so this would allow a reduced thickness of material to be used in the AKS. Tungsten was chosen because the photons will be incident over an angular range of ± 10 mrad and the theory predicts a radiation length reduction over a wider angular range for higher Z materials. Using the H2 beam line at CERN, in collaboration with the NA43 experiment, data was taken for photons incident near the $< 100 >$ axis of a 3.17 mm thick tungsten crystal. Figure 2 shows the results obtained when photons were incident along the axis. The results of these runs are that the theory agrees with the data within errors and that the effect is large enough to be of use in NA48. More data has been taken this summer with an iridium crystal and again with tungsten but this time around the $< 111 >$ axis. Both of these are predicted to have a greater effect that $< 100 >$ tungsten. After analysis of these data a crystal will be installed this summer for testing in the NA48 K_S beam itself.

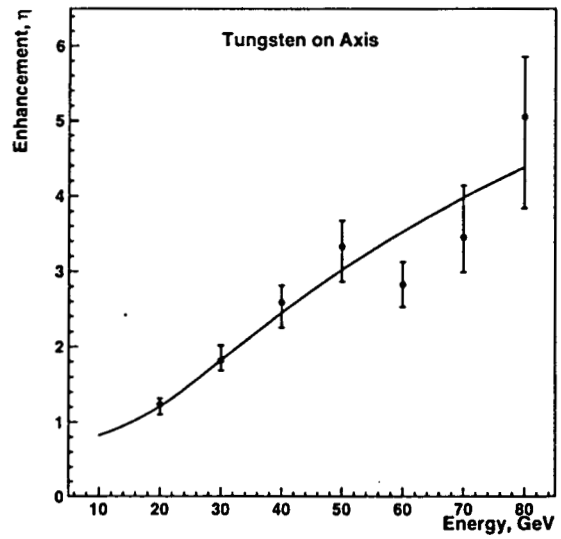

Figure 2: *Plot of the change in radiation length of tungsten as a function of the incident photon energy; η is the ratio of the crystal radiation length over the amorphous radiation length. The line indicates the theoretical prediction.*

Publications and Theses

1. N.E. McKay *An Input Buffer for the NA48 Experiment at CERN*, Edinburgh (1995)
2. R. Moore *et al*, *Measurement of Pair-Production by High Energy Photons in an Aligned Tungsten Crystal*, to be published in NIM

STUDY OF LEAD LEAD INTERACTIONS AT 160 GeV/c PER NUCLEON

WA97 **Proposal 285**

Athens; Bari; Bergen; Birmingham; CERN; Genoa; Košice; Legnaro; Oslo; Padova; Paris; Prague; Protvino; Rome; Salerno; Strasbourg.

The study of strange baryon spectra in heavy ion collisions is a useful probe of the dynamics of hadronic matter under extreme conditions. The relative abundances for different baryon and antibaryon species allow the degree and nature of flavour equilibration to be studied, while the transverse mass (m_T) spectra provide independent information on the temperatures achieved in the collision [1]. In particular, the onset of a Quark-Gluon Plasma (QGP) phase during the collisions is expected to enhance the antihyperon yield with respect to normal hadronic interactions and to give rise to a large $\overline{\Xi^-}/\overline{\Lambda}$ ratio [2]. The WA85 and WA94 experiments have high statistics data on strange baryon antibaryon spectra [3], and both measure the $\overline{\Xi^-}/\overline{\Lambda}$ ratio to be significantly larger in S-W and S-S collisions than in p-p interactions.

The advent of Pb beams at CERN gives us the opportunity of searching for a phase transition to a QGP in the interactions of truly heavy nuclei with larger reaction volumes. However it presents us with additional experimental problems due to the very high track densities. The main challenge is to reconstruct strange particle decays in this high multiplicity environment.

The WA97 experiment [4] aims to measure the spectra of hyperons and antihyperons ($\Lambda, \overline{\Lambda}, \Xi^-, \overline{\Xi^-}, \Omega^-, \overline{\Omega^-}$) produced in Pb-Pb interactions at 160 GeV/c per nucleon using the Omega Spectrometer at the CERN SPS. The principal aim is to compare the production of baryons carrying one unit of strangeness (Λ) with those carrying two (Ξ^-) and three units of strangeness (Ω^-). The possiblity of a comprehensive study of the spectra of various hyperon and antihyperon species constitutes a unique feature of the experiment.

The 1994 setup for WA97 is shown in fig. 1. The target was followed by three stations of multiplicity detectors: one scintillator station and two microstrip stations. The scintillators were used at trigger level to select central Pb-Pb collisions (typically 30% of the inelastic cross section). More accurate multiplicity information for off-line use is provided by the two microstrip stations, each sampling the multiplicity about one unit of rapidity, with 34% azimuthal coverage.

The silicon telescope is placed above the beam line, and is inclined to point back to the target. The angle is chosen in such a way as to have good acceptance for the decays of hyperons produced at central rapidity and $p_T > 0.5$ GeV/c. Each plane is 5 cm by 5 cm and the length of the telescope is 60 cm. For the 1994 Pb run the telescope started at 90 cm from the target (120 cm for the first part of the run) and

consisted of six doublets of silicon detectors (8 microstrip planes and 4 pixel planes). The pixel dimensions are 500 μm x 75 μm, and the four planes had a total of 300 000 channels. Additional lever-arm tracking was provided by a further doublet consisting of a plane of silicon pads and a microstrip plane at 180 cm from the target, and three planes of multi-wire proportional chambers with pad cathode read-out at 4 m from the target.

During November and December 1994 we obtained 60 million triggers of central Pb-Pb interactions and also took p-Pb data for comparison. Fig. 2 shows the display of a Pb-Pb event taken without magnetic field. The event is viewed looking down the telescope towards the target. The squares represent hits on the four pixel planes, and the straight lines represent the 40 fitted tracks. All tracks except two (shown by dashed lines) point back to the primary vertex, and no clean-up of non-associated hits has been performed.

Preliminary results from part of the 1994 Pb run are shown in fig. 3. Signals corresponding to $\Lambda, \overline{\Lambda}$ and K^0 are clearly seen, and the resolution of the silicon telescope is good. During 1995 we have recorded 200 million p-Pb events and will take Pb-Pb data during November and December.

REFERENCES

1. J. Rafelski and B. Müller, Phys. Rev. Lett. **48** (1982) 1066; **56** (1986) 2334.
   P. Koch, B. Müller and J. Rafelski, Phys. Rep. **142** (1986) 167.
   J. Ellis and U. Heinz, Phys. Lett. **262B** (1991) 223.
2. J. Rafelski, Phys. Lett. **262B** (1991) 333.
3. Proposal 275,this volume.
4. WA97 Proposal. N. Armenise et al., CERN/SPSLC 91-29, SPSLC/P263.

PUBLICATIONS

1. First Results from the 1994 Lead Beam Run of WA97.

   A.C. Bayes, J.N. Carney, J.P. Davies, D. Evans, P. Jovanovic, J.B. Kinson, K. Norman, O. Villalobos Baillie and M.F. Votruba (Birmingham) + Athens, Bari, Bergen, CERN,Collège de France, Genoa, Košice, Legnaro, Oslo, Padua, Prague, Protvino, Salerno, Rome and Strasbourg.

   Nuclear Physics **A590** (1995) 139c-146c.

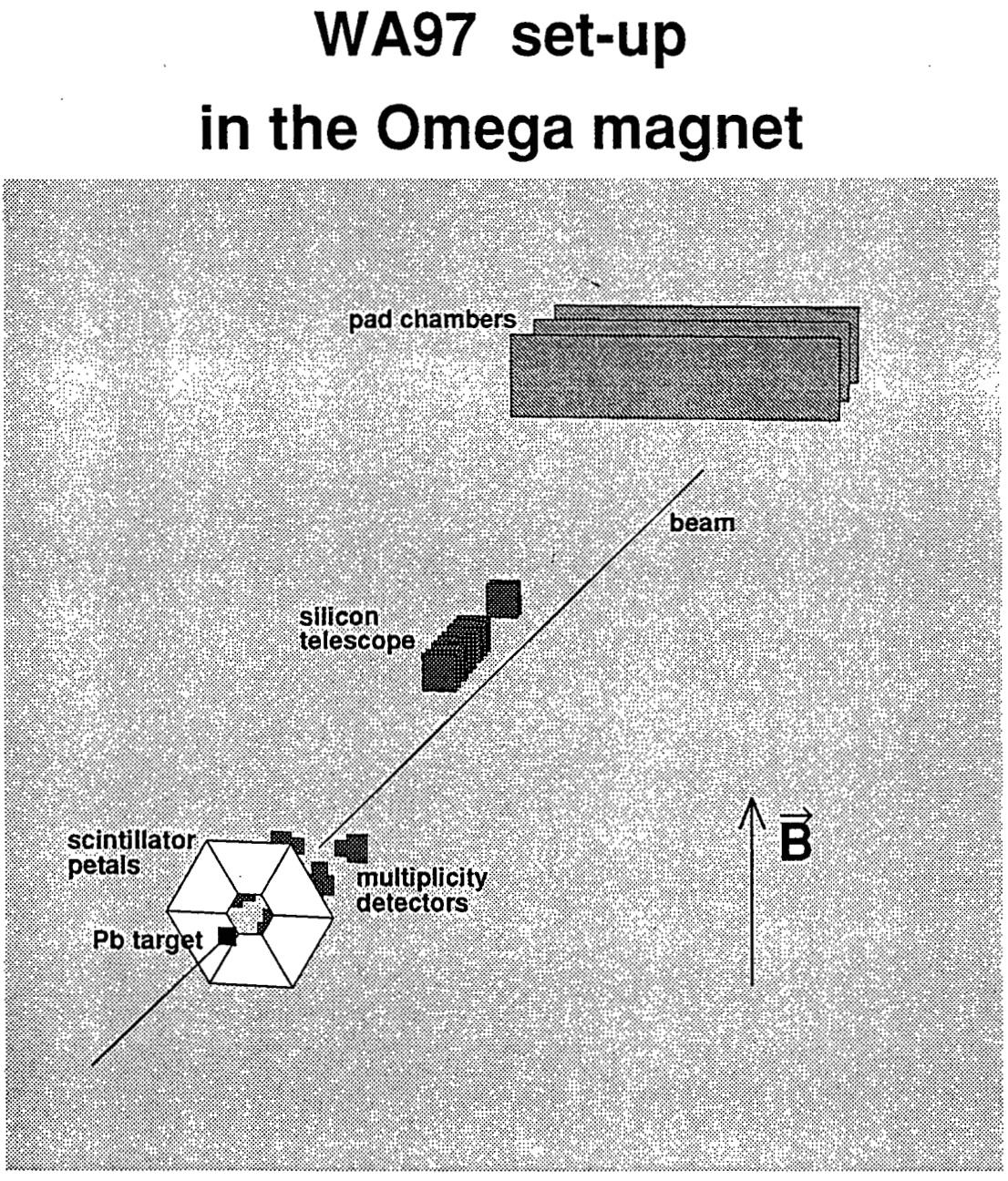

Fig. 1. Perspective view of WA97.

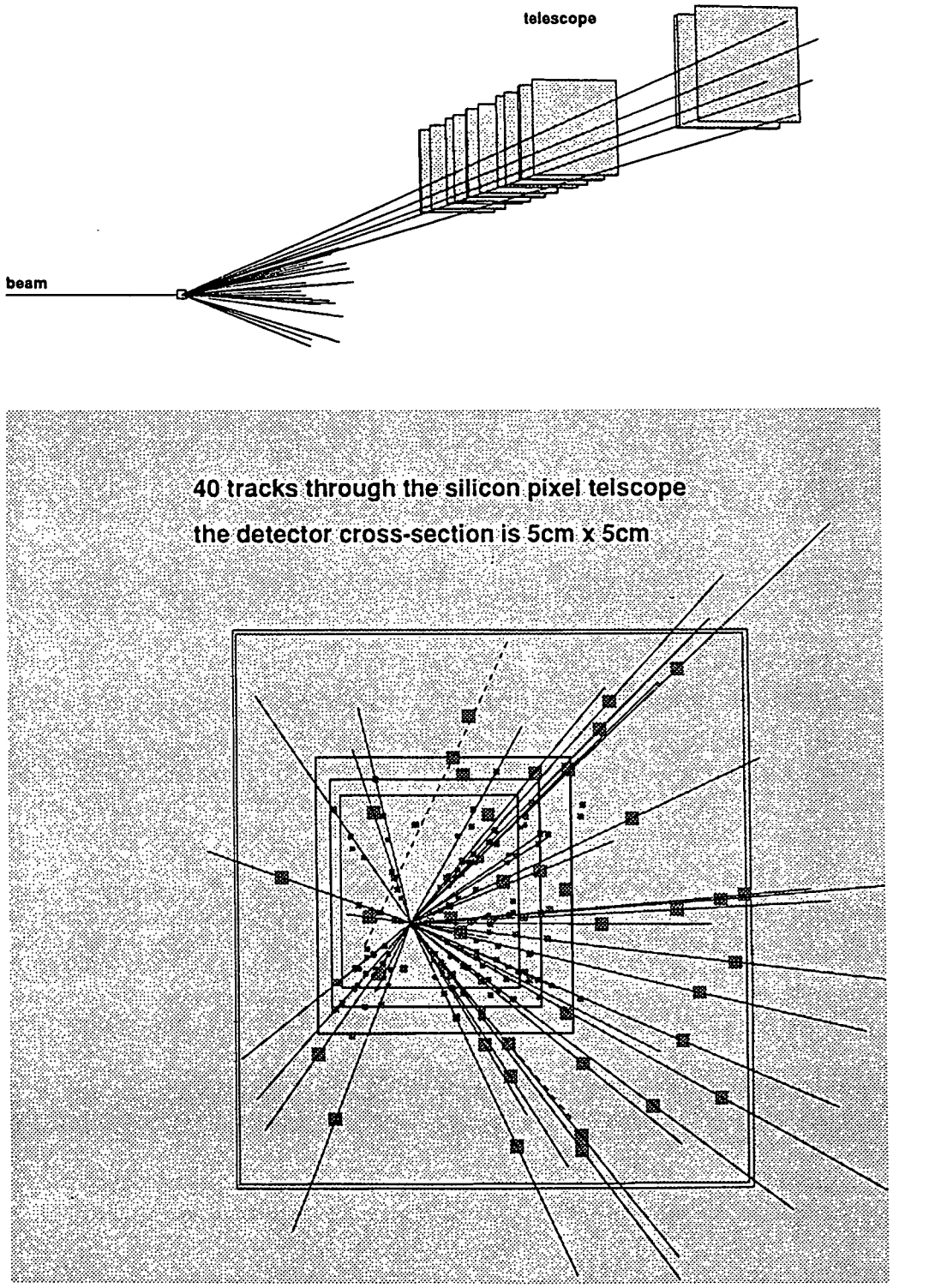

Fig. 2. A Pb-Pb event with 40 reconstructed tracks as seen by the 4 pixel planes. The magnetic field is off.

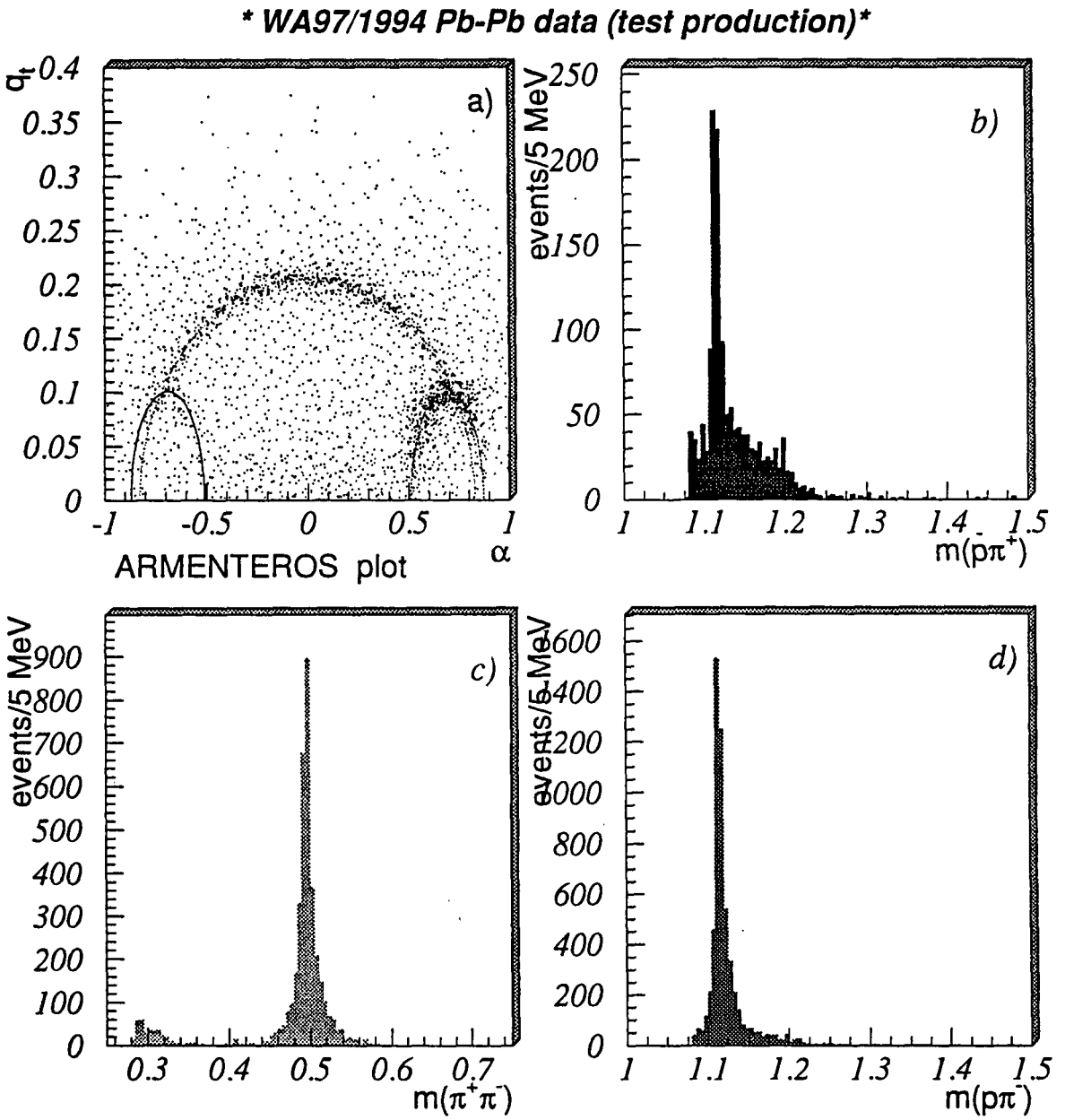

Fig. 3 Results from Pb-Pb test production data.

ANGULAR AND POLARIZATION CORRELATION COEFFICIENTS IN NEUTRON DECAY

Proposal FD286

ILL, Sussex, Glasgow, Rutherford Appleton Laboratory

Nuclear beta-decay is governed by two independent coupling constants; a vector coupling constant G_V and an axial coupling constant G_A. The conventional notation for the ratio of these constants is $G_A/G_V = \lambda$. The current experimental status of these numbers is that the absolute values of both have been determined to better than 1% accuracy by combining data on the neutron lifetime which provides a value for $G_V^2 + 3G_A^2$ [1], and the ft-values of pure Fermi superallowed beta-decays which yield a value for $|G_V|$ [2]. However to avoid uncertainties due to nuclear structure effects it is preferable to derive values for the coupling constants from data on neutron decay alone. To this end a number of rather precise measurements of the electron asymmetry coefficient in polarized neutron decay have recently been carried out. This parameter determines both the sign and magnitude of λ.

Unfortunately there is a conflict in the experimental data [2,3] which it is the objective of the present program to resolve. We proposed therefore to measure both the proton spectrum,which provides a value for $|\lambda|$, and the proton asymmetry coefficient in polarized neutron decay, which, like the electron asymmetry coefficient, determines both the sign and magnitude of λ. The proton asymmetry coefficient has not previously been measured. Both these measurements would be carried out using modified versions of the 5 tesla Penning trap apparatus used to determine the neutron lifetime [4].

In 1994 it was anticipated that the experiments to measure the proton asymmetry coefficient could begin in May 1995 on the polarized neutron beam PF1 at the ILL, Grenoble. However, following the four year shut-down of the reactor, a number of unexpected technical problems arose, as a result of which all experiments on PF1 were re-scheduled. Our program was allocated beam time in both the August-October cycle and in the November-December cycle, and the apparatus was therefore moved out to Grenoble in July. In the event, due to continuing difficulties with the beam, the first three weeks of the August cycle were not available and, during the second half of the cycle, there was only time to align the apparatus with the beam and have a single day's run with the cooled cryomagnet. With the start of the new cycle in November, although initially the experiment encountered some severe background problems which took time to resolve, it has been established that polarized neutron decays are recorded at the rate of about one per second, which is in line with the rate predicted in the original proposal. The supermirror polarizer-analyser combination and current sheet spin-flipper assembly have now been brought into full operation, and data collection on the proton asymmetry coefficient has begun, although in rather higher backgrounds than might have been anticipated.

The experiment has also been allocated beam time during the first half of the January-March cycle in 1996 to make up for the time lost in August, and there is every reason to expect that at least a preliminary measurement of the proton asymmetry coefficient can be completed during this period.

[1] Review of Particle Properties, Phys. Rev. D50 (1994) 1173.
[2] D H Wilkinson, Z. Phys. A248 (1994) 129.
[3] K Schreckenbach et. al., Phys. Lett. B349 (1995) 427.
[4] J Byrne et. al., Phys. Rev. Lett. 65 (1990) 289.

Publications 1994-1995

J Byrne, On the neutron lifetime and the weak coupling constants. Physica Scripta T59 (1995) 311.
J Byrne et. al., A revised value for the neutron lifetime measured using a Penning trap. Europhysics Letters (1995) (in press).

CHARMED BARYON STUDIES IN THE CERN HYPERON BEAM

CERN WA89 proposal 287

Bristol University – CERN Geneva – Genova University/INFN – ISN Grenoble
Max-Planck-Institut Heidelberg – Heidelberg University – Mainz University
Lebedev Institute Moscow

WA89 uses the Omega spectrometer in the CERN West Hall, with a special hyperon beam. This provides 10^5 Σ^- and 2.5×10^5 π^- per spill (2.5 s) at 330 GeV/c. The experimental layout is shown in figure 1. The incident Σ^- are selected on-line by 10 modules of transition radiation detectors. The beam strikes targets of copper and diamond (and the silicon detectors). The vertex detector consists of 29 planes of either 25 or 50 μm pitch. Since we are interested in charmed baryons, we must recognise hyperons and also protons and neutrons in the final state. The decay region is equipped with 40 planes of drift chambers and 32 planes of MWPC. This allows the identification of the $\Lambda \rightarrow p\pi^-$ decay. Protons, kaons and pions are recognised in the RICH detector, after the Omega spectrometer. Finally, there is a lead-glass calorimeter for π^0 and γ measurement and a hadronic calorimeter for neutrons.

Almost 500 million events were accumulated in the 1993 and 1994 runs. Analysis of these is continuing, to achieve maximum efficiency of charm reconstruction. During 1995 we published results on the lifetime of the Ω_c^0 seen in the $\Omega^-\pi^+\pi^-\pi^+$ and $\Xi^- K^-\pi^+\pi^+$ final states. Figure 2 shows the histograms of vertex separation for background and signal band events for the first of these; the combined result is

$$\tau(\Omega_c^0) = 55^{+13}_{-11}(stat.)^{+18}_{-23}(syst.)\ \text{fs}$$

This is the shortest lifetime of all charmed hadrons observed to date.

Publication since October 1994:

M I Adamovich *et al.*,
Measurement of the Ω_c^0 Lifetime
Physics Letters **B 358**, 151 – 161 (1995)

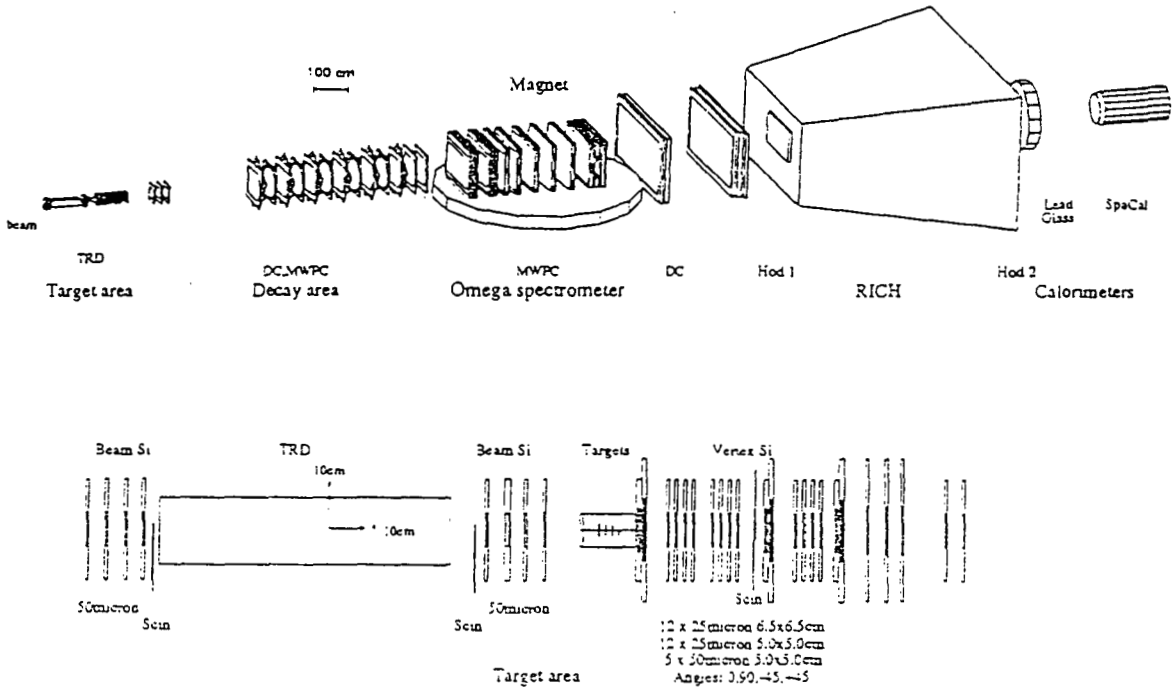

Figure 1

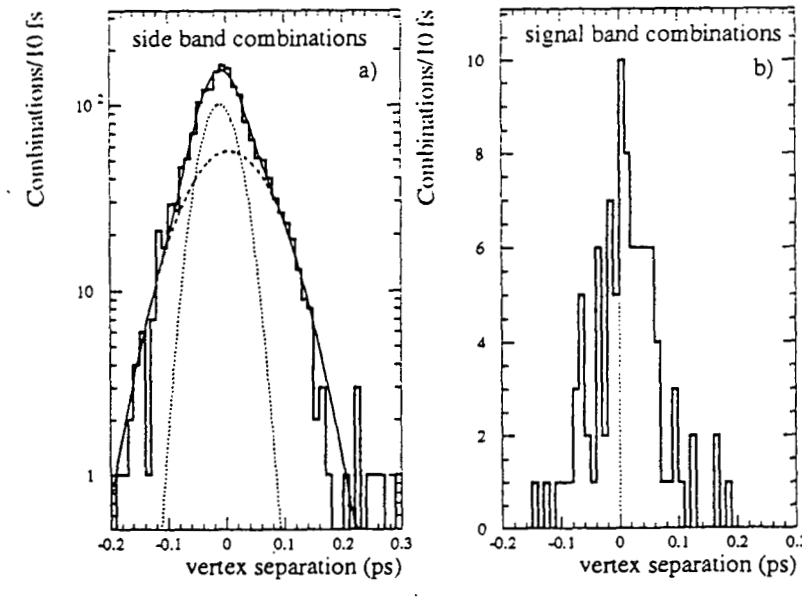

Figure 2: $\Omega^-\pi^+\pi^-\pi^+$ sample : vertex separation (ps) for a) background events, b) for signal band.

CENTRAL PRODUCTION OF MESONS USING THE CERN OMEGA SPECTROMETER AND THE GAMS 4000 ELECTROMAGNETIC CALORIMETER

WA102 Proposal 291

Annecy LAPP, Athens, Birmingham, CERN, Dubna JINR, IISN Belgium, Los Alamos LANL, Manchester, Protvino IHEP, Tsukuba KEK

The study of central meson production is motivated by the search for non $q\bar{q}$ mesons. QCD predicts that whole spectra of non $q\bar{q}$ mesons of different types (gg, ggg, $q\bar{q}g$ ...) should exist [1]. Although several candidates exist, no definite state has yet been identified. Central meson production is considered to be a promising mechanism for the production of these states. In particular, meson states decaying to ηs and η/s are of interest because glueball states are likely to decay preferentially into states with the emission of these particles [2]. Available statistics are low, owing to the difficulty in identifying exclusive final states involving these particles. The WA102 experiment [3] is a continuation of the program of study of central production of mesons initiated by WA76 and continued by WA91. The aim of the WA102 experiment has been to exploit the improvements in the Omega data acquisition system to obtain very high statistics data samples, suitable for detailed spin analyses of meson resonances.

The first run of the experiment, performed in the summer of 1995, was aimed at collecting high statistics data with good acceptance for channels involving neutral particles. In order to achieve this, the Omega Spectrometer was run in conjunction with the GAMS-4000 calorimeter. This combination combines the best features of the WA76/91 and NA12 programmes: high rate data-taking with an effective central trigger and proven charged particle tracking, and excellent detection of states with multiple photons. As a result of the ability of the combined detector to measure final states with both charged and neutral particles, several thousand centrally produced $\eta\eta\prime$ events are expected, allowing the mass spectrum for this final state to be investigated thoroughly. The previous world total for events in this channel was about 100.

The layout for the experiment is shown in figure 1. The direction of the incident beam is measured using a system of 20μ pitch silicon microstrips. The beam is incident on a 60 cm. H_2 target. The trigger for central production requires a "fast" proton and a "slow" proton. The "fast" proton must hit the two downstream counters A1 and A2, and its direction after deflection in the Omega field is measured using eight planes of 25μ pitch microstrips plus 1 mm pitch MWPCs. The "slow" proton trigger requires a track to give hits in two planes of scintillators (BOX and SPCL, SPCR, depending on direction) and in two planes of MWPCs from the eight placed between the scintillators. At the

same time there should be no other activity in the box counter encircling the target, *i.e.* only one track in the rapidity region corresponding to the slow proton. Tracks at mid-rapidity are measured using the Omega MWPCs, and the photons using GAMS-4000, with the OLGA electromagnetic calorimeter for large-angle photons. A hadron calorimeter behind GAMS is used to veto hadron showers in the GAMS calorimeter.

Some 200 million triggers were obtained in the 1995 run. Preliminary event reconstruction has been performed for about 40% of the data sample so far. A preliminary study of the reaction

$$pp \rightarrow p_f(\pi^+\pi^-\gamma\gamma\gamma\gamma)p_s \qquad (1)$$

with two γs constrained to form a π^0 shows that GAMS and Omega are both working properly. The $\pi^+\pi^-\pi^0$ effective mass spectrum for events where the $\gamma\gamma$ effective mass is in the η band is shown in fig. 2a Peaks corresponding to η and ω production can be seen. Figure 2b shows the $\gamma\gamma$ spectrum if the $\pi^+\pi^-\pi^0$ system lies in the η band, after removal of the π^0 peak. Again, a clear η peak is seen. The clear peaks in these two spectra indicate that in these preliminary data GAMS and Omega are already quite well matched. Finally, fig. 2c shows the scatter plot of $M(\pi^+\pi^-\pi^0)$ vs $M(\gamma\gamma)$ for this reaction, where an accumulation corresponding to $\eta\eta$ events can be seen. Further tuning is in progress.

The second data taking period for WA102 takes place in 1996; the Omega Spectrometer will be closed at the end of 1996, making this the final data taking period for the experiment. In view of the topical interest in states with decays to kaons, in particular the need to establish the spin of the $\theta/f_J(1720)$[4] we propose to use the C1 Cerenkov counter with a CO_2 filling downstream of the Omega magnet, in order to have kaon identification for charged tracks. The GAMS and OLGA electromagnetic calorimeters would also be used, but set further back from the target. This layout has been chosen because it minimizes both the amount of material in front of GAMS and the loss of geometrical acceptance for the calorimeters.

References

[1] M. Chanowitz and S. Sharpe, Nucl. Phys. **B222** (1983) 211.

[2] S.S. Gershtein et al., Z. Phys. C **24** (1984) 305.

[3] WA102 proposal, J.P. Peigneux et al., CERN/SPSLC 94-22 P281, August 1994.

[4] M.R. Pennington, Proc *Hadron '95 Conf.*, Manchester, July 1995, to be published.

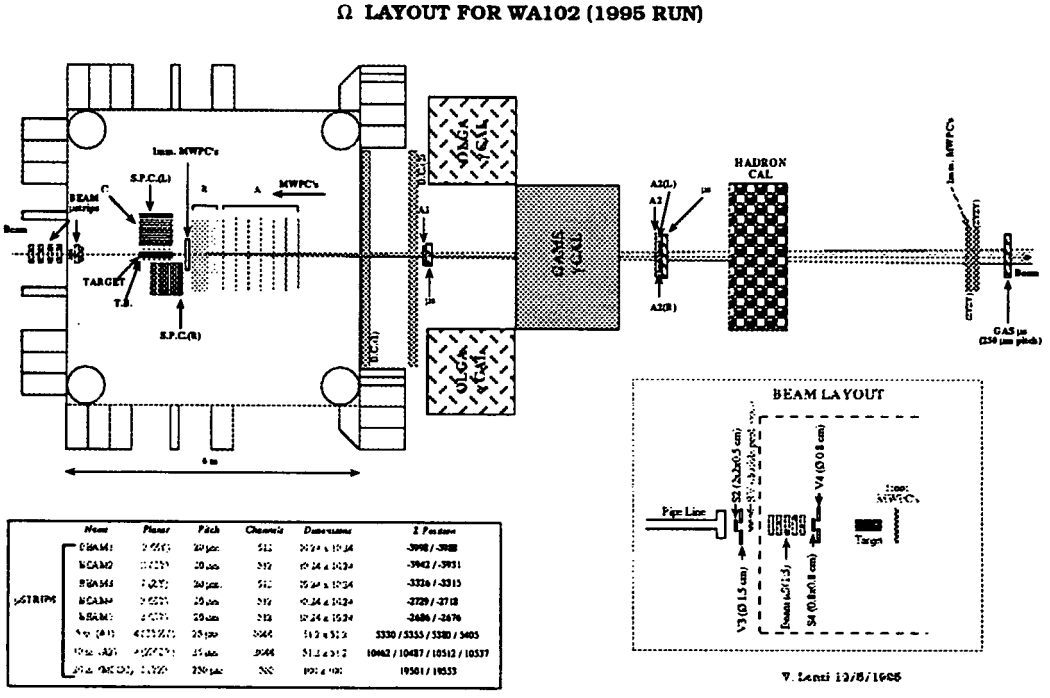

Figure 1: Layout of the WA102 experiment

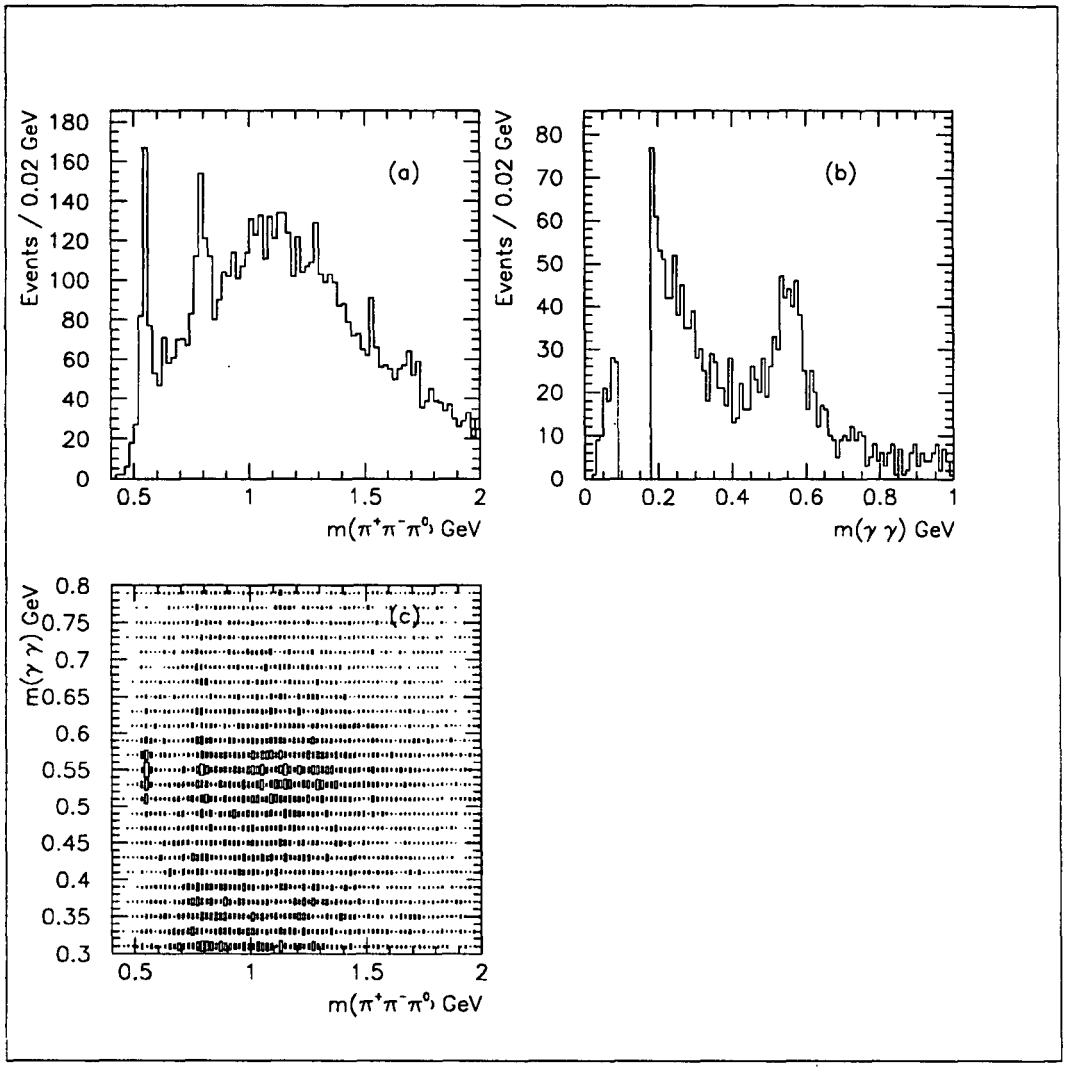

Figure 2: Reaction $pp \rightarrow p_f(\pi^+\pi^-\gamma\gamma\gamma\gamma)p_s$, (a) $M(\pi^+\pi^-\pi^0)$ for events with $M(\gamma\gamma)$ in η band, (b) $M(\gamma\gamma)$ for events with $M(\pi^+\pi^-\pi^0)$ in η band, after removal of π^0 band, and (c) scatter plot of $M(\gamma\gamma)$ vs $M(\pi^+\pi^-\pi^0)$.

BaBar - Physics at the SLAC B factory

Bristol, Brunel, Edinburgh, Imperial College, Lancaster, Liverpool, Manchester, Queen Mary and Westfield College, Royal Holloway College, Rutherford Laboratory

The principal aim of the BaBar experiment is to make precision measurements of CP violation in decays of the B^0 meson, specifically the unitarity triangle relations between the CKM matrix elements via the angles α and β and the side V_{ub} of the triangle. The standard model makes predictions for these quantities from measurements of other CKM matrix elements and any new physics will invalidate these predictions. Hence the experiment is a critical probe of the standard model. Moreover CP violation appears to be an important element in understanding the baryon asymmetry of the universe and the current lack of an explanation of the asymmetry through this mechanism provides added incentive for these measurements.

The experiment will be performed at SLAC where the asymmetric collider PEP-II is being built. In this machine 9 GeV electrons will collide with 3.1 GeV positrons leading to Y(4S) production at a $\beta\gamma$ of 0.56. The initial luminosity will be 3×10^{33} $cm^{-2}s^{-1}$ rising ultimately to 10^{34} $cm^{-2}s^{-1}$. The coherent B^0B^0 pair produced in the decay of the Y(4S) are given a Lorentz boost such that they travel a measurable distance before themselves decaying. CP violation modifies the exponential decay distribution of the B decays by a factor which depends on the difference of the proper times of the two B decays. Different decay modes of the B meson measure different angles of the CP triangle. This feature, together with the small branching ratio of any single decay mode, requires that as many different final states as possible are detected. With 30 fb^{-1} of data expected after three years of running BaBar will measure the angles α and β with a precision better than 0.1. In addition to these CP violation measurements the high luminosity and the asymmetry of the beam energies will allow other important physics studies including rare B decays, charm and tau physics, and two-photon physics.

The proper time difference between the two B decays will be measured using a low-mass silicon vertex detector consisting of five doubled sided cylindrical layers. The vertex resolution in the z direction is typically 50 μm for the most important B decay modes. Charged particle momenta will be measured in a drift chamber of 40 planes in a 1.5T magnetic field. Charged particles will be identified using a ring-imaging Cerenkov detector in the barrel region and a threshold detector in the forward endcap region. Muons and neutral hadrons will be identified using 21 planes of resistive plate chambers between the iron plates of the magnetic flux return.

The need to reconstruct CP eigenstates containing π^0s makes excellent electromagnetic calorimetry essential to the experiment. In particular a high efficiency and excellent energy resolution for photons with energy below 100 MeV/c is required to allow reconstruction of final states containing several π^0s. BaBar has chosen a highly segmented electromagnetic calorimeter of 6780 Thallium-doped CsI crystals to satisfy these requirements. The design resolution is for a stochastic term of 1% and a constant term of 1.2%. The BaBar-UK groups are responsible for the front-end electronics, trigger and DAQ for the whole electromagnetic calorimeter and for the design and construction of the calorimeter endcap. The calorimeter barrel is being built by groups from Dresden and SLAC.

The endcap calorimeter will be built in two C-shaped halves each containing ten modules with 45 crystals (see figure) arranged to have a projective geometry. The crystals will be 32 cm long (17.5 radiation lengths) and approximately 5 x 5 cm in cross-section at the front and slightly tapered. Each crystal will be held in a separate compartment of a honeycomb structure. The design of the mechanical structure is now essentially complete. Orders for the crystals are expected to be placed by the end of 1995. During 1996 a prototype module will be built and construction of the final calorimeter will begin in 1997.

In October 1995 a prototype consisting of 25 crystals was built and a very successful test was carried out in a mixed pion and electron beam at PSI, Zurich by the UK, Dresden and SLAC groups. The beam momentum covered the range 100 to 500 GeV/c with good separation of electrons and pions at momenta centred around 100, 215 and 405 GeV/c. The principal aims of the test were to measure the energy and position resolutions of the detector and to determine the effects of different amounts of material between individual crystals. Analysis of these data is currently in progress. Meanwhile further laboratory tests to determine optimum wrapping procedures and to understand the radiation tolerance of the crystals are continuing in the UK and elsewhere.

An amplifier with two gain stages of unity and 32 is mounted on the rear of each crystal. A custom IC receives the two analogue signals and provides two additional gain stages giving an output which is sent to an ADC close to the crystal at one of four possible gains. Readout modules in the counting house receive the data from the ADC, store them in a VRAM buffer for later analysis and form trigger sums for the calorimeter trigger. The design of the electronics is now essentially complete and a single channel demonstrator will be built in 1996.

Teams to write the event reconstruction program and the definitive simulation program began to form in 1995 with UK participation. Both will be written using Object Oriented techniques with C++ as the recommended language. UK physicists have continued studies of different physics channels with particular emphasis on the $B^0 \rightarrow J/\psi$ modes which were our contribution to the physics chapter of the Technical Design Report.

During 1995 the project has made much progress at a political and financial level. The Technical Design Report was submitted in March 1995 and has now been approved by US committees responsible for considering the technical design and the costings. In the UK the PPESP has recommended PPARC support for the UK groups at an initial level of £2.472M for capital items with an additional sum of £768k in 1997 if the financial circumstances at that time permit. Financial approval has now been obtained in a majority of the participating countries. The current schedule is for the detector to be completed by 31 December 1998 and for data-taking to begin in spring 1999.

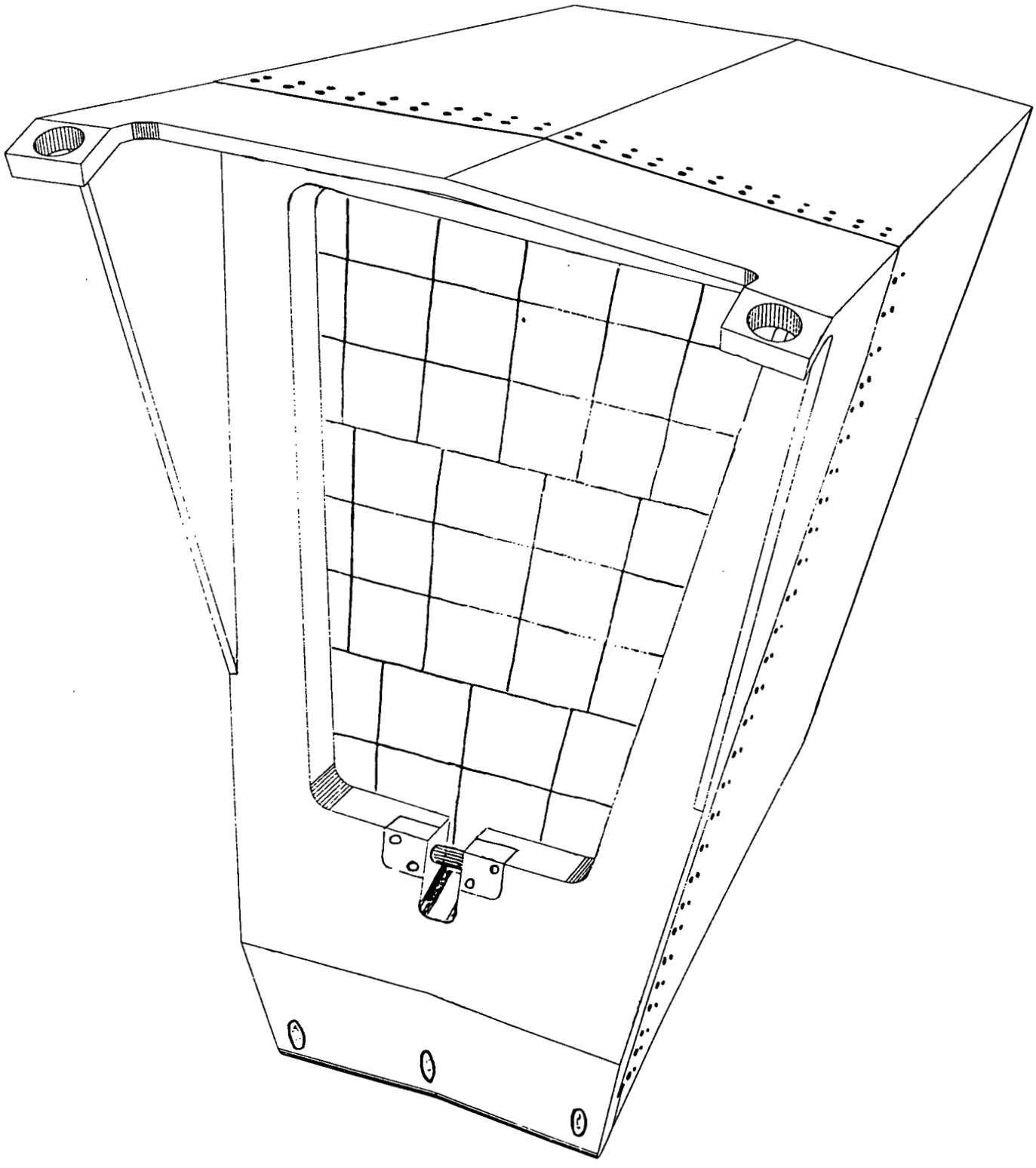

A module of the forward endcap calorimeter.

The ALEPH Experiment at LEP

Annecy; Barcelona; Bari; Beijing; CERN; Clermont-Ferrand; Copenhagen; Demokritos; Ecole Polytechnique; Edinburgh; Florence; Florida; Frascati; Glasgow; Heidelberg; Imperial College; Innsbruck; Lancaster; Mainz; Marseilles; MPI Munich; Orsay; Pisa; Royal Holloway and Bedford New College; Rutherford Appleton Laboratory; Saclay; Santa Cruz; Sheffield; Siegen; Trieste; Wisconsin.

1 Introduction

This year LEP1 running at the Z resonance officially ended on October 5th. The collider was operated at this energy in a new multi-bunch mode corresponding to 4 trains of 3 bunches each 277ns apart. After an initial period of running at the peak of the resonance (91.2 GeV) to establish stable conditions, the remaining time was allocated to a three-point scan over the resonance with the principal aim of measuring the Z width with the best possible precision ($\sim$ 2 MeV). Altogether, ALEPH recorded 35.7 nb^{-1} before and during the scan which is 92% of the integrated luminosity delivered by LEP: the best achieved of any year to date. Due to the new mode of running and the scan, the accumulated Z statistics were significantly less than 1994. However, the total number of off-line hadronic Z decays from all data collected since 1989 is now expected to be about 4.5 million.

Then, after a short shutdown to install more superconducting cavities LEP declared stable colliding beams for physics at a CM energy of 130 GeV on October 31st. Dubbed LEP1.5, this event heralded the start of the LEP2 programme and the excitement of a new energy frontier for e^+e^- physics was quite evident in the control rooms! Subsequently, the energy was raised further to 136 GeV and by the end of running for 1995 ALEPH had collected 6.2 nb^{-1} at the higher energies with an efficiency of 97.9%! This was due to the superbly low backgrounds in the LEP machine as well as the excellent functioning of the detector. All the precautions made to cope with unforeseen high backgrounds were not required even when the machine achieved luminosities of $2.6 \times 10^{31} cm^{-2} sec^{-1}$.

During the above short shutdown, ALEPH removed its old Silicon micro-vertex detector and installed a completely new one with a more uniform thickness in ϕ, improved angular coverage in θ, and radiation hard electronics. It was intended as a trial run since a quarter of the detector modules (from Italy) were still not available for installation. Working for the first time in this area, UK groups played a major rôle in the provision of this detector. The trial turned out to be extremely successful and the missing parts will be added next year before running starts in June 1996.

Over the past year the other long-standing apparatus commitments of the UK groups have been maintained: namely to the inner tracking chamber (ITC), the electromagnetic calorimeter endcaps (ECAL), the second level trigger, parts of the TPC

laser system and to which will now be added the front-end electronics of the new vertex detector. The main DAQ-VAX computers have been replaced by a VAX-ALPHA cluster which involved significant UK effort. Overall, this is a large and continuing responsibility, carried out increasingly by heavy commuting rather than LTA. Also, the UK groups continue to play a very substantial rôle in the running of the experiment especially run co-ordination, apparatus co-ordination and shifts. More complete details of these activities are given in the following sections.

Since the last report, ALEPH has published a further 19 papers and contributed several written papers to International Conferences in Brussels and Beijing based on physics analyses of LEP1 data. Also, five UK physicists have given presentations at International Conferences. This report will focus on analyses completed and in progress since the major report presented to the UK PPESP in April.

2 Experimental Commitments

2.1 New Vertex Detector (Glasgow, Imperial, RAL, Royal Holloway)

The basic building block of the new detector is a "module" consisting of three double-sided silicon wafers glued end-to-end. The total area is approximately $5 \times 20 cm^2$. The strips running along the length (ϕ) are wire-bonded together to form individual readout elements on one side of the detector whereas the transverse strips (z) are connected via fine tracks on a "kapton" film to the readout electronics similarly mounted on the other. There are 1021 longitudinal strips and 960 pairs of transverse strips read out by 128 channel MX7-RH amplifier multiplexer chips mounted on identical hybrid assemblies. These are glued to each side of a ceramic support which in turn are also glued to the silicon. Altogether 1600 chips were selected and tested at RAL of which approximately 900 were found satisfactory after mounting on the hybrids. Some 7000 bonds per module were necessary to connect the strips to the hybrids. To date, 26 of the 48 modules required to build the detector have been assembled and wire-bonded by automatic machines at RAL, and 4 remain to complete our recently agreed contribution to the fabrication. Italian groups are responsible for the remainder. Tooling for these operations was designed and produced at Imperial for all the groups.

Following the design of the hybrid printed circuit in the Glasgow group, the first production batch was made in the microfabrication laboratory at CERN using a Dupont-photosensitive technique. GEC, Lincoln had been unable to achieve the fine-line resolution necessary and significant delays had been incurred. However, they have now succeeded in making 50 units using a comparable technique and these are being used to complete the production. RAL have surface mounted and wire-bonded all components on to these hybrid PCs.

Twenty-four of the modules have been tested and mapped at Imperial College. Following basic signal-to-noise measurements performed with a radio-active source. Systematic functionality checks of all channels were made by scanning a finely focussed light spot across the detectors. The average number of defective channels was found to be below 1% after curing "pin-hole" problems due largely to "shorts" in the capacitor chips coupling the detector strips to the electronics. Glasgow have so far tested 2

modules in a similar facility.

The online software for the new VDET was completed by an RAL physicist early in the year and incorporated very successfully into the ALEPH data acquisition system whilst the old VDET was in operation. In addition, this software was used extensively to test the detector elements before final installation. This effort was rewarded by a very smooth first operation at 130 GeV inside ALEPH. The VDET data were soon incorporated into the full data-stream and off-line analysis of tracks from real Z events has enabled a satisfactory local alignment of the detector faces to be achieved. Figure 1 shows an early event with hits recorded as expected from all tracks reconstructed by the ITC and TPC. Contrary to expectation, the new detector is already providing invaluable input into the physics being derived from the first high energy run.

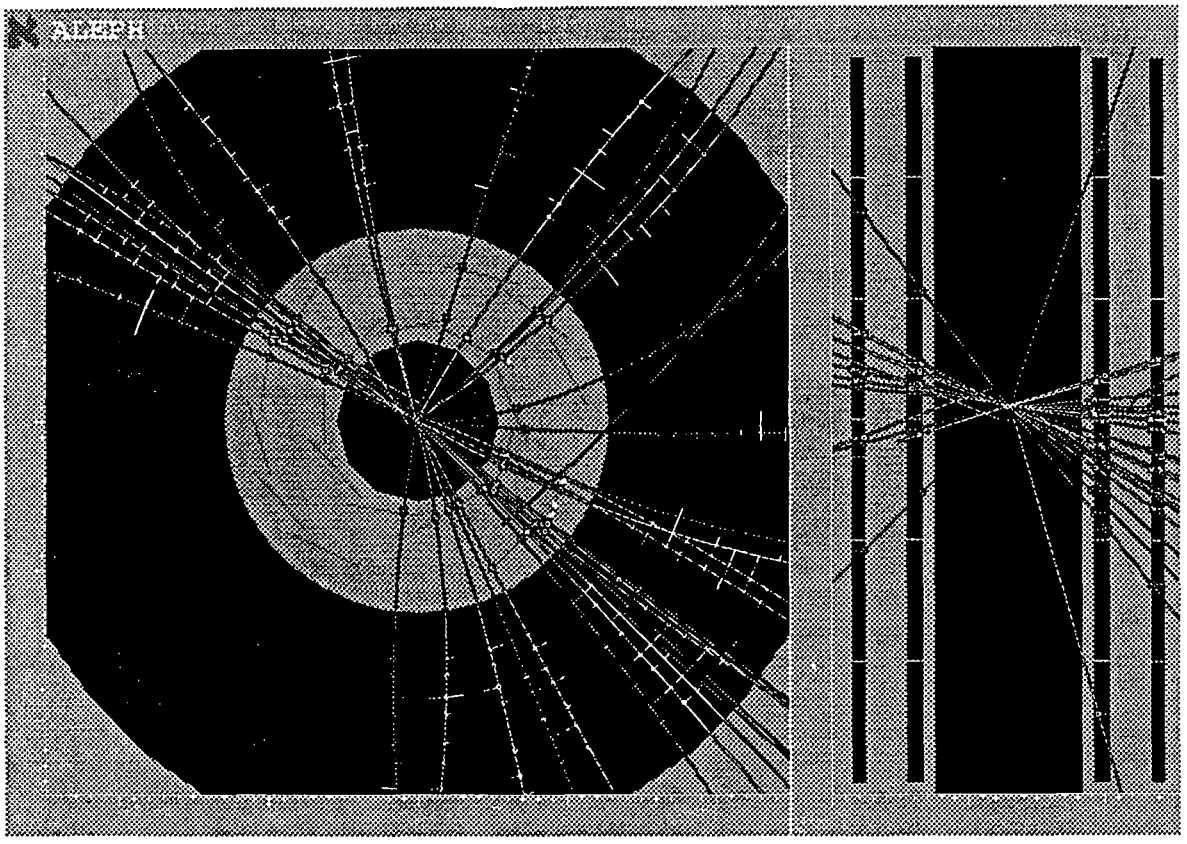

Figure 1: Reconstructed tracks using VDET hits.

2.2 TPC Laser System (Glasgow)

The TPC laser calibration system is used routinely to monitor the electron drift velocity in the TPC gas, and to determine the track distortions caused by inhomogeneities in the TPC electric field and the solenoid's magnetic field. The Glasgow group are responsible for maintaining the laser, and parts of the beam transport, as well as analysing most of the calibration data. This year Glasgow students have played a major rôle in perfecting the regular operation of a laser trigger during normal data taking. Figure 2 shows a

Laser Calibration event recorded during the 130 GeV run. It has been shown that precise monitoring and tuning of TPC parameters can continue despite the paucity of multi-track events at LEP2. This means that valuable time at high energy will not be compromised by the need to run often at the Z for calibration purposes.

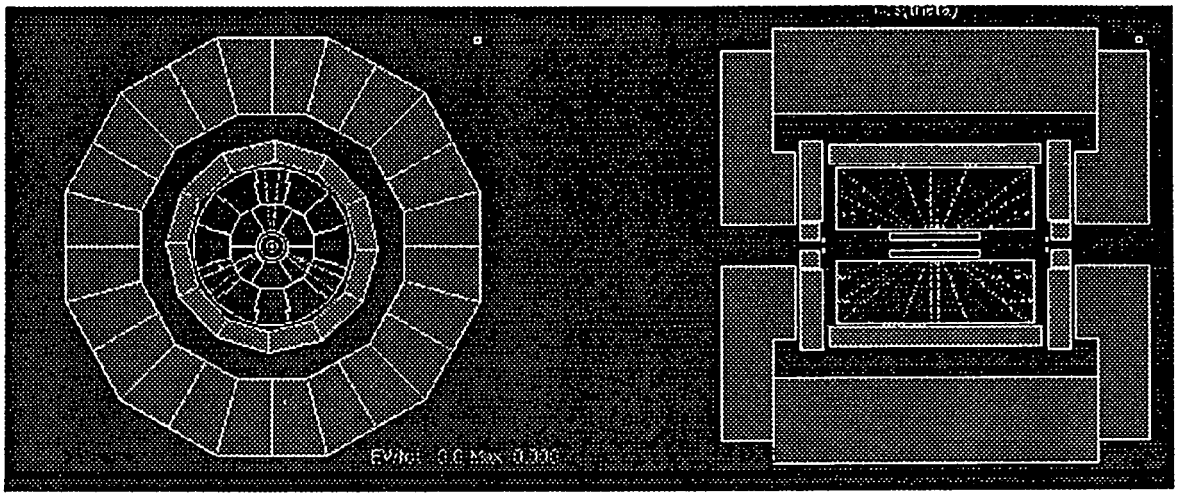

Figure 2: TPC laser calibration event.

2.3 Inner Tracking Chamber (Imperial College)

The Inner Tracking Chamber has continued to perform excellently during 1995. At LEP2 the ITC trigger may be even more vital than at LEP1 as the backgrounds in the calorimeters at the highest energies are still unknown. Plans for operating the chamber with only the outer layers on at the start-of-fill were set up as well as reducing maximum current limits in the chamber. So far, the LEP background has been very satisfactory and no problems have arisen requiring any permanent change in conditions.

Preparations are well in hand for the insertion of the mask and shield during the coming winter shutdown. An IC engineer is currently based at CERN leading the removal operations of the ITC which will then be used to support these devices symmetrically round the beam pipe.

2.4 2nd Level Trigger (Royal Holloway)

The second level trigger has continued to perform with high reliability during 1995. Before the 130 GeV run, a special study was made of the effect of reducing the TPC gas gain on Level 2 track finding efficiency. This might be necessary if backgrounds are very high. A new set of threshold conditions for the Level 2 electronics were established and are ready for implementation if required.

2.5 ECAL endcaps (Glasgow, RAL)

The marked improvement in performance and reliability in 1994 has continued this year fully justifying the replacement of the front-end electronics by monolithic chips.

However, coherent noise effects are still a problem occasionally, and are very difficult to trace since they disappear when the detector is opened for maintenance. Recently, new diagnostic cards have been added to aid in the search for the origin of these transients.

2.6 New Small-Angle Luminosity Monitor (RAL, Lancaster)

An upgrade of the ALEPH Bhabha calorimeter (BCAL) has been proposed. The BCAL consists of four small calorimeter modules positioned $\pm 7.7m$ from the interaction point at the centre of ALEPH, and monitors the rate of low-angle Bhabha scattering to provide an online measurement of the luminosity. With the upgraded detector, the accuracy of luminosity monitoring will be improved and it will also be possible to use BCAL signals as possible low angle tags of $\gamma\gamma$ events.

The new BCAL will have a larger volume, and therefore increased acceptance. With double the number of sampling layers and a layer of finely-segmented silicon pads, it will also have improved energy and position resolution. Whereas previously the BCAL has always operated independently of the main ALEPH detector, a new readout and DAQ system for the BCAL will allow its signals to be incorporated in the ALEPH data stream and associated with ALEPH-accepted events. Hence it will be possible to use BCAL information in $\gamma\gamma$ events to identify very low angle lepton tags - these correspond to low virtuality of the emitted photon and this kinematic region is currently of great theoretical interest.

The BCAL upgrade is the responsibility of the Barcelona group in ALEPH, but the detector design and readout scheme have been devised with input from RAL and Lancaster physicists to optimise the detector for $\gamma\gamma$ physics.

3 Physics Analyses

The analyses of LEP1 data continue to be organised in 5 areas: namely electroweak physics (couplings of the Z), τ physics (decays and polarisation), QCD including $\gamma\gamma$ interactions, Searches and Heavy Quark physics. The latter topic has been subdivided into (i) properties of the b hadrons and (ii) the electroweak couplings of b quarks to the Z. One senior UK physicist still coordinates the remaining Searches studies and another is a member of the Editorial Board which oversees the publication of all papers. Work in progress is described below where there has been significant UK involvement in the last months since the PPESP review.

For several months preparations have been made for the analysis of the events expected at 140 GeV. UK physicists have been involved in this work especially in QCD, Electroweak and Searches.

3.1 Heavy Flavour physics

Measurement of $R_b = \Gamma(Z \rightarrow b\bar{b})/\Gamma(Z \rightarrow hadrons)$ remains one of the most challenging, but potentially most rewarding results which can be extracted at LEP1. A strong team from Imperial is still very active in trying to push the accuracy on this quantity significantly below the 1% level to exploit the current 3.8σ discrepancy reported with the Standard Model prediction at the summer conferences. One of the most important

methods of identifying $b\bar{b}$ decays relies on "impact parameter tagging" and a student at Imperial has succeeded after much painstaking work in sorting out problems in the simulation of the vertex detector performance on a year-by-year basis. After reprocessing all the data affected, it is hoped to improve on the result reported at Beijing which was:

$$R_b = 0.2187 \pm 0.0022(stat) \pm 0.0025$$

The alternative heavy flavour tag is a high p_t lepton. An Imperial RA has now completed the measurement of the branching ratios for $b \rightarrow lepton$ and $b \rightarrow c \rightarrow lepton$ so reducing the systematic uncertainty in the R_b determination.

An equally important heavy flavour electroweak quantity is the forward-backward asymmetry in $Z \rightarrow b\bar{b}$ decays which is likely to remain as the most sensitive LEP determination of $\sin^2\theta_W$ and hence the Higgs mass. Using both "lifetime tagging" and hemisphere charge algorithms to construct the b quark charge and direction a Glasgow/Lancaster team lead a major part of this effort aimed at reducing the systematics in the "tagging" efficiency when all '92 to '94 data are combined. Currently when the independently measured lepton analysis is combined with the "lifetime" result, the ALEPH value for A^b_{FB} is 0.0953 ± 0.0080 at the Z peak.

A member of the Imperial group has also produced a new measurement of the mean b hadron lifetime using the 3-d impact parameter of high p_t leptons coming from semileptonic b decays. The data sample is 1.5 million hadronic Zs collected from 1991-1993 with the full power of the ALEPH vertex detector operational and the benefits of the excellent lepton identification of ECAL over the full solid angle. Figure 3 shows the impact parameter distribution obtained. The value of $1.533 \pm 0.013 \pm 0.022$ psec, which was presented at the 1995 summer conferences, has been sent for publication.

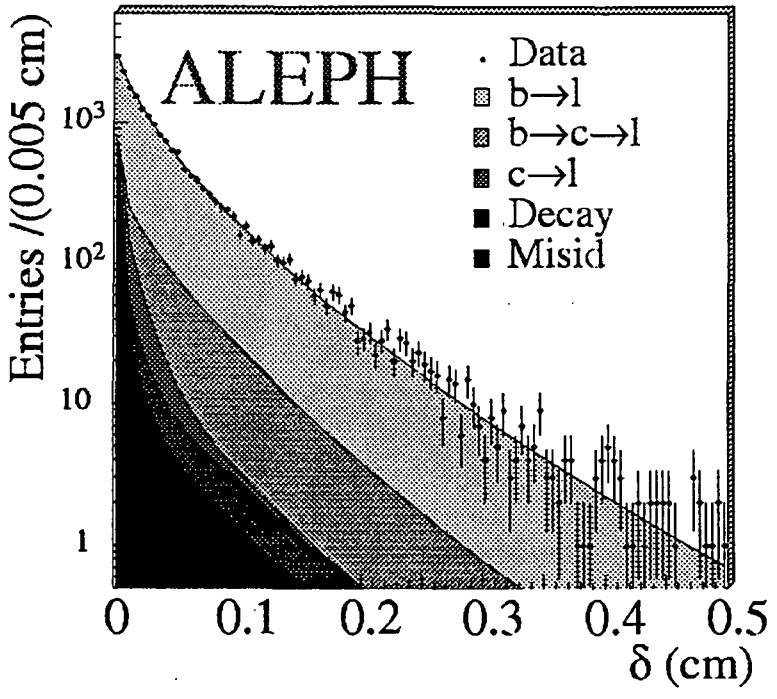

Figure 3: Impact parameter distribution.

Imperial group members have been investigating the degree to which it is possible to establish the proportion of b quarks produced in Z decay resulting from B^{**} resonances and, in particular, which of the four predicted states are formed. Along with the other experiments ALEPH has shown direct evidence for B^{**} production by looking at the inclusive spectrum of the soft pion from the B^{**} decay. However, it is very difficult with this measurement to separate the components of the signal. The only realistic way to do this is to exclusively reconstruct the $B^{**} \rightarrow B\pi$ system and this in turn demands a substantial clean sample of fully reconstructed B states. ALEPH presented a paper to the Brussels conference from an analysis of 186 fully reconstructed charged B's and 198 neutral B's including a background of $18 \pm 5\%$. After selecting *right-sign* tracks which could only have originated from the decay of a resonance, a narrow structure is observed above background with a mass of $5703 \pm 14 MeV/c^2$ and a narrow width (Figure 4). There is also a hint of a broader structure at lower mass. The total production fraction is estimated to be $30 \pm 8\%$. It has also been shown that a B-tag based on a $\pi^{\pm}$ with the highest longitudinal momentum relative to the B direction is efficient and may supplement the armoury of tags used in CP violation and mixing studies in the future.

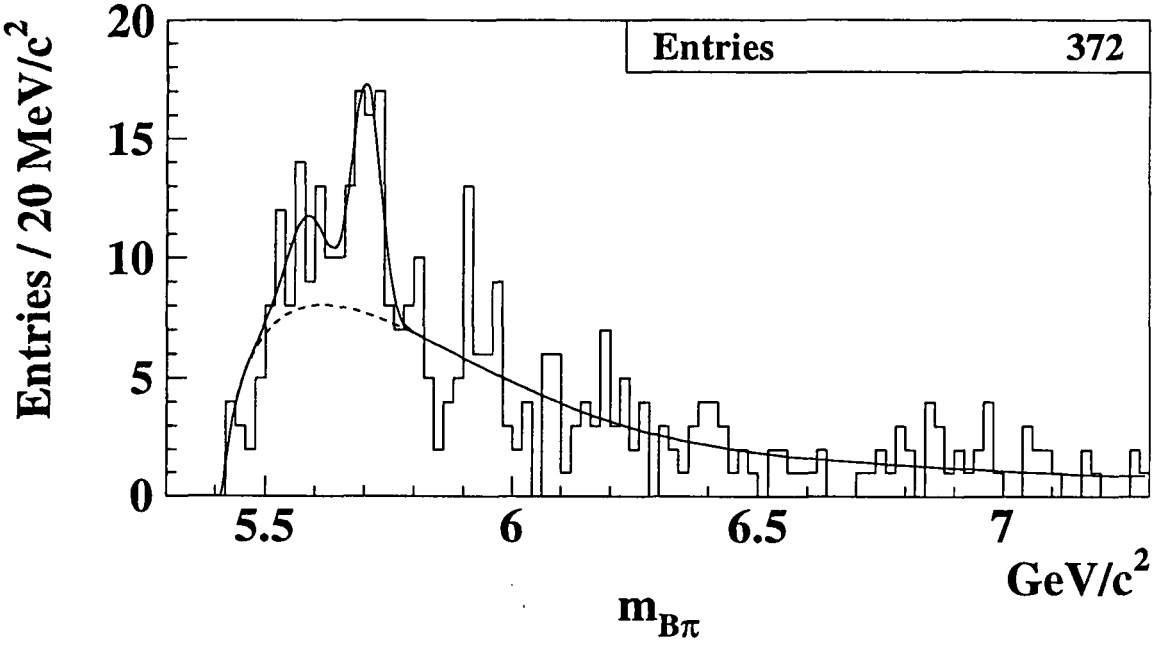

Figure 4: The right-sign $B\pi$ mass distribution.

3.2 Other Electro-weak physics

The propagation of initial quark charges to their final state particles has been long studied in ALEPH with the active involvement of the Glasgow group. Momentum weighted charge estimators are used to determine the charge of the outgoing primary quarks and hence enable the mean forward-backward asymmetry of all quark-antiquark states from the Z to be determined. This provides a sensitive measurement of the

electroweak mixing angle. Differences between the individual light quark charge values have been determined using hadronisation models, constrained by better measurements of inclusive identified particle production. A final draft paper is now almost ready including data off-resonance collected up to the end of 1993 with the result:

$$sin^2\theta_W = 0.2323 \pm 0.0010 \pm 0.0010$$

which is the most accurate at LEP from this kind of analysis.

The RAL group have continued to analyse the single photon counting process where the only observed particle in an event is a solitary photon with at least 1.5 GeV energy. In the Standard model this photon is emitted from the incoming electrons and tags the s-channel Z and the t-channel W exchange processes to neutrino pairs. All data up to the end of 1994 have been analysed to yield 1335 candidate events. With the addition of the SiCAL luminosity calorimeter in 1993, the background from other processes is now very low. Accepting the Standard Model values for the $W.Z$ interference cross section through the resonance region, the number of light neutrino families by this *direct* method is found to be:

$$N_\nu = 2.97 \pm 0.09 \pm 0.11$$

in excellent agreement with the well known more precise result of the indirect method. However, the variation of the measured cross section through the resonance region (see Figure 5) deviates in shape from the Standard Model prediction for three neutrino families as described by the current Monte Carlo generators. Further studies are in progress to understand this phenomenon as well as the new results at 130 GeV.

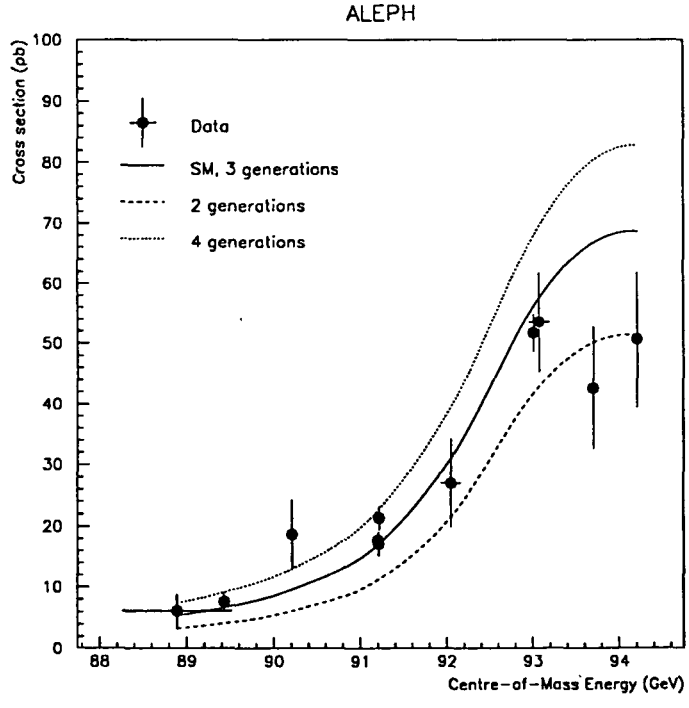

Figure 5: Variation of the $e^+e^- \rightarrow \nu\bar{\nu}\gamma$ cross section with centre-of-mass energy.

In ALEPH, an upper limit on the τ neutrino mass is determined from the distribution in reconstructed energy and invariant mass of the observed hadrons from selected 5 prong decays which are close to the allowed phase space boundaries. A Royal Holloway RA has been involved in this work for some years and has now added the 1994 data to earlier samples of $5\pi(\pi^0)$ candidates to give 38 $\tau \rightarrow 5\pi\nu_\tau$ and $3\pi\pi^0\nu_\tau$ events altogether. Figure 6 shows the 1994 selected events in the E_{had}/E_{beam} versus M_{had} plane. Only the event appearing between the $m_\nu = 31MeV/c^2$ and $m_\nu = 0MeV/c^2$ lines makes a significant contribution to improving the upper limit on the ν_τ mass which is now 23.1 MeV/c^2 at 95% confidence level.

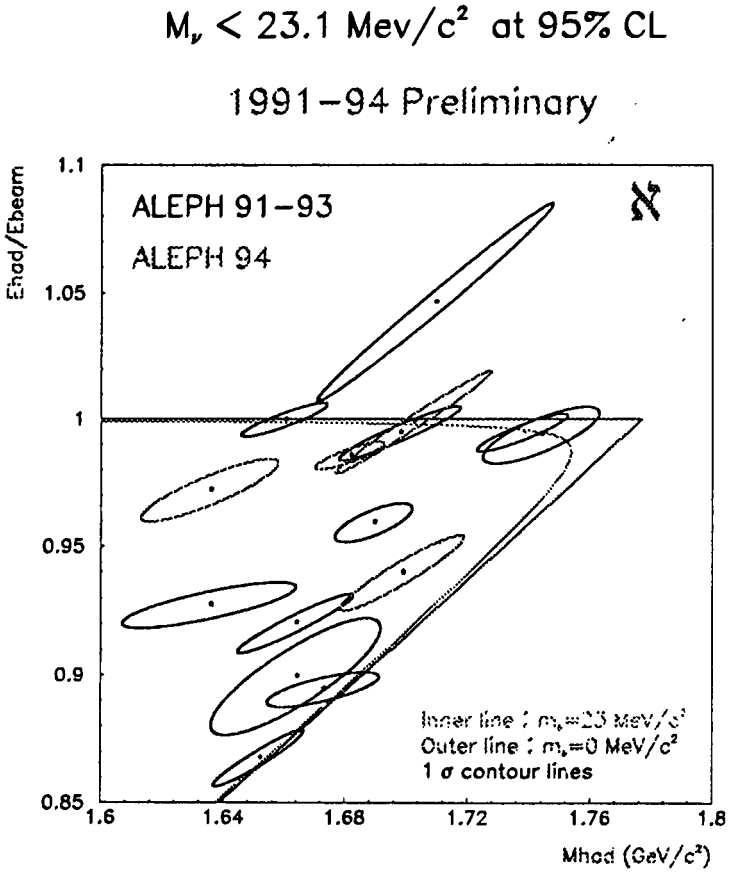

Figure 6: Current limit on tau neutrino mass.

3.3 QCD topics

The UK institutes have continued to play an important rôle in QCD analyses in ALEPH. Several analyses involving or performed solely by UK physicists have now been finalised: results were presented at the Brussels Conference and now await formal publication.

The study of quark and gluon jet properties by Imperial and Edinburgh physicists compared jets produced with almost equal energy($\sim 24GeV$) in symmetric three-jet events - such an environment allows the direct comparison of the jets without the

model dependence suffered by previous analyses. Two b jet identification techniques (impact parameter lifetime tag and a lepton tag) were used to identify quark jets and hence anti-tag gluon jets, and significant differences between quark and gluon jets were observed: as expected by QCD, gluon jets were found to have a higher multiplicity then quark jets, to have a softer fragmentation function and to be less collimated around the jet axis. In particular the analysis of a b jet sample showed that the above differences are markedly reduced if gluon jet properties are compared to the corresponding b jet properties, implying that, for the current energy scale, the non-leading fragmentation of the heavy flavour quark dominates the development of the jet profile.

The Glasgow and RAL groups have made the first measurement of the quark-to-photon fragmentation function carried out at LEP. Hard photons, radiated from the final state quarks in Z decays, are separated statistically from non-prompt hadronic backgrounds to produce a photon fragmentation function ($D(z)$), where z is the fractional energy of the photon within its own hadron jet. It is then shown that the measured $D(z)$ function , limited to $z \geq 0.7$ by background, can be described by a factorisation scale independent QCD leading order prescription (Glover and Morgan) with non-perturbative contributions in which the *only* free parameter is a cut-off mass scale μ_0. After fitting this prescription to the data, μ_0 was found to be $0.14^{+0.21}_{-0.08}$ GeV which might be interpreted as the effective mass of the radiating quark. The isolated photon component of the fragmentation function is now described adequately without the need to invoke next-to-leading order corrections.

The mechanism by which baryons are created in e^+e^- annihilations into hadrons is poorly understood. Single particle spectra are reproduced by many phenomenological models and provide little discriminating power, but considering two particle correlations should provide a clearer insight into baryon production. A Glasgow RA has studied correlations between protons and antiprotons in rapidity, azimuth and $cos\theta^*$, where θ^* is the angle between proton and sphericity axis in the proton-antiproton rest frame. A strong local compensation of baryon number is observed: given a tagging proton, 70% of the excess of additional antiprotons over additional protons is found within one unit of rapidity from the proton. No evidence for an anticorrelation in azimuth is seen, while a prominent peak at $|cos\theta^*| = 1$ is observed, in contrast to the expectation for an isotropic cluster decay mechanism, such as implemented in the HERWIG Monte Carlo program.

Further studies of correlations in hadronic events have been performed by a senior Imperial physicist: a significant, positive, transverse momentum correlation, hitherto unreported, has been observed between the two sides of hadron events. This correlation cannot be explained by energy-momentum conservation, flavour conservation, the imposition of an event axis or imperfect event reconstruction. However a similar type of correlation is found in reconstructed events generated by the JETSET Monte Carlo program, although the magnitude is only $\sim 2/3$ of that seen in the ALEPH data. In JETSET the correlation forms non-perturbatively after the parton shower, as the coloured partons separate and hadronise via the Lund "string" mechanism. A correlation is also seen in events generated by ARIADNE, but this forms perturbatively, early in the parton shower: the correlation predicted by ARIADNE is $\sim 30\%$ above the measured value. A technique in which the correlation is examined as a function of a jet-clustering parameter $m_y = \sqrt{y_{cut}.s}$ was introduced and was shown to give some discrimination between a string-induced correlation and one at the harder, parton level:

although correlations introduced in the parton cascade are closest to describing the data, the need for some additional string-like component is indicated.

A Sheffield student has recently concluded an analysis of ω production in hadronic Z decays. The ω is detected via its three pion decay mode $\omega \rightarrow \pi^+\pi^-\pi^0$ and was observed to have a total rate of 1.07 ± 0.14 per event. The rate of ω production is expected to be almost the same as for the ρ^0 since the two have essentially the same flavour content, the same spin and nearly the same mass, only differing in isospin. The ratio of the measured production rate of the ρ^0 to that of the ω is 1.36 ± 0.27. This agrees within errors with the value of 1.07 from JETSET 7.3, which does not distinguish isospin states. Therefore no evidence for isospin dependence is seen.

During the year, a Glasgow RA was one of the convenors of the LEP2 QCD Event Generators workshop and also worked on the standardisation of the particle codes and decay tables used by the major Monte Carlo programs. In addition, a RAL physicist provided a summary of the current understanding of prompt photon production in hadronic events at LEP as provided by the principle event generators.

The QCD group have been quick to analyse the $6pb^{-1}$ of data at $\sqrt{s} = 130-140GeV$ collected in the last few weeks of LEP's 1995 running period. Initial studies of this data, for example the measurement of the mean charged particle multiplicity (see Figure 7) indicate consistency with the predictions of QCD.

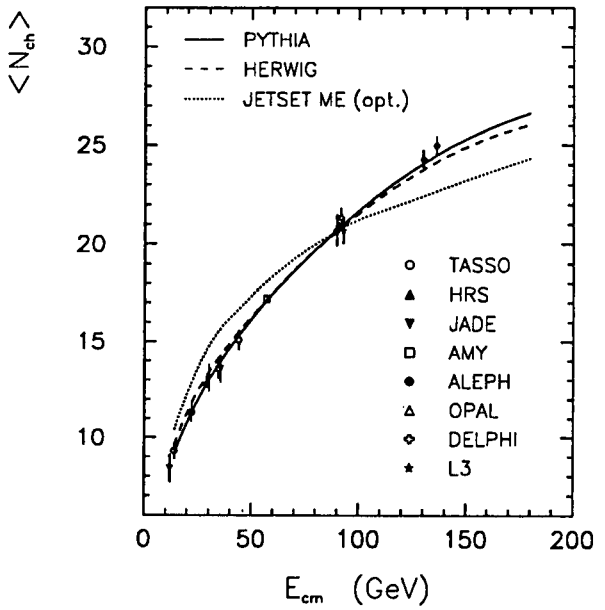

Figure 7: Charged particle multiplicity as a function of centre-of-mass energy.

3.4 $\gamma\gamma$ Physics

Interest has grown significantly in this field in the past year, particularly because of the great potential for $\gamma\gamma$ physics at LEP2. Members of the Lancaster, RAL and

Sheffield groups have formed an ALEPH $\gamma\gamma$ working group, membership of which is now expanding to include other groups from the UK and abroad.

Analysis of LEP1 data continues: measurements of the real photon structure function, F_2^γ at both high and intermediate Q^2 are in progress; high-$p_\perp$ jet production and the optimisation of jet-finding algorithms for $\gamma\gamma$ interactions are being studied; and the azimuthal asymmetry seen in the process $e^+e^- \rightarrow e^+e^-\mu^+\mu^-$ is also being analysed.

Much of the group's effort in the past year has been dedicated to preparations for LEP2, within the framework of the LEP2 Workshop held at CERN from January to November 1995. The cross section for $\gamma\gamma$ collisions dominates all other processes at LEP2, and so interest in $\gamma\gamma$ physics springs not only from the increased statistics for photon studies but also from the need to understand the $\gamma\gamma$ background to other physics studies such as supersymmetric particle searches. UK physicists have been active participants in the $\gamma\gamma$ subgroup of the workshop, particularly in the areas of heavy flavour production and structure function measurements.

Heavy flavour production is useful for the study of the anomalous behaviour of the photon since the soft VDM component does not significantly contribute as the heavy quark mass sets a hard scale for the interaction. At LEP2 the total charm production cross section in $\gamma\gamma$ interactions is $870pb$, compared with $468pb$ at the Z. In the first published D^* paper ALEPH observed 33 events from $70pb^{-1}$. Assuming similar acceptance at LEP2 implies the observation of approximately 400 events. It is intended to apply other methods for charm tagging, namely soft pion analysis and electron tagging. Preliminary studies of vertex tagging methods at LEP1 suggest this is not helpful but this deserves further study using the upgraded vertex detector and tracking software in the different kinematic regime. Given the higher statistics the aim would be to extract the single resolved gluonic structure of the probed photon.

The increased energy and luminosity of LEP2 will allow a measurement of the real photon structure function F_2^γ to be made at low x ($< 10^{-2}$) - a new kinematic region where photon structure is poorly understood. However, measurements at such low x are experimentally difficult. To measure x (the fraction of the target photon's momentum involved in the scattering process) in an event tagged by just one of the beam leptons requires the reconstruction of the final state invariant mass from hadrons observed in the detector. $\gamma\gamma$ events are typically boosted in the very forward direction and much of the final state is lost in the beam pipe, but unfolding techniques can be used to recover some information and reconstruct the true x distribution for the sample of events. At LEP2 energies, the forward boost is more severe and much work has been done to improve the reconstruction of the final state mass, particularly by improving our understanding of the hadronic response of ALEPH's low angle luminosity calorimeters (LCAL, SiCAL).

A completely new measurement at LEP2 will be that of the virtual photon structure function, $F_2^{\gamma^*}$ - here both beam leptons must be tagged to measure the virtuality of the probe and target photons, and this will be possible with the increased rate and acceptance for these events envisaged at LEP2: the planned upgrade of the low angle bhabha calorimeter (BCAL) will make this small detector capable of lepton tagging for $\gamma\gamma$ events, measuring photon virtuality in the range $0.1 - 0.8GeV^2$. There is theoretical interest in measuring $F_2^{\gamma^*}$ at intermediate Q^2 and low P^2 (where Q^2 is the virtuality of the probe photon and P^2 is the virtuality of the target), to understand the evolution of the structure function as P^2 increases. AT LEP2, $\sim$ 800 events suitable for this

analysis are expected: these will be double-tagged events where one tag is in either the main luminometers (SiCAL or LCAL) or the electromagnetic calorimeter (ECAL) endcap (ie. $> 34mrad$) and the other tag is identified in BCAL ($< 10mrad$).

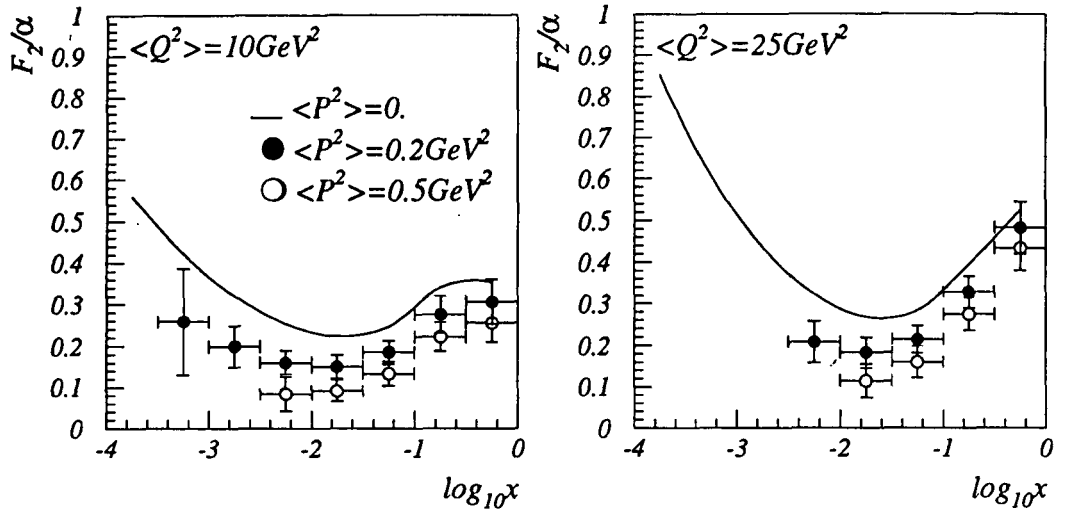

Figure 8: The evolution of the photon structure function with P^2.

Figure 8 shows the photon structure function predicted by the Schuler-Sjöstrand parametrisation (set 1D) for $< P^2 >= 0$ (the real photon structure function) and non-zero $< P^2 >$ (the virtual photon structure function). The error bars show the predicted statistical error on each point. So it is expected that, for the LEP2 data sample, the virtual photon structure function, $F_2^{\gamma^*}$ can be measured in perhaps two Q^2 and P^2 bins and the evolution away from real photon structure will be clearly seen.

3.5 Searches

The Royal Holloway group have continued their long standing search for excited quarks and leptons by radiative decays, and the radiative decay of the Z to a scalar particle, S, which would occur if both particles consisted of the same preonic constituents. These results have now been updated using 1.8×10^6 hadronic Zs from 1990 to 1993 data for inclusion in a comprehensive paper on compositeness searches in ALEPH. The group is also working on improved limits for the possible rare decays $Z \rightarrow \gamma gg$, $Z \rightarrow \nu N$ where N is a heavy neutrino above the W mass which mixes with one or more light neutrinos. In addition, a Royal Holloway student has completed a search for an anomalous magnetic moment of the τ and also possible deviations in $\mu\mu\gamma(\gamma)$ cross sections from the Standard Model.

In another search for compositeness in leptons, the Sheffield group have continued their study of the reaction $e^+e^- \rightarrow \gamma\gamma$ with all the statistics available up to the end of 1993. This process is expected to be pure QED with negligible weak corrections even at the Z mass. If the electron is composite, then there would be a form factor correction to the QED predicted cross section of the form:

$$F(q^2) = 1 \pm q^4/\Lambda_\pm^4$$

where the Λs are the so-called QED cut-off parameters which set the limits of the theory. Using 1552 good events, a fit is made to the polar angular distribution from which limits at 95% confidence level are set on the minimum values of Λ_+ and Λ_- separately of about 145 GeV. A comprehensive review of these and other searches limits from LEP1 has been compiled by an Royal Holloway physicist.

At the LEP2 workshop, a Royal Holloway physicist led the study on the detection strategies for non-SUSY particles. He reported on the topologies and expected cross sections for the pair production of sequential heavy leptons, excited leptons, lepto-quarks and other exotics.

4 ALEPH Publications since last year's report

1. Production of K^0 and Λ in hadronic Z decays
   Z. Phys. C64 (1994) 361

2. Measurement of the $b \to \tau^- \overline{\nu}_\tau X$ branching ratio and an upper limit on $B^- \to \tau^- \overline{\nu}_\tau$
   Phys. Lett. B343 (1995) 444

3. Study of the four-fermion final state at the Z resonance
   Z. Phys. C66 (1995) 3

4. Performance of the ALEPH detector at LEP
   NIM A360 (1995) 481

5. A study of $D^{*+}\pi^-$ production in semileptonic B decay
   Phys. Lett. B345 (1994) 103

6. Search for CP violation in the decay $Z \to \tau^+\tau^-$
   Phys. Lett. B346 (1995) 371

7. Inclusive $\pi^\pm, K^\pm$ and $(p, \overline{p})$ differential cross-sections at the Z resonance
   Z. Phys. C66 (1995) 355

8. Study of the subjet structure of quark and gluon jets
   Phys. Lett. B346 (1995) 389

9. Michel Parameters and τ neutrino helicity from decay correlations in $Z \to \tau^+\tau^-$
   Phys. Lett. B346 (1995) 379

10. An upper limit for the τ neutrino mass from $\tau \to 5\pi(\pi^0)\nu_\tau$ decays
    Phys. Lett. B349 (1995) 585

11. Search for supersymmetric particles with R-parity violation in Z decays
    Phys. Lett. B349 (1995) 238

12. Test of the flavour independence of α_s
    Phys. Lett. B355 (1995) 381

13. Measurement of the $D^{*\pm}$ cross section in two photon collisions at LEP
    Phys. Lett. B355 (1995) 595

14. The Forward-Backward Asymmetry for charm quarks at the Z pole
Phys. Lett. B352 (1995) 479

15. Measurements of the b baryon lifetime
Phys. Lett. B357 (1995) 685

16. Limit on B_s^0 oscillation using a jet charge method
Phys. Lett. B356 (1995) 409

17. A measurement of $|V_{cb}|$ from $\overline{B}^0 \rightarrow D^{*+} l^- \overline{\nu}_l$
Phys. Lett. B359 (1995) 236

18. Measurement of α_s from scaling violations in fragmentation functions in e^+e^- annihilation
Phys. Lett. B357 (1995) 487

19. Measurement of the effective b quark fragmentation function at the Z resonance
Phys. Lett. B357 (1995) 699

5 International Conference Presentations by UK Physicists

M. Green	"ALEPH Calorimetry"	Oct '94	Int.Symp., Beijing
P. Dornan	"Heavy Flavours"	Dec '94	Cambridge Conf.
P. Reeves	"Review on α_s"	Mar '95	QCD, Moriond
F. Foster	"D^* production in $\gamma\gamma$"	Apr '95	Photon '95, Sheffield
A. Moutoussi	"$q-g$ jets"	Jul '95	Hadron '95, Manchester

6 PhDs awarded in the past year

Imperial College

A. Moutoussi "Quark and gluon jet properties in symmetric three-jet events"

G. San Martin "Cross-section and A_{FB} for $Z \rightarrow \mu\mu$ at ALEPH"

N. Konstantinidis "Resonant structure and charge-flavour correlations in the $B\pi\pm$ system using fully reconstructed B decays"

Sheffield

I. Dawson "Inclusive production of the ϕ vector meson in hadronic Z decays"

THE OPAL EXPERIMENT AT LEP

PROPOSAL 720

Aachen; Alberta; Birmingham; Bologna; Bonn; Brunel; Budapest; California (Riverside); Cambridge; Carleton; CERN; Chicago; CRPP Canada; Debrecen; Duke; Freiburg; Hamburg/DESY; Heidelberg; Indiana; Manchester; Maryland; Montreal; Oregon; Queen Mary and Westfield College, London; Rutherford Appleton Laboratory; Saclay; Technion; Tel Aviv; Tokyo; University College, London; Vancouver (UBC); Victoria; Weizmann Institute.

INTRODUCTION

The LEP machine has operated very successfully during 1995, in spite of a series of changes. Early in the year, bunch train running, with 4 trains of up to 4 bunchlets spaced by 250 ns, was fully commissioned, allowing record luminosities to be delivered to the experiments. This bodes well for LEP2 in future years. During May, June and July, LEP ran at the Z^0 peak, and in August and September a final precision scan, with data recorded at energies 2 GeV above and below the Z^0 peak, was performed. Over 70% of the off-peak fills had their beam energy accurately calibrated by resonant depolarisation. A total luminosity of 40 pb^{-1}, split equally between on-peak and off-peak, was delivered to each of the experiments, thereby doubling the total amount of off-peak data. The analysis of these data, now under way, will result in a significant improvement in our knowledge of the Z^0 parameters, particularly the total width.

To give an example of the precision of the beam measurements: not only is the beam energy in LEP sensitive to the tides and to the level of the water in Lac Leman (from distortions of the LEP ring), but the measurements are able to detect that, between 00:00 and 05:30 each day, trains stop running on the local railway lines half a mile away.

During the October technical stop, additional superconducting RF cavities were installed and commissioned in LEP. For the last month's running in 1995, the beam energy has substantially increased, from 45 GeV to 65-70 GeV, en route for 80 GeV next summer (LEP2). Background conditions in the machine are spectacularly good. At these high energies many events radiatively return to the Z^0 peak by emitting a photon. Figure 1 shows an example of a distinctive subset of such events, a 4-fermion event, where a virtual radiative photon has materialised as a quark and anti-quark (forming one combined jet) and the Z^0 has decayed to a $\mu^+\mu^-$ pair. LEP has now achieved its goal of delivering 5 pb^{-1} to the experiments before the end of 1995, which will be sufficient to allow initial physics measurements to be made at these energies.

OPAL has made full use of the excellent accelerator performance this year. By the end of September, 850k Z^0 events had been recorded in 1995, bringing OPAL's total at LEP1 to 5.2 M Z^0 events on disk. The challenge now is to complete the full analysis of this dataset over the next 12-18 months. OPAL was also delighted to be the first experiment to see collisions at 65 GeV per beam, on the evening of 31 October. By 20 November over 1400 multihadronic events had been recorded at high energies. The distinctive topologies of the high energy data are forcing the physicists to think afresh about their event selection criteria - an excellent preparation for the future.

DETECTOR OPERATION

Barrel Muon Detector

The Barrel muon chambers, for which Manchester is responsible, have run consistently, reliably, and efficiently throughout the OPAL datataking periods. Virtually all the chambers are working well, and the designed 4-layer redundancy takes care of the handful

that are not. The hardware has also been kept running smoothly and efficiently, which requires continual monitoring of the HV and gas systems and readout diagnostics. A crucial task for the succeeding years is to ensure that this record of reliability and high performance continues.

A substantial upgrade of the online monitoring and calibration software is currently underway. Following the decision of OPAL no longer to support Vaxes in the online system, the software is being transferred to an HP environment.

End Cap Muon Detector

The Endcap Muon Detector, which is the responsibility of the University of Birmingham, has been in operation now for seven years, with no measurable deterioration in performance. Over this period the LEP machine has moved from 4 on 4 to 8 on 8 bunch mode operation, then to 4 on 4 bunch-trains and very recently to high energy running at 130 GeV. Throughout these changes the readout and triggering has continued to function well, and increased processing power has reduced the deadtime. In the 1994/1995 shutdown the VME HV control crate had a new processor installed and this has enhanced its performance. During physics running the detector performance is monitored daily from the Birmingham office at the main CERN site.

Vertex Drift Chamber & Track Trigger

The precision Vertex Drift Chamber and the Track Trigger, both responsibilities in the UK of the Cambridge, QMW and RAL (Electronics) groups, have continued to operate with good efficiency under both LEP1 and LEP1.5 conditions.

The chamber provides (r-ϕ) coordinates with a precision around 50 μm, as well as z co-ordinates with σ(z) around 700 μm from stereo wires.

End Cap Electromagnetic Calorimeter

The end cap electromagnetic calorimeter, consisting of 2264 instrumented lead glass blocks, is the responsibility of RAL together with Cambridge and QMW. The calorimeter is a crucial component of OPAL, both at the trigger and reconstruction level. It has continued to perform extremely reliably throughout the 1995 run. No change to the trigger or reconstruction thresholds have been needed to cope with the high energy running in November 1995.

The main challenge for the calorimeter in 1995 has been to cope with bunch train running of LEP, ie operation with 4 trains of up to 4 bunchlets spaced by 250 ns. To achieve good noise performance, the preamplifiers of the calorimeter have shaping times which are long compared to the ADC gate width. Thus the calorimeter response changes as the time of the signal is varied relative to the gate and hence depends on which bunchlet in a train gives rise to an event. For most physics events, the bunchlet causing the event can be tagged from the time-of-flight system or the tracking chambers before full offline reconstruction, allowing the calorimeter response to be corrected. Using the LED and LASER monitoring data, the necessary channel-by-channel correction factors were available well before the start of the 1995 LEP data-taking.

Forward Detector and End Cap Time of Flight System

The Forward Detector, components of which are the responsibility of the UCL and Brunel groups, has continued to run as a tagger for two photon physics and to contribute to the selection of hadronic events. Furthermore, with the start of high energy running in LEP, it is being used once more as the main OPAL luminometer. The Forward Proportional Tube Chambers are vital for both the photon tagging and the luminosity measurement, since they provide the precise radius of impact of electromagnetic showers in the Forward Calorimeter.

During the past year essential maintenance has been carried out on the Proportional Tubes and work has started on upgrading the readout electronics. In the 94/95 shutdown, the UCL/Brunel team unpacked one of the calorimeter segments to access the associated Proportional Tube module and repair a high voltage contact. In the forthcoming shutdown a new 14 bit ADC readout system, developed at UCL and based on a system used elsewhere in OPAL, will be installed.

UCL is also playing an important part in preparing the fibre-optic and wavelength shifter readout for the new Time of Flight Endcap system of OPAL, the TE, which is needed to help identify bunchlets in the LEP2 bunch trains. UCL designers are responsible for the routing of the fibres to the photomultipliers and the UCL/Brunel team will undertake a major part of the installation during the 1995/6 shutdown.

UPGRADE PROJECTS

The Silicon Microvertex Detector

The silicon microvertex detector project is moving to its third phase with a leading contribution continuing to come from the UK collaboration of Birmingham, Cambridge, QMW and RAL. This final upgrade is designed to maximise the B-tagging efficiency within OPAL, in readiness for Higgs boson searches during the period of LEP2 running that will begin in 1996.

The new detector has improved azimuthal coverage and increased length to provide a greater angular acceptance for charged particle tracking. All existing ladder modules are re-used in the revised geometrical configuration and are joined end to end with newly constructed ladders of similar design. All ladders are made with single-sided FoxFET biased microstrip wafers, 250 μm thick, in an orthogonal back-to-back configuration to provide both (r-ϕ) and z co-ordinates, with precisions of between 5 and 10 μm.

The construction of the new ladders required for the upgrade, together with all necessary spares, has been led by the UK and is now very near completion. Installation of this final detector will take place next Easter, ready for the first LEP2 running. The new tilted azimuthal geometry and half the new ladders were in fact already included in the detector installed for the 1995 data taking, together with all the power supplies and readout electronics necessary for the complete system. Alignment techniques have therefore now been established for this geometry, and valuable experience has been gained in running for the first time the radiation hard MX7 amplifier chips used on the new ladders.

Cambridge and QMW physicists continue to have responsibilities in the daily monitoring of device data, DAQ software, off-line reconstruction of data, and Monte Carlo simulation. They have also carried out all the software alignment for silicon data from the 1995 running and from previous years, and have continued to be very productive in the physics analyses that are dependent on data from the detector in the areas of b- and c-quark and τ-lepton studies.

PHYSICS ANALYSIS

The OPAL collaboration has submitted 31 letters and papers for publication during the last year, many of which already include analysis of the data collected in 1994. Significant improvements in precision have been obtained in electroweak and τ physics, and qualitatively new analyses have been developed in the heavy quark, QCD and $\gamma\gamma$ areas. Preparations for analysis of LEP2 data, as well as of that collected in the intermediate energy run at the end of 1995, are also proceeding apace. The UK groups continue to play a central part in all of these fields, as summarised below.

Precision Electroweak Physics

The OPAL results for the Z^0 lineshape and leptonic forward-backward asymmetries, including 1994 data, were presented at the spring and summer conferences during 1995. The results are based on a total of 412 000 leptonic and 3 357 000 hadronic Z^0 decays. Significant improvements in the accuracy of measurements of M_Z (91.1846 ± 0.0035 GeV) and Γ_Z (2.4959 ± 0.0053 GeV) are obtained. The lineshape and lepton pair forward-backward asymmetries are consistent with the predictions of the Standard Model and within this model yield the constraints $M_{top} = 158^{+19}_{-22}{}^{+18}_{-17}$ GeV, consistent with the measured value from CDF and D0, and $\alpha_s(M_Z^2) = 0.132 \pm 0.006 \pm 0.002$. The precision of tests of the lepton universality of the neutral current coupling is also improved (see Figure 2). The new silicon-tungsten luminosity detector, to which the Birmingham, Brunel, RAL and UCL groups have contributed, provides a measurement with an experimental accuracy of 0.075%. This significantly improves the OPAL measurement of the invisible width of the Z^0, which may be used to estimate the number of light neutrino flavours ($N_\nu = 2.984 \pm 0.024 \pm 0.005$).

Analysis of lepton pair final states continues to be a focus of UK effort: a Brunel student was responsible for a large part of the analysis of the $Z^0 \rightarrow \mu^+\mu^-$ channel and, in particular, provided many detailed checks of systematic errors and biases in the asymmetry analysis. The Manchester group has maintained its strong activity in the analysis of the Z^0 lineshape and lepton pair forward-backward asymmetries. Since 1993, members of this group have contributed to the estimation of the systematic errors in the selection of $Z^0 \rightarrow \mu^+\mu^-$ and $Z^0 \rightarrow \tau^+\tau^-$ events, the inclusion of endcap $e^+e^- \rightarrow e^+e^-$ events into the electroweak fits and studies of events consisting of four final-state fermions. OPAL members from Manchester and Cambridge have played important roles in the LEP energy working group.

An independent analysis has been provided by the UCL group, in which the cross-sections, asymmetries and important correlations are fully taken into account when extracting the electroweak parameters. Fits to the lineshape and asymmetry data have been used to measure the ε parameters which separately parametrise the corrections to the lowest order electroweak diagrams due to Standard Model effects (primarily loops involving the top quark and Higgs boson) and effects from beyond the Standard Model.

Several UK members of OPAL, from Birmingham, Manchester and UCL, are active in the LEP electroweak working group (EWWG) which brings together physicists from each experiment. The aim of the EWWG is to ensure that all electroweak results from the four experiments are combined correctly, taking into account any correlations. The results from this group are then provided as an important definitive source, for use in conference presentations and other derived analyses.

Electroweak measurements in the heavy flavour sector have also made substantial progress during 1995. New preliminary measurements of the fraction of hadronic Z^0 decays into $b\bar{b}$ or $c\bar{c}$ pairs (R_b and R_c) have both been presented at conferences. There is a strong UK involvement in both measurements.

The R_b measurement, published last year with 1992 and 1993 data, has been updated, by inclusion of the 1994 data, to give a new preliminary result of $R_b = 0.2197 \pm 0.0014 \pm 0.0022$, with R_c set to its Standard Model value of 0.172. The analysis uses a 'double tagging' technique which allows a simultaneous determination of $\Gamma_{b\bar{b}}$ and the b-tagging efficiency, improving substantially the overall accuracy. Vertex and lepton tags are combined to improve the precision. The dominant vertex tagging component remains the responsibility of Cambridge, and the muon identification that of Birmingham.

Several new preliminary R_c measurements have been presented by OPAL at conferences in 1995. Of particular note is a novel analysis, originated by the QMW group, which derives R_c by measuring the production rates in hadronic Z^0 decays, of four species of weakly decaying charm hadron D^+, D^0, D_s^+, Λ_c. Since these four species almost saturate the weak

charm decay rate, the sum of their production rates gives R_c, free from most of the hadronisation uncertainties which afflict, for example, measurements of R_c using the observed yield of a single D meson species. This analysis yields the preliminary value $R_c = 0.168 \pm 0.016$, one of the most precise determinations available. Work is in progress to add the 1994 and 1995 data, which should improve the error significantly. Combining with the other published and preliminary OPAL R_c measurements gives $R_c = 0.1550 \pm 0.0112$. The OPAL results for R_b and R_c and the Standard Model expectation (marked SM) for a range of top masses are compared in Figure 3.

Forward-backward asymmetries of quarks are also interesting electroweak observables, as they are sensitive to $\sin^2 \theta_w$. The measurements of A^b_{FB} and A^c_{FB} have been updated during 1995 to include 1994 data. Recent developments in measuring quark asymmetries using jet charge estimates to separate quark and anti-quark directions have led to a measurement of A^b_{FB} performed by the Birmingham group, in collaboration with colleagues from CERN and Italy, and a determination of $\sin^2 \theta_w$ from an inclusive hadronic event sample, performed partly by the Manchester group. These two analyses include 1993 and 1994 data, and give $\sin^2 \theta_w = 0.2313 \pm 0.0012 \pm 0.0006$ and $\sin^2 \theta_w = 0.2326 \pm 0.0012 \pm 0.0013$ respectively. The Manchester group is currently extending this analysis to include information on the charge of tracks associated with tagged vertices.

The UCL and Brunel groups have developed a new analysis to search for the possible presence of an extra high mass neutral gauge boson. A Z' could manifest itself through direct exchange, interference with the standard Z^0 or by mixing, resulting in a modification of the values extracted from electroweak fits. Mixing angles of the order of 10 mrad have so far been excluded and this represents a substantial improvement over previous results.

A high-precision energy scan was performed during 1995, to improve the accuracy of the Z^0 mass and width measurements further. Collaborators from Manchester and UCL played a leading role both within OPAL and in the wider LEP community in establishing the technical and physics case for the scan.

b Quark Physics

The UK groups have continued to play a central part in b quark studies. A number of new results have been published, and others presented at conferences.

The updated B^+ and B^0 lifetimes ($1.52 \pm 0.14 \pm 0.09$ ps and $1.53 \pm 0.12 \pm 0.08$ ps respectively) obtained by the Cambridge and QMW groups, have been published in 1995. The measured ratio of $0.99 \pm 0.14^{+0.05}_{-0.04}$ is consistent with the expectation that the lifetimes are similar.

Measurements of $B^0 - \bar{B}^0$ oscillations continue to improve. A determination of the oscillation frequency for B^0_d mesons using events with two identified leptons has been published, and others using jet charge measures in concert with reconstructed D^{*+} mesons and leptons have been presented at conferences. The most recent, the lepton-jet-charge measurement, yields $\Delta m_d = 0.439 \pm^{0.030}_{0.029} \pm^{0.020}_{0.019}$ ps^{-1} and places a limit on Δm_s, which determines the frequency of B^0_s oscillations. A Birmingham physicist leads the $B^0 - \bar{B}^0$ oscillations working group and has played a leading role in many of these measurements. The Birmingham group is also working on measuring the average B mixing using lepton tagging and jet charge measurement, applying the techniques used in the A^b_{FB} measurement.

The sample of semileptonic B hadron decays with a reconstructed charm meson has been used by the QMW group in an analysis, submitted for publication, to measure b quark fragmentation into B^0 and B^+ mesons, and compare the fragmentation functions observed with different phenomenological models. The mean scaled energy of B^0 and B^+ mesons was determined to be $\langle x_E \rangle = 0.695 \pm 0.006 \pm 0.003 \pm 0.007$, where the errors are statistical, systematic, and due to model dependence. This analysis is more complete than previous ones in that the effect of production of P-wave B mesons is explicitly taken into account.

The QMW group has also pioneered the study of inclusive charm production. Results have been obtained for D^0, D^+, D_s^+ and Λ_c^+ hadrons. In each case, statistical separation between prompt production and $B \rightarrow DX$ decays was achieved using lifetime information. Together these measurements represent the first comprehensive study of charm hadron production at LEP. The relative rates for the different charmed hadrons formed from primary c quarks has been found to be in good agreement with lower energy data. The measurements of primary charm production have also been used to study charm fragmentation and to measure $\Gamma_{c\bar{c}}/\Gamma_{had}$. The measured rates of these four charmed hadrons in b hadron decays is found to account for $(1.018 \pm 0.046^{+0.067}_{-0.065} \pm 0.036)$ c or $\bar{c}$ quarks per b hadron decay where the errors arise from statistical, systematic, and branching ratio uncertainties respectively. This is the first such 'charm counting' result obtained at LEP, where the systematic errors are different to measurements made in Y(4S) decays.

The rate of production of J/ψ mesons in Z^0 decays, and in $b\bar{b}$ decays of the Z^0, has been measured by the Cambridge group in collaboration with colleagues from CERN and Italy. The values obtained for the branching ratios are $B(Z^0 \rightarrow J/\psi\, X) = (3.9 \pm 0.2 \pm 0.3) \times 10^{-3}$ and $B(b \rightarrow J/\psi\, X) = (1.15 \pm 0.06 \pm 0.12) \times 10^{-2}$.

Exclusive reconstruction of B meson decays to states including J/ψ were further attempted, and signals reported in the $B^0 \rightarrow J/\psi\, K_s^0$ and $B^+ \rightarrow J/\psi\, K^+$ channels.

The Cambridge group is working on updating its previous analysis of rare B decays, such as $B^0 \rightarrow \pi^+\pi^-$, which give information about 'penguin' diagrams.

τ Lepton Physics

OPAL has updated its measurements of τ lifetime, polarisation and many decay branching ratios during the year. A measurement by the Birmingham group of the leptonic branching ratios of the τ was published during 1995, and already an update of the electron channel, performed by Canadian colleagues, has been submitted for publication. Birmingham continues to work on improving the muon decay branching ratio measurement.

The τ polarisation has been measured in many channels by OPAL. The first OPAL measurement of the τ polarisation in the difficult $\tau \rightarrow a_1\nu$ channel has been made by the RAL group using 1990 to 1994 data, and presented at conferences during the year. Combining the result with those from other τ-decay channels yields preliminary results of $A_e = 0.134 \pm 0.015 \pm 0.004$ and $A_\tau = 0.134 \pm 0.010 \pm 0.009$, consistent with e/τ universality. In the Standard Model framework these results can be used to give a value $\sin^2\theta_W = 0.2331 \pm 0.0013$. The UCL group continues to work on improving the τ polarisation measurement in the muon channel.

Birmingham and RAL have also been working together with Canadian colleagues to measure the topological branching ratios of the τ lepton.

QCD

A determination of $\alpha_s(M_{Z^0}^2)$ has been made by Cambridge and Birmingham by comparing experimental data with $O(\alpha_s^2)$ QCD calculations including all-order resummed leading and next-to-leading logarithms. The published value, averaging over results from study of several variables, is $\alpha_s(M_Z^2) = 0.120 \pm 0.006$. The analysis has been further extended by Cambridge into a region dominated by two-jet events, with consistent results. This analysis was submitted for publication in the first half of 1995.

The longitudinal, transverse and asymmetry fragmentation functions for the process $e^+e^- \rightarrow h + X$ have been separated and measured by Cambridge using 3 million events. Comparisons have been made with QCD predictions and the measured value of the longitudinal cross-section $\sigma_L/\sigma_{tot} = 0.057 \pm 0.005$ is in agreement with the expectation of

the JETSET parton shower model. It is, however, considerably above the $O(\alpha_s)$ QCD prediction of 0.038 ± 0.002 owing to hadronization and higher-order perturbative effects. The gluon fragmentation function has been extracted from the transverse and longitudinal functions. This offers a complementary approach to other methods (Figure 4). The asymmetry fragmentation function grows in importance towards large x, and its behaviour may be understood in terms of standard electroweak asymmetries and a simple valence quark dominance model.

Studies of isolated photons in hadronic events led to the publication of measurements of electroweak couplings of up and down-type quarks and recently to comparisons of event properties with predictions of matrix elements calculations. Following its previous work in this area, the RAL group is now addressing the measurement of photon production inside jets. Photons emitted by partons provide information about the development of the parton shower and the parton-photon fragmentation function. Knowledge of the latter, not predicted by theory, is important for the interpretation of the measurement of the prompt photon production in hadronic colliders, especially for estimates of the background to the $H \rightarrow \gamma\gamma$ channel at the LHC. The RAL group is investigating methods of reducing the important π^0 background.

In the field of non-perturbative strong interactions, Manchester is responsible for the co-ordination within OPAL of measurements of inclusive particle production and fragmentation. Measurements made in Manchester of the production of the strange vector mesons $\phi(1020)$ and $K^*(892)^0$ in hadronic Z^0 decays have been published during 1995. The results included a measurement of the rate of production of the $K_2^*(1430)^0$, the first observation of a strange tensor meson at LEP. The position of the peak (ξ_{peak}) in the distribution of $\ln(1/x_p)$ for $\phi(1020)$ and $K^*(892)^0$ has been measured and compared with measurements from other species of hadrons. In the framework of the modified leading log approximation, the ξ_{peak} values are expected to depend only on the mass of the produced hadron, but OPAL measurements have suggested that baryons and mesons lie in two separate bands. It has been shown that this apparent discrepancy is probably due to the production and decay of higher mass resonances.

In Manchester, the production and spin-alignment of $\phi(1020)$ in gluon jets has been investigated, and results were presented at the summer conferences. Another long standing interest has been the residual effects of Bose-Einstein correlations on the mass spectra of unlike-sign pairs of hadrons. An understanding of these effects is necessary before a reliable measurement of the production of the ρ^0 meson can be performed.

A measurement is underway in Manchester of the probability for strange quark-antiquark pairs to be produced in the fragmentation process. This uses the novel technique of measuring the forward-backward asymmetry of $K^*(892)^0$ and K^+ mesons.

The QMW group have used reconstructed D^* mesons and secondary vertices in jets to measure the hemisphere charged particle multiplicity in $Z^0 \rightarrow u\bar{u}$, $d\bar{d}$, $s\bar{s}$, $Z^0 \rightarrow c\bar{c}$ and $Z^0 \rightarrow b\bar{b}$ events. The results are $\bar{n}_{uds} = 10.41 \pm 0.06 \pm 0.09 \pm 0.19$, $\bar{n}_c = 10.76 \pm 0.20 \pm 0.14 \pm 0.19$, and $\bar{n}_b = 11.81 \pm 0.01 \pm 0.12 \pm 0.21$. The differences in total charged particle multiplicity between c and b quark events and light (u, d, s) quark events are found to be $\delta_{cl} = 0.69 \pm 0.51 \pm 0.35$ and $\delta_{bl} = 2.79 \pm 0.12 \pm 0.27$. The QMW and Cambridge groups are now using the same techniques to study scaling violations.

$\gamma\gamma$ Physics

The UCL analysis of the photon structure function $F_2^\gamma(x)$ was the first to be performed at LEP. As a second stage to the analysis, the unfolding of the true Bjorken x distribution has now been done on a logarithmic scale which refines the measurement at low x values - extending it into a region which lower energy experiments could not reach. Down to x values of 0.01, there is no sign of any rise in the photon structure function. This has already ruled out a number of theoretical models. We look forward to LEP2, where the reach in x will be

sufficient to see whether the photon has a rise in the same region of x as the rise seen in the proton structure function at HERA.

The RAL group has measured F_2^γ using electrons tagged in the end cap lead glass calorimeter, thereby extending the Q^2 range to 200 GeV^2. This work was presented at the Sheffield Photon '95 conference. A RAL physicist is joint convenor of the OPAL $\gamma\gamma$ working group.

Higgs Searches

UCL have been in charge of the search for Higgs events with a recoiling muon or electron pair, published in 1994, and including 1990 to 1993 data. They have found what is probably the best candidate yet seen at LEP; an event which passes the $Z^* \rightarrow \mu^+\mu^-$ selection criteria with one well resolved b decay vertex. However, four-fermion production gives rise to an irreducible background in this channel which, for masses above 50 GeV, is estimated to be 0.3 ± 0.1 events.

The Intermediate Energy Run ('LEP 1.5')

During November 1995, LEP ran at higher beam energies, from 65 to 70 GeV, as a step towards the LEP2 operations, scheduled for 1996. This short high energy run is of interest both to search for possible new physics signatures at a new energy frontier for e^+e^- colliders, and as a test of expected physics processes, machine backgrounds and overall performance at higher energy. The UK groups are preparing themselves for LEP2 by involving themselves fully in the analysis of LEP1.5 data.

Physics Preparations for LEP2

Preparations for LEP2 analysis have been proceeding at full steam during 1995, particularly in the context of the LEP2 workshop at CERN. A Manchester physicist is on the organising committee of the workshop, and colleagues from Cambridge and UCL summarised LEP-wide experimental work on the W mass and triple-gauge coupling measurements for the final plenary session of the workshop.

The measurement of M_W is one of the fundamental measurements to be performed at LEP 2, and one of the most promising techniques appears to be the direct reconstruction of the W mass from its decay into $q\bar{q}$. This may be done independently in two channels, $W^+W^- \rightarrow q\bar{q}q\bar{q}$ and $W^+W^- \rightarrow q\bar{q}\,\ell\bar{\nu}_\ell$. At Cambridge and UCL, studies have been performed of the selection of events in these channels, and of techniques for the subsequent mass reconstruction (Figure 5). For example the $W^+W^- \rightarrow q\bar{q}q\bar{q}$ reaction may be selected with an efficiency of ~ 80% and a purity of ~ 75%. Kinematic fitting provides an important tool for further reducing background and refining the W mass resolution; present studies predict a statistical precision of 55 MeV for 500 pb^{-1} of data, and future work is likely to improve on this. In 1996 M_W will be determined from measurements of the W-pair cross section at threshold. Physicists from Cambridge and Manchester are currently studying the systematic uncertainties of this measurement.

The production of pairs of W bosons at LEP2 will provide a chance to measure the properties of the triple-gauge boson coupling between Z^0WW and also γWW. There is a small sensitivity to these couplings in $\bar{p}p$ collisions, but this will be greatly improved at LEP2. The Birmingham, UCL and Brunel groups are studying how these measurements can best be made at LEP2, considering both the resolution effects of the detector, and the effects of the W width and initial-state radiation, on the measured W-pair properties. Several different electroweak generators are being studied, and alternative fitting strategies considered.

The Cambridge group is also participating in the QCD working group for LEP2. In contrast to LEP1, one of the main problems for QCD studies is to select a sample of $Z^0 \rightarrow q\bar{q}$ events

close to the full c.m. energy, without contamination from radiative $Z^0\gamma$ or $W^+W^- \rightarrow q\bar{q}q\bar{q}$ final states. At present, efficiencies of around 85% with a purity close to 87% seem to be achievable, but with significant bias to the selected event sample. Work continues to optimise the event selection procedure. The distributions of event shape variables such as Thrust may be used to measure α_s at LEP2. Monte Carlo studies indicate that the influence of hadronization on such distributions will be greatly reduced relative to LEP1, and will be less dependent on the model used. In particular, this will allow the use of resummed QCD calculations to determine α_s in the two-jet region of the distributions, where the LEP2 data should be most plentiful and least biased. A statistical uncertainty of ± 0.001 on α_s should be achievable. (An assessment of the likely systematic uncertainties has not yet been completed).

In the $\gamma\gamma$ part of the workshop, the convenor of the structure function study group is from UCL. This sub-group has made considerable progress in establishing the need for Monte Carlo models, particularly PYTHIA and HERWIG, to incorporate $\gamma\gamma$ processes in a formally correct way, replacing the ad hoc models used for LEP1 analysis. This should allow systematic errors due to modelling and unfolding to be reduced to match the increased statistics at LEP2.

In addition to the above activities, investigations have also progressed on obtaining the best sensitivity to possible Higgs boson production and decay at LEP2. From the UK, the UCL and RAL groups have participated in the studies for the workshop.

In summary, OPAL is eagerly anticipating LEP2 data-taking next year. Furthermore the UK groups confidently expect to play an important role in the analysis of the higher energy data, capitalising on their leadership of current preparatory work and on the central roles they have played at LEP1, particularly in electroweak, QCD, and two-photon analyses.

OPAL PUBLICATIONS

1 A Test of CP-Invariance in $Z^0 \rightarrow \tau^+ \tau^-$ Using Optimal Observables
The OPAL Collaboration, R Akers et al
Zeit fur Phys. **C66,** (1995) 31-44.

2 Combined Preliminary Data on Z^0 Parameters from the LEP Experiments and Constraints on the Standard Model
The LEP Electroweak Working Group and The LEP Collaborations: ALEPH, DELPHI, L3, OPAL
CERN-PPE/94-187 (25 November 1994).

3 Observations of π-B charge-flavor correlations and resonant B π and BK production
The OPAL Collaboration, R Akers et al
Zeit fur Phys. **C66,** (1995) 19-30.

4 A Measurement of the Production of $D^{*\pm}$ Mesons on the Z^0 Resonance
The OPAL Collaboration, R Akers et al
Zeit fur Phys. **C67,** (1995) 27-44.

5 A Study of Charm Meson Production in Semileptonic B Decays
The OPAL Collaboration, R Akers et al
Zeit fur Phys. **C67,** (1995) 57-68.

6 Measurement of the Leptonic Branching Ratios of the τ lepton
The OPAL Collaboration, R Akers et al
Zeit fur Phys. **C66,** (1995) 543-554.

7 A Study of B Meson Oscillations Using Dilepton Events
The OPAL Collaboration, R Akers et al
Zeit fur Phys. **C66,**(1995) 555-565.

8 Comparisons of the Properties of Final State Photons in Hadronic Z^0 Decays with Predictions from Matrix Element Calculations
The OPAL Collaboration, R Akers et al
Zeit fur Phys. **C67,** (1995) 15-26.

9 Improved Measurements of the B^0 and B^+ Meson Lifetimes
The OPAL Collaboration, R Akers et al
Zeit fur Phys. **C67,** (1995) 379-388.

10 An Improved Measurement of the B_s^0 Lifetime
The OPAL Collaboration, R Akers et al
Phys. Lett. **B350,** (1995) 273-282.

11 Search for Heavy Charged Particles and for Particles with Anomalous Charge in e^+e^- Collisions at LEP
The OPAL Collaboration, R Akers et al
Zeit fur Phys. **C67,** (1995) 203-211.

12 Measurement of the Hadronic Decay Current in $\tau \rightarrow \pi^-\pi^-\pi^+ \nu_\tau$
The OPAL Collaboration, R Akers et al
Zeit fur Phys. **C67,** (1995) 45-55.

13 The Production of Neutral Kaons in Z^0 Decays and their Bose-Einstein Correlations
The OPAL Collaboration, R Akers et al
Zeit fur Phys. **C67,** (1995) 389-401.

14 Inclusive Strange Vector and Tensor Meson Production in Hadronic Z Decays
The OPAL Collaboration, R Akers et al
Zeit fur Phys. **C68,** (1995) 1-12.

15 A Measurement of Charged Particle Multiplicity in $Z^0 \rightarrow c\bar{c}$ and $Z^0 \rightarrow b\bar{b}$
The OPAL Collaboration, R Akers et al
Phys. Lett. **B352,** (1995) 176-186.

16 A Search for Lepton Flavour Violating Z^0 Decays
The OPAL Collaboration, R Akers et al
Zeit fur Phys. **C67,** (1995) 555-564.

17 A Measurement of the Forward-Backward Asymmetry of $e^+e^- \rightarrow b\bar{b}$ by Applying a Jet Charge Algorithm to Lifetime Tagged Events
The OPAL Collaboration, R Akers et al
Zeit fur Phys. **C67,** (1995) 365-378.

18 A Measurement of the Λ_b Lifetime
The OPAL Collaboration, R Akers et al
Phys. Lett. **B353,** (1955) 402-412.

19 Measurement of the Multiplicity of Charm Quark Pairs from Gluons in Hadronic Z^0 Decays
The OPAL Collaboration, R Akers et al
Phys. Lett. **B353,** (1955) 595-605.

20 Measurement of the Longitudinal, Transverse and Asymmetry Fragmentation Functions at LEP
The OPAL Collaboration, R Akers et al
Zeit fur Phys. **C68,** (1995) 203-213.

21 A Study of QCD Structure Constants and a Measurement of α_s (M_Z0) at LEP Using Event Shape Observables
The OPAL Collaboration, R Akers et al
Zeit fur Phys. **C68,** (1995) 519-530.

22 Measurement of the $\tau \rightarrow h^-h^+h^-\nu_\tau$ and $\tau \rightarrow h^-h^+h^- \geq 1\pi^0\nu_\tau$ branching ratio
The OPAL Collaboration, R Akers et al
Zeit fur Phys. **C68,** (1995) 555-567.

23 A Model Independent Measurement of Quark and Gluon Jet Properties and Differences
The OPAL Collaboration, R Akers et al
Zeit fur Phys. **C68,** (1995) 179-201.

24 Investigation of the String Effect Using Final State Photons
The OPAL Collaboration, R Akers et al
Zeit fur Phys. **C68,** (1995) 531-540.

25 Measurement of the Average b-Baryon Lifetime and the Product Branching Ratio $f(b \rightarrow \Lambda_b) \cdot BR\ (\Lambda_b \rightarrow \Lambda\ \ell\overline{\nu}\ X)$
The OPAL Collaboration, R Akers et al
CERN-PPE/95-090 (23 June 1995)
Submitted to Zeit fur Physik

26 Δ^{++} Production in Hadronic Z^0 Decays
The OPAL Collaboration, G Alexander et al
Phys. Lett. **B358** (1995) 162-172.

27 A study of b Quark Fragmentation into B^0 and B^+ Mesons at LEP
The OPAL Collaboration, G Alexander et al
CERN-PPE/95-122 (3 August 1995)
Submitted to Phys. Lett. **B**.

28 A comparison of b and uds quark jets to gluon jets
The OPAL Collaboration, G Alexander et al
CERN-PPE/95-126 (22 August 1995)
Submitted to Zeit fur Physik.

29 Measurement of the $\tau \rightarrow \bar{\nu}_e \nu_\tau$ Branching ratio
The OPAL Collaboration, G Alexander et al
CERN-PPE/95-142 (28 September 1995)
Submitted to Phys. Lett. **B**.

30 J/Ψ and Ψ' production in hadronic Z^0 decays
The OPAL Collaboration, G Alexander et al
CERN-PPE/95-153 (26 October 1995)
Submitted to Zeit fur Physik.

31 Test of the Exponential Decay Law at Short Decay Times using τ leptons
The OPAL Collaboration, G Alexander et al
CERN-PPE/95-155 (1 November 1995)
Submitted to Phys. Lett. **B**.

CONFERENCE CONTRIBUTIONS AND REVIEW ARTICLES BY UK PHYSICISTS

Measurements of B hadron Lifetimes at LEP
J R Batley
6th International Conference on Hadron Spectroscopy, Manchester, 10 - 14 July 1995.

Electroweak Measurements using Heavy Quarks at LEP
T Behnke and D G Charlton
Physics Scripta 52 (1995) 133.

Measurements of R_b using Lifetime Tags
D G Charlton
International Europhysics Conference on High Energy Physics, Brussels,
27 July - 2 August 1995.

Lepton Flavour Violation and CP Invariance in τ Decays
T Geralis
International Europhysics Conference on High Energy Physics, Brussels,
27 July - 2 August 1995.

Review of b-hadron physics at LEP
M Jimack
XXXth Rencontres de Moriond, Electroweak Interactions and Unified Theories,
11-18 March 1995.

Measurements of the photon structure function F_2^γ using two-photon events tagged in the OPAL endcaps
B W Kennedy
Photon'95 Conference, Sheffield, 8 - 13 April 1995.

Multiplicities and Fragmentation Functions with OPAL at LEP
S Kluth
Symposium on Multiparticle Dynamics, Stara Lesna, Slovakia, September 1995.

Recent Particle Searches at LEP
P Sherwood
Four Seas Conference, Sissa, Trieste, 25 June - 1 July 1995

Measurement of Tau Lepton Decays to Kaons at OPAL
C P Ward
XXXth Rencontres de Moriond, Electroweak Interactions, Les Arcs, March 1995.

Measurement of Fragmentation at LEP
J A Wilson
6th International Conference on Hadron Spectroscopy, Manchester, 10 - 14 July 1995.

OPAL-RELATED PAPERS BY UK AUTHORS

A method for measuring strangeness suppression in light quark fragmentation at LEP
G Lafferty, Phys. Lett. **B353,** (1995) 541-546.

Where to stick your data points: the treatment of measurements within wide bins
G Lafferty and T Wyatt, NIM **A355,** (1995) 541-547.

The OPAL Muon Barrel detector
R J Akers et al NIM **A357,** (1995) 253-273.

OPAL RESEARCH THESES BY UK STUDENTS

Determination of the tau pair production cross section at the Z^0 resonance
R Akers, Ph.D. Thesis, Manchester, 1995.

A search for the standard model higgs boson using the OPAL detector at LEP
K Ametewee, Ph.D. Thesis, UCL, Autumn 1995.

A measurement of the forward-backward asymmetry of $Z^0 \rightarrow \mu^+\mu^-$ and a search for an additional neutral vector gauge boson using electroweak observables at OPAL
P Bright-Thomas, Ph.D. Thesis, Brunel, May 1995.

Measurement of the leptonic branching ratios of the tau lepton using the OPAL detector at LEP
J Clayton, Ph.D Thesis, Birmingham, January 1995.

Studies of QCD using event shape observables in e^+e^- annihilation at the Z^0 energy
S Kluth, Ph.D. Thesis, Cambridge, 1995.

A search for lepton-flavour violating decays at OPAL
W Matthews, Ph.D. Thesis, Brunel, submitted but not yet awarded.

A measurement of the tau polarization asymmetry from acolinearity at OPAL
N Tresilian, Ph.D. Thesis, Manchester, 1995.

A measurement of the B^+ and B^0 meson lifetimes and lifetime ratio using the OPAL detector at LEP
T Shears, Ph.D. Thesis, Cambridge, August 1995.

A study of Λ^0 and K^0 production in bottom quark events at LEP
A Yeaman, Ph.D Thesis, QMW, submitted but not yet awarded.

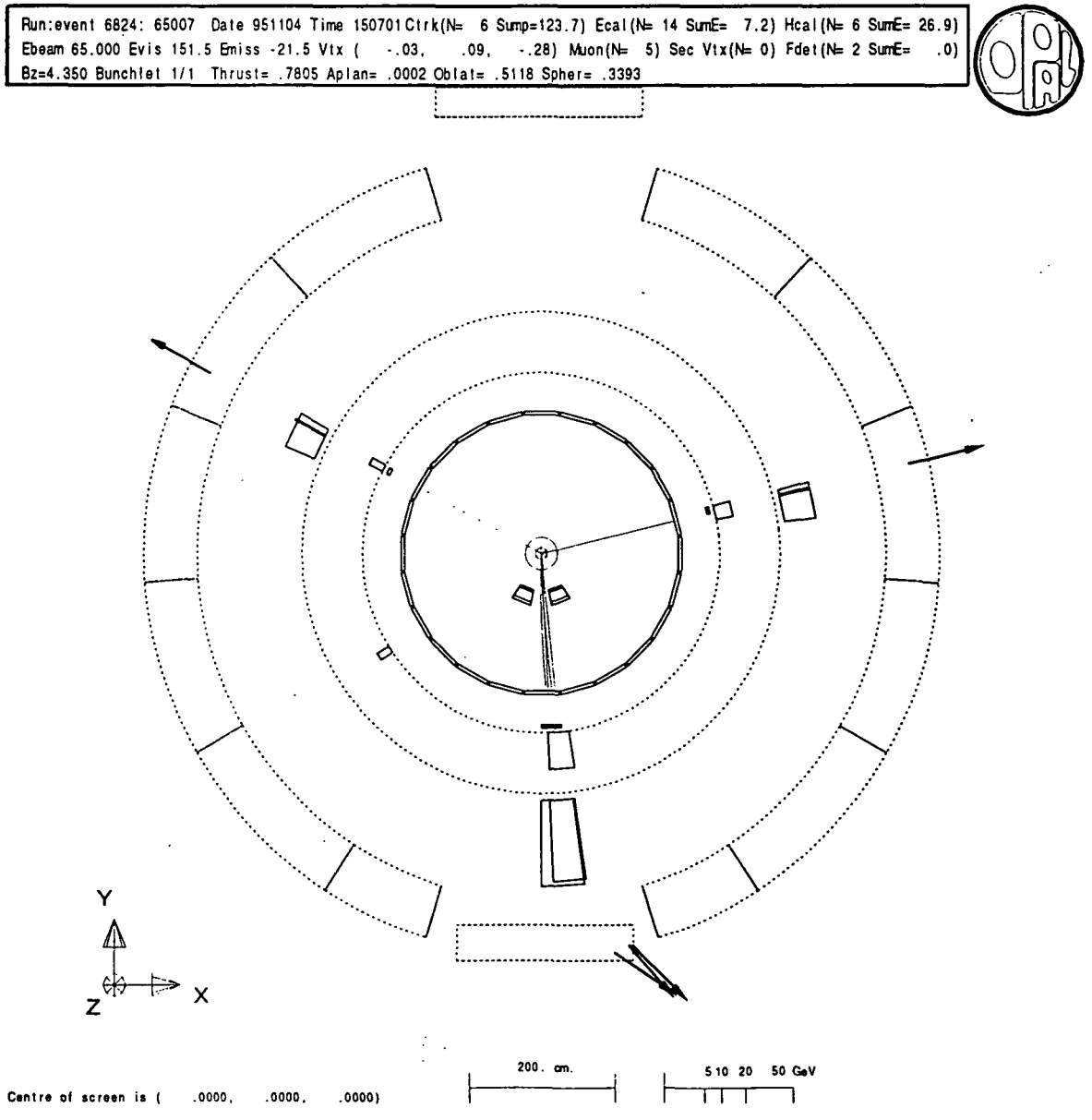

Figure 1 An example of a 'radiative return' event recorded by OPAL during LEP operation at 130 GeV. A virtual radiative photon has materialised as a quark and anti-quark (forming one combined jet) and the Z^0 has decayed to a $\mu^+\mu^-$ pair.

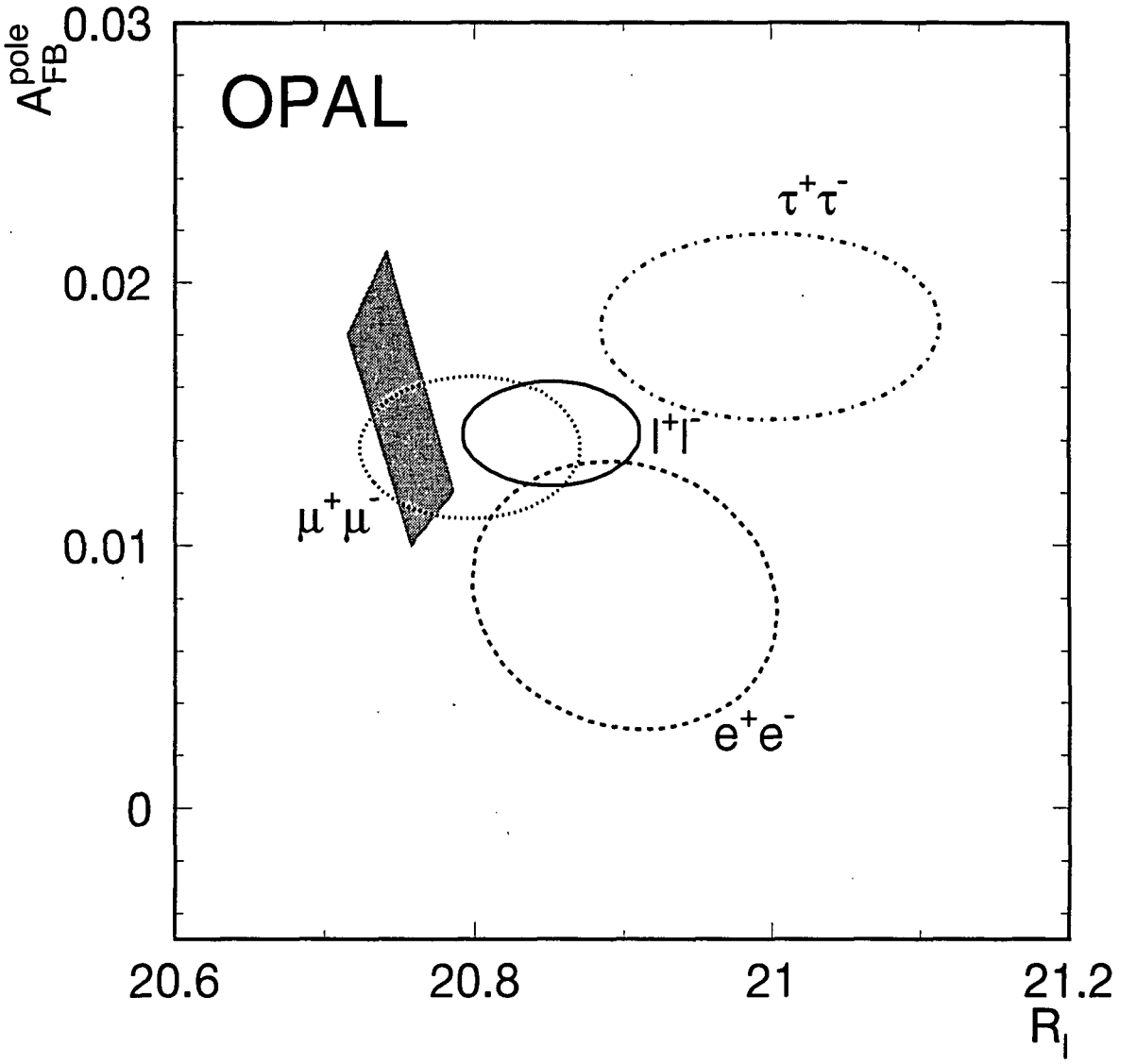

Figure 2 One standard deviation contours (39% probability content) in the $R_\ell - A_{FB}^{pole}$ plane for each lepton species and for all leptons assuming lepton universality. The shaded area is the Standard Model prediction for $50 < M_{top} < 230$ GeV and $60 < M_{Higgs} < 1000$ GeV for $\alpha_s(M_Z^2) = 0.120$.

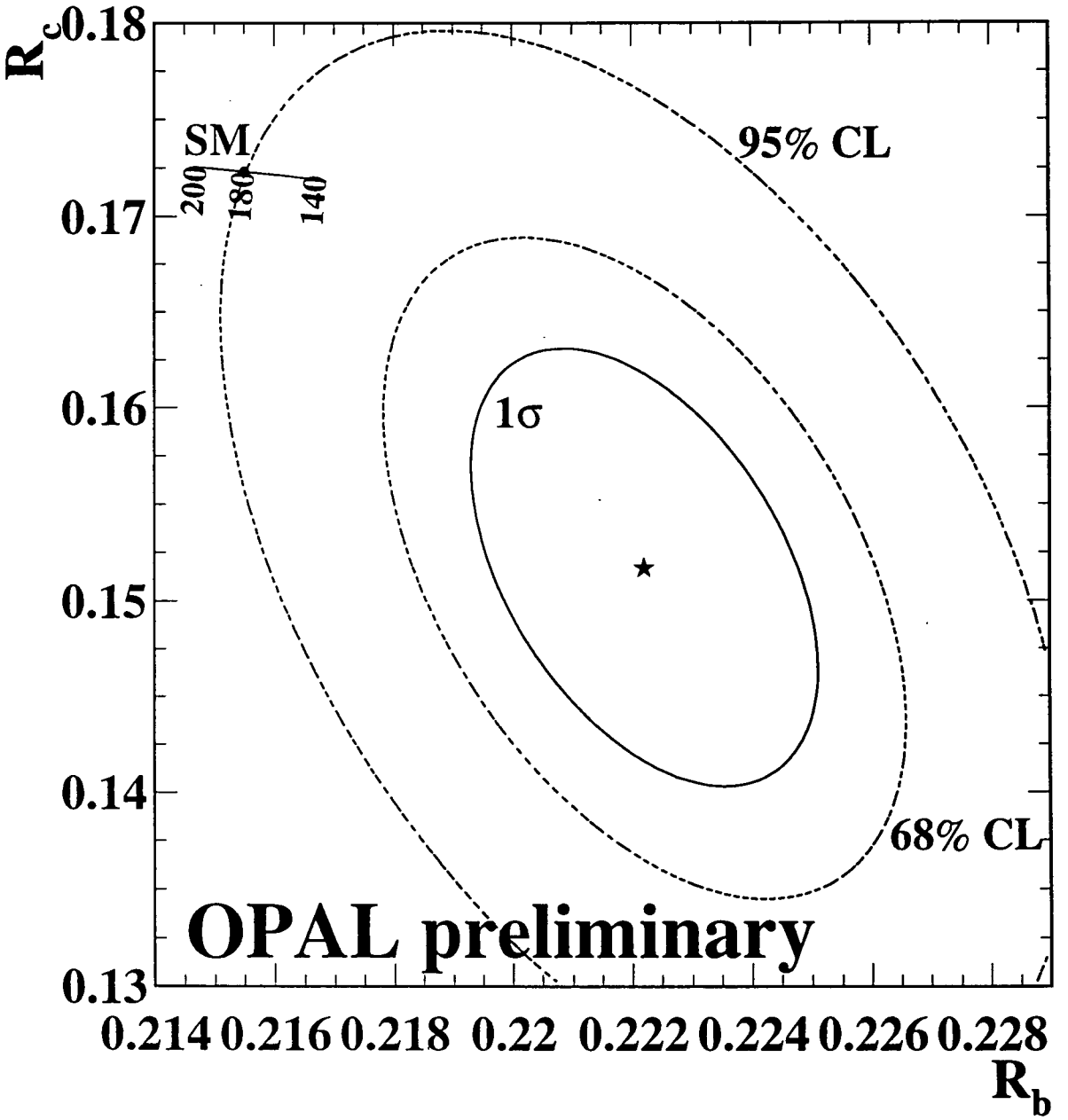

Figure 3 Comparison of OPAL measured R_b and R_c values with the Standard Model prediction (SM) for the range of top masses indicated. The central measured value is shown as a star, the 1 standard deviation contour has a 39% probability content.

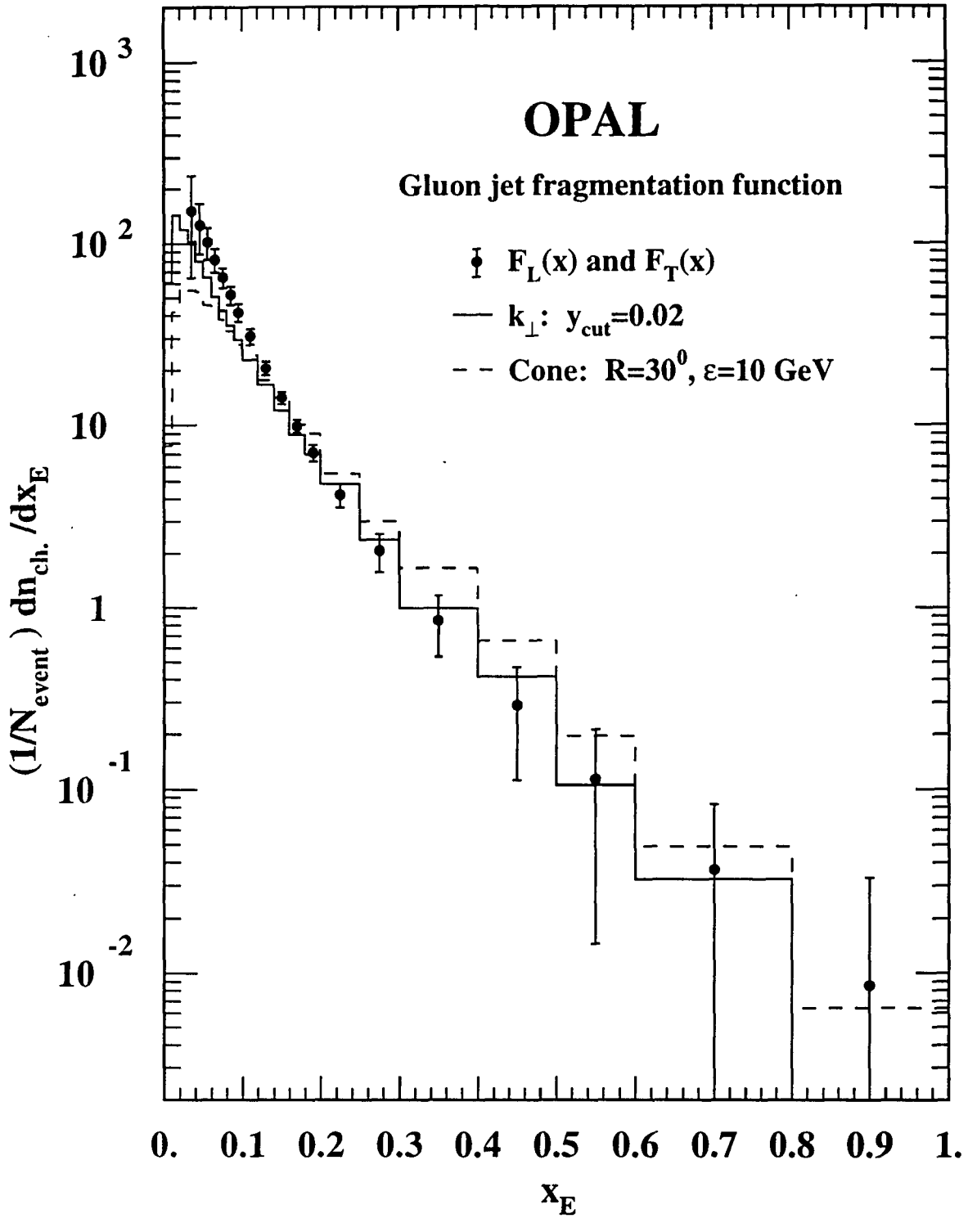

Figure 4 Gluon fragmentation function as measured by OPAL via transverse and longitudinal fragmentation functions (points) and from three-jet events with secondary vertex tag identification of quark jets (histograms) for two different jet-finders.

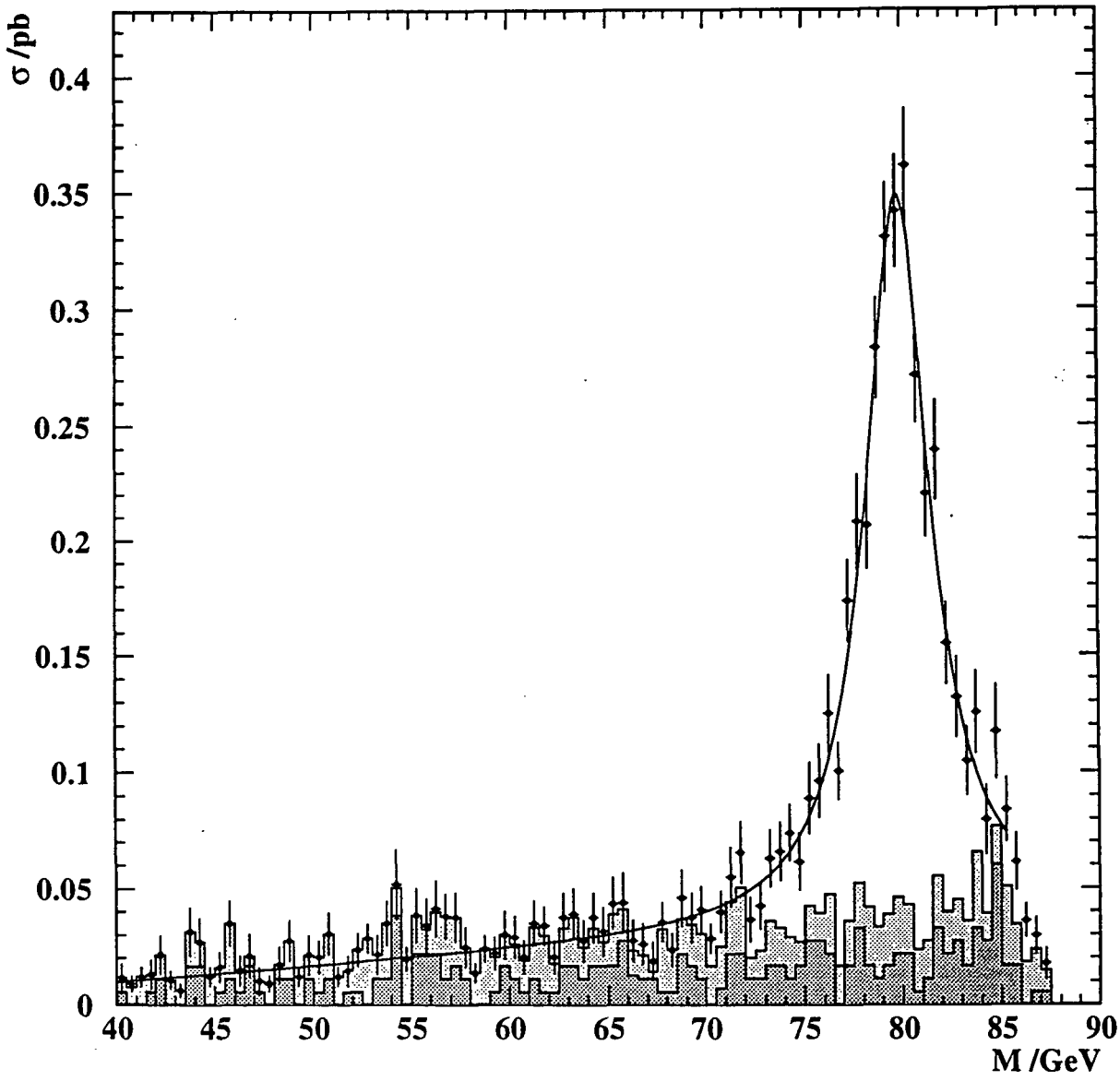

Figure 5 Simulated reconstructed jet-jet mass distribution for events selected as $W^+W^- \to q\bar{q}q\bar{q}$ candidates. The dark shaded area shows background from $e^+e^- \to (Z^0/\gamma)^*(\gamma) \to q\bar{q}(\gamma)$ and $W^+W^- \to q\bar{q}\,\ell\bar{\nu}_\ell$ events, the light shaded area shows incorrect jet-jet combinations in W^+W^- $q\bar{q}q\bar{q}$ events.

Ames; Antwerp; Athens; Bergen; Bratislava; Bologna; College de France; CERN; CRN (Strasbourg); Demokritos; Genova; Grenoble; Helsinki; IIHE (Brussels); JINR Dubna; KFK (Karlsruhe); Krakow; LAL (Orsay); Lisbon; **Liverpool**; Ljubljana; LPNHE (Paris VI); Lund; Lyon; Marseille; Milano; Mons; NBI (Copenhagen); NIKHEF (Amsterdam); Oslo; **Oxford**; Padova; Prague; **RAL**; Rio de Janeiro; Rome; Saclay; Sanita (Rome); Santander; Serpukhov; Stockholm; Tech Univ Athens; Torino; Trieste; Udine; Uppsala; Valencia; Vienna; Warsaw; Wuppertal.

Physics Results in 1995:

Publications on physics topics studied with the DELPHI detector this year have again covered a wide range of topics (see publications list attached). In addition, approximately 50 further papers were presented at the International Conferences on High Energy Physics in Brussels and Beijing, held in July and August, and are currently being prepared for publication. The following briefly summarizes some of the studies in which UK physicists have been most recently and most heavily involved:

1) Standard Model Tests :

Measurements of the mass and the partial and total widths of the Z^0 together with the forward-backward asymmetries in Z^0 decay provide a powerful test of the Standard Model. During the last year, further refinements have taken place in the determination of these quantities, and a preliminary sample of 1.14 million hadronic Z^0 decays and 54000 $Z^0 \rightarrow \mu^+\mu^-$ events, recorded at the Z^0 peak in 1994, has been added to the 1.8 million events accumulated between 1990 and 1993 at the peak and at several energies around it. This has resulted in an improvement in precision of up to 40% in the values of several parameters.

The following values of the mass and the total width of the Z^0 and of the unfolded Born cross section at the Z^0 pole have been obtained from fits to the hadronic and leptonic cross-sections and the leptonic asymmetries:

$$M_Z = 91.1849 \pm 0.0034 \text{ GeV},$$
$$\Gamma_Z = 2.4913 \pm 0.0053 \text{ GeV},$$
$$\sigma_0 = 41.39 \pm 0.10 \text{ nb}.$$

The ratios R of hadronic to leptonic decay rates were determined to be

$$R_{ee} = 20.88 \pm 0.16,$$
$$R_{\mu\mu} = 20.70 \pm 0.09,$$
$$R_{\tau\tau} = 20.61 \pm 0.16,$$

and the forward-backward asymmetry parameters for $Z^0 \rightarrow \ell\bar{\ell}$ decays were found to be

$$A^0_{ee} = 0.0233 \pm 0.0069,$$
$$A^0_{\mu\mu} = 0.0166 \pm 0.0030,$$
$$A^0_{\tau\tau} = 0.0210 \pm 0.0057.$$

These values have been combined with those of the other LEP experiments to give overall precision in M_Z of ± 2.2 MeV and in Γ_Z of ± 3.2 MeV. They have also been used to derive more precise values of additional electroweak parameters. The squares of the vector and axial vector couplings of the Z^0 to charged leptons are determined to be

$$V_l^2 = 0.00154 \pm 0.00021,$$

$$A_l^2 = 0.2507 \pm 0.0007,$$

corresponding to a value of the weak mixing angle of

$$\sin^2 \theta_{eff}^{lept} = 0.2304 \pm 0.0014.$$

The invisible and hadronic Z^0 widths have been derived to be

$$\Gamma_{\rm inv} = 503.9 \pm 4.1 \text{ MeV},$$

$$\Gamma_{\rm had} = 1736.0 \pm 5.2 \text{ MeV},$$

and, using the Standard Model prediction $\Gamma_{\nu\nu}/\Gamma_{\ell\ell} = 1.992 \pm 0.002$ and the DELPHI result $\Gamma_{\rm inv}/\Gamma_{\ell\ell} = 6.010 \pm 0.046$, the number of light neutrino species has been deduced to be

$$N_\nu = 3.017 \pm 0.023.$$

UK groups continue to be responsible for all the work on the $\mu\mu$ channel and for much of the global fitting and interpretation of the data. The asymmetry determined from the muon data taken in 1992–4 is shown in figure 1 as a function of centre-of-mass energy.

An original study has been performed by UK groups in 1994 of the interference between initial and final state radiation in the process $e^+e^- \to \mu^+\mu^-$. The effects of this interference are small when only loose cuts are placed on the phase space available to the radiated photons. However, when the radiated photon energy is restricted to be less than Γ_Z, the interference can lead to large shifts in the forward-backward asymmetry A_{FB} of the final state $\mu^+\mu^-$. This can be understood by considering the space time structure of the process and suggests that it should be possible to measure Γ_Z by examining this effect. In the analysis performed, the photon energy is restricted by indirect cuts on the acoplanarity angle of the muons. Figure 2 compares the data with theoretical predictions for A_{FB} as a function of acoplanarity, with and without interference effects. Fits to this distribution show clear evidence for radiative interference, and a value of

$$\Gamma_Z = 2.26 \pm 0.19\,(\text{stat.}) \pm 0.06\,(\text{syst.}) \text{ GeV}$$

has been extracted. This result is subject to a further theoretical error due to as yet uncalculated higher order interference terms.

2) τ physics :

UK groups continue to be deeply involved in studies of τ physics, and several new results have been derived this year.

A paper describing the measurement of the τ lifetime has been completed, in which three different methods have been used. The first two methods use events with two one-prong τ decays: in the first, the miss distance between the two tracks is measured, thus cancelling the dependence of the lifetime determination on the Z^0 decay point reconstruction, while the second method uses the correlation between the difference of the two signed impact parameters and the acoplanarity of the tracks to determine the lifetime, thus avoiding dependence on Monte Carlo simulation. Since these methods both use events of the same topology, their results are highly correlated, and they have been combined to give the value

$$\tau_\tau = 291.8 \pm 3.3\,(\text{stat.}) \pm 2.0\,(\text{syst.}) \text{ fs}.$$

In the third method, the τ decay point is reconstructed in $Z^0 \to \tau\tau$ events with 3-prong decays. Using a new tracking pattern recognition algorithm, the efficiency in reconstructing such decay vertices has been increased by 75%, and a value of

$$\tau_\tau = 286.7 \pm 4.9\,(\text{stat.}) \pm 3.3\,(\text{syst.}) \text{ fs}$$

has been determined. The combined value, $\tau_\tau = 290.3 \pm 2.7(\text{stat.}) \pm 1.8(\text{syst.})$fs, may be compared with the value of 285.7 ± 4.1fs predicted assuming lepton universality and using $BR(\tau \to e\nu\nu) = 17.50 \pm 0.25\%$ and m_τ=1777.1 $\pm$ 0.4 MeV/c^2. Alternatively, the measured lifetime may be used to determine the relative strengths of the Fermi coupling constants (g_τ/g_μ). This ratio is found to be 0.990 ± 0.009, consistent with lepton universality.

In a second published analysis in the field of τ physics, the leptonic branching ratios of the τ have been determined. The method involves a careful study of the separation of signal from background in $\tau \to e\nu\bar{\nu}$ and $\tau \to \mu\nu\bar{\nu}$ decay modes. The signal for the electron decay mode is separated from hadronic backgrounds using the distributions of ionization loss in the TPC and of the ratio of the associated electromagnetic energy deposited in the HPC to the particle momentum. Muonic τ decays are separated from hadronic background by looking at the differential energy deposition in the layers of the hadron calorimeter. Branching fractions

$$BR(\tau \to e\nu\nu) = (17.51 \pm 0.39)\,\% \text{ and}$$

$$BR(\tau \to \mu\nu\nu) = (17.02 \pm 0.31)\,\%$$

have been determined, and the ratio of the muon and electron couplings to the weak charged current is derived as

$$\frac{g_\mu}{g_e} = 1.000 \pm 0.013,$$

in conformity with $e-\mu$ universality. Alternatively, $e-\mu$ universality may be assumed, and the $e\nu\nu$ and $\mu\nu\nu$ branching fractions combined to give a value $BR(\tau \to \ell\nu\nu) = 17.50 \pm 0.25\%$ for the average branching fraction into a massless lepton.

An additional activity of the τ physics team is the measurement of the mass of the ν_τ using τ hadronic decays into three charged particles; m_{ν_τ} can be determined from the shape of the invariant mass spectrum of the seen decay products in the region of its end-point. The spectrum is shown in figure 3; it has been used to derive a preliminary value:

$$m_{\nu_\tau} \leq 37\text{MeV}.$$

3) Heavy quark physics :

UK groups have continued their activities in the field of heavy quark physics, with several new analyses in progress.

In the field of B spectroscopy, the observation of correlated $\Lambda^0 e^\pm$ and $\Lambda^0 \mu^\pm$ pairs in hadronic Z^0 decays has yielded a value for the production rate per b-quark of weakly decaying B-baryons followed by their leptonic decay of

$$f(\text{b} \to \Lambda_b^0) \times BR(\Lambda_b^0 \to \Lambda^0 \ell^- \bar{\nu} X) = (0.30 \pm 0.05\,(\text{stat.})\,^{+0.06}_{-0.05}\,(\text{syst.})\,)\%.$$

A fit to the impact parameter distribution of the muon in the $\Lambda^0\mu$ sample has been made and the lifetime of weakly decaying B-baryons measured as

$$\tau_{\Lambda_b^0} = (1.07^{+0.19}_{-0.17}\,(\text{stat.}) \pm 0.08\,(\text{syst.})\,)\text{ps}.$$

Also in progress is a search for the hitherto unobserved B_c ($\bar{b}c$) meson, predicted to have mass around 6.2-6.5 GeV/c^2 and a high branching ratio to $J/\psi + X$. A method has been developed to look for the B_c meson decay into 3 leptons and no other charged particles, which would indicate the $B_c \to J/\psi\,\ell\,\nu$ decay in events with a clear secondary vertex. The mass of the B_c would be fixed by observing the decay $B_c \to J/\psi + X$, where X is an odd number of charged hadrons.

The production of vector B^* mesons has been studied by observation of their radiative decays to pseudoscalar B mesons. In such a decay, the energy of the observed photon is below 0.8 GeV and is normally poorly measured in the electromagnetic calorimeters. However, about 5% of such photons convert to e^+e^- pairs in the detector before the TPC, and an algorithm has been developed to reconstruct them, achieving resolutions of 1% in energy and 1.5 mrad in angle. The mass difference $\Delta m_{(B^*-B)}$ is to a good approximation estimated as $E_\gamma \gamma_B (1 - \beta_B \cos\theta_{B\gamma})$, where E_γ is the measured energy of the photon, γ_B and β_B are the boost factor and velocity of the b-hadron system and $\theta_{B\gamma}$ is the angle between the b-hadron and the photon. Figure 4 shows the distribution of this quantity from analysis of the 1991–94 data. From the clear peak seen, a value

$$\Delta m_{(B^*-B)} = 0.0456 \pm 0.0003 \text{ (statistical only) GeV/c}^2$$

has been determined, and the mean B* yield is estimated as 0.25 ± 0.01(statistical only) per hadronic Z^0 decay.

The rate of b hadron decays into neutral strange particles has been determined in a study of events tagged as $Z^0 \to b\bar{b}$ by a successful b-tag in one hemisphere (defined by the event thrust axis) and with a K^0 or Λ^0 observed in the opposite hemisphere. The strange hadrons can originate either from b hadron decays or from fragmentation, but these two sources have very different rapidity distributions, the shapes of which are predicted by standard hadronization routines. From fits to the rapidity distributions, branching ratios

$$BR(\text{b}-\text{hadron} \to K^0_s X) = 0.290 \pm 0.011\,(\text{stat.}) \pm 0.027\,(\text{syst.}),$$
$$BR(\text{b}-\text{hadron} \to \Lambda^0 X) = 0.059 \pm 0.007\,(\text{stat.}) \pm 0.009\,(\text{syst.}) \text{ and}$$
$$BR(\text{b}-\text{baryon} \to \Lambda^0 X) = 0.28^{+0.17}_{-0.12}$$

have been determined.

The study of strange particle production has continued with a new publication of the observed rates of Ξ^-, $\Xi^0(1530)$ and $\Sigma^\pm(1385)$ production in Z^0 decays. In addition, the rates of K^0, Λ^0 and Ξ^- production have been determined as a function of the event topology, and compared with the predictions of the JETSET hadronization program for the relative rates of production of each of these particles in events with two or more than two jets. Significant disagreement is observed in some rates. The study will continue with the addition of more data, and the final results used to adjust the tuning of strange particle production parameters in JETSET.

The search for the Higgs boson, which will be one of the major activities at LEP2, and the heightened interest in the measurement of the ratio $\Gamma_{b\bar{b}}/\Gamma_{had}$ in Z^0 decays make it of great importance to develop the most efficient and purest possible b quark tag. Up to now, this has generally been considered to be that based on the Borisov method, in which the probability that the event contains a b decay vertex is estimated by combining the probabilities that each track comes from the Z^0 decay point, using their measured impact parameters. An improved method has been devised, in which probabilities are estimated using not only the impact parameter of each track, but also other kinematic variables, such as momentum and angle with respect to the jet axis. The expected distributions of these variables in the DELPHI detector for b quarks, c quarks and light quarks are derived from the detector simulation program, and hence the separate probabilities of the event containing any of these quark species can be evaluated. The curves of efficiency versus purity obtained by varying the cut on the combined b confidence are shown for the two methods in figure 5; the improvement achieved with the new method is evident.

Physics at LEP2

During 1995, intensive preparations have been made for the forthcoming upgrade of LEP to run at energies above the WW threshold. Much of the activity has centred around a CERN workshop with participation from all the LEP experiments as well as from theorists, for which a detailed report is in preparation. UK DELPHI physicists have played a prominent role in this work.

The opening of the $e^+e^- \rightarrow W^+W^-$ channel will allow two measurements, those of the W mass and of the trilinear couplings of gauge bosons (TGCs), to be made with considerably greater accuracy than has hitherto been possible. Both of these measurements are of great importance in tests of the Standard Model and in the search for the physics which lies beyond it. The importance of a precise measurement of M_W, for instance, has been quantified using the model-independent parameters of Altarelli et al. The parameter ϵ_2 can only be improved by a precise measurement of M_W. The current error, corresponding to $\delta M_W = 180$ MeV/c^2, is $\delta\epsilon_2 = \pm 0.0040$. The range of precision on M_W which can be expected from LEP2, assuming an integrated luminosity of about 500 pb^{-1} per experiment, is from ± 25 to ± 50 MeV/c^2; for $\delta M_W = 25$ MeV/c^2, the error on ϵ_2 would be reduced to $\delta\epsilon_2 = \pm 0.0011$.

In both W mass and TGC studies, the availability of reliable Monte Carlo generators is of great importance. A detailed comparison of the predictions of different codes has been carried out, resulting in an essential standardization of their running parameters. A particular study has been made of the 4-fermion generator ERATO, in which the three Feynman diagrams responsible for on-shell WW production are supplemented by the (up to 20) diagrams needed to describe the general $e^+e^- \rightarrow f_1\bar{f}_2f_3\bar{f}_4$ final state. This code has been interfaced to the JETSET hadronization program, and hence to the DELPHI detector simulation code.

Studies of TGC measurements at LEP2 have included an examination of whether it will be possible to distinguish different models of deviations from Standard Model predictions in maximum likelihood fits to all the available kinematic information in each event. Figure 6 indicates that this can indeed be achieved for values of TGC parameters differing from the SM predictions by a few times the expected LEP2 statistical precision. The method uses the known statistical property that a χ^2 distribution can be derived from the ratio of likelihoods of two hypotheses applied to the same data if the parameters of the two hypotheses belong to the same parametric family. In the figure, χ^2 probability distributions are shown when such tests are applied to event samples generated with non-SM values of one TGC and analyzed with a model corresponding to the same, "true" hypothesis, and with a "wrong" one. It can be seen that a simple comparison of the values of these probabilities indicates the correct model in the majority of cases and, in addition, the absolute probability value indicates the goodness of the fit.

The analysis of the final states $jj\ell\nu$, $jjjj$ and $\ell\nu\ell\nu$ from WW production (where j represents the jet fragmentation of a quark or antiquark, and $\ell\nu$ a charged lepton-antilepton pair) will proceed in several stages: the selection of event samples of acceptable efficiency and purity; the possible use of kinematic fitting to impose energy and momentum conservation (and, possibly, W mass constraints); and extraction of the TGC parameters using a statistical technique such as the maximum likelihood method mentioned above. Each of these stages has been studied in detail using fully simulated data. It has been concluded that good efficiency and purity can be achieved in each of the final states; for instance, in the $jj\ell\nu$ channel, $\epsilon \sim 70\%$ and $P \sim 95\%$ can be expected. The effect of kinematic fitting can be seen in figure 7, where distributions of the jet energy residuals and of the W production angle in reconstructed $jj\ell\nu$ events are shown before and after application of the fit. It is of great importance to understand and correct the biases in parameters determined from the data, incurred by application of the analysis procedure. These have been quantified — they amount to $\sim$ a few times the expected statistical precision, — and methods of dealing with them in the analysis are being studied.

Detector upgrades and performance

The performance, reliability and understanding of all the DELPHI detector components have continued to improve this year. In particular, the hardware items for which UK groups have responsibility, namely the Outer Detector, Barrel Muon Chambers and Micro–Vertex Detector, all continue to perform excellently and have been tested to be compatible with LEP bunch train operation. The Outer Detector has been shown able to provide a reliable tag of the bunch number within the train. In parallel, the Data Acquisition control system and Slow Control system, for which UK physicists are responsible, have performed very efficiently throughout the 1995 data-taking period.

UK physicists have continued their involvement with the upgrading of the Micro–Vertex Detector. The inclusion in 1994 of a layer to provide z as well as $R\phi$ measurements has resulted in much improved precision in both primary and secondary vertex reconstruction. Plans for a further upgrade during the 1994-5 shutdown were postponed due to late delivery of the detectors; however, this development will take place, ready for data-taking in 1996, in conjunction with the installation of a Very Forward Tracking device. The upgrade of the Micro–Vertex Detector involves extending the outermost layer down to 25°. Because of the large area involved, pairs of single-sided detectors glued back-to-back will be used instead of double-sided ones. The readout will again be routed over a second metal layer integrated onto the detector. This development has been carried out by the UK groups in collaboration with Micron Semiconductor (UK) Ltd, and the construction and testing of one half of the modules is being carried out in UK laboratories.

At the start of data-taking in 1995 DELPHI was equipped with a new extended Inner Detector. The development included the replacement of the Inner Detector trigger chambers by a five layer straw tube detector with angular coverage down to 15°. UK physicists participated in the commissioning of this detector, which subsequently ran successfully during the year.

During 1995, a substantial amount of development work was carried out on the LEP machine in order to prepare it for high energy running in 1996. In addition to this, however, LEP provided e^+e^- collisions at the Z^0 peak and at energies at 2 GeV on either side of it, and DELPHI collected $16.7pb^{-1}$ at the peak and $9.1pb^{-1}$ and $9.3pb^{-1}$ at 89.2 and 93.2 GeV, respectively. The final LEP running period, although designated primarily a technical run, proved to be a very successful first venture into high energy running, with a peak of 70 GeV per beam achieved. With the DELPHI detector performing extremely well, $6.0pb^{-1}$ were collected, mainly at a centre-of-mass energy of 136 GeV. Figure 8 shows one of the beautiful events recorded in this new energy regime.

DELPHI Publications in the last year:

1. First evidence of hard scattering processes in single tagged $\gamma\gamma$ collisions
   P. Abreu et al.
   Phys. Lett. B342 (1995) 402

2. Measurement of $\frac{\Gamma_{b\bar{b}}}{\Gamma_{had}}$ using Impact Parameter Measurements and Lepton Identification
   P. Abreu et al.
   Zeit. Phys. C66 (1995) 323

3. Measurement of the Forward-Backward Asymmetry of charm and bottom Quarks at the Z Pole using $D^{*\pm}$ Mesons
   P. Abreu et al.
   Zeit. Phys. C66 (1995) 341

4. Observation of Orbitally Excited B Mesons
   P. Abreu et al.
   Phys. Lett. B345 (1995) 598

5. First Measurement of the Strange Quark Asymmetry at the Z^0 Peak
   P. Abreu et al.
   Zeit. Phys. C67 (1995) 1

6. Search for heavy neutral Higgs bosons in two-doublet models
   P. Abreu et al.
   Zeit. Phys. C67 (1995) 69

7. Measurements of the τ Polarisation in Z^0 decays
   P. Abreu et al.
   Zeit. Phys. C67 (1995) 183

8. Strange baryon production in Z hadronic decays
   P. Abreu et al.
   Zeit. Phys. C67 (1995) 543

9. Production of Charged Particles, K^0_S, $K^{\pm}$, p and Λ in $Z \to b\bar{b}$ Events and in the Decay of b Hadrons
   P. Abreu et al.
   Phys. Lett. B347 (1995) 447

10. Inclusive Measurements of the $K^{\pm}$ and $p/\bar{p}$ Production in Hadronic Z^0 Decays
    P. Abreu et al.
    Nucl. Phys. B444 (1995) 3

11. A Measurement of B^+ and B^0 Lifetimes using $\overline{D}\ell^+$ events
    P. Abreu et al.
    Zeit. Phys. C68 (1995) 13

12. B^* Production in Z Decays
    P. Abreu et al.
    Zeit. Phys. C68 (1995) 353

13. Lifetimes of Charged and Neutral B Hadrons using Event Topology
W. Adam et al.
Zeit. Phys. C68 (1995) 363

14. Lifetime and production rate of beauty baryons from Z decays
P. Abreu et al.
Zeit. Phys. C68 (1995) 375

15. Production of strange B-baryons decaying into $\Xi^{\mp} - \ell^{\mp}$ pairs at LEP
P. Abreu et al.
Zeit. Phys. C68 (1995) 541

16. Study of Prompt Photon Production in Hadronic Z^0 Decays
P. Abreu et al.
Zeit. Phys. C69 (1995) 1

17. Observation of short range three-particle correlations in e^+e^- annihilations at LEP energies
P. Abreu et al.
Phys. Lett. B355 (1995) 415

18. Search for exclusive charmless B meson decays with the DELPHI detector at LEP
P. Abreu et al.
Phys. Lett. B357 (1995) 255

19. A Measurement of the τ Leptonic Branching Fractions
P. Abreu et al.
Phys. Lett. B357 (1995) 715

20. Upper limits on the branching ratios $\tau \to \mu\gamma$ and $\tau \to e\gamma$
P. Abreu et al.
Phys. Lett. B359 (1995) 411

21. The DELPHI Silicon Strip Microvertex Detector With Double Sided Readout
V. Chabaud et al.
CERN PPE/95-86
Submitted to **Nucl. Instrum. Methods A (1995)**

22. A measurement of the photon structure function F_2^{γ} at an average Q^2 of 12 GeV^2/c^4
P. Abreu et al.
CERN PPE/95-87
Submitted to **Zeit. Phys. C (1995)**

23. Measurement of $\Delta^{++}(1232)$ Production in Hadronic Z Decays
P. Abreu et al.
CERN PPE/95-130
Submitted to **Phys. Lett. B (1995)**

24. Measurement of Inclusive π^0 Production in hadronic Z^0 Decays
W. Adam et al.
CERN PPE/95-144
Submitted to **Zeit. Phys. C (1995)**

25. Search for Promptly Produced Heavy Quarkonium States in Hadronic Z Decays
P. Abreu et al.
CERN PPE/95-145
Submitted to **Zeit. Phys. C (1995)**

26. A Precise Measurement of the Tau Lepton Lifetime
P. Abreu et al.
CERN PPE/95-154
Submitted to **Phys. Lett. B (1995)**

27. Energy Dependence of the Differences between the Quark and Gluon Jet Fragmentation
P. Abreu et al.
CERN PPE/95-164
Submitted to **Zeit. Phys. C (1995)**

International conference presentations by UK physicists in last year:

Electroweak results at LEP
G.R. Wilkinson,
Invited review talk,
Rencontres Internationales de La Vallee D'Aoste,
La Thuile, Italy,
March 1995.

WW Physics at LEP2
R.L. Sekulin,
Invited review talk,
International Europhysics Conference on High Energy Physics,
Brussels,
July 1995.

Production of heavy flavours by neutrinos
J. Guy,
Invited review talk,
International Europhysics Conference on High Energy Physics,
Brussels,
July 1995.

Review of experimental results on precision tests of electroweak theories
P.B. Renton,
Invited review talk,
XVIIth International Symposium on Lepton-Photon Interactions,
Beijing, China,
August 1995.

Recent DELPHI results on differences between quark and gluon jets
J. Guy,
Invited review talk,
XXV International Symposium on Multiparticle Dynamics,
Slovakia,
September 1995.

Experimental topics in B physics
W. Venus,
Invited review talk,
Workshop on Weak Interactions and Neutrinos WIN95
Talloires, France,
September 1995.

B hadron decay rates
W. Venus,
Invited review talk,
Workshop on e, b, t physics
Rio de Janiero, Brazil,
February 1995.

Talks by UK students at the Telford IOP conference, April 1995

P.J. Holt (Oxford)
A first study of the interference between initial and final state radiation at Z energy.

I. Last (Liverpool)
Observation of B* mesons at DELPHI.

Theses completed by UK students in the last year:

J.D. Richardson (Liverpool)
The Design and Evaluation of an LHC Prototype Double-sided Silicon Microstrip Detector and Measurement of the Tau Lifetime.

R.A. Campion (Liverpool)
A Study of Strange and Charm Particle Production in Heavy Quark Decays using the Delphi Detector at LEP.

J. Davies (Liverpool)
A Measurement of the Cross-section and Forward-Backward Asymmetry of the Tau Lepton using the Delphi Detector at LEP.

S. Bosworth (Oxford)
A measurement of the B-baryon lifetime.

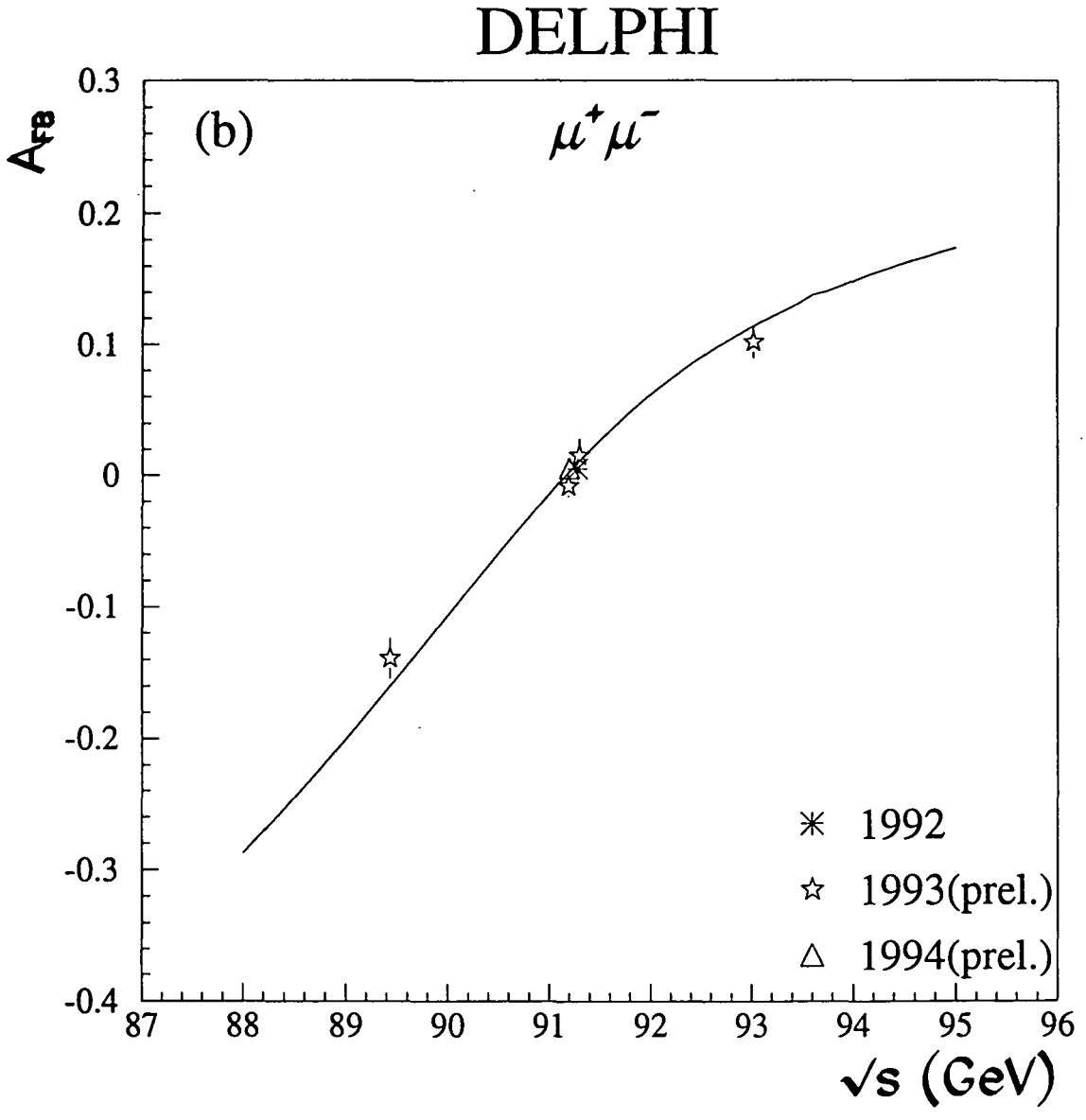

Figure 1: Forward-backward asymmetry in the $\mu^+\mu^-$ channel as a function of centre-of-mass energy with data taken from 1992–4. The asymmetry has been extrapolated to the full solid angles and corrected for acollinearity and momentum cuts. The curve is the result of a 5-parameter fit of electroweak parameters to the data shown and to other DELPHI hadronic and leptonic data.

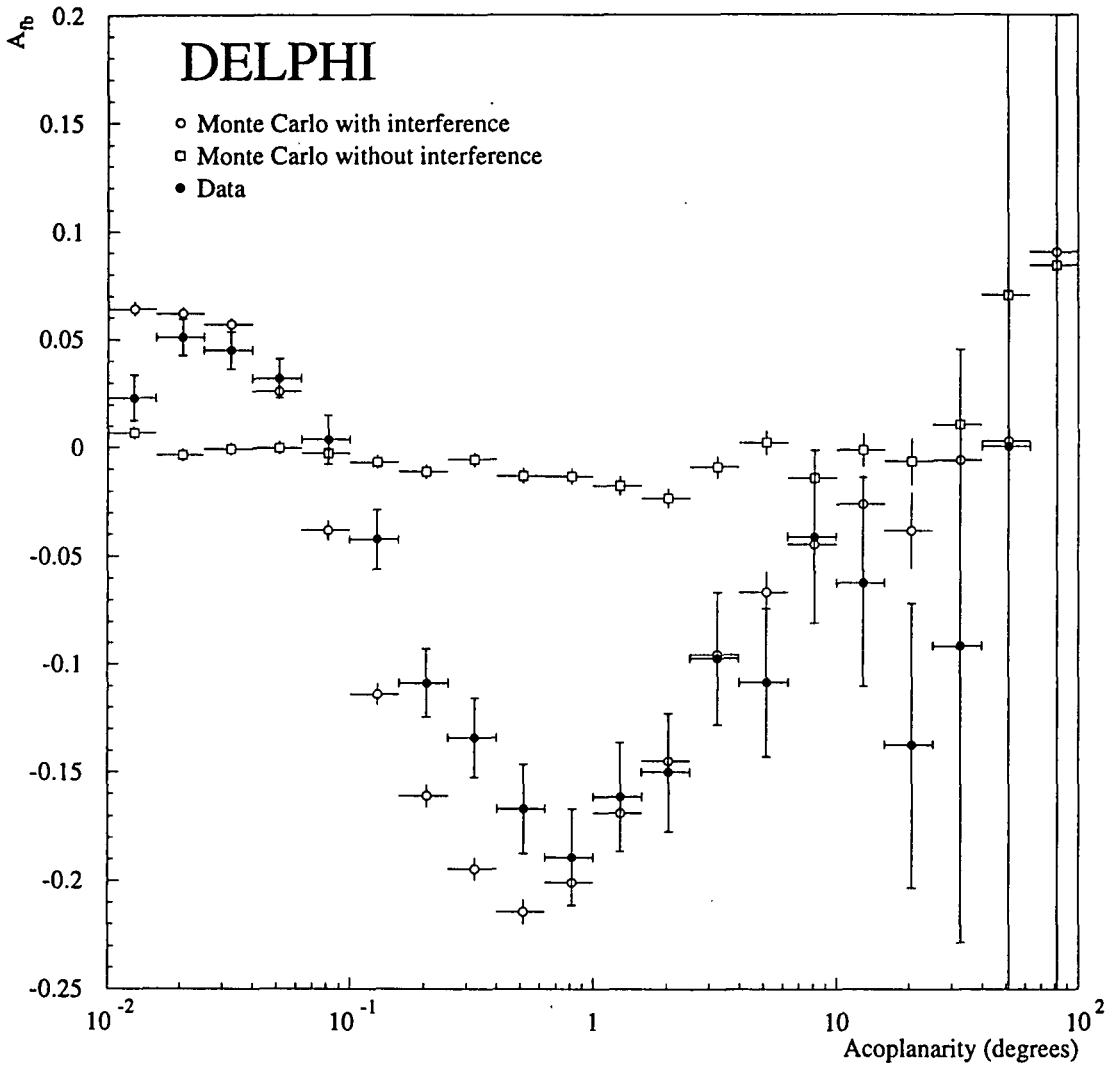

Figure 2: The forward-backward asymmetry observed in $e^+e^- \to \mu^+\mu^-$ at centre-of-mass energy $\sim M_Z$ as a function of acoplanarity, compared with theoretical predictions from the generator KORALZ, with and without interference between initial state and final state radiation.

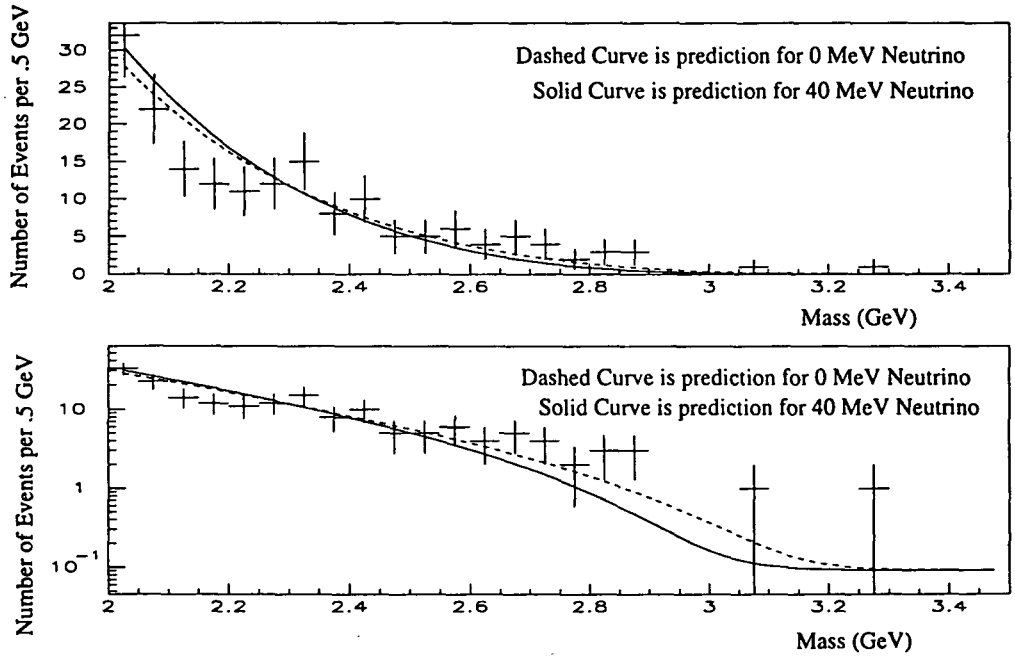

Figure 3: Invariant mass spectrum of the charged tracks from 3-prong τ decays plotted (top) linearly and (bottom) logarithmically. The curves show the predictions for two values of m_{ν_τ}.

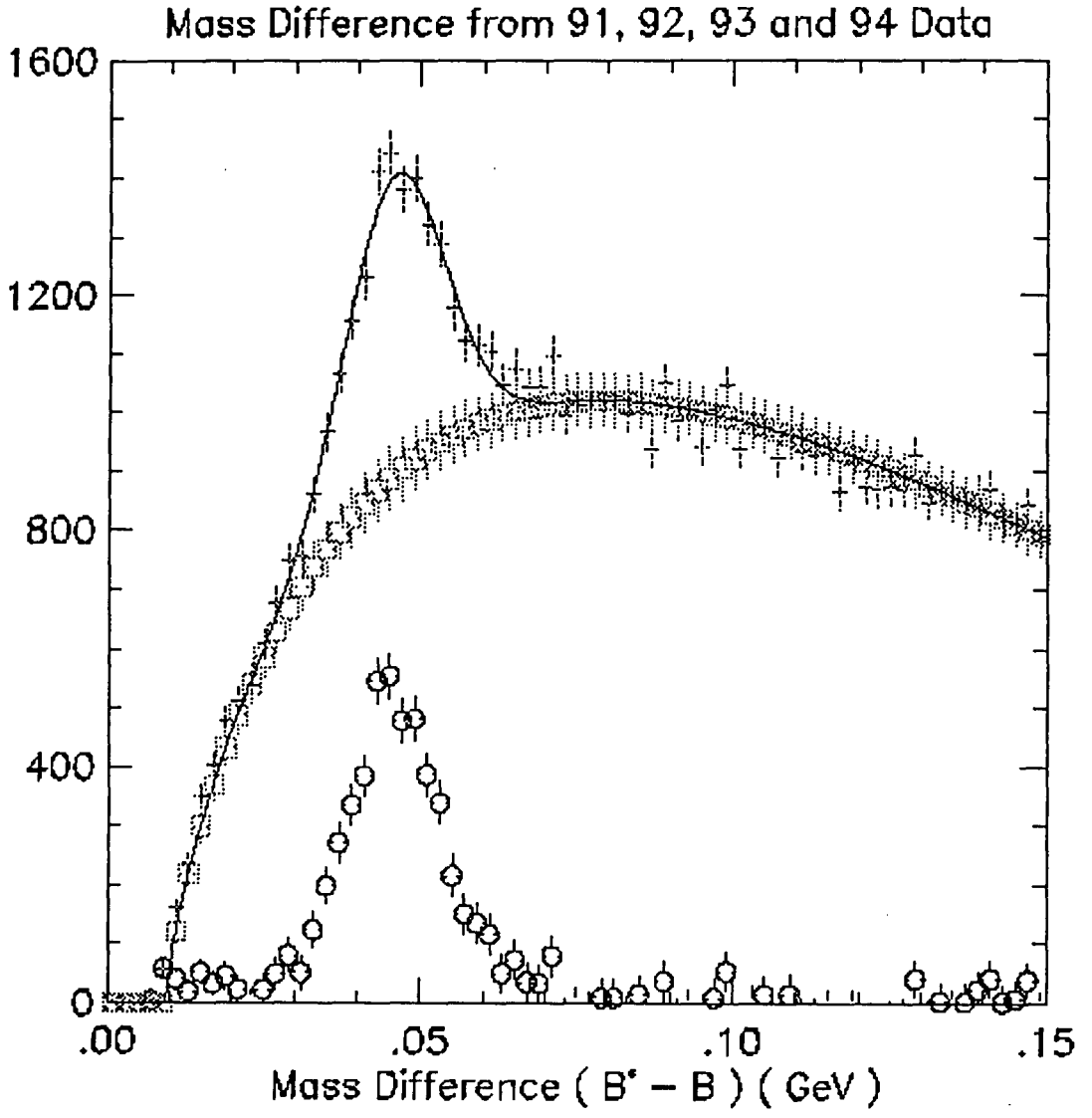

Figure 4: $B^* - B$ mass difference for reconstructed candidates in the 1991–1994 data sample. The points represent the data, the open squares correspond to the predicted background, and the open circles show the background–subtracted signal.

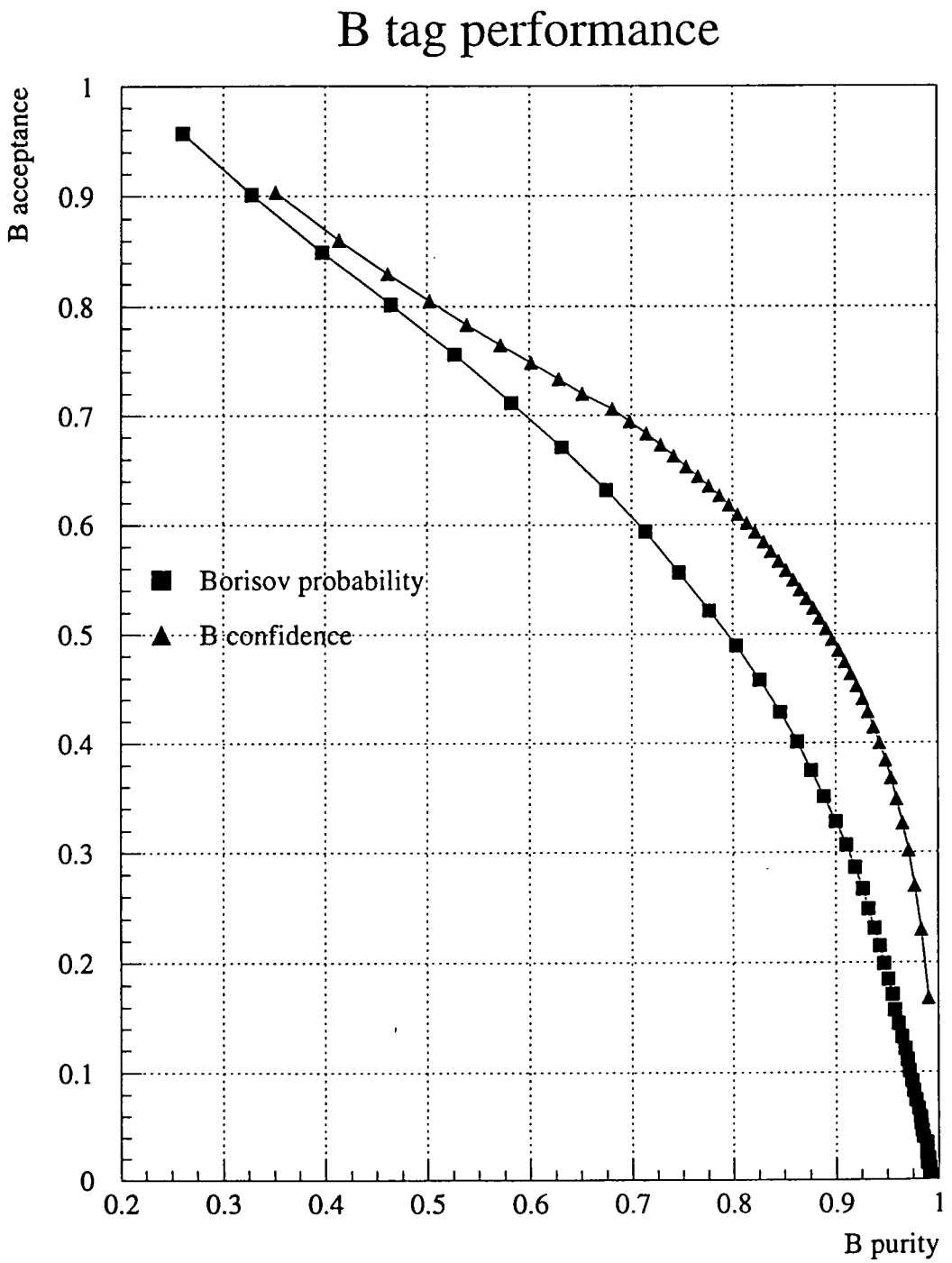

Figure 5: Efficiency as a function of purity obtained for the event b tag described in the text, compared with that obtained the Borisov tagging method.

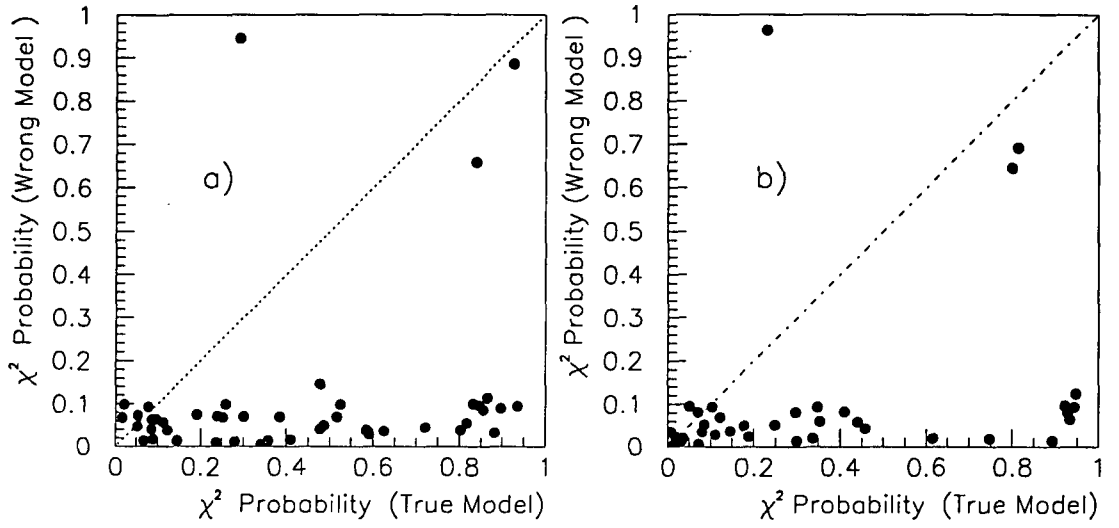

Figure 6: Two methods of hypothesis testing applied to maximum likelihood fits of TGC parameters to simulated $e^+e^- \to jj\ell\nu$ events at 190 GeV: a) the likelihoods of fits to P_1, (the "correct" hypothesis) and P_2, (the "wrong" hypothesis) are compared with that of the 2-parameter fit to P_1 and P_2; b) the likelihoods of the 1-parameter fits are compared with that of a fit to the hypothesis that the data is described by the models parametrized by P_1 OR P_2. Each data set consists of about 2500 events generated with TGC parameters deviating from Standard Model values by one to five times the expected LEP2 precisions.

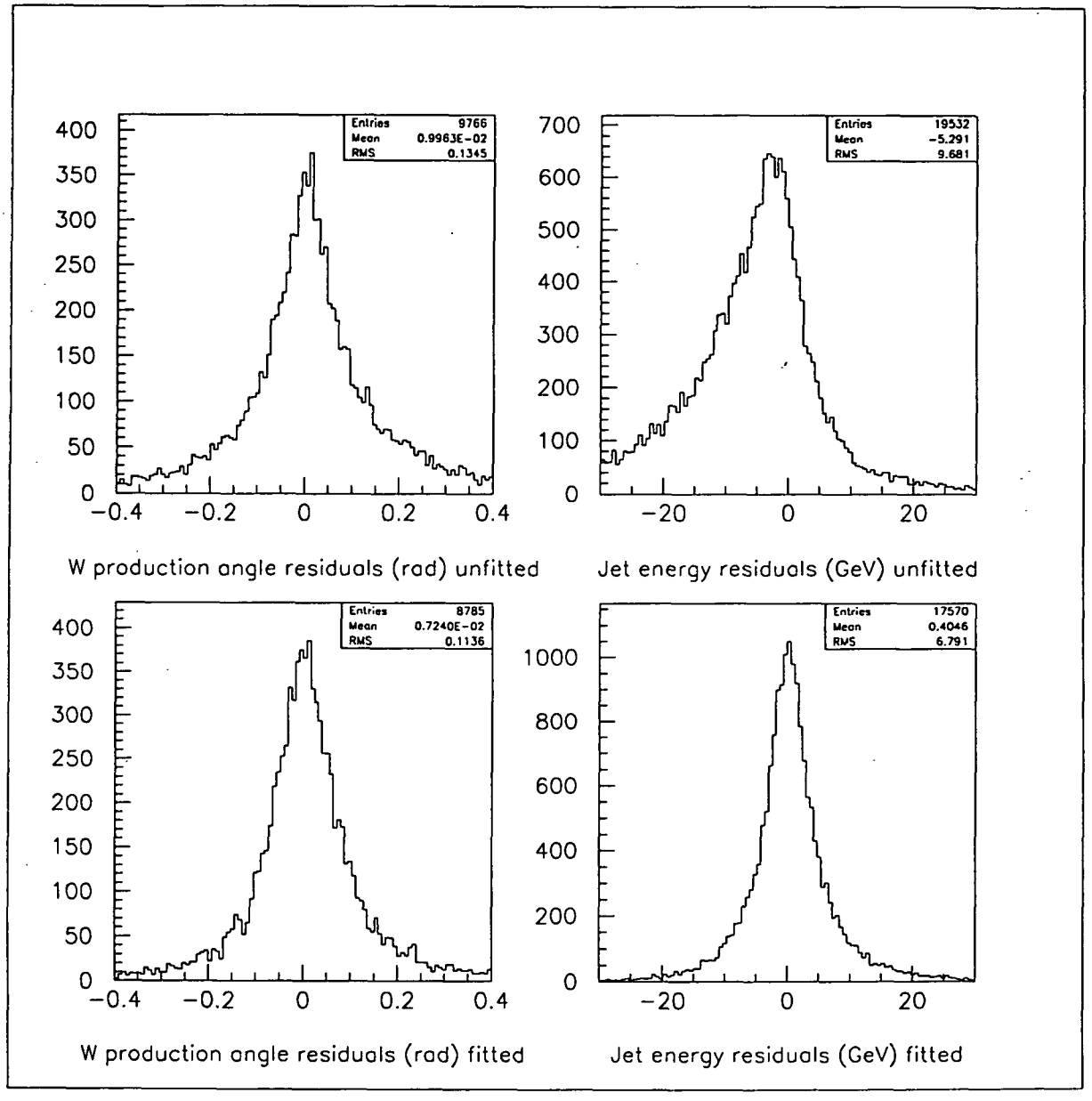

Figure 7: Resolutions in the W production angle (left-hand plots) and in the jet energies (right-hand plots) from simulated $e^+e^- \to jj\ell\nu$ events at 190 GeV. The resolutions are estimated as the differences between reconstructed and generated values of the variables. They are shown evaluated before (upper row) and after (lower row) application of a kinematic fit to the data, imposing 4-momentum conservation and constraining M_{jj} and $M_{\ell\nu}$ to be compatible with the W mass.

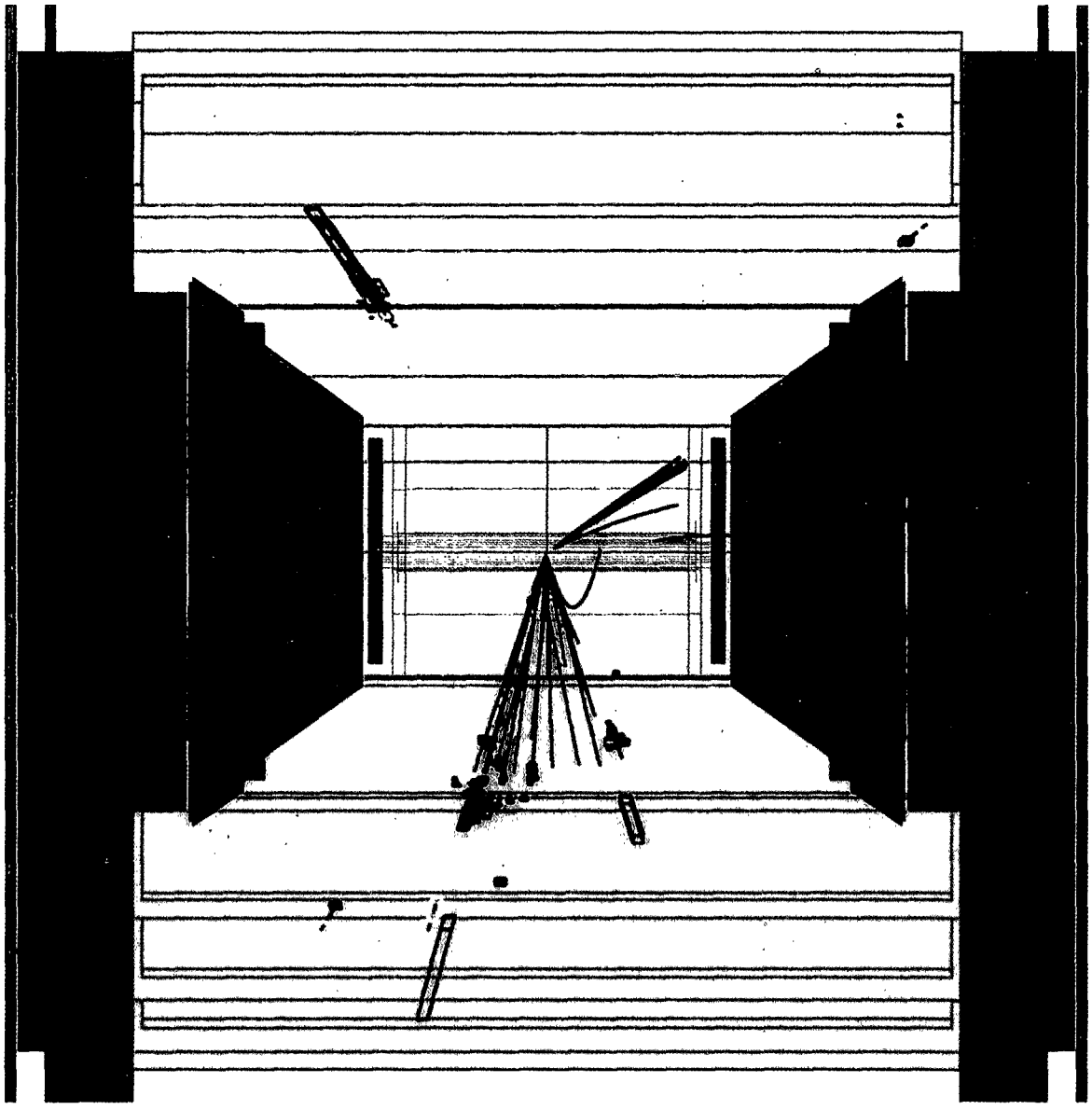

Figure 8: An event corresponding to the reaction $e^+e^- \rightarrow Z^0\ \gamma$ at centre-of-mass energy of 140.2 GeV observed in the DELPHI detector. The two jets from Z^0 decay and the deposition of energy in the HPC (barrel electromagnetic calorimeter) from the large-angle γ can be clearly seen.

High Energy Electron–Proton Physics at HERA

H1 COLLABORATION PROPOSAL 750

The Universities of Birmingham, Glasgow, Lancaster, Liverpool, and Manchester, Queen Mary and Westfield College, University of London, and Rutherford Appleton Laboratory

with

RWTH Aachen (I and III Inst.), Humboldt Univ. Berlin, Universities of Brussels, Cracow, California (Davis), and Dortmund, CEA Saclay, DESY–Hamburg, DESY–Zeuthen, Universities of Hamburg (I and II Inst.) and Heidelberg, MPI Heidelberg, Universities of Kiel, Kosice, and Lund, CPPM-Marseille, ITEP Moscow, LPI Moscow, MPI Munich, LAL Orsay, Ecole Polytechnique, Universities of Paris VI, Paris VII, Prague, and Rome, PSI-Villigen, University of Wuppertal, ETH Zürich and University of Zürich

1 Introduction and Overview

HERA commenced operation in 1995 in April with the usual period of machine physics. By mid-May, positron-proton luminosity was achieved for physics, and H1 commenced data taking. Peak luminosity at the beginning of electron fills regularly reached about 20% of design. For the first time, HERA delivered simultaneously luminosity for physics in three interaction regions, for the H1 and ZEUS collider experiments and in the East Hall for the newly installed HERMES polarised gas jet experiment. Data–taking in the H1 interaction region took some time to establish with conditions of low background. In the subsequent months to the beginning of November data were accumulated with daily integrated luminosity sometimes reaching $100\,\mathrm{nb}^{-1}$. At the time of writing (end October 1995), HERA had delivered $8\,\mathrm{pb}^{-1}$ of integrated luminosity to H1. The on–going status of HERA operation is in < http : //www – mpy.desy.de/desy – acc.html > on World Wide Web.

Throughout 1995 data taking, all of the H1 detector components which were designed and built by the UK groups were operational. These include the Superconducting Solenoid (RAL), the Forward Track Detector which extends the reconstruction of charged particles down to within about 5° of the proton beam (RAL, Glasgow, Lancaster, Liverpool, Manchester), the H1 Central Data Acquisition System (RAL), the H1 central trigger control (RAL), and the Forward Muon Detector (Manchester) and Trigger (Birmingham, QMW) which provide muon identification and reconstruction also in this forward region. In addition the first parts of the H1 upgrade program were operational for the first time. The on–going status of H1 operation is in < http : //dice2.desy.de/ >.

The new backward calorimeter (SPACAL) took data with all its advertised features working, namely excellent energy resolution, fast inter-bunch timing response, and triggering. Parts of the tracking upgrade using silicon microvertex detectors in both the central and the forward regions, also took data. The Forward Proton Spectrometer (FPS) was operational throughout the 1995 running period. The UK groups from Birmingham and QMW, with support from RAL,

are responsible for the timing monitoring of the SPACAL. The H1 group at RAL is responsible for the read-out and data acquisition of the silicon detectors. Lancaster contributed to the construction of the FPS. In addition scintillator detectors were added in the forward direction by Manchester and QMW to enhance both ToF and proton remnant tagging.

Throughout 1995, analysis of the data taken both in 1993 and in 1994 has continued. Work is in progress on many aspects of photoproduction and electroproduction in the kinematic regions to which HERA provides unique experimental access. The accumulation of data in 1994 and the development of appropriate analysis techniques have meant that now first measurements of the partonic sub-structure of the proton, of the photon, and of diffractive exchange are complete. These, plus initial studies of neutral and charged current ep physics at high Q^2 and searches for new phenomena, form the backbone of the present physics program at of H1 at HERA. As the luminosity increases, the scope and precision of this program grows as the unique challenges posed by the operation of HERA, the world's first collider of different particle species, continue to be met and the operational luminosity and duty cycle continue to improve. The on-going status of H1 physics in the form of publications is in < http : //dice2.desy.de/psfiles/papers/list.html >.

2 Deep–Inelastic Physics

H1's first measurements of the proton structure function F_2 in the new kinematic region of deep–inelastic ep scattering at low Bjorken–x [1, 2, 3] have now been analysed in the context of DGLAP QCD evolution to isolate and quantify the dominant parton contribution due to gluons [4]. With this in mind the interests and activities of the H1–UK groups are concerned with related physics which probes further the way QCD governs the structure of the proton, the way it interacts, and the dynamics of hadronisation. These activities are reported on below.

2.1 Quark Fragmentation in Deep–Inelastic Scattering

The comparison of the fragmentation of quarks in deep–inelastic ep collisions with e^+e^- collisions provides a unique insight into parton dynamics. QCD drives quark fragmentation and so a careful experimental comparison helps our understanding of the complex nature of the process. Distributions of the final state charged hadrons are compared with their equivalent distributions in e^+e^- collisions [5, 6]. The underlying processes are shown schematically in figures 1a and b). H1's analysis has demonstrated that the quarks emerging from within the proton, in ep interactions, as a result of large momentum transfer (Q^2) from a virtual photon, reveal themselves in an essentially identical manner to those which are pair-produced in e^+e^- collisions. For example, the distribution of final state charged hadrons (the fragmentation function) can be expressed in terms of the variable $\ln\frac{1}{z}$, where $z = P_{hadron}/P_{max}$, with P_{max} being the maximum possible momentum available to a single hadron. For e^+e^- interactions, in the CMS frame, this maximum momentum is $\frac{E}{2}$ (i.e. to lowest order, the momentum of either of the pair-produced quarks). In the case of ep collisions, choosing the Breit, or "brick wall" frame of reference, the momentum of the outgoing quark in the simple quark-parton model (i.e. figure 1b) is $\frac{Q}{2}$, where Q is the modulus of the virtual photon's 4–momentum. Figure 1c shows the most probable value of $\ln\frac{1}{z}$ as a function of Q for H1's data and, as a function of E, for various e^+e^- experiments, together with some theoretical predictions and fits. It is clear that, with the above choice of reference frame, Q is the ep variable which is equivalent to E and that, with this choice, the evolution of the maximum in the fragmentation function is the same for both processes.

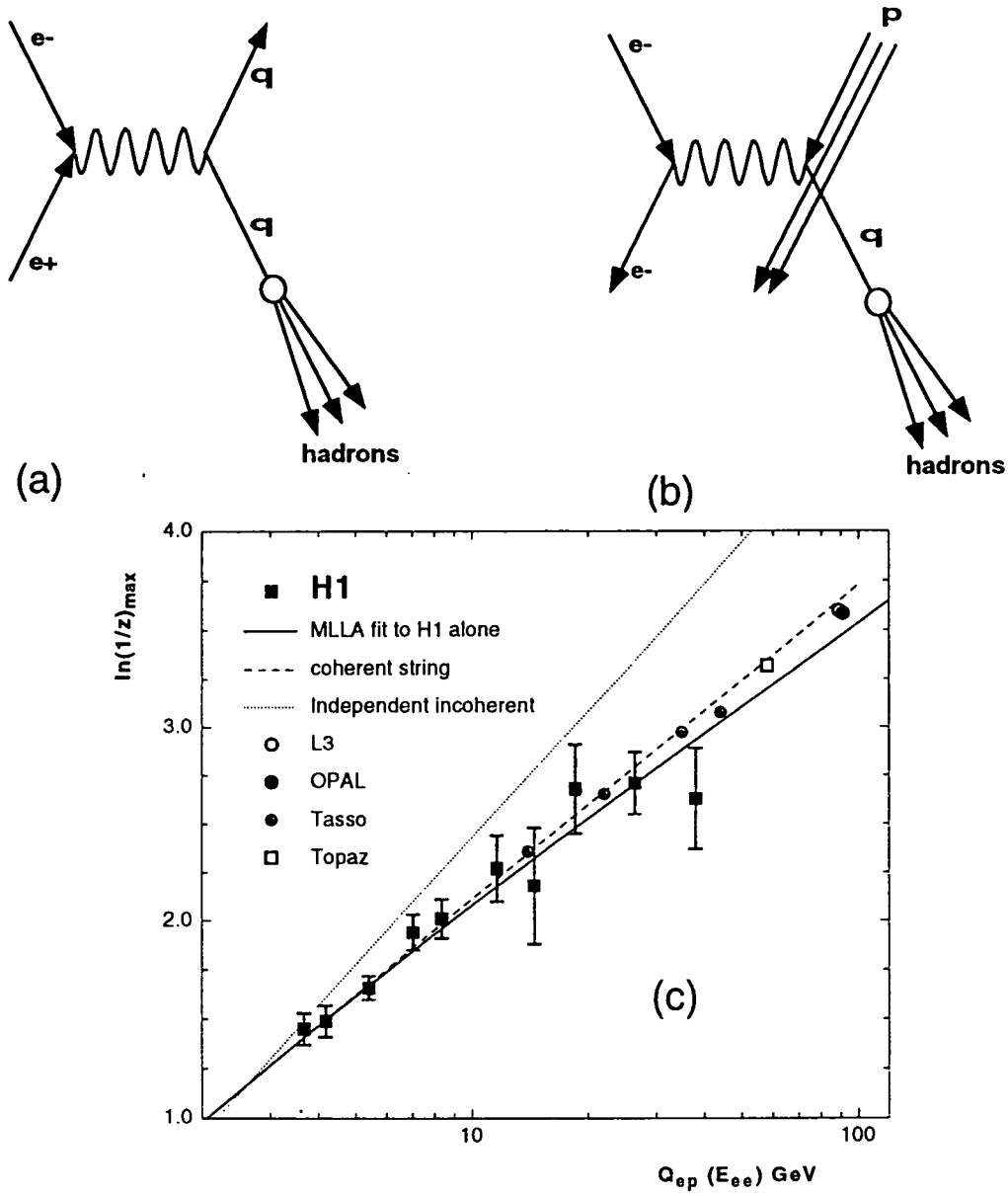

Figure 1: Schematic Feynman diagrams for quark production and fragmentation in the naive Quark Parton Model (QPM) for a) e^+e^- annihilation and for b) deep–inelastic ep scattering; c) variation of the maximum of the fragmentation distribution in $\ln \frac{1}{z}$ with Q (see text).

2.2 Strangeness Production in Deep–Inelastic Scattering

An interesting question, which always arises whenever the structure of the proton can be probed with enhanced precision, is whether there is a contribution to it of strange quarks (s), as well as up (u) and down (d) quarks. Measurements of the dependence of strange hadron production, such as K^0 and Λ^0, on $z = (p_{K^0_{//}} + E_{K^0})/(2p_q)$ can be examined for evidence of such a contribution in the form of "leading production" at large z ($\rightarrow 1$). Here E_{K^0}, $p_{K^0_{//}}$ and p_q are respectively the K^0 energy, lab momentum parallel to the direction of the struck parton, and the lab momentum of the struck parton. The results for K^0 production can be understood entirely in terms of u and d quark fragmentation (figure 2). There is no evidence yet of an excess at large z over models which assume only fragmentation contributions from u and d [7, 8]. Furthermore the evidence suggests that the models of u and d fragmentation invoke a "strangeness suppression factor" in fragmentation which is too large, much as has been observed in e^+e^- annihilation to hadrons at LEP.

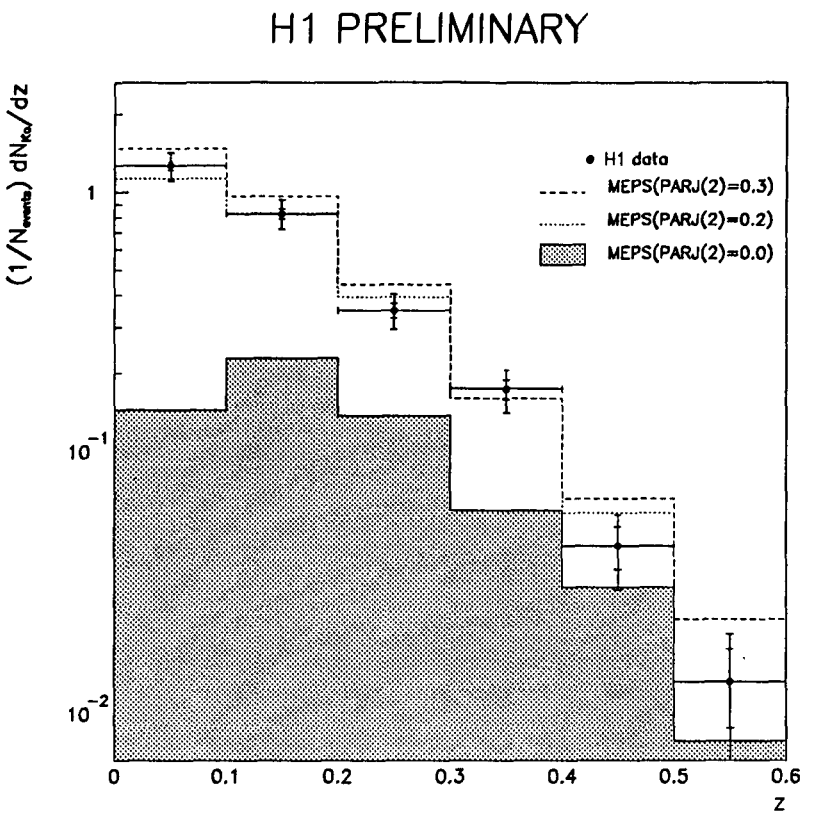

Figure 2: Corrected K^0 multiplicity in non-diffractive deep-inelastic events as a function of the fragmentation variable z; the results are compared with Monte Carlo simulations (MEPS) for different values of strangeness suppression in quark fragmentation to hadrons; the inner error bars are statistical and the outer error bars are the full error due also to systematic uncertainty.

2.3 Hadronic Energy Flow and QCD Evolution in Deep–Inelastic Scattering

No understanding of proton structure is adequate if the global features of hadron production in deep-inelastic scattering are not understood in terms of it. At low Bjorken-x, the dominant parton dynamics are based on virtual photon-gluon fusion to quark and antiquark (shown in figure 3a with additional QCD contributions from a "ladder" of parton exchange). Attempts have been made to understand the features of final state transverse hadronic energy flow E_T given the understanding of the partonic structure of the proton from QCD analyses of F_2, of the leading and next-to-leading order QCD dynamics, and of hadronic fragmentation. To date the results indicate that E_T flow, measured with respect to the virtual photon–proton axis in their overall centre of mass system, is not well understood in terms of our present abilities to calculate all of these influences.

In figure 4, $< E_T >$ is shown as a function of Bjorken-x for different Q^2 together with a theoretical approach which models as closely as possible "BFKL motivated" QCD evolution. A distinguishing characteristic of the latter is that the partons (mainly gluons) in the ladder diagram (figure 3a) are not ordered in decreasing transverse momentum as one moves "up the ladder" from the proton remnant to the current or struck quark. The result is that BFKL QCD expects more E_T between the remnant and the current than other schemes. The curves shown in figure 4 include a Colour Dipole Model (CDM) prediction (with and without parton hadronisation) in which there is explicitly no ordering in transverse momentum of the partons,

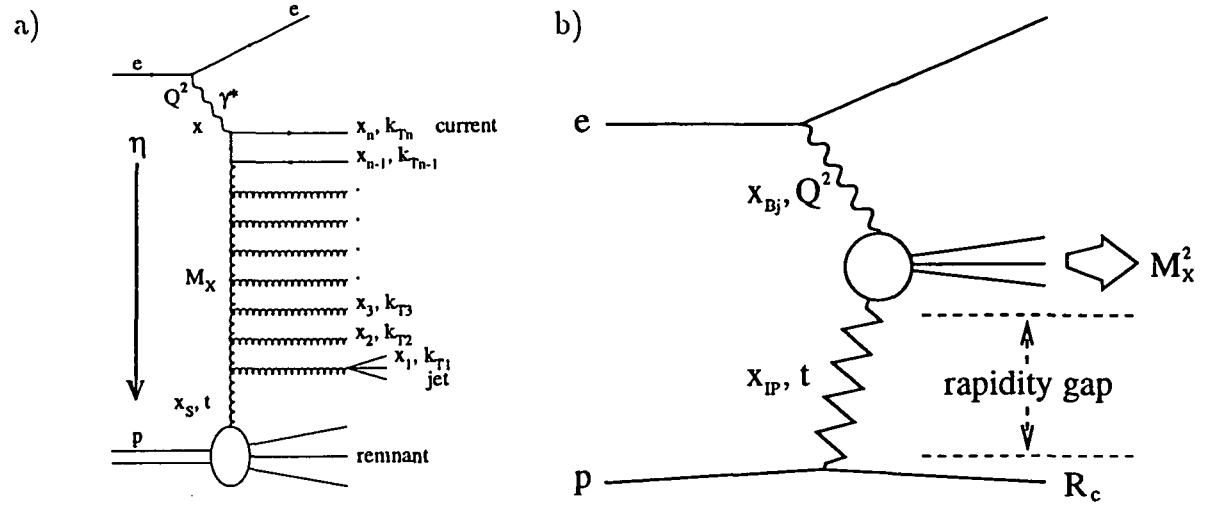

Figure 3: Schematic Feynman diagrams for a) ep DIS at low Bjorken–x illustrating how QCD can give rise to hadron production from partons produced between the "struck" or "current" quark at $x = x_n = x_{Bj}$ and the proton remnant; increasing pseudo–rapidity η from the current quark towards the remnant corresponds roughly to increasing the fractional momentum $x_{i/p} = x_i$ of the parton which forms the side of the "ladder"(usually a gluon at low Bjorken–x) as a fraction of the incident proton; the transverse momenta of the ith parton is k_{Ti}; and for b) a deep–inelastic ep interaction in which there is a forward diffractive "rapidity gap" devoid of hadronic energy; the high Q^2 virtual photon interacts with a colourless entity of space–like mass t whose momentum as a fraction of the target proton is $x_{I\!P}$; a (colourless) remnant of the proton R_c continues close to the incident direction of the target proton in the laboratory frame.

and an explicit BFKL calculation, but ignoring parton hadronisation. There is an intriguing possibility that the "qualitative" agreement of the "CDM hadrons" expectation with the measurement may be a first hint of evidence for BFKL motivated QCD evolution. The difficulties associated with the application of the more familiar "DGLAP motivated" QCD evolution mean however that the interpretation in terms of "BFKL evolution" remains at present only one of many possibilities [9, 10].

2.4 Diffractive Deep–Inelastic Scattering

One of the most significant observations by both HERA experiments has been the presence of events with a "rapidity gap" in deep–inelastic scattering. These events are interpreted naturally as the interaction of the probing virtual photon with a colourless piece of the proton which carries very little of its parent's momentum (figure 3b). Some of the time in ep interactions, the violently scattered electron probes the means by which this small momentum transfer from the proton takes place, rather than the proton itself which consequently emerges relatively unscathed from the interaction.

A first measurement has been made of the contribution $F_2^{D(3)}$ to the proton structure function F_2 of deep–inelastic interactions in which the proton remnant R_c carries nearly all of the incident proton momentum. The striking result is shown in figure 5 in which are shown the dependences of $F_2^{D(3)}$ on a variable called $x_{I\!P}$. This variable measures the momentum transfer in the diffractive proton interaction (as a fraction of that of the incident proton). The dependence on $x_{I\!P}$, shown as measured data points with a superimposed dependence, is obviously universal, irrespective of the values of the variables β and Q^2. The form of the dependence ($\propto x_{I\!P}^{-1.19}$) is exactly as expected for diffractive proton interactions. Because β and Q^2 describe the way the electron probes the colourless piece of the proton, and because $x_{I\!P}$ specifies the way the diffractive energy/momentum transfer from the proton takes place, the universality

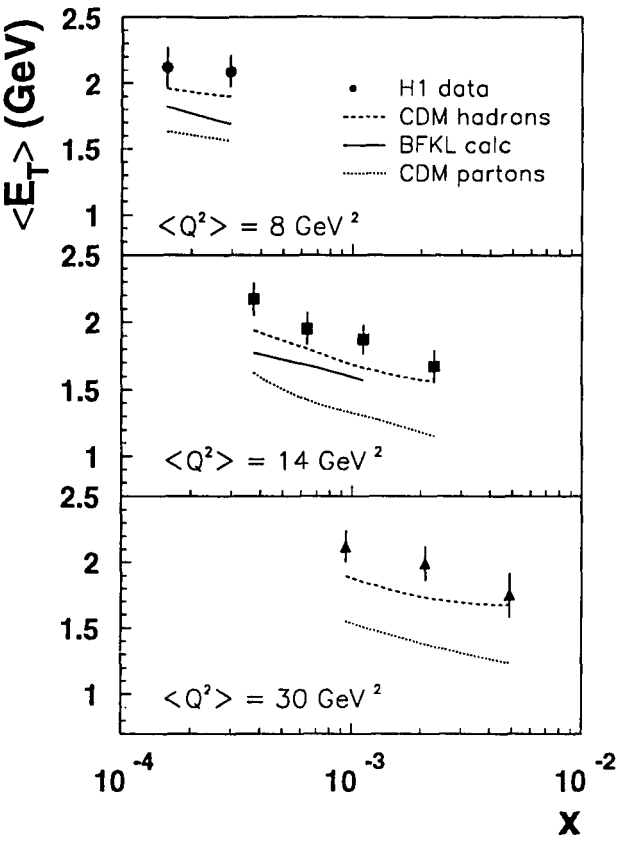

Figure 4: Mean transverse energy in the virtual photon–proton centre of mass rest frame as a function of Bjorken–x for different Q^2; also shown are the expectations from theoretical calculations; "CDM hadrons" refers to the Colour Dipole Model in which there is no ordering in transverse momentum of partons in the ladder diagram, BFKL to an explicit QCD calculation which ignores parton hadronisation, and CDM partons to a Colour Dipole Model calculation in which parton hadronisationis ignored.

of the slope of the $x_{I\!P}$ dependence demonstrates unambiguously that the electron is probing the means by which this small energy/momentum transfer takes place, that is the diffractive proton interaction, rather than the proton itself [11, 12, 13].

These results can then be used to deduce the structure function of the diffractive exchange, for many years considered phenomenologically to be the exchange of the pomeron, and this is shown in figure 6. The dependence on β and Q^2 of $\tilde{F}_2^D$ in figure 6 can be analysed using DGLAP QCD evolution. Though the accuracy of this first measurement is limited, the results already demonstrate that an understanding of the energy/momentum transfer in proton diffraction, that is of the pomeron, is possible in terms of the exchange of gluons, and that there is a suggestion that one gluon likes to carry most of the momentum transfer [14].

3 Production of Heavy Flavour Quark Systems

In all theoretical supposition, production of heavy SU_3 flavour quark systems (charm c and beauty b) is predicted to be substantial in ep interactions by virtue of the large gluon content of the proton at low Bjorken–x [4]. The detection of these events, either in which there is evidence for c or b decay through leading lepton (μ or e) production, or in which there is evidence for resonance production (e.g. J/ψ, ψ', D, D^* for c, Υ, Υ', B, B^* for b), is complicated by the difficulties of low leptonic decay branching ratios and peak signal to noise respectively. Though, with one exception, measurements are presently concerned with ep collisions in which Q^2 is small, nevertheless they are motivated by dependence of the cross sections on the gluon

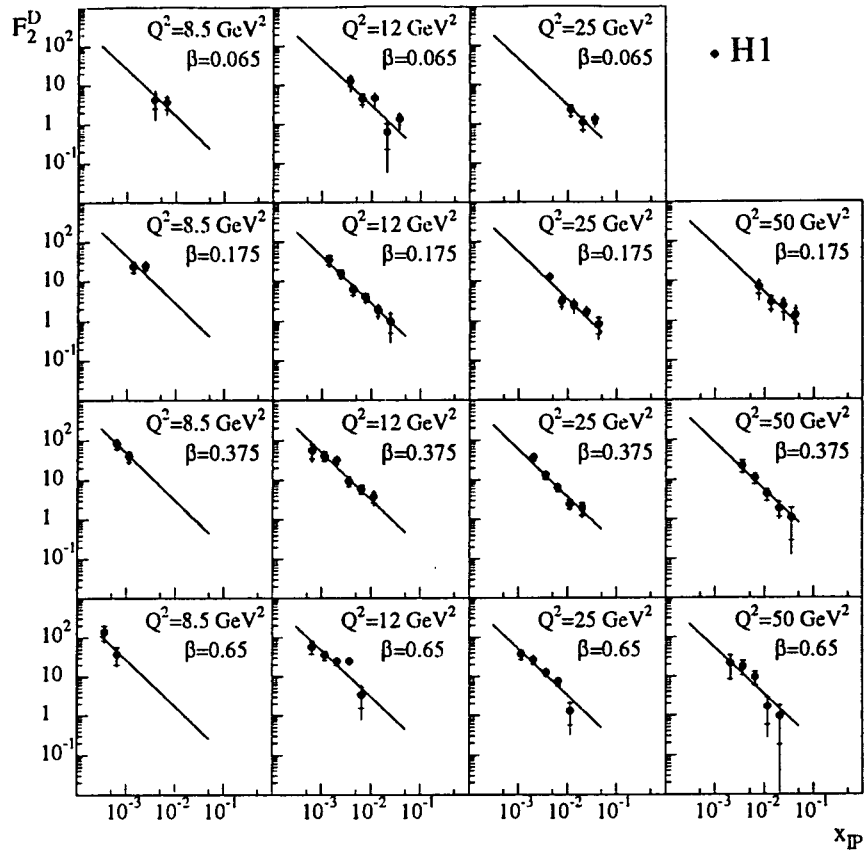

Figure 5: The diffractive contribution $F_2^{D(3)}(\beta, Q^2, x_{I\!P})$ to the proton structure function F_2 as a function of $x_{I\!P}$ for different β and Q^2; the inner error bar is the statistical error; the full error shows the statistical and systematic error added in quadrature; superimposed is the result of the fit establishing a factorisable dependence of the form $\propto x_{I\!P}^{-n}$. Note that an overall normalisation uncertainty of 8% is not included.

content of the proton, and therefore as such have particular relevance to the low x domain of proton structure probed in ep deep–inelastic scattering.

With the present level of integrated luminosity first measurements have been made of the cross sections for J/ψ production [15, 16, 17]. In addition signals are now visible for ψ' production (figure 7a) and for D/D^* production. The latter is shown in figure 7b in deep–inelastic diffractive events where it has been observed for the first time [18]. Though a cross section has yet to be evaluated, observation of a signal is interesting because the QCD analysis of the structure function $\tilde{F}_2^D$, shown in figure 6, favours a significant contribution to diffractive exchange from c–quarks [19].

4 Forward Track Detector

Throughout 1995 the Forward Track Detector has functioned well, with its day-to-day operation and maintenance being the responsibility of DESY based UK physicists. By contrast, most monitoring and all calibration of the detector are performed remotely by physicists based in the UK. Histories of the most interesting monitored quantities, along with more general FTD information and documentation [20], are now made available to all H1's collaborating institutes via the H1 FTD World-Wide-Web home pages < http : //dice2.desy.de/h1/www/h1det/list.html >.

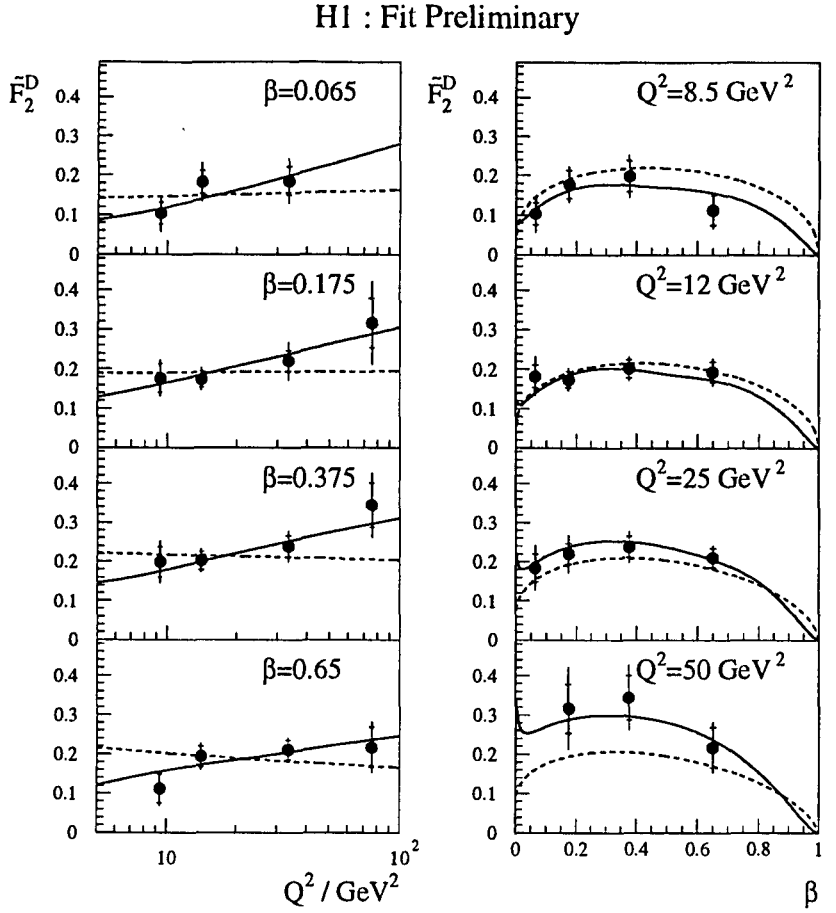

Figure 6: Dependence of $\tilde{F}_2^D$ on Q^2 and β; superimposed are the results of two LO $\log Q^2$ DGLAP QCD fits. The dashed line shows a fit in which at the starting scale, $Q_0^2 = 4\,\mathrm{GeV}^2$, diffraction is attributed to the exchange of only quarks (χ^2/dof of 13/12, 37%C.L.). The solid line shows a fit in which both quarks and gluons may contribute to the diffractive mechanism at $Q_0^2 = 4\,\mathrm{GeV}^2$ (χ^2/dof = 4/9, 91%C.L.). In the latter, the gluons carry $\sim$ 90% of the momentum of the pomeron at $Q_0^2 = 4\,\mathrm{GeV}^2$.

5 Central Data Acquisition and Central Trigger

RAL have been responsible for the project leadership of the central data acquisition system. During the whole of 1995 the system once more performed without any breakdown or serious incident. The system consists of a dual-fibre optic ring which co-ordinates the readout of the detector sub-components in VMEbus over distances of several hundred metres. An array of R3000 RISC processors, equivalent to 20 IBM-3090 units, provides event filtering, data processing, event reconstruction and histogram monitoring in real-time. By embedding the full data acquisition functionality in VMEbus, the complete system can be operated from the latest generation of user-interactive workstations.

During 1995 the Central Trigger Control was expanded to include the new Level-2 interfaces (topological and neural-net) which add more flexibility in event selection prior to the final event filtering array.

6 Silicon Tracker Data Acquisition and Readout

Groups from RAL, DESY-Hamburg, DESY-Zeuthen and Zürich, have been collaborating to provide silicon detectors located inside the central jet chamber. The Central Silicon Tracker (CST) is to provide high resolution tracking and vertex reconstruction in the central region,

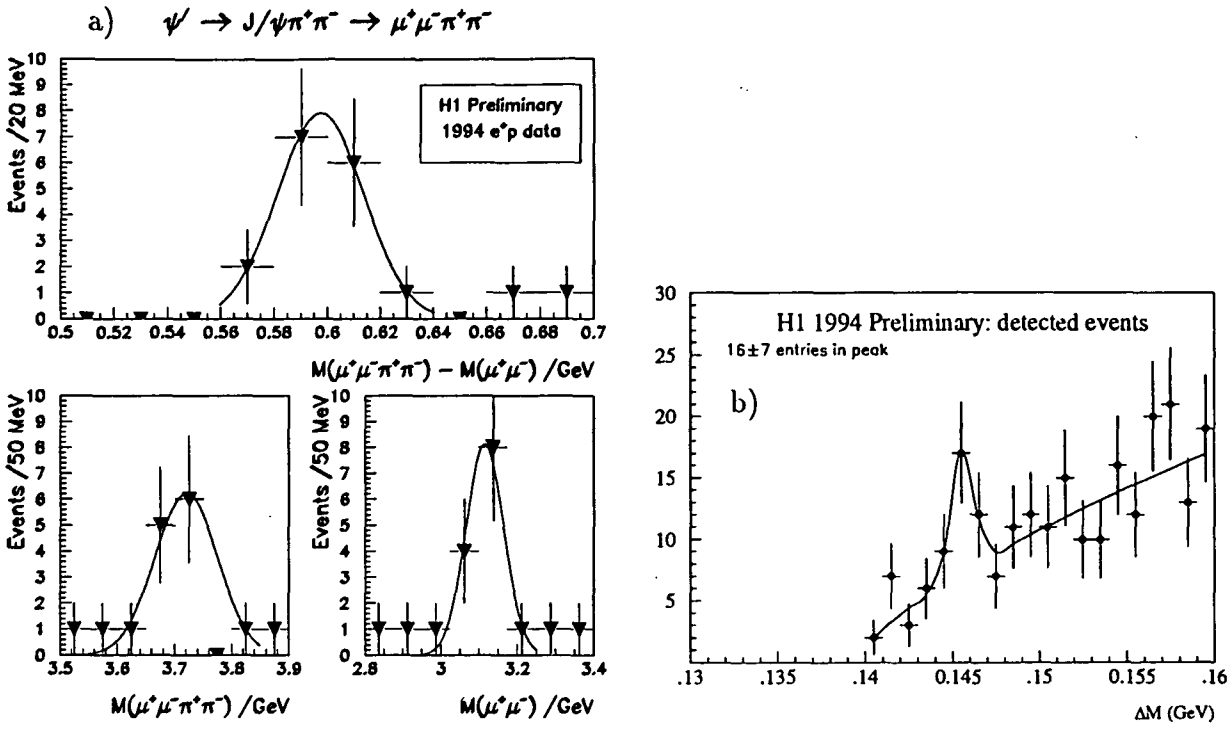

Figure 7: a) Evidence for ψ' production in ep interactions; b) The invariant mass combination $\Delta M = M(K^{\pm}\pi^{\mp}\pi^{\mp}_{slow}) - M(K^{\pm}\pi^{\mp})_{D^0}$ in diffractive deep-inelastic scattering events showing evidence for $D^{*\mp}$ production.

and the Backward Silicon Tracker (BST) will extend this coverage to small backward angles. RAL are responsible for providing the data acquisition readout chain.

During 1995 the first stage of the detector was successfully commissioned and tested within the H1 experiment, together with a full DAQ chain, including custom amplifier-pipeline chips integrated on the detector and read into VMEbus. The architecture of the readout follows that of the central DAQ by using fibre-optics and fast integer processing within a modular framework. Parasitic monitoring and reconstruction tasks can be executed in parallel using R3000 and 68040 processor cards. Graphics-oriented workstations cater for software development and operator-intervention.

During the winter shutdown, 1995-6, the remainder of the Silicon Tracker will be added, the final system contributing a total of a quarter of a million electronic channels. In preparation for this next round, and as a result of the evaluations done during 1995, an on-going optimised readout enhancement is being implemented by RAL engineers. This involves the integration of custom ADC mezzanines with the latest commercial PowerPC processor boards, by both PCI and VME busses. This will ensure sufficient digital and data processing capacity well into the coming years as the HERA luminosity further increases.

7 Backward Calorimeter Upgrade

The new upgraded H1 backward calorimeter (SPACAL) was installed during the 1994-5 winter shutdown. This device uses scintillating fibres encased in lead, and is read out by mesh-dynode photomultiplier tubes that work well in the 1 T H1 field. The electromagnetic part of the calorimeter has excellent energy resolution ($7\%/\sqrt{E(GeV)} \oplus 1\%$), and both e.m. and hadronic parts have < 1 ns timing resolution. It also has good spatial resolution, and provides valuable electron/pion discrimination.

The good timing resolution is needed to reject beam-induced backgrounds, which are fre-

quently very large in H1. Most of this rejection must be done in the level-1 trigger in order to minimise dead-time. Good efficiency and minimal rejection of physics are essential. The accurate online and offline timing information needed in order to adjust the trigger gates, which are set individually on each photomultiplier's signals, comes from 1400 time-to-digital converters (TDCs) designed and built by Birmingham, QMW and RAL. This compact system of only two VME crates is based on the TMC1004 chip, which provides four TDCs with < 1 ns timing resolution and pipelined readout per chip. This allows 64 TDC channels per module, along with large memories that provide automatic on-board histogramming of each channel for up to 16 programmable types of trigger. In addition, the modules include rate scalers that can be used in several different ways.

The TDC system was installed on time and works well and reliably. It has been essential in commissioning the SPACAL trigger electronics and in fine-tuning the performance of the front-end electronics. The rate information has also proven to be a very useful beam diagnostic. Online test and monitoring programs, as well as offline reconstruction software for the timing information, have been provided. The online monitoring program, which was written using object oriented techniques in common with the Central DAQ and Trigger interfaces, includes a wealth of crisp displays and flexible operator-interfaces. Extensive use of networking features is added, including full documentation for the TDC system available over the World Wide Web.

References

[1] H1 Collaboration, Nucl. Phys. **B439** (1995) 471.

[2] T. Ahmed, "First Measurements of the Neutral Current Deep-Inelastic Cross Sections and the Proton Structure Function $F_2(x, Q^2)$ at HERA", PhD Thesis (University of Birmingham), 1994 (unpublished) and Rutherford Appleton Laboratory report RALT-008-94.

[3] R. Martin, "A Measurement of the Structure Function of the Proton $F_2(x, Q^2)$ at Low Bjorken-x", PhD thesis (University of Liverpool), 1994 (unpublished) and Rutherford Appleton Laboratory report RALT-022-94.

[4] H1 Collaboration, Phys. Letts. **354B** (1995) 494.

[5] D. Kant, "A Study of the Fragmentation of Quarks in ep Collisions at HERA using the H1 Detector", PhD Thesis (Queen Mary and Westfield College), 1995, in litt.

[6] H1 Collaboration, Nucl. Phys. **B445** (1995) 3.

[7] D. Milstead,"Production of neutral strange particles in deep inelastic scattering and a search for instantons.", PhD Thesis (University of Liverpool), 1995, in litt.

[8] H1 Collaboration, "Strangeness in Photoproduction and Deep-Inelastic Scattering at HERA", paper EPS0479 submitted to the 1995 Europhysics Conference, Brussels, and to the 1995 Lepton Photon Symposium, Beijing.

[9] T. R. Ebert,"Hadronic Energy Flow in Deep-Inelastic Electron-Proton Scattering and Proton Structure at low Bjorken-x", PhD thesis (University of Liverpool), 1995 (unpublished) and Rutherford Appleton Laboratory report RALT-009-95.

[10] H1 Collaboration, Phys. Letts. **356B** (1995) 118.

[11] A. Mehta, "Measurement of the Diffractive Proton Structure Function and Calibration of the Forward Muon Detector at H1", PhD thesis (University of Manchester), 1994 (unpublished) and Rutherford Appleton Laboratory report RALT-037-95.

[12] J. Phillips, "The Deep-Inelastic Structure of Diffraction", PhD thesis (University of Manchester), 1995 (unpublished).

[13] H1 Collaboration, Phys. Letts. **348B** (1995) 681.

[14] H1 Collaboration, "The Partonic Structure of Proton Diffraction", paper EPS0491 submitted to the 1995 Europhysics Conference, Brussels, and to the 1995 Lepton Photon Symposium, Beijing.

[15] H1 Collaboration, Phys. Letts. **B338** (1994) 507.

[16] H1 Collaboration, "Photoproduction of J/ψ Mesons at HERA", paper EPS-0468 submitted to the 1995 Europhysics Conference, Brussels, and to the 1995 Lepton Photon Symposium, Beijing.

[17] H1 Collaboration, "J/Psi Production inf Deep Inelastic Scattering at HERA", paper EPS-0469 submitted to the 1995 Europhysics Conference, Brussels, and to the 1995 Lepton Photon Symposium, Beijing.

[18] J. B. Dainton "Deep-Inelastic Diffraction", in Proc. of the VIth Recontre de Blois "Frontiers in Strong Interactions", Château de Blois, France, April 1995, in litt.

[19] J. P. Phillips "Photoproduction at HERA", invited talk at the 1995 Institute of Physics Conference on Nuclear and Particle Physics, Telford, UK, April 1995.

[20] S. Burke et al. "Track Finding and Fitting in the H1 Forward Track Detector", DESY 95-132, July 1995, accepted for publication in Nucl. Inst. Meth.

H1 Publications 1995

1. T. Ahmed et al. (H1 collaboration), "Observation of hard processes in rapidity gap events in γp interactions at HERA", Nucl. Phys. **B435** (1995) 3-20, DESY 94-198.

2. T. Ahmed et al. (H1 collaboration), "Determination of the strong coupling constant from jet rates in deep-inelastic scattering", Phys. Letts. **346B** (1995) 415-425, DESY 94-220.

3. T. Ahmed et al. (H1 collaboration), "Observation of an $e^+p \rightarrow \mu + X$ event with high transverse momenta at HERA", DESY 94-248.

4. T. Ahmed et al. (H1 collaboration), "A measurement of the proton structure function $F_2(x, Q^2)$" , Nucl. Phys. **B439** (1995) 471-502, DESY 95-006.

5. T. Ahmed et al. (H1 collaboration), "Experimental study of hard photon radiation processes at HERA", Zeit. Phys. **C66** (1995) 529-542, DESY 95-024.

6. T. Ahmed et al. (H1 collaboration), "First measurement of the deep-inelastic structure of proton diffraction", Phys. Letts. **348B** (1995) 681-696, DESY 95-036.

7. T. Ahmed et al. (H1 collaboration), "Inclusive parton cross sections in photoproduction and photon structure", Nucl. Phys. **B445** (1995) 195-215, DESY 95-062.

8. S. Aid et al. (H1 collaboration), "A study of the fragmentation of quarks in $e-p$ collisions at HERA", Nucl. Phys. **B445** (1995) 3-21, DESY 95-072.

9. S. Aid et al. (H1 collaboration), "Leptoquarks and compositeness scales from a contact interaction analysis of deep inelastic e^+p scattering at HERA", Phys. Letts. **353B** (1995) 578-588, DESY 95-079.

10. S. Aid et al. (H1 collaboration), "The gluon density of the proton at low x from a QCD analysis of F_2", Phys. Letts. **354B** (1995) 494-505, DESY 95-081.

11. S. Aid et al. (H1 collaboration), "A direct determination of the gluon density in the proton at low x", DESY 95-086.

12. S. Aid et al. (H1 collaboration), "Measurement of the e^+ and e^- induced charged current cross sections at HERA", Zeit. Phys. **C67** (1995) 565-575, DESY 95-102.

13. S. Aid et al. (H1 collaboration), "Transverse energy and forward jet production in the low x regime at HERA", Phys. Letts. **356B** (1995) 118-128, DESY 95-108.

14. S. Aid et al. (H1 collaboration), "Comparison of deep-inelastic scattering with photoproduction interactions at HERA", accepted for publication in Phys. Letts. **B**, DESY 95-156.

15. S. Aid et al. (H1 collaboration), "Measurement of the total photon proton cross section and its decomposition at 200 GeV centre of mass energy", accepted for publication in Zeit. Phys. C, DESY 95-162.

16. T. Ahmed et al. "A Pipelined First-Level Trigger for the H1 Forward-Muon Spectrometer", Nucl. Inst. Meth. **A364** (1995) 456-472.

17. E. Eisenhandler et al. "The H1 SPACAL Time-to-Digital Converter System", IEEE Trans. Nucl. Sc. **42** (1995) 688-692.

18. S. Burke et al. "Track Finding and Fitting in the H1 Forward Track Detector", accepted for publication in Nucl. Inst. Meth. DESY 95-132.

PhD Theses

All PhD theses which are concerned with ep physics at H1 and which have been submitted since October 1994 are listed below.

1. S. M. Robertson "Hadronic Energy Flow and Inclusive Charged Particle Production at HERA", PhD thesis (University of Birmingham), 1995.

2. L. Johnson, "Jet production in deep inelastic scattering and the separation of quark and gluon jets using a neural network technique", PhD thesis (University of Lancaster), 1995.

3. T. R. Ebert,"Hadronic Energy Flow in Deep-Inelastic Electron-Proton Scattering and Proton Structure at low Bjorken-x", PhD thesis (University of Liverpool), 1995 and Rutherford Appleton Laboratory report RALT-009-95.

4. A. Mehta, "Measurement of the Diffractive Proton Structure Function and Calibration of the Forward Muon Detector at H1", PhD thesis (University of Manchester), 1994 and Rutherford Appleton Laboratory report RALT-037-95.

5. J. Phillips, "The Deep–Inelastic Structure of Diffraction", PhD thesis (University of Manchester), 1995.

6. A. E. Wright, "Event Classification at HERA and The development of the Resistive Plate Chamber for LHC", PhD thesis (University of Manchester), 1994 and Rutherford Appleton Laboratory report RALT-034-95.

7. J. Heatherington, "ToF, The Time-of-Flight device for H1, PhD thesis (Queen Mary and Westfield College, University of London), 1995.

8. D. Kant, "A Study of the Fragmentation of Quarks in ep Collisions at HERA using the H1 Detector", PhD Thesis (Queen Mary and Westfield College, University of London), 1995, in litt.

9. A.K.Mavroidis, "A QCD Analysis of Structure Function Data from Electron-Proton Collisions in the H1 Experiment", PhD thesis (Queen Mary and Westfield College, University of London), 1995.

H1 Conference Presentations 1995

Conference presentations by members of the H1–UK groups which are concerned with all aspects of H1 physics and operation are listed below.

1. G. Thompson "Physics from H1", XXIV International Conference on Multiparticle Dynamics, Salerno, Italy, September 1994, World Scientific.

2. S. Prell et al. "The readout system of the new H1 silicon detectors", DESY 95–049, presented at the 1995 Vienna Wire Chamber Conf., Feb. 1995, Austria, to appear in proceedings.

3. S. J. McMahon et al. "$e^{\pm}$ Identification for Particles produced at Small Angles to the Incident Proton Beam at HERA using the Drift Chambers and Transition Radiator of the H1 Forward Track Detector", presented at the 1995 Vienna Wire Chamber Conf., Feb. 1995, Austria, to appear in proceedings.

4. P. Biddulph "Rapidity Gap Events in DIS at HERA", in Proc. of the 2nd Workshop on Small x and Diffractive Physics at the Tevatron, ed. M. Albrow and A. White Fermilab report.

5. A. Mehta "Comparison of Diffractive and non-Diffractive Deep–Inelastic Scattering", in Proc. of the International Workshop on Photon–Photon and Photon–Hadron Interactions "Photon95", Sheffield, UK, April 1995, ed. S. L. Cartwright and D. J. Miller, in litt.

6. J. P. Phillips "Photoproduction at HERA", invited talk at the 1995 Institute of Physics Conference on Nuclear and Particle Physics, Telford, UK, April 1995.

7. J. B. Dainton "Deep–Inelastic Physics with H1 at the HERA ep Collider", in Proc. of the International Workshop on Deep–Inelastic Scattering and Related Topics, Paris, France, April 1995, ed. J-F. Laporte and Y. Sirois, in litt.

8. J. P. Phillips "Rapidity Gap Events at HERA and the Structure of the Pomeron", in Proc. of the International Workshop on Deep-Inelastic Scattering and Related Topics, Paris, France, April 1995, ed. J-F. Laporte and Y. Sirois, in litt.

9. I. R. Kenyon "J/ψ AND ρ^o Meson Production at H1", in Proc. of the VIth Recontre de Blois "Frontiers in Strong Interactions", Château de Blois, France, April 1995, in litt.

10. J. B. Dainton "Deep-Inelastic Diffraction", in Proc. of the VIth Recontre de Blois "Frontiers in Strong Interactions", Château de Blois, France, April 1995, in litt.

11. J. P. Phillips invited talk "Deep-Inelastic *ep* Diffraction", at the IoP Half Day Meeting "New Light on the Pomeron", Imperial College, London, UK, June 1995.

12. J. B. Dainton invited talk "Summary Talk", at the IoP Half Day Meeting "New Light on the Pomeron", Imperial College, London, UK, June 1995.

13. T. Greenshaw "Diffraction at HERA and the Pomeron", invited talk at the International Conference "Hadron Spectroscopy", Manchester, UK, July 1995, to appear in proceedings.

14. J. B. Dainton "Pomeron Puzzles in Proton Diffraction - a Discussion", talk at the meeting "Low x Physics", Christ's College, Cambridge, July 1995.

15. P. R. Newman "*ep* Diffraction in H1", talk at the meeting "Low x Physics", Christ's College, Cambridge, July 1995.

16. S. Burke "Measurement of the Deep-Inelastic Structure of Proton Diffraction", talk presented to the Parallel Session PA04 "Structure Functions", 1995 International Europhysics Conference on High Energy Physics, Brussels, 1995.

17. R. Martin "Diffractive Dynamics in Deep-Inelastic *ep* Scattering", talk presented to the Parallel Session PA17 "Soft Interactions At High Energy", 1995 International Europhysics Conference on High Energy Physics, Brussels, 1995.

18. S. J. Maxfield "Measuring the Structure of the Photon at HERA", to appear in Proc. of the XXVth International Symposium on Multiparticle Dynamics, Stara Lesna, Slovakia, 1995.

19. S. J. Maxfield "Some Aspects of Photoproduction at HERA", to appear in Proc. of the Phenomenology Workshop "Proton, Photon and Pomeron Structure", Durham, UK, September 1995, to be published in J. Phys. **G**.

20. J. P. Phillips "Report of the Diffractive Working Group", to appear in Proc. of the Phenomenology Workshop "Proton, Photon and Pomeron Structure", Durham, UK, September 1995, to be published in J. Phys. **G**.

21. G. Thompson "The Hadronic Final State in Deep-Inelastic Scattering", to appear in Proc. of the Phenomenology Workshop "Proton, Photon and Pomeron Structure", Durham, UK, September 1995, to be published in J. Phys. **G**.

H1 Conference Submissions 1995

The following papers were submitted by the H1 collaboration to the two major international conferences in 1995, namely the 1995 Europhysics Conference, Brussels (to which the paper number refers), and to the 1995 Lepton Photon Symposium, Beijing.

1. "A Search for Leptoquarks in H1 at HERA", EPS0462.
2. "First Search for the Minimal Supersymmetric Model at HERA", EPS0463.
3. "A Search for Heavy Leptons in ep Scattering at HERA", EPS0464.
4. "Measurement of Differential Cross sections for Charged Current and Neutral Current Interactions at HERA", EPS0466.
5. "Photoproduction of D^* Mesons in Electron-Proton Collisions at HERA", EPS0467.
6. "Photoproduction of J/ψ Mesons at HERA", EPS0468.
7. "J/ψ Production inf Deep Inelastic Scattering at HERA", EPS0469.
8. "Measurement of the Proton Structure Function F_2 at HERA", EPS0470.
9. "The Structure Function F_2 at low Q^2 from Radiative Events at HERA", EPS0472.
10. "Elastic Photoproduction of ρ–mesons at HERA", EPS0473.
11. "Jets and energy flows in γp collisions at HERA", EPS0476.
12. "Strangeness Production in Deep Inelastic Scattering at HERA", EPS0479.
13. "Bose-Einstein Correlations in Deep Inelastic Scattering at HERA", EPS0481.
14. "Charged Particle Multiplicities in Deep Inelastic Scattering at HERA", EPS0483.
15. "Determination of the Strong Coupling Constant α_S in Deep Inelastic Scattering", EPS0486.
16. "Exclusive ρ^0 Production in Deep Inelastic Scattering Events at HERA", EPS0490.
17. "The Partonic Structure of Proton Diffraction", EPS0491.
18. "Studies of the Hadronic Final State in Diffractive Deep-Inelastic Scattering Interactions at HERA", EPS0494.
19. "A Search for Squarks of R_p-Violating SUSY in H1 at HERA", EPS0784.
20. "Inclusive D^0 and D^* Production in Deep Inelastic ep Scattering at HERA", EPS0785.
21. "Observation of $ep \to \mu^+ X$ and $ep \to e^- X$ Events with High Transverse Momenta at HERA", EPS0786.

THE ZEUS EXPERIMENT AT HERA.

Proposal 760

Bristol, Glasgow, Imperial College London, University College London, Oxford, Rutherford Appleton Laboratory

in collaboration with

Argonne, Bologna, Bonn, Brookhaven, Calabria, Columbia, DESY, DESY-Zeuthen, Florence, Frascati, Freiburg, Hamburg, Iowa, Jülich, Krakow, Louisiana, Madison (Wisconsin), Madrid, Manitoba, McGill, Moscow, NIKHEF, Ohio, Padova, Pennsylvania, Rome, Santa Cruz, Seoul, Siegen, Tel Aviv, Tokyo, Tokyo Metropolitan Univ., Torino, Toronto, Virginia, Warsaw, Weizmann Inst., Yokohama, York (Ontario).

Introduction

During 1995 HERA ran with 174 colliding bunches of 820 GeV protons and 27.5 GeV positrons. Approximately 6 pb^{-1} of usable data were accumulated by the ZEUS experiment, roughly twice as much as in 1994. Major contributions to the improved performance were the achievement of higher proton currents and the extended running period in 1995. As in most of 1994, it was decided to run HERA mainly with positrons, since these give a much longer beam lifetime than that obtained using electrons. It is believed that the replacement of some of the vacuum pumps should make an electron beam viable for the 1997 running.

The ZEUS detector as a whole continued to function well. The increase in luminosity made it necessary to employ more stringent triggers than in previous years – in particular, making much tighter use of the tracking information – and the collaboration is beginning to have to be more selective on the physics data that it is able to record on tape. Analysis of the 1993 data is now essentially complete, that of the 1994 data is well progressed, and first results are appearing from the 1995 running.

Hardware developments.

The ZEUS apparatus was improved in a number of ways for the 1995 running. These particularly assist the coverage in the region of the beamline.

1. An improved version of the beampipe calorimeter (BPC) has been in operation, following the group's experience with the 1994 prototype. The full planned azimuthal coverage is now obtained, so as to maximise the acceptance for electrons that tag virtual photons in a Q^2 range 0.1–0.7 GeV^2. In conjunction with this, the two halves of the central column of cells in the rear uranium calorimeter (RCAL) have each been moved 5 cm towards the beamline to improve the Q^2 coverage of the RCAL.
2. Scintillator arrays have been installed in front of the forward and rear calorimeters to act as presampler devices which improve the energy measurement of forward jets and scattered beam leptons. An extension of this system to the barrel calorimeter is planned.
3. The Leading Proton Spectrometer is now fully installed and instrumented. A trigger involving this device was brought into operation to enhance the measurement of diffractive processes.
4. Readout of the forward and rear trackers and the transition radiation detector is now complete, and information from these detectors can be incorporated into the track measurements. Progress is continuing on the analysis of the TRD signals.

CTD performance.

The Central Tracking Detector, together with its associated readout and trigger electronics, has been the major contribution made by the UK groups to the ZEUS detector, and it remains our joint task to operate it effectively and obtain the optimum results from it. In data taking the CTD has performed very reliably, with less than 2% of dead channels and little contribution to the experimental running downtime. No signs of aging are apparent. A much improved data quality monitoring system has been of great assistance.

At the offline level, a number of detailed improvements to the corrections have enabled the (r, ϕ) resolution to be brought down to the 190 μm level. Such a value is close to reasonable expectations, but we shall continue to seek further improvement. Much progress has been made on the extraction of dE/dx (ionisation density) measurements, which are now being used to assist particle identification in a number of physics analyses. Both the previous and present ZEUS tracking coordinators are ZEUS-UK members.

Trigger and running.

ZEUS operates a three-level trigger, of which the first level is a hardware-based system whose principal aim is to reduce backgrounds from processes that do not come from the interaction point. Information from the CTD makes an important contribution to this, by means of dedicated pipelined processor cards which enable (r, z) information from track segments in the first drift chamber superlayer to be incorporated into the trigger. This system gives fast recognition of the point of origin of tracks, and is currently used by 28 of the 33 active first level triggers. It is to be extended and improved by using information from superlayers 3 and 5, by means of the so-called CP3 and CP5 cards. These are now installed and read out, and work is taking place to integrate the information into the trigger system for the 1996 running.

The second level trigger applies software cuts to clean the event sample further and identify certain classes of physics event. The CTD component to this has been in operation since 1994, and enables detailed information on the tracking and vertexing to to be used in the event selection. It is used by five of the six physics filters at this level. At the third trigger level, all the event information is available, and many different types of physics selection can be made using software algorithms similar to those used offline. All the physics analysis groups contribute here.

A programme of continued improvement to all three levels of the trigger will remain of paramount importance over the coming years if ZEUS is to exploit effectively the expected increases in HERA luminosity. The UK groups plan to maintain a central role in this essential activity.

ZEUS data taking has become an increasingly smooth operation, and the collaboration has decided to reduce the number of regular shift personnel required from four to three. The UK groups have continued to play a full part here, and have provided several of the designated shift leaders. We also provided one of the four ZEUS Run Coordinators for 1995.

Physics analysis.

During 1995 a large number of analyses were completed and published by the ZEUS collaboration. This has been made possible to a large extent by the ZARAH computing system and environment, which was designed and implemented by the collaboration. It is based on the rapid accessibility of events on disk storage, which together with an Ampex tape system and high CPU power provides an outstandingly versatile and fast data handling capability. The facilities at the ZEUS member institutions, including the UK groups, are now being increasingly exploited in conjunction with those at DESY to carry out Monte Carlo simulations. In this way the use of resources is maximised in performing the massive amounts of computation which the physics analyses demand.

In the following summary, we concentrate especially on those physics areas where the UK members of ZEUS have been particularly active. During 1994-95, the Deep Inelastic Scattering (DIS) analysis group was coordinated by a UK physicist, and ZEUS-UK also currently provide deputy coordinators for the Structure Function and the Hard Photoproduction analysis groups. From Autumn 1995, a UK physicist has been the collaboration's overall Physics Coordinator.

1. *Proton structure.* A major focus of activity has been the measurement of the structure function $F_2(x, Q^2)$ for Deep Inelastic Scattering off the proton. Measurements now reach down to x values well below 10^{-4}. The extended coverage was made possible by using events with initial state radiation, and also a special period of running of HERA with the interaction point moved 60 cm upstream to allow smaller $e^{\pm}$ scattering angles to be measured in ZEUS. Two important features are seen in the data. One is that F_2 continues to rise with decreasing x; the other is that this rise still occurs at Q^2 values as low as 1.5 GeV^2. The latter comes as a slight surprise as it contradicts Regge-based predictions at this Q^2 value, although perturbative QCD-based predictions are still able to describe the data.

   Fig. 2 shows the rise in the gluon density in the proton that is implied by the F_2 data. The F_2 values can alternatively be expressed as total $\gamma^* p$ cross sections (Fig. 1). Here it is apparent that quite a rapid transition in behaviour needs to occur in the region $Q^2 < 1.5$ GeV^2 if the curves for constant Q^2 values are not to cross. However there is no known theoretical argument that prohibits the latter. The intermediate region between quasi-real photons and $Q^2 = 1.5$ GeV^2 is thus of considerable interest for further study.

2. *Photon structure in the intermediate Q^2 region.* One contribution to our understanding of this region may come from the study of direct and resolved hard photoproduction, with particular reference to the behaviour of the resolved component. The newly installed BPC has enabled first measurements to be made in the range $0.1 < Q^2 < 0.55$ GeV^2. The expectation that the resolved component should fall with Q^2 is found to be fulfilled. The results, as presented at the 1995 Brussels conference, are shown in Fig. 3.

3. *Charm states in low Q^2 photoproduction.* Clear signals for D^* production have been found in inclusive photoproduction, and the total inclusive cross section has been measured at a mean centre of mass energy of 163 GeV. The results are substantially higher than those found at lower energies, but are well described by NLO QCD calculations with rising gluon distributions at low x in the proton, such as are obtained from the HERA F_2 data. Figs. 4 and 5 illustrate charm signals seen in the 1994 data with the help of the dE/dx measurements in the CTD. Cross sections have also been determined for elastic J/ψ photoproduction (Fig. 6). Here too, a substantial rise compared with lower energy experiments is found, leading to similar conclusions as with the D^* data, and again confirming the general picture of the proton which HERA is presenting to us.

4. *High Q^2 DIS.* At the opposite extreme, deep inelastic scattering at Q^2 values of $O(10^4)$ GeV^2 is sensitive to electroweak effects, and this was indeed one of the original prime motivations for constructing HERA. First measurements of neutral and charged current cross sections in this region have now been published. As shown in Fig. 7, agreement with the standard model is good. This provides a direct confirmation of the unification of the electromagnetic and weak forces, which should be further reinforced with the use of beam polarisation and high statistics data from both electron and positron beams.

5. *Determination of α_s.* A measurement of the strong coupling constant α_s has been made from DIS events containing two high-p_T jets. The necessary NLO calculations at the parton level require that the JADE jet definition scheme be applied to the data. On this basis, the observed jet rates can be fitted to extract α_s, which is found to decrease with

Q^2 in agreement with expectations (Fig. 8). Expressed at the Z^0 mass, our result is: $\alpha_s = 0.117 \pm 0.005\ (stat)\ ^{+0.004}_{-0.005}\ (sys_{exp}) \pm 0.007\ (sys_{theory})$; this value is consistent with other determinations, and the already competitive errors should be significantly improved with further development of this approach.

6. *Properties of final states in DIS.* At a range of Q^2 values above 10 GeV^2, the collaboration have published a study of inclusive particle distributions in the Breit frame, where direct comparisons can be made with e^+e^- annihilation data (Fig. 9). No significant differences are suggested at this global level. An analysis has also been made of inclusive K^0 cross sections in DIS final states; the K^0s are expected to be observed mainly as products of hadronisation in the struck parton jet, so that the measurements test our detailed understanding of this process. Here, fewer K^0s are found than expected from predictions based mainly on the parameterisation of e^+e^- data. These are clearly topics which merit more detailed investigation. A study of K^0s in hard photoproduction is well advanced.

7. *Diffractive processes.* The collaboration have continued to place much effort in investigating processes whose energy flow displays a large rapidity gap. Three types of such process have been studied: diffractive processes in DIS and in low-Q^2 hard photoproduction, and processes with a centrally occurring rapidity gap. Present data have not yet resolved the debate as to whether or not the processes in these kinematic regimes are fundamentally similar, in particular whether a common "pomeron" is involved. In DIS, the diffractive structure function is found to show no variation with Q^2 or with the fraction of the proton momentum taken by the diffractively exchanged object, thus respectively displaying scaling and factorisation. The errors are at present substantial, however, and although a particle-like pomeron is supported, there is also consistency with other models. From the DIS studies it is apparent that such an object must have a quark substructure, while the low-Q^2 results confirm that if the same pomeron is involved, it must in addition contain gluons. Centrally occurring rapidity gaps have also given first evidence for "colour singlet exchange" in hard photoproduction, providing yet another perspective on this area.

8. *Other topics.* In hard photoproduction ZEUS have also published further studies of jet properties, in particular those of dijet events, where the direct component gives information on the gluon content of the proton while the resolved is also sensitive to the photon structure. Other measurements in this area have included inclusive jet cross sections, and angular distributions of the scattered partons in their centre of mass system.

   Searches for exotic states also continue. They have so far proved unsuccessful but not unfruitful, since accounting for the candidate events which are found demands an increasingly rigorous understanding of lepton and jet physics in ZEUS.

HERA still remains a unique instrument for the study of lepton-hadron interactions at the highest energies, and its potential is only gradually becoming realised. We expect higher luminosities for some years yet, and eventually polarised electron and positron beams. It is evident that the results so far have opened up many interesting questions which future running should help to solve. The ZEUS collaboration thus looks forward to a very healthy future, with a continuing rich diversity of physics.

Publications.

1. *Measurement of total and partial photon proton cross sections at 180 GeV center of mass energy.* M Derrick et al., Z. Phys. C63 (1994) pp391-408.
2. *Comparison of energy flows in Deep Inelastic Scattering with and without a Large Rapidity Gap.* M Derrick et al., Phys. Lett. B338 (1994) pp483-496.

3. *Measurement of the proton structure function F_2 from the 1993 HERA Data.* M Derrick et al., Z. Phys. C65 (1995) pp379-398.
4. *A Search for excited fermions in electron-proton Collisions at HERA.* M Derrick et al., Z. Phys. C65 (1995) pp627-647.
5. *Inclusive jet differential cross sections in photoproduction at HERA.* M Derrick et al., Phys. Lett. B342 (1995) pp417-432.
6. *Extraction of the gluon density of the proton at small x.* M Derrick et al., Phys. Lett. B345 (1995) pp576-588.
7. *Observation of hard scattering in photoproduction events with a large rapidity gap at HERA.* M Derrick et al., Phys. Lett. B346 (1995) pp399-414.
8. *Dijet cross sections in photoproduction at HERA.* M Derrick et al., Phys. Lett. B348 (1995) pp665-680.
9. *Study of $D^*(2010)^{\pm}$ production in ep collisions at HERA.* M Derrick et al., Phys. Lett. B349 (1995) pp225-237.
10. *Measurement of charged and neutral current ep deep inelastic scattering cross sections at high Q^2.* M Derrick et al., Phys. Rev. Lett. 75 (1995) pp1006-1011.
11. *Measurement of the cross section for the reaction $\gamma p \rightarrow J/\psi p$ with the ZEUS detector at HERA.* M Derrick et al., Phys. Lett. B350 (1995) pp120-134.
12. *Jet production in high Q^2 deep-inelastic ep scattering at HERA.* M Derrick et al., Z. Phys. C67 (1995) pp81-92.
13. *Measurement of multiplicity and momentum spectra in the current fragmentation region of the Breit frame at HERA.* M Derrick et al., Z. Phys. C67 (1995) pp93-107.
14. *Inclusive transverse momentum distributions of charged particles in diffractive and non-diffractive photoproduction at HERA.* M Derrick et al., Z. Phys. C67 (1995) pp227-237.
15. *Study of the photon remnant in resolved photoproduction at HERA.* M Derrick et al., Phys. Lett. B354 (1995) pp163-177.
16. *Diffractive hard photoproduction at HERA and evidence for the gluon content of the pomeron.* M Derrick et al., Phys. Lett. B356 (1995) pp129-146.
17. *Exclusive ρ^0 production in Deep Inelastic electron-proton scattering at HERA.* M Derrick et al., Phys. Lett. B356 (1995) pp601-616.
18. *Measurement of the diffractive structure function in Deep Inelastic Scattering at HERA.* M Derrick et al., accepted by Z. Phys. C.
19. *Neutral strange particle production in Deep Inelastic Scattering at HERA.* M Derrick et al., Z. Phys. C68 (1995) pp29-42.
20. *Measurement of α_s from Jet Rates in Deep Inelastic Scattering at HERA.* M Derrick et al., DESY-95-182, accepted by Phys. Lett. B.
21. *Optimization of the pulse arrival time determination in the ZEUS central tracking detector FADC system.* D.G. Cussans and H.F. Heath, NIM A 362 (1995) pp277-282.
22. *A Measurement of the proton structure function $F_2(x, Q^2)$ at low x and a determination of the low-x gluon distribution.* M Lancaster in proc. XXVII International Conference on High Energy Physics, Glasgow (ed. P J Bussey, I G Knowles), IOP (1995) pp641-644.
23. *Proton structure functions and diffraction in Deep Inelastic Scattering at HERA.* A Prinias in proc. XXIV International Symposium on Multiparticle Dynamics, Vietro sul Mare, (ed. A Giovanni, S Lupia, R Ugoccioni), World Scientific (1995) pp503-516.

Ph.D Theses.

1. A F Byrne (Oxford) *An initial study of diffractive physics in ep collisions at HERA and performance of the tracking trigger for the ZEUS experiment.*
2. C Catterall (UCL) *Measurement of charged particles from the hadronic final state of electron proton deep inelastic scattering at a centre of mass energy of 296 GeV.*
3. S George (Bristol) *SDC trigger studies and measurement of $\sigma(K^0)$ in DIS.*
4. P Kaziewicz (UCL) *Energy flows in deep inelastic scattering at HERA.*
5. J O'Mara (Bristol) *NLO QCD fit to ZEUS and NMC DIS data.*
6. A Prinias (IC) *Measurement of the proton structure function F_2 using the ZEUS detector.*

The thesis by V. Jamieson *(Measurement of scaled momentum distributions in the Breit Frame at HERA)*, shared a prize with two others for the best experimental Ph.D. theses submitted in 1994 on work done at DESY.

Talks on ZEUS and ZEUS-related physics given at International Conferences.

1. N Brook, *Energy flow, forward jets (ZEUS),* DIS Workshop, Cambridge 1995.
2. P Bussey, *A comparison of prompt photon processes and two jet processes in hard photoproduction,* Photon '95, Sheffield.
3. R Cashmore, *Prospects for very high luminosity at HERA,* DIS '95, Paris, and Zeuthen Meeting on Spin Physics at HERA, 1995.
4. R Devenish, *Recent results on proton structure,* DESY Theory Workshop 1995.
5. A Doyle, *Diffraction (ZEUS),* DIS Workshop, Cambridge 1995.
6. A Doyle, *Diffraction at HERA: Experimental Perspective,* Durham workshop on proton, photon and pomeron structure, 1995.
7. I Fleck, *Measurement of F_2 of the proton in ZEUS data and extraction of the gluon density at small x,* Photon '95, Sheffield.
8. B Foster, *Recent results from ZEUS,* DIS '95, Paris.
9. M Lancaster, *A measurement of the proton structure function F_2 in DIS at low x and low Q^2,* DIS '95, Paris.
10. M Lancaster, *Proton structure at HERA: F_2, QCD fits and Beyond,* Durham workshop on proton, photon and pomeron structure, 1995.
11. L Lindemann, *Latest ZEUS results on F_2,* DIS Workshop, Cambridge 1995.
12. V Noyes, *Results from the searches for new particles at HERA,* XVth Workshop on Weak Interactions and Neutrinos, Talloires.
13. H Uijterwaal, *The ZEUS central tracking detector second level trigger,* CHEP95, Brazil.
14. M Utley, *Direct and resolved photoproduction at HERA with virtual and quasi-real photons,* EPS Conference on High Energy Physics, Brussels 1995.
15. R Walczak, *W and Z boson production at HERA,* International Symposium on Vector Boson Self Interactions. Los Angeles, 1995.
16. A Whitfield, *Vector mesons in Deep Inelastic Scattering at HERA,* DIS '95, Paris.
17. A Whitfield, *Photo- and Electroproduction of Vector Mesons (ZEUS),* DIS Workshop, Cambridge 1995.
18. R Yoshida, *Deep Inelastic Scattering at HERA: Recent results from H1 and ZEUS,* Rencontres de Phys. de la Vallée d'Aosta, La Thuile.

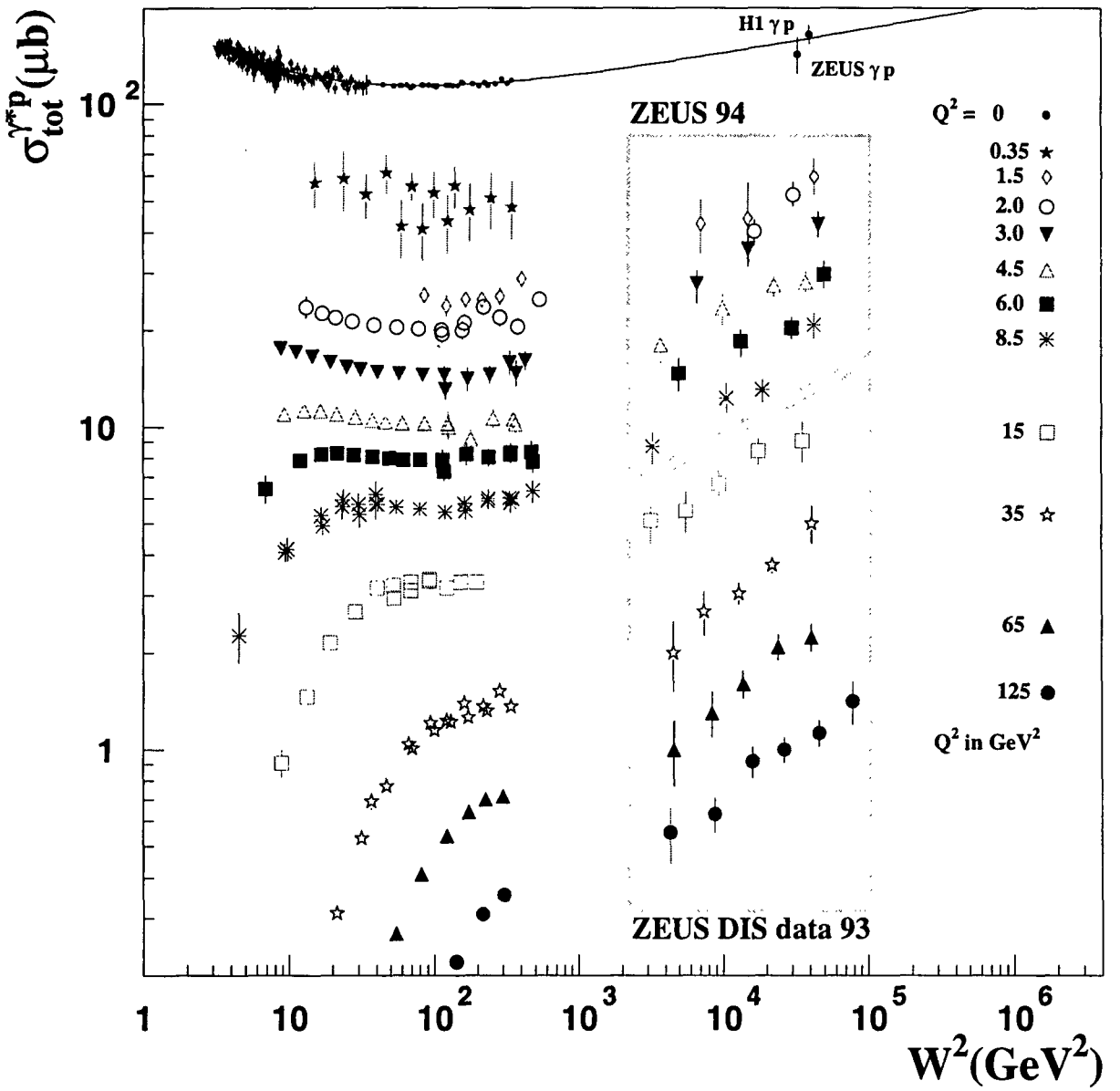

Figure 1: Total $\gamma^* p$ cross sections for photons of varying degrees of virtuality as a function of $\gamma^* p$ centre of mass energy W squared. It can be seen that at high W^2, the trend of each set of $Q^2 > 0$ points with W^2 is a much steeper rise than for the "real" photoproduction data parameterised by the top curve.

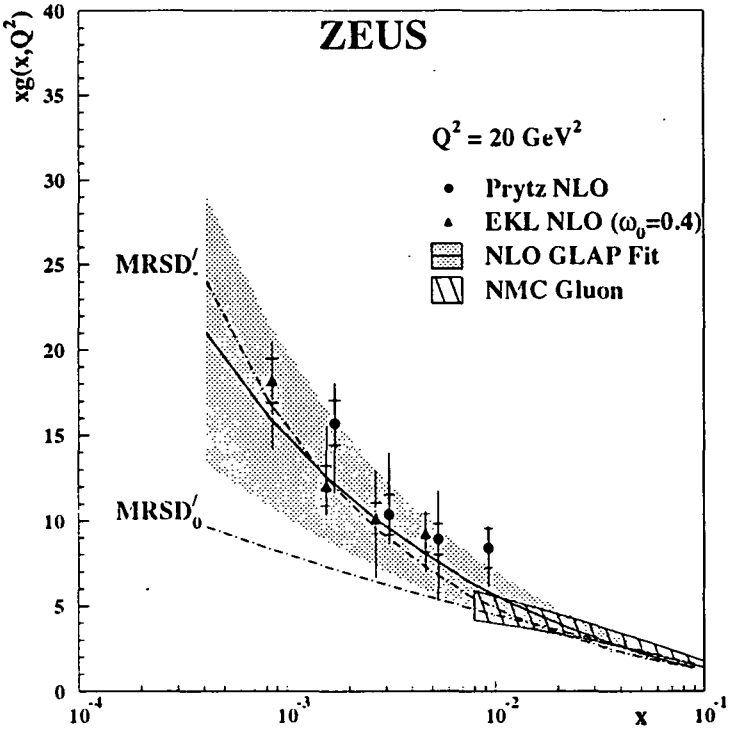

Figure 2: Gluon density in the proton, as extracted using methods of Prytz and EKL and compared with the MRSD–′ and MRSD0′ global fits [6].

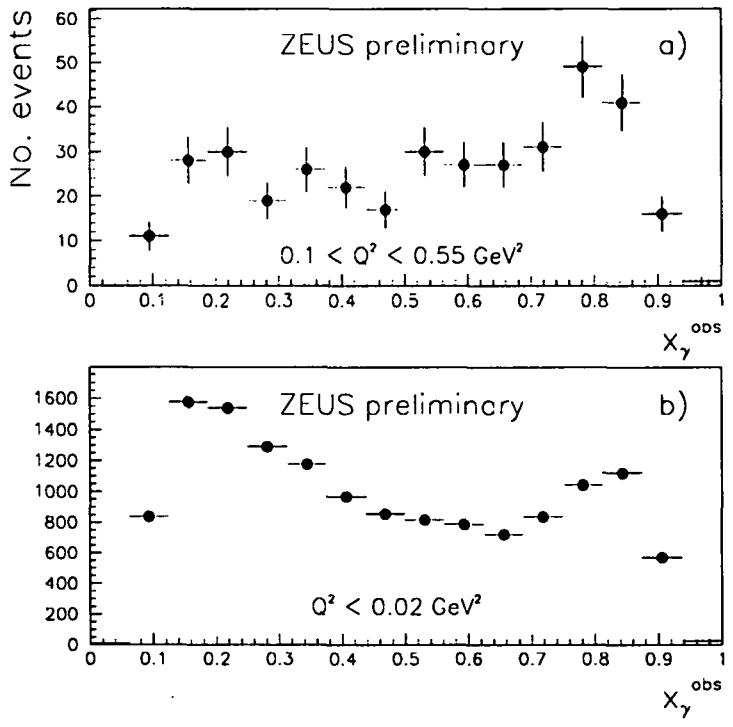

Figure 3: Distributions of x_γ for hard photoproduction as measured using dijet events for (a) $0.15 < Q^2 < 0.55\,\mathrm{GeV}^2$, (b) $Q^2 \approx 0$. The resolved component (i.e. for $x_\gamma < 0.7$) is proportionately much reduced in (a) compared to (b).

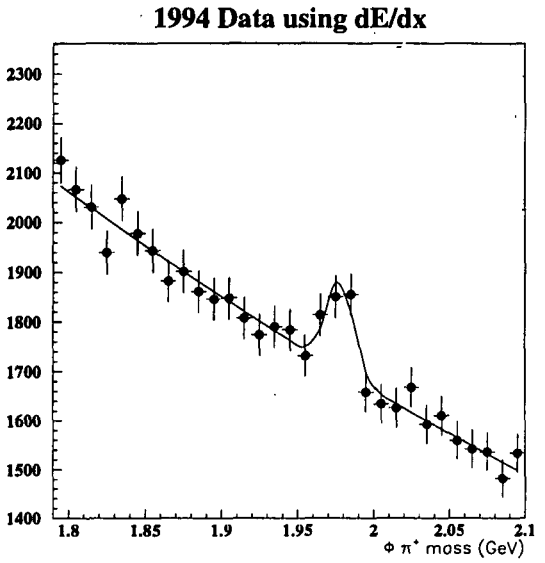

Figure 4: D_S signal in $\phi\pi^+$ decay mode in low Q^2 photoproduction.

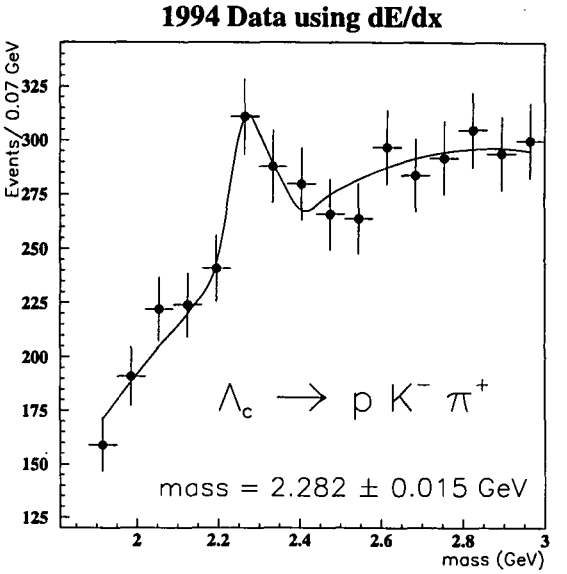

Figure 5: Λ_c signal in $pK^-\pi^+$ channel.

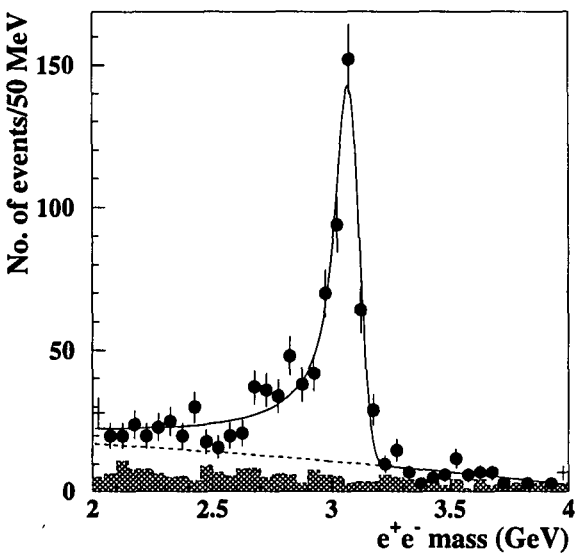

Figure 6: Elastically produced J/ψ signal in e^+e^- decay channel.

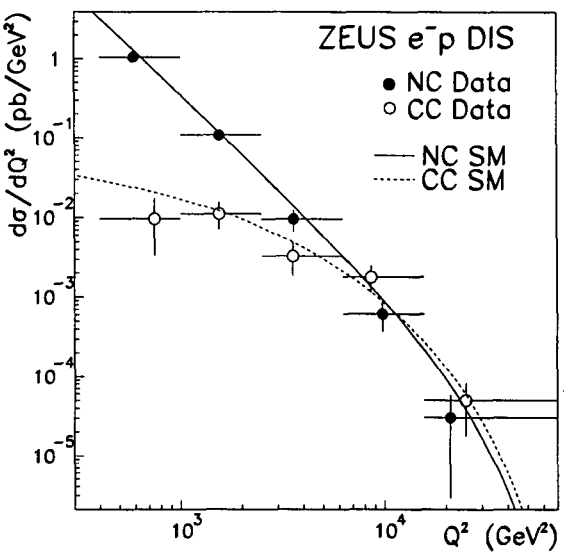

Figure 7: Cross sections for neutral and charged current e^-p scattering at very high Q^2, compared with Standard Model predictions [10].

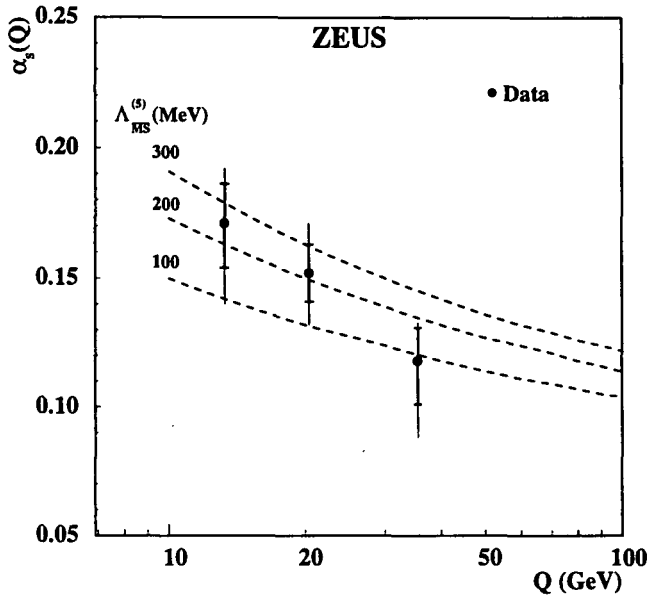

Figure 8: Measured values of α_s as a function of Q, together with predictions using different values of the QCD scale parameter Λ, as determined from the rate of two-jet events in DIS in the ZEUS 1994 data [20].

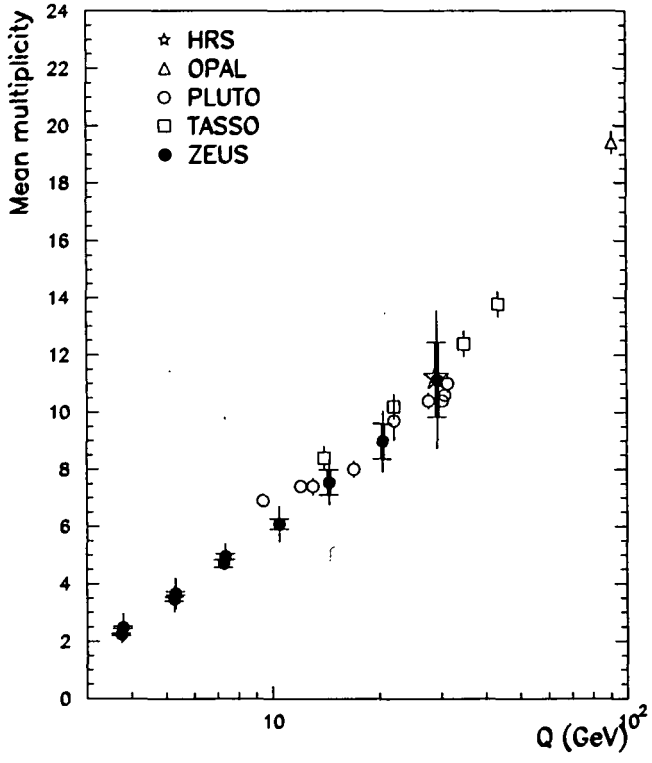

Figure 9: Charged hadron multiplicities in the current region of the Breit frame in ep scattering, scaled by a factor of two. These are compared with corresponding multiplicities in e^+e^- annihilation events on an equivalent energy scale [13], and demonstrate a similarity in quark hadronisation properties in the two classes of event.

The ATLAS Project

Albany; Alberta; Alma Ata; Amsterdam (NIKHEF); Annecy; Argonne; Arizona; Arlington; Athens (Univ and NTU); Baku; Barcelona; Bergen; Berkeley (LBL and UC); Bern; **Birmingham**; Bochum; Bonn; Boston; Brandeis; Bratislava; Brookhaven; Bucharest; **Cambridge**; Carleton; CERN; Chicago; Clermont-Ferrand; Columbia; Copenhagen; Cosenza; Cracow (INP and FPNT); Dortmund; Dubna; Duke; **Edinburgh**; Frascati; Freiburg; Fukui; Geneva; Genoa; **Glasgow**; Grenoble; Haifa; Hamburg; Harvard; Hawaii; Heidelberg; Helsinki; Hiroshima; Indiana; Innsbruck; Irvine; Istanbul; Jena; KEK; Kobe; Kosice; Kyoto; **Lancaster**; Lecce; Lisbon; **Liverpool**; **QMW**; **RHBNC**; **UCL**; Lund; Madrid; Mainz; **Manchester**; Mannheim; Marseille; MIT; Melbourne; Michigan; Milan; Minsk; Montreal; Moscow (ITEP, Lebedev, MEPHI, MSU); Munich (LMU and MPI); Naples; Naruto; New Mexico; Nijmegen; Northern Illinois; Novosibirsk; Oklahoma; Orsay; Oslo; **Oxford**; Paris VI and VII; Pavia; Pennsylvania; Pisa; Pittsburgh; Prague (CAS, CU and TU); Protvino; Rio de Janeiro; Rochester; Rockefeller; Rome (I,II and III); **RAL**; Saclay; Santa Cruz; Sao Paulo; **Sheffield**; Shinshu; Siegen; Southern Methodist; St Petersburg (IFMO and NPI); Stockholm (Univ and KTH); Sydney (Univ and ANSTO); Tbilisi (AS and SU); Tel-Aviv; Thessaloniki; Tokyo (CU, ICEPP, MU and AT); Toronto; TRIUMF; Tufts; Udine; Uppsala; Urbana; Valencia; Vancouver; Victoria; Washington; Weizmann; Wisconsin; Wuppertal; Yerevan.

1 Introduction

The year 1995 has seen steady progress in the ATLAS project. The Technical Proposal [1] was submitted in December 1994 and throughout 1995 the project was reviewed at CERN by the LHCC and in the UK by the PPESP. In November ATLAS was recommended for approval by the LHCC, a recommendation subsequently endorsed by the CERN Research Board in December. ATLAS is pleased by the confidence expressed by these two bodies.

Because of some remaining uncertainty in non-member-state financial contributions, both the LHC machine and the experiment will be reviewed again in 1997. Between now and then preparation for ATLAS will continue at full speed.

The overall detector concept remains unchanged (fig 1). It combines a high resolution muon spectrometer with robust and fine-grained calorimetry and high precision inner tracking with very good pattern-recognition capabilities.

The extensive R&D programme launched some years ago in anticipation of physics at LHC has now been fully absorbed into the ATLAS subdetector development programme.

The main activities undertaken by groups in the UK have been:

1. The air cored endcap superconducting toroids.
2. The inner detector.
3. The level-1 trigger.
4. The level-2 trigger.
5. Software development.

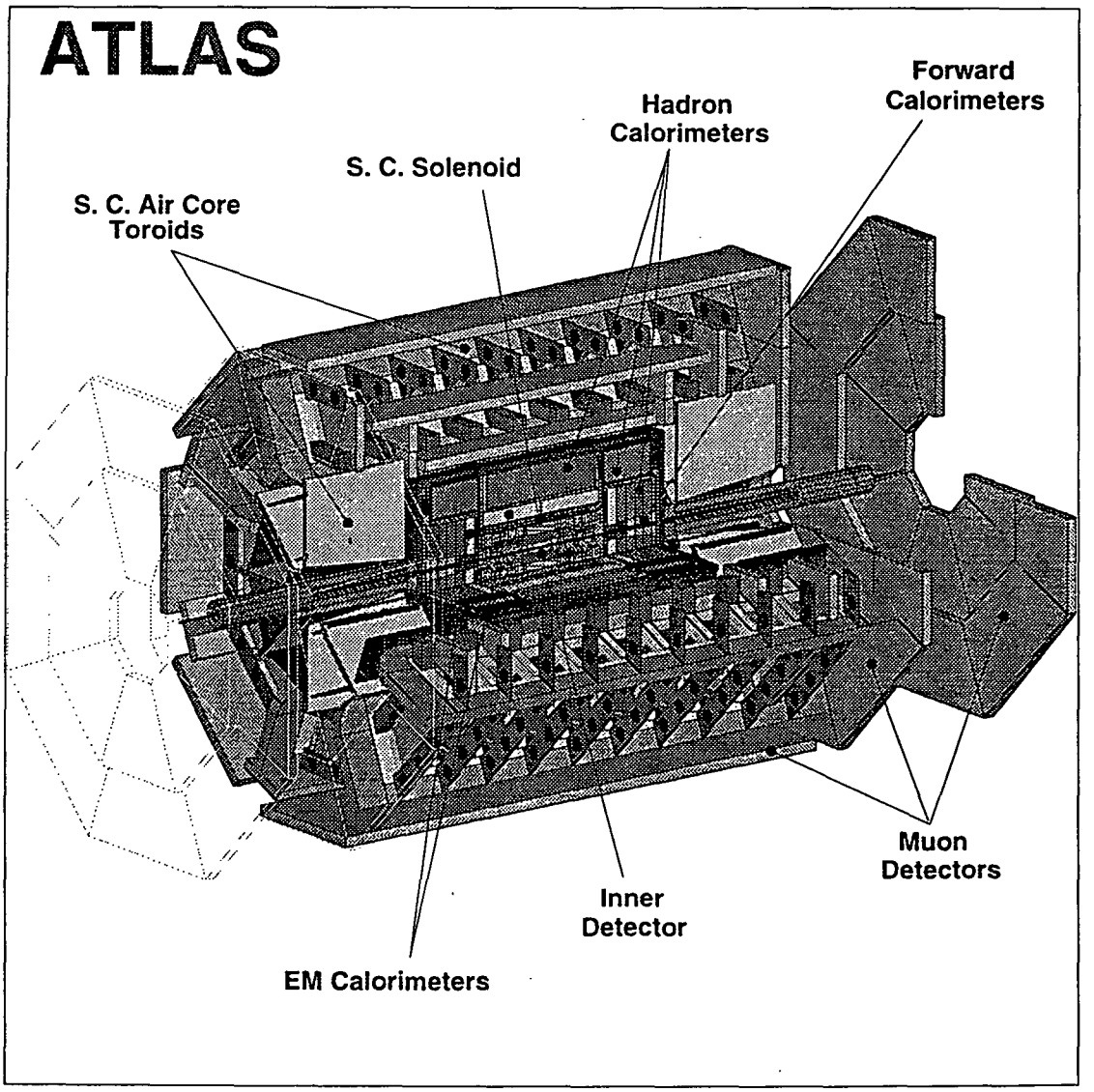

Figure 1: Three dimensional schematic of the ATLAS detector.

2 The Endcap Toroids

The air cored endcap superconducting toroids are being designed at RAL. Following a review at the end of 1994, further progress has been made on the specification, and conceptual designs have been developed and evaluated, taking particular account of the interaction with the rest of the detector and of the implications for the muon spectrometer resolution. Each endcap is constructed from eight symmetrically distributed coils enclosed in a single large cryostat (fig 2). Considerable progress has been made in 1995 on the design and stress analysis of the cold mass, the design of the cryostat, cryogenic specifications, fault conditions and their prevention, and installation and assembly procedures.

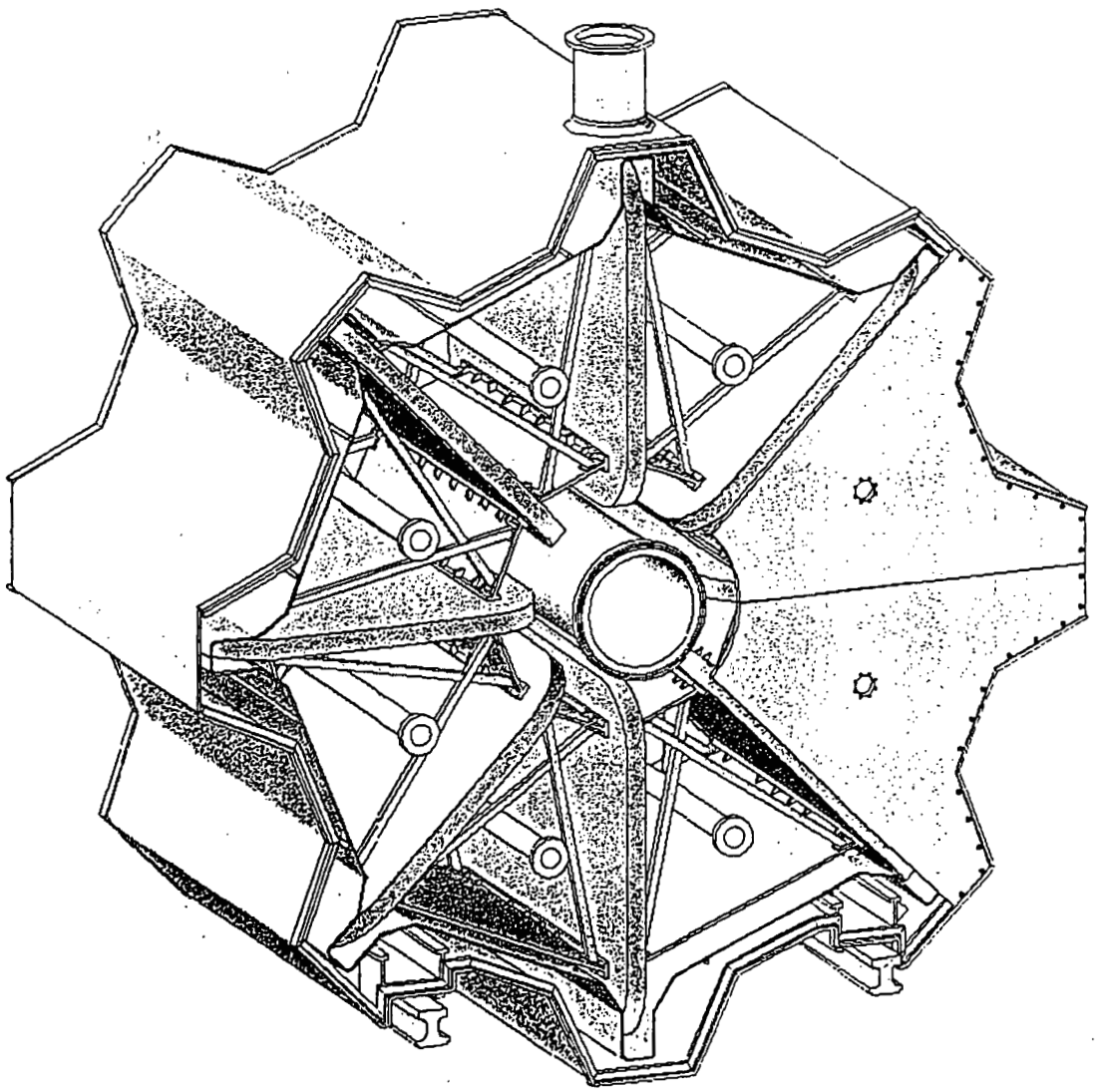

Figure 2: Three dimensional schematic of an ATLAS endcap toroid.

3 The Inner Detector

3.1 Overview

At design luminosity, the ATLAS Inner Detector (ID) is designed primarily to help identify high p_T leptons produced in the decays of heavy *Higgs* or arising from new physics such as a massive Z'. This involves measuring particle momenta, checking their isolation and distinguishing between prompt electrons, photons, conversions and bremsstrahlung. At low luminosity, the emphasis will be on b-tagging using identified leptons and vertexing techniques for *top* physics and light *Higgs* searches, along with the reconstruction of exclusive B decays to study CP violation.

Despite significant advances in the understanding of gas microstrip detectors (MSGCs), in September the ID community decided to replace the MSGC wheels proposed for the forward tracking by silicon detectors. The main reasons for this choice were: the simplification achieved by reducing the number of technologies, the reduced risk associated with a more familiar technology, less material, the ability to achieve higher spatial resolution and correspondingly better two-track separation. The result is an integrated barrel and forward tracker with many design features in common.

The current layout is illustrated in figures 3 and 4. The aim is to provide ≥ 6 precision hits over the range $|\eta| < 2.5$. This is achieved by 2 pixel hits at small radii, with 4 stereo hits provided by silicon strips up to $r \leq 54$ cm. At smaller r in the forward region, the latter are replace by GaAs strips. These stereo strip layers constitute the Semi-Conductor Tracker (SCT). Beyond the precision layers, continuous tracking is provided by up to 36 layers of straw tubes. At low luminosity, a vertexing layer of pixels or crossed-strips is envisaged. This design will be frozen to permit extensive simulations and detailed costings. Some refinements of the barrel-forward overlap may be required. This layout will be reviewed in Spring 1996 to ensure that it is within the cost ceiling.

3.2 Prototyping and Test-beam for Silicon detectors

Much of the effort of the community (especially Birmingham, Cambridge, Liverpool, QMW, Oxford, RAL) in 1995 has gone into prototyping for and running in the H8 test-beam at CERN. To aid measurements, a very precise telescope was built with UK participation (Cambridge, Liverpool, RAL)

Along with a variety of other schemes, detectors are being designed based on n^+-strips in n-type bulk. These are likely to be more robust after high doses of radiation. Masks were designed (Cambridge, Liverpool, QMW, RAL) and fabricated by CMF (RAL), with detectors being made by Micron Semiconductor (UK) Ltd. Results demonstrating charge sharing in these devices can be seen in figure 5.

Studies with the Oxford/RAL designed DDR2 binary read-out chip yielded resolutions $\approx \frac{pitch}{\sqrt{12}}$. Subsequent analysis (Liverpool) of analogue data indicates that using this scheme to read out every other channel of an AC-coupled detector could yield significantly better resolution with a small loss in signal.

To test the concept of a module along with the analogue solution, two prototype

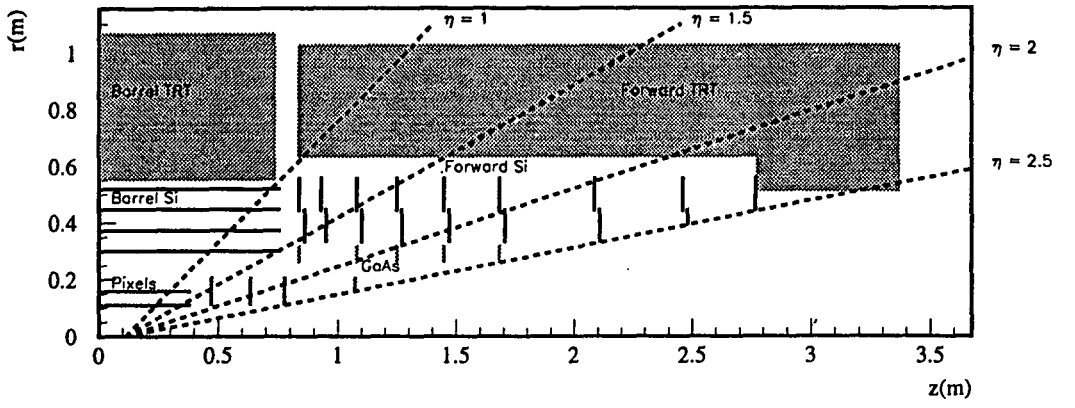

Figure 3: Inner Detector layout showing pixels, silicon stereo layers, GaAs stereo layers and TRT. The rays originate from a collision point displaced by 2σ in z.

z-modules were constructed. These include two pairs of single-sided silicon detectors mounted back-to-back with a 40 mrad stereo angle. The APV5 analogue FE chips sit on a hybrid located to the side of the detectors and connected by kapton fan-ins. The driver electronics, APV5s and LED based opto-links were supplied by RAL; the mechanics by QMW and RAL; the hybrids were designed at Liverpool and the detectors were tested and bonded at Cambridge, Liverpool and RAL. Successful tests were made of the Multi-Quantum Well readout (Birmingham) and a pulse height modulation scheme designed for the distribution of the clock and control data (Oxford). The latter scheme has been adopted as the SCT baseline. While the prototype provided a successful full system test of the z-module, the APV5 did not permit measurements at LHC-speeds. However, tests with the FElix-128 front-end (Liverpool) yielded $\sigma = 16$ μm (deconvoluted) from a pitch of 112.5 μm.

Tests were also made with a 32-channel version of the ADAM architecture, which is currently the only digital front-end chip working at LHC-speeds. signal/noise (S/N) of ~ 11 was achieved. Experience gained with this is being used in the development (RAL) of the AROW digital design which incorporates a bipolar front-end amplifier with an integrated Wilkinson ADC on a 128-channel chip.

An exhaustive review process has begun, and will conclude at the end of 1996. The baseline decisions taken in 1995 are: AC-coupled detectors with n^+-strips in n-type bulk and LED read-out. Next year, decisions will be made on: pitch; analogue, digital or binary read-out; single or double sided detectors; and r-ϕ or z module type.

Following tests at ISIS-RAL, Oxford in collaboration with Bern have shown that LEDs have a good lifetime even after irradiation. LEDs have been adopted as the baseline solution for data transmission for the SCT.

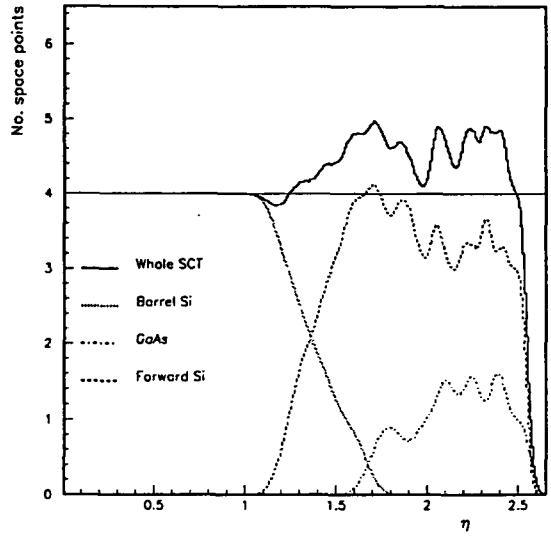

Figure 4: Number of space points from SCT as a function of pseudo-rapidity.

3.2.1 Silicon detectors in the Forward region

ATLAS has been pursuing the concept of silicon detectors in the forward region - this project has an additional impetus following its selection as the baseline. A 12 cm long module with keystone geometry has been designed and tested (Liverpool) in H8. The detectors used were simple DC-coupled devices with p-strips in n-bulk. The active area of the module was full length but half width, with read-out pitches varying between 103 and 145 μm. Using APV5 front-end chips, efficiencies of 99.5% were achieved with a cut at 4 times rms noise. The resolution was compatible with $\frac{pitch}{\sqrt{12}}$, but not better due to the lack of charge sharing in a DC device.

3.2.2 GaAs detectors

The Glasgow, Lancaster and Sheffield groups have led the development of GaAs detectors for ATLAS. Commercial detectors have been obtained from EEV (UK) Ltd and Alenia SpA, while in-house detectors have been produced by Glasgow. These were read out in H8 using LEP-speed electronics. The 11 mm EEV detectors gave S/N 20:1 with resolutions of $\frac{pitch}{\sqrt{12}} = 14$ μm (1-hit clusters), 9 μm (2-hit clusters) with an average of 12 μm. Work is underway to increase the breakdown voltage beyond the 180V currently observed, where charge collection efficiency is around 45%. The 25 mm Alenia and Glasgow detectors had comparable resolution but lower S/N due to greater capacitive load arising from their length.

Further studies with neutrons (ISIS-RAL) have confirmed the radiation hardness of GaAs, however new studies with protons (CERN) and pions (PSI) suggest that charged particles may be much more damaging than expected. Studies are underway to understand this in terms of non-ionising energy loss and more irradiations will be performed in 1996.

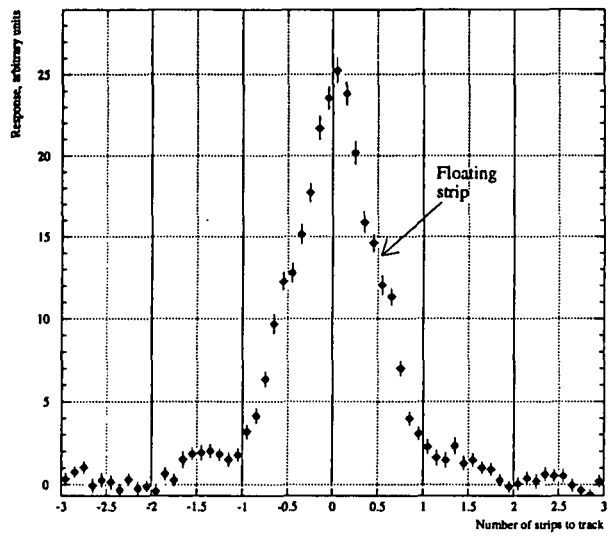

Figure 5: The response of a readout strip in an AC-coupled detector as a function of the distance to a track (in units of strip pitch). The 'shoulder' due to the intermediate diode, where half of the charge is collected on one strip, can be clearly seen.

3.3 Engineering and Electronics development

The silicon barrel structure incorporating beryllium staves is in an advanced stage of design (RAL) including finite-element analysis (FEA) (Oxford, RAL) of the stresses and work is underway to understand the integration of the complete ID (including pixels and TRT) into ATLAS. In parallel, much work (Liverpool, RAL) is going on to bring the mechanical design of the forward wheels and corresponding support structure up to the same level as that currently achieved for the barrel - see figure 6.

Detailed designs have been produced for the barrel silicon z-module (RAL) (see above) along with FEA (Oxford, RAL) of the heat-flow. These have been confirmed using a prototype attached to a stave segment. Detailed maps have been built up (RAL) of the radiation lengths of all components in the barrel modules. The design (Glasgow, Lancaster, Sheffield, RAL) of the GaAs modules has been brought more into line with the forward silicon modules: detectors will have a keystone geometry with one of the pair of detectors rotated from radial by a stereo angle of 40 mrad and with pitches varying from 50 to 62 μm.

Binary-ice has been chosen for cooling the SCT and will be operated somewhere in the range -15 to $0°$C. The desire is to run the system 'leakless', ie. sub-atmospheric pressure. Tests have been done (RAL) on flow, viscosity and the cooling of heat sources attached to a prototype barrel stave.

Consideration is now being given (RAL, QMW) to the procedures which will be used to assemble silicon detectors, front-end chips, fan-ins etc into modules. First attempts have been made (RAL) to understand the service requirements (high-voltage, read-out,

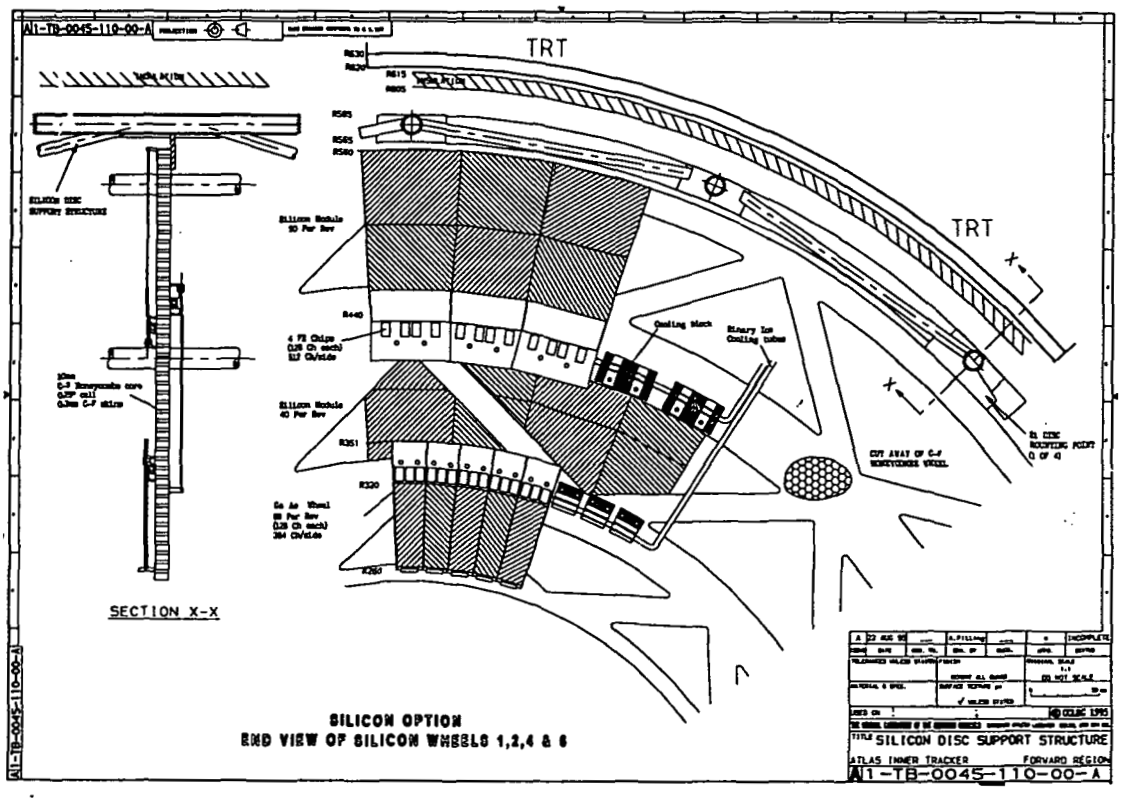

Figure 6: Forward wheel design showing two rings of silicon modules and an inner ring of GaAs.

clock-and-control, cooling) and their impact on the rest of the ATLAS integration.

Substantial work on hardware alignment has been carried out at Oxford. The ultimate alignment precisions ($\Delta_{r\phi} \leq 10\mu$m) will come from reconstructed tracks. To assist in the initial alignment and continuous monitoring, absolute measurements will be made in situ at many references points using Frequency Scan Interferometry. An Electron Speckle Pattern Interferometry (ESPI) system has been set up in Oxford. ESPI will be an invaluable tool for understanding the deformations of complete components (eg. modules, staves, cylinders) in real time under thermal and mechanical loads. The ESPI facility has already been used to understand the RAL z-module and will be used by many ATLAS groups next year.

Work continues at RAL on analogue readout solutions (APVn). Work on binary and digital (AROW) FE chips will continue at Oxford and RAL. In addition, development work is being done on the DORIC clock-and-control chip (with Oxford) and the AROMA readout module (with Cambridge), aimed at digitising analogue information off-detector.

3.4 Microstrip Gas Chambers

Whilst at the start of the year MSGCs were the baseline choice for the forward precision tracker, there was an option to replace MSGCs by silicon microstrip detectors as used in the barrel precision tracker. The ATLAS collaboration set up a decision path to choose between these technologies. This consisted of a set of criteria against which the technologies would be judged by the Inner Detector Review Panel, the Inner Detector Steering Group and the Inner Detector Working Group in September.

The criteria for the MSGC included a demonstration that the detectors would survive for at least 10 years in ATLAS and measurements of position resolution, two track resolution and efficiency as a function of track angle. The charge collection time for the MSGCs is of the order of two LHC bunch crossings (50 ns), so an additional requirement was a measurement of the ability to correctly tag the bunch crossing from which the track originated.

By the time of the September review the ageing characteristics of MSGCs built on semiconducting glass had been measured using both an x-ray source and a Sr^{90} β source. These measurements show that, although a detectors with aluminium electrodes show rapid deterioration under irradiation, detectors with gold metallisation survive a dose equivalent to 10 years in ATLAS with little or no loss of gas gain. The results of gain measurements as a function of integrated dose from a Sr^{90} source are shown in figure 7 for two Ar/DME gas mixtures. A 50:50 mixture was the baseline for ATLAS.

At the beginning of 1995 two full sized MSGC detectors were built with the fan shaped electrodes needed for the forward tracker. The performance of these detectors was evaluated in a test beam at CERN. These measurements demonstrated uniform gain and efficiency along the full 15 cm electrode length up to within 1 mm of the end of the strips, see figure 8. Also measured were the two track resolution, efficiency as a function of angle and the bunch crossing tagging efficiency. All measurements demonstrated that the MSGCs envisaged would satisfy the ATLAS requirements.

An agreed cost comparison of the MSGC and silicon microstrip detectors for the forward region showed that the MSGC based tracker would be approximately 4 MCHF less expensive.

While the Inner Detector Review Panel at the September review recognised that MSGCs would perform satisfactorily in ATLAS they considered that the silicon option would have better stand alone capability and offers the advantage of a reduced number of detector technologies in the tracker. They did not consider the cost saving to outweigh the advantages of the silicon option, and recommended ATLAS to choose the latter. This recommendation was endorsed by the Inner Detector Steering Group, the Inner Detector Working Group, and the Collaboration Board.

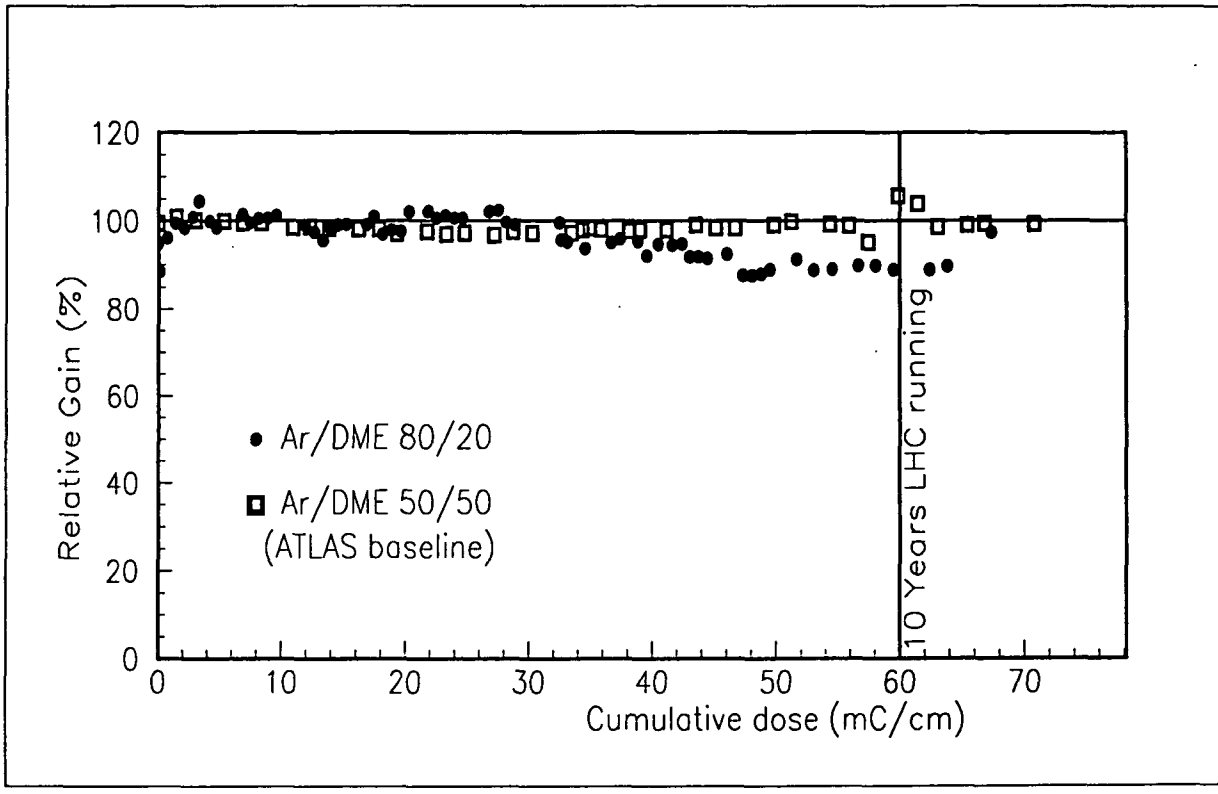

Figure 7: Ageing of a MSGC detector with a S8900 glass substrate and gold electrodes. Operating voltages were kept constant. Measurements have been corrected for temperature and pressure variation.

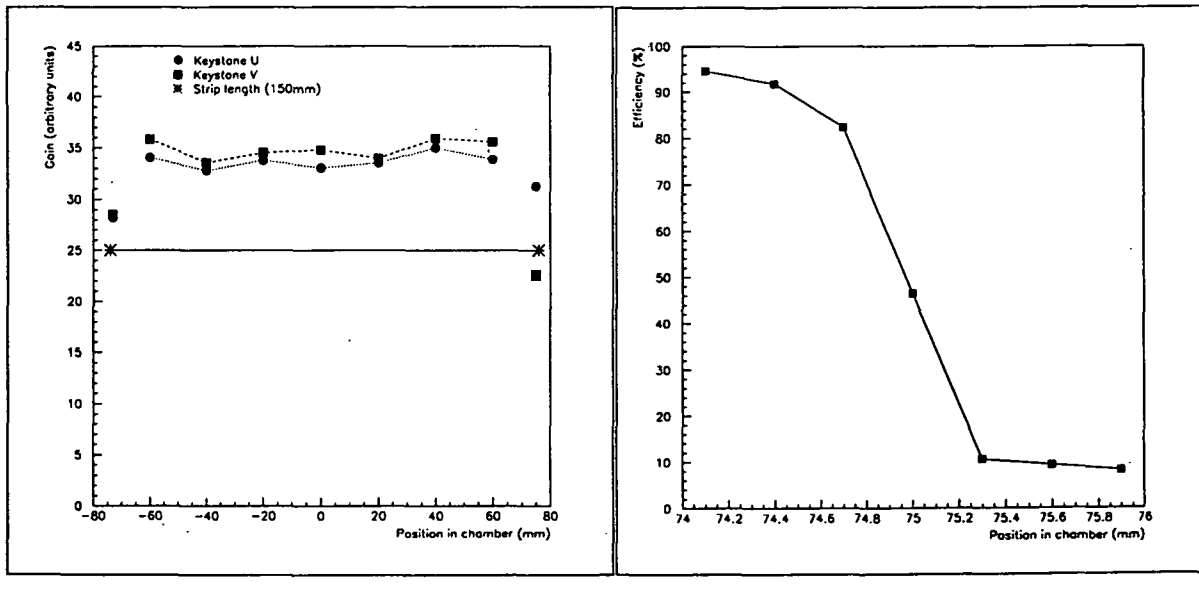

Figure 8: Test beam measurements on a full size 'fan-shape' prototype. Left: Gain measurements along the strips. Right: Efficiency measurements within $\pm$1mm of the end of the electrodes.

3.5 TRT

Activity on straw tube electronics for ATLAS at RAL, initiated in the RD6 collaboration, was completed in 1995. A new version of the front end electronics was produced providing better cancellation of the ion tail in the signal (essential for high rate operation) and a more uniform discrimination threshold. This front end chip was tested in the beam and achieved its performance goals. Previous work on straws has now been published [4], relying very substantially on analysis performed at Glasgow.

3.6 Physics simulation

UK groups (Glasgow, Manchester, Sheffield, RAL) have contributed significantly to the ATLAS effort to develop simulation code which reflects the current design of the apparatus. Realistic geometries and material distributions, along with detector response appropriate to analogue or binary read-out is now included. Various modifications and improvements to the layout have been made.

The b-tagging capabilities of the detector have been investigated (Oxford, RAL) using both simple simulations and more recently, full GEANT simulation, incorporating sophisticated pattern-recognition algorithms. Gluon-jet rejection of 10^2 should be obtainable for b-jet efficiencies $\geq 50\%$.

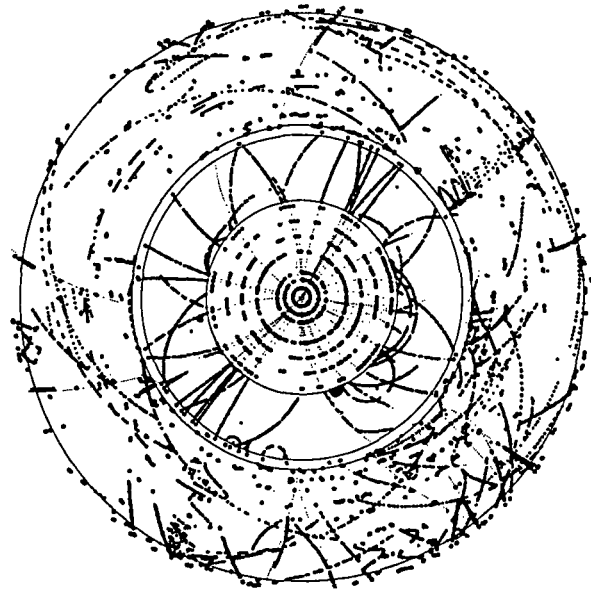

Figure 9: Example of $H \rightarrow b\bar{b}$ at low luminosity with full GEANT simulation. The inner part of the picture corresponds to the barrel of the ID. Open circles represent precision measurements (pixel, SCT); filled circles represent TRT hits. Generated tracks are shown as dotted curves. Similarly, the outer ring corresponds to the forward regions where the z information has been transformed into a radial position.

4 Level-1 Trigger

The ATLAS level-1 trigger is based on calorimetry and muon detectors. The trigger system operates synchronously at the LHC bunch crossing frequency of 40 MHz, reducing the rate of accepted events to a maximum of 75 kHz. Birmingham, QMW and RAL are involved in development of a purpose-built digital processor which will provide electron, photon, jet, and missing transverse energy triggers from calorimeter data [5].

The calorimeter trigger consists of front-end summation, digitisation and bunch-crossing identification (BCID) logic, a high speed data transmission system, and specialised processors identifying e.m. clusters, jets, and missing-E_T. The electromagnetic processing algorithm was incorporated into an ASIC which was demonstrated in 1993 at the full LHC bunch crossing frequency of 40 MHz.

The emphasis in 1995 has been on demonstration of BCID algorithms, and on design of the phase-II demonstrator system for use in 1996.

4.1 Bunch Crossing Identification

The calorimeters proposed for ATLAS produce output signals extending over several 25 ns bunch crossing periods. For the level-1 trigger these pulses present a problem which has to be solved in real time. The problem is two-fold. Firstly, the LHC bunch crossing corresponding to the energy deposition that produced the pulse has to be identified, and secondly, an energy measurement must be extracted. The pulse heights of the calorimeter signals are digitised every 25 ns by a system of FADCs. The function of the bunch-crossing identification (BCID) logic is to identify, for each calorimeter pulse, the digitised value which corresponds to the pulse peak, to pass this on to the calorimeter trigger processor and to set all other digitisings to zero.

Candidate BCID algorithms must maintain good efficiency for all pulse sizes - BCID is harder for small pulses with lower signal-to-noise ratio, and for large pulses which saturate the FADCs. Algorithms must also be simple enough to permit an economic and low-latency hardware implementation. With these requirements in mind, many digital BCID algorithms have been evaluated by software simulation, using calorimeter data recorded during previous test beam runs. The data include both hadrons and electrons with a range of beam energies up to 300 GeV.

Several efficient BCID algorithms have been identified in simulation studies [for details, see ref [5]]. For pulse heights above 7 counts (7 GeV), all algorithms performed with 100% efficiency. Below this level, even the most complex algorithms start to fail. However, it can be noted that even in the low pulse height regime, the peak finder, the simplest of all the algorithms, gives results comparable to the best of the more complex algorithms. From these results it was concluded that BCID could be performed with good efficiency using relatively simple algorithms.

4.2 The 36-Channel BCID Demonstrator System

A hardware demonstrator was designed, built and used in a test beam to check the real-time BCID performance. The system performed BCID on 36 channels of calorimeter trigger data, with algorithms implemented in Xilinx Field-Programmable Gate Arrays (FPGAs). The re-programmable nature of these devices allowed a variety of BCID

algorithms to be evaluated. Figure 10 shows the complete system as installed in the test beam.

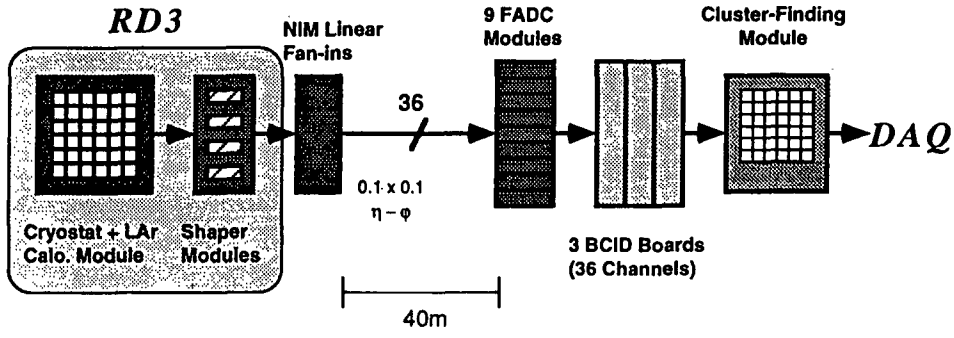

Figure 10: BCID evaluation system used in 1995 test beam running.

After digitisation, 8-bit data from the 36 trigger towers were passed to the BCID system consisting of three 12-channel modules. Inside the modules, pedestal subtraction was performed using a look-up table, followed by BCID processing in Xilinx FPGAs and transmission to the e-γ trigger processing module. Eleven different BCID algorithms were tried.

4.3 Test Beam Results

The main test beam runs took place in September 1995 during tests of front-end electronics for the ATLAS barrel calorimeter prototype. Data were recorded with beam energies from 20 GeV to 300 GeV and with a range of different front-end electronics, which produced analogue pulses with a range of different shapes. Initial analysis has concentrated on checking the system hardware performance. Apart from minor problems, the system behaviour was as expected. This is illustrated in figure 11, which shows the performance of the BCID system using a peak-finding algorithm on a typical 50 GeV electron pulse. The pedestal has been subtracted in the hardware, and the pulse peak correctly identified and passed through the system. The Xilinx implementation of this algorithm has a latency of eight clock cycles.

In the interests of reduced latency as well as cost, the BCID function will ultimately be incorporated into an ASIC. A first prototype BCID ASIC was developed by the Heidelberg group and successfully used with the UK BCID modules by means of a daughter card which was plug-compatible with the Xilinx chip. As expected, this operated with a latency of 7 clock ticks. Further detailed analysis of the data is still underway.

4.4 Phase-II Demonstrator

At the heart of the trigger system is a synchronous pipelined processor identifying e.m. clusters. A prototype of this processor was successfully operated in 1993 and 1994 at the full LHC bunch-crossing rate of 40 MHz.

The trigger also relies on some new technologies which have not yet been tested together as a system. Digitised data from the detector are transferred on optical links as high-speed digital bit-streams in the commercial HP G-link protocol, and requires compact

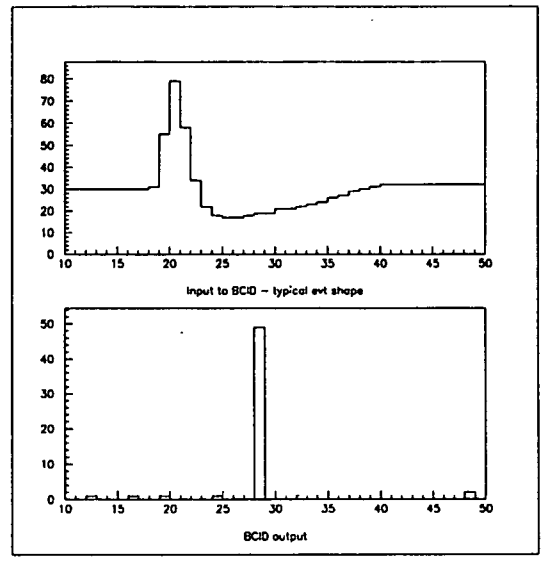

Figure 11: Peak-finding ($S_{n-1} < S_n \geq S_{n+1}$) BCID operation with a 50 GeV e^- pulse.

optical receivers on the e.m. cluster-processing modules. Data are fanned out using optical splitters to span crate boundaries and at 160 Mbit/s on high-speed backplanes within crates. Transmission and reception of the 160 Mbit/s data streams requires new ASIC circuitry. Sophisticated timing arrangements are necessary to ensure that data from all trigger channels enter the processing ASICs at the same time, even though the hadronic and electromagnetic calorimeters have significantly different pulse peaking times.

The purpose of the phase-II demonstrator programme is to show that a complete and usable system can be built, with reliable working examples of all the required new optical, ASIC and backplane technologies.

4.4.1 Phase-II Demonstrator Structure

The demonstrator structure is illustrated in figure 12.

Incoming analogue data are digitised by the 9 four-channel FADC modules previously used with the BCID demonstrator. The digital data are passed over short links to 9 four-channel transmit modules for conversion to serial format by HP G-link chipset and transmission on multi-mode optical fibres by Finisar transmitters. After 80 m of optical fibre, the data are received on 9 cluster-processing modules, converted back to an electrical bit-stream, and returned to parallel format by a G-link receiver. A multiplexing ASIC converts the parallel data to and from the 160 Mbit/s serial format, such that each pair of outputs conveys one 8-bit digitisation each 25 ns. This ASIC also includes the pipeline delays needed for channel-channel synchronisation. Four of the nine Cluster Processing Modules are equipped with phase-I cluster-processing ASICs. The data required to populate these are obtained in part directly from incoming optical fibres, and in part from other Cluster Processing Modules via a transmission-line backplane operating at 160 Mbit/s. The backplane and connector technology closely emulate the proposed design of the full trigger system required for ATLAS.

Limited space is available for electronics on the ATLAS detector, and there is intense debate over the choice of data transmission from the detector. Digital and analogue transmission are both regarded as possibilities, and the final choice will depend on

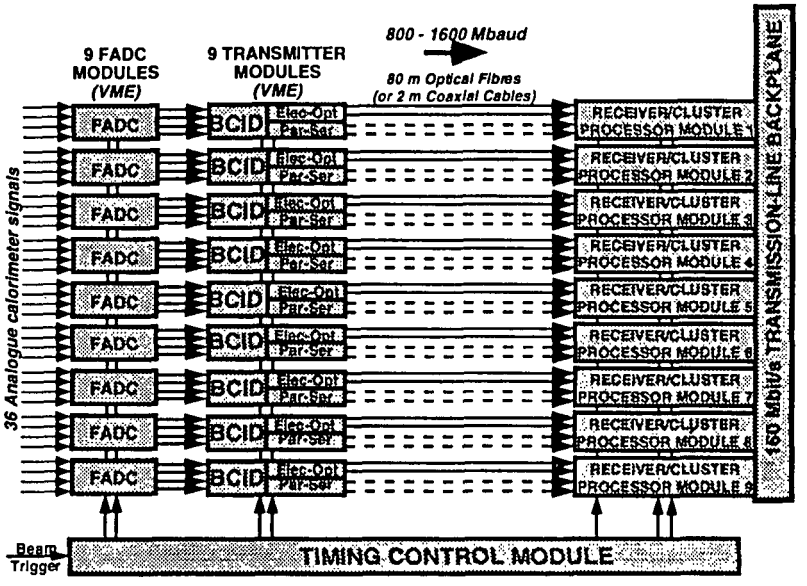

Figure 12: Structure of the Phase-II demonstrator.

the options open to the Liquid Argon calorimeter group as well as the outcome of tests performed within the trigger community. The phase-II demonstrator is therefore structured to allow comparison of several long-distance transmission options before concentrating on the eventual ATLAS choice for detailed study.

To enable studies to start before the transmission method is chosen, transmitting and cluster-processing modules are both equipped with daughter boards on which the transmission components are mounted. The first generation of daughter boards will be equipped with discrete Finisar and G-link devices, and will be replaced by a compact multi-chip module (MCM) once the final transmission method has been chosen.

4.4.2 Demonstrator Status

The demonstrator will be constructed in two stages. The first stage will cover 8 trigger towers. This will check that the complete chain of modules and data transformations work correctly for the technical proposal architecture, but without MCMs. Following this, the remaining modules will be built for a full 36-channel system. It is expected that the transmission-line backplane will be delivered before Christmas, with the first modules arriving in January and February 1996. The first multiplexing ASIC chips have been tested and fully conform to specification. The schedule should allow comprehensive laboratory evaluation prior to beam tests scheduled for June 1996.

The demonstrator will include provision for the fast readout required when the trigger is running in ATLAS. A new ASIC is under design in Heidelberg which will incorporate look-up tables, BCID and fast readout. This will be incorporated into the demonstrator system when available.

5 Level-2 Trigger

Within the three level trigger system proposed for ATLAS, the level-2 trigger has to reduce the trigger rate from that accepted by level-1 (up to 100 kHz) to approximately 1 kHz, the maximum rate to be passed to level-3. During the level-2 decision time the data from the complete event are kept in level-2 Read-out Buffers. If these buffers are to be kept reasonably small, the level-2 system latency should be no more than a few milliseconds. Key features of the system proposed are: restricting the volume of data to be used in level-2 by using data only from regions of interest as indicated by the level-1 trigger; extracting 'feature parameters' (e.g. a track segment) from each region of interest within each sub-detector, with parallel processing of these 'local' features; combining all of the features from the complete event in a 'global' system for the final level-2 decision.

The work on level-2 is split into studies of the local and global sub-systems, discrete event simulation of the entire system, algorithm development, trigger performance and physics studies. The UK contributes to all of these areas with participation from RHBNC, UCL, Manchester, Oxford and RAL, plus Liverpool who have recently joined this effort.

The UK groups constitute some 20% of the total level-2 effort and although the base line solution for level-2 in the technical proposal encapsulates many of the ideas put forward by the UK groups there remains much diversity of opinion on the exact system to be built. In June the UK hosted at Cosener's House a strategy meeting for the whole ATLAS level-2 community. At this meeting several initiatives were agreed. First a group was set-up to define milestones, not only for the final system and the prototypes, but also for the architecture and technology choices. A second group are investigating how formal methods might be applied to this work with its mixture of both hardware and software. A third group (initially using the ESA methodology) is producing a User Requirements Document and will then move on to a Systems Requirement Document. These initiatives will enable the large number of groups involved to work together on the level-2 system, to produce a coherent system which satisfies the many requirements of the different communities. The UK has been well represented on these groups. Draft reports are now in advanced stages and it is planned that they will be submitted to the wider ATLAS community early in 1996. Since the meeting other sections of the ATLAS Trigger/DAQ community have followed these initiatives and are producing similar documents themselves.

The demonstrator programme of the UK groups has been broadened and there is close collaboration with many more non-UK groups - now in addition to CERN and Cracow, the programme includes groups from NIKHEF, Niels Bohr Institute, Argonne National Lab, Michigan State University and Valencia.

Previously the components used in local sub-system tests were based on C40 digital signal processors mounted on commercial boards. During 1995 UK groups commissioned a number of board designs to give C40 based components more optimised to the needs of the local level-2 demonstrator systems. A key design for this work was a VME board with an embedded C40 processor. Fig 13a shows one of these boards, and fig 13b shows the board with the prototype level-2 buffer. Other boards which have been designed and produced within the UK include: a Link VME Interface (LVI) to give VME access to C40 communication links; a new C40/SCI interface; a fan-out for C40 communication link signals. These various boards have been produced in sufficient numbers to allow modest sized test systems to be run in the UK, with some modules being used by non-UK

collaborators to check inter-operability with their equipment. Early in 1996 it is planned to set up larger scale combined tests in CERN.

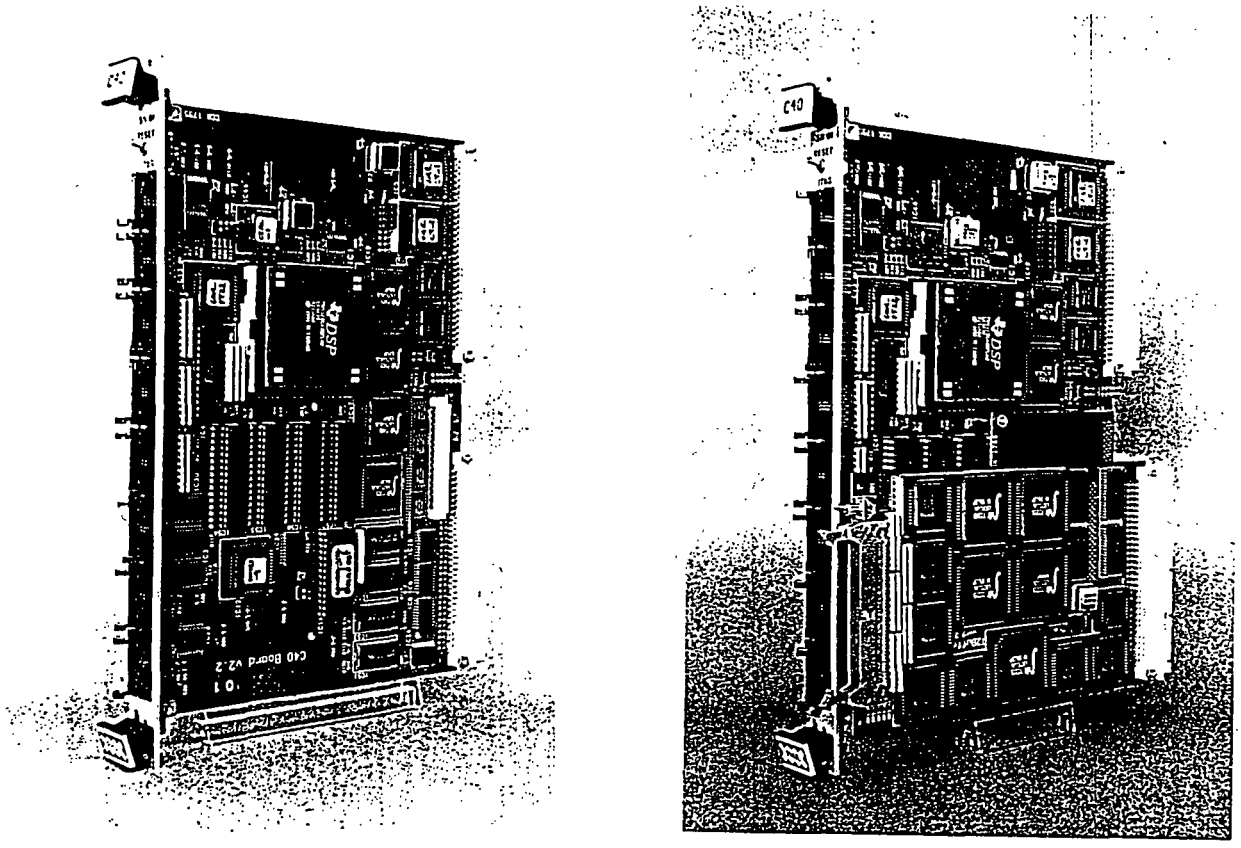

Figure 13: A VME module with an embedded C40 processor. The left hand picture shows the basic board. The right hand picture shows the board with a prototype level-2 buffer attached.

Much of the laboratory tests have been to confirm earlier tests with these new boards, but one particularly significant result has been the demonstration with a prototype level-2 Buffer of the handling of event data (i.e. buffer management and output of part of the data to the level-2 processors) at the rates expected at LHC.

Similarly, laboratory tests of SCI have led to a much deeper understanding of SCI and have identified ways to improve the performance of the current SCI interfaces, several of these improvements have already been implemented. In addition there have also been combined laboratory tests with the CERN/Valencia groups and more extensive combined tests are planned for 1996, including the use of SCI switches, which are essential to realise a scalable system.

During 1995 two designs of 'commodity' DEC Alpha boards were obtained, these boards aimed at the price sensitive PC market promise a particularly cost effective solution. For the global processing the boards are run as embedded processors, with code down-loaded from a host work-station. The tools for using these boards in this mode are, however, still under development and tests continue on the best solution for this work.

For the modelling work, 1995 has seen extensive additions and improvements to the discrete event simulation program (SIMDAO) ready for future use of detailed simulations

of both future demonstrators and complete systems.

The ability to trigger on high transverse momentum isolated electrons is of vital importance to the study of many physics processes at the LHC. The ATLAS inner detector has a crucial role in selecting events with isolated single electrons from the background, mainly QCD jets. The tracker is also vital to providing a trigger to study b-physics channels in the initial low luminosity phase of LHC running.

UK groups have taken a leading role in the work for the precision tracker part of the level 2 trigger. Algorithms had already been developed for the barrel part of the tracker, based on a fitting method, and the forward region (MSGC option), using a histogramming technique. During 1995 data from a full detector simulation were used to study the physics performance in the forward region. A similar study had already been made for the SCT barrel, this was extended to include the region of transition from barrel to forward geometry.

Following the decision in September 1995 to adopt the Si option in the forward region, work has started to develop common strategy for the whole precision tracker. A promising technique is to use a coarse binned histogram to identify a smaller region in which a fit will be performed. This combines the speed advantage of the histogramming technique with the greater precision of a fitting method. Work has also started to study triggers for the b-physics channels.

6 Software development (Object Orientation)

It has become clear from the presentations at the CHEP95 conference, and from the reports of the OO R&D projects at CERN that Object Orientation (OO) is the way forward in particle physics software.

Birmingham, Edinburgh and RAL are all working in the ATLAS OO subgroup which is part of Moose, one of the R&D projects. Moose is studying the viability of the Object Oriented approach for software development for High Energy Physics reconstruction and analysis code at the LHC and has just submitted its first status report [6].

The ATLAS OO group within Moose have produced an OO model of the semiconductor tracker and electromagnetic calorimeter, coded it in Eiffel and tested it with events from GEANT to satisfy one of the milestones set for Moose by the LCRB.

6.1 Future work

The list of criteria for CASE tool selection will be completed and criteria will be established for selection of methods and languages.

Most of the Eiffel code which has been written so far will be converted to C++ in order to compare the languages and to define some criteria to apply when selecting a programming language. Language inter-operability between different OO languages will be studied as will the interfacing to non-OO legacy code.

It is planned to try out an OO database to provide object persistence (i.e. when the object lives longer than the program which created it), and compare it with the simple persistency scheme currently used which was developed at RAL.

The application code will be developed further and more detectors added to produce a part of a useful OO framework for ATLAS.

7 Publications and Conference Papers

1. 'ATLAS SCT Technical Proposal Backup Document', ATLAS SCT Community, ATLAS INDET-No-085.

2. 'The Sensitivity of GaAs Particle Detectors to fast Neutrons', A.Chilingarov, P.Ratoff, T.Sloan, contributed paper at International Europhysics Conference on High Energy Particle Physics, Brussels '95.

3. 'Optical Links for ATLAS', C.B.Brooks et al., contributed paper at First Workshop on Electronics for LHC Experiments, Lisbon '95. CERN/LHCC/95-56.

4. 'ATLAS Silicon Strip Beam Test Results', P.Allport et al., contributed paper at Conference on Development and Application of Semiconductor Tracking Detectors, Hiroshima '95. ATLAS INDET-No-117.

5. 'Silicon Detectors for Forward Tracking in ATLAS', P.Allport et al., contributed paper at Conference on Development and Application of Semiconductor Tracking Detectors, Hiroshima '95.

6. 'ATLAS Semiconductor Tracker', M.Tyndel, contributed paper at Conference on Development and Application of Semiconductor Tracking Detectors, Hiroshima '95.

7. 'MQW-Modulator Based Optical Links for Atlas Tracking Detectors', I.Dawson et al., ATLAS INDET-No-119.

8. 'The Level-1 Calorimeter Trigger System for ATLAS', I.Brawn et al., ATLAS DAQ-No-30.

9. 'A first-level calorimeter trigger for the ATLAS experiment', V.Perera et al., Presented by V.Perera at IEEE 1994 Nuclear Science Symposium, Norfolk, Virginia, USA, Oct 30 - Nov 5, 1994.

10. 'Bunch-Crossing Identification for the ATLAS First-Level Calorimeter Trigger', I.Brawn et al., contributed paper at First Workshop on Electronics for LHC Experiments, Lisbon '95. CERN/LHCC/95-56, pp. 293-296.

11. 'A first-level calorimeter trigger for the ATLAS experiment.' V.Perera et al. Proc. first workshop on electronics for LHC experiments, CERN/LHCC/95-56, p. 297.

12. 'Data Transfer in the ATLAS Level-1 Calorimeter Trigger System.', C.N.P.Gee, Invited talk at Detector Data Link Workshop, CERN, November 1995

13. 'SIMDAQ – a system for modelling DAQ/Trigger systems.', S.Hunt et al., Real-Time 95, Michigan, 1995.

14. 'Object Oriented Tracking Software for the ATLAS Experiment', Julius Hřivnáč et al., contributed paper at CHEP 95, Rio de Janeiro

15. 'MOOSE: Software developments for LHC' Christian Arnault et al., contributed paper at CHEP 95, Rio de Janeiro

8 Thesis

K.A.Webster, (Birmingham,1995), 'Investigation of the use of optical modulators for analogue data readout from particle physics detectors'

References

[1] *The ATLAS Technical Proposal, June 1995* (CERN/LHCC/94-43)

[2] *The ATLAS UK Technical Proposal, June 1995* (PPESP/95/39)

[3] *ATLAS UK Resource Planning, October 1995.* (PPESP/95/46)

[4] RD6 collaboration NIM A 361 (1995) 440

[5] I.P.Brawn et al, The Level-1 Calorimeter Trigger System for ATLAS, ATLAS DAQ Note 30 (1995)

[6] *Status Report of MOOSE* (CERN/LHCC/95-60)

THE COMPACT MUON SOLENOID (CMS) DETECTOR

PROPOSAL 892

UNITED KINGDOM

Bristol University; Brunel University; Imperial College, London; Rutherford Appleton Laboratory

OTHER CERN MEMBER STATES

AUSTRIA: HEPHY, Vienna; **BELGIUM**: Univ. Libre, Brussels; Vrije Univ., Brussels; Univ. cath. Louvain, Louvain; Univ. Antwerpen, Wilrijk; Univ. Mons Hainaut, Mons; **CERN**; **CZECH REPUBLIC**: Charles Univ., Fac. of Math. and Physics, Prague; Inst. of Sci. Instr., Brno; Czech Tech. Univ., Prague; Inst. of Computing Machines, Prague; NRI, Rez; **FINLAND**: Phys. Dept., Helsinki Univ., Helsinki; HTI, Helsinki Univ. of Technology, Espoo; Jyväskylä Univ., Jyväskylä; Oulu Univ., Oulu; SEFT, Research Inst. for HEP, Helsinki; Tampere Univ. of Technology, Tampere; **FRANCE**: LAPP, Annecy; Inst. Phys. Nucl., Lyon; LPNHE Ecole Polytechnique, Palaiseau; DAPNIA, Saclay; CRN-ULP, Strasbourg; **GERMANY**: I. Phys. Inst., RWTH Aachen, Aachen; III. Phys. Inst. A, RWTH Aachen, Aachen; III. Phys. Inst. B, RWTH Aachen, Aachen; Humboldt University, Berlin; **GREECE**: NRCPS Democritos, Attiki; Univ. Athens, Athens; Univ. Ioannina, Ioannina; **HUNGARY**: KFKI, Hung. Acad. Sci., Budapest; Kossuth Lajos Univ., Debrecen; **ITALY**: Dip. fisica dell'Univ. and Sez. dell'INFN, Bari; Bologna; Catania; L'Aquila; Firenze; Genova; Padova; Pavia; Perugia; Pisa; Roma I; **POLAND**: Inst. Experim. Physik, Univ. Warsaw, Warszawa; Inst. Nuclear Studies, Warszawa; **PORTUGAL**: LIP, Lisbon; **SLOVAK REPUBLIC**: Inst. of Computing Machines, Zilina; **SPAIN**: CIEMAT, Madrid; Univ. Autonoma, Madrid; Cantabria Univ., Santander; **SWITZERLAND**: EPFL, Ecole Polytechnique Fédérale, Lausanne; PSI, Paul Scherrer Institute, Villigen; ETH, Eidgen. Techn. Hochschule, Zürich; Univ. Basel, Basel; Univ. of Zurich, Zurich

NON-MEMBER STATES (Except USA)

ARMENIA: YerPhI, Yerevan; **BELARUS**: INP, Inst. of Nucl. Problems, Byelorussian State Univ., Minsk; NSEC, Nat. Sci. and Educ. Centre of P'cle and High Energy Physics, Minsk; RIAPP, Research Inst. Appl. Phys. Probl., Minsk; Dept. of Physics, Byelorussian State Univ., Minsk; **BULGARIA**: Inst. Nucl. Res. + Nucl. Energy, Sofia; Univ. of Sofia, Fac. of Phys., Sofia; **CHINA**: Institute of High Energy Physics, Beijing; Univ. of Science & Technology of China, Hefei; **CROATIA**: Univ. of Split, FESB, Elect. and Mech. Eng. Dept; Univ. of Split, PMF, Dept. of Natural Sciences; **CYPRUS**: Univ. of Cyprus, Nicosia; **ESTONIA**: Inst. Chemical Physics and Biophysics, Tallinn; **GEORGIA**: Inst. Phys. Academy of Science, Tbilisi; Inst. HEP, Tbilisi State Univ., Tbilisi; **INDIA**: Tata Institute (HECR), Tata Institute (EHEP), Bombay; Exp. HEP Group, Inst. of Physics, Bhubaneshvar; Panjab Univ., Chandigarh; Univ. of Delhi South Campus, Delhi; **LATVIA**: Inst. Electronics and Comp. Science, Riga; **PAKISTAN**: Quaid-I-Azam Univ., Islamabad; **RUSSIA**: JINR, Dubna; INR, Moscow; ITEP, Moscow; Lebedev Physics Institute, Moscow; MSU, Moscow; BINP, Budker Inst. of Nuclear Physics, Novosibirsk; IHEP, Protvino; Petersburg Nucl. Physics Inst., St. Petersburg; **UKRAINE**: Kharkov State Univ., Dept. of Physics and Tech; NSC-KIPT, Kharkov Inst. of Ph. and Tech., Kharkov; Institute of monocrystals, Kharkov; **UZBEKISTAN**: INR, Uzbekistan Acad. of Sciences, Tashkent

USA

Univ. of Alabama, Tuscaloosa; Boston University; Brookhaven Nat. Lab., Upton; Caltech, Pasadena; Univ. of California at Davis, Davis; Univ. of California at Los Angeles, Los Angeles; Univ. of California at Riverside, Riverside; Univ. of California at San Diego, La Jolla; Carnegie Mellon Univ., Pittsburgh; Fairfield Univ., Fairfield; Fermilab, Batavia; HEPG, Florida State Univ., Tallahassee; SCRI, Florida State Univ., Tallahassee; Univ. of Florida, Gainesville; Johns Hopkins Univ., Baltimore; Univ. of Illinois, Chicago; Univ. of Iowa, Iowa City; Iowa State Univ., Ames; Lawrence Livermore Nat. Lab., Livermore; Los Alamos Nat. Lab., Los Alamos; Univ. of Maryland, College Park; Massachusetts Institute of Technology, Boston; Univ. of Minnesota, Minneapolis; Univ. of Nebraska, Lincoln; Northeastern Univ., Boston; Northwestern Univ., Evanston; Univ. of Notre Dame, Notre Dame; Ohio State Univ., Columbus; Princeton Univ., Princeton; Purdue Univ., West Lafayette; Rice Univ., Houston; Univ. of Rochester, Rochester; Rockefeller Univ., New York; Univ. of Mississippi, Mississippi; State Univ. of New York, Stony Brook; Univ. Texas, Dallas; Texas Tech Univ., Lubbock; Virginia Polytech. Inst. and State Univ., Blacksburg; Univ. of Wisconsin, Madison

INTRODUCTION

The CMS (Compact Muon Solenoid) experiment is a general purpose detector designed to run at the highest luminosity at LHC. It has been optimized for the search for the Standard Model Higgs boson over a mass range from 90 GeV/c^2 to 1 TeV/c^2, but it will also be sensitive to a wide range of possible signatures from alternative electro-weak symmetry breaking mechanisms. Muons, photons, and electrons will be identified and measured with high precision.

The past year has been a particularly rewarding one for the CMS collaboration, with major milestones passed on the road towards full approval of the project. The Technical Proposal, submitted to the LHCC at the end of 1994, was presented to a packed auditorium at CERN in an open meeting of the LHCC in January. Scientists in outside institutes were able to follow the proceedings via an audio-video link.

October saw the first meeting of the Resources Review Board, chaired by the CERN Research Director and attended by almost all of the 30 funding agencies supporting the experiment. This meeting established that the assumptions on which the financial planning of the experiment had been based were entirely reasonable, thus paving the way for approval of the project. Finally, in November the LHCC formally recommended the experiment for approval. It is anticipated that the Director General of CERN will endorse this recommendation early in 1996.

Within the UK the project also made important progress towards acceptance by PPARC. An open presentation was made to the PPESP in May, which was warmly received by the panel, who subsequently endorsed without reservation the physics aims of CMS.

In the following sections we report on the significant technical advances made by the UK groups during the year towards the realisation of the electromagnetic calorimeter and the readout of the central tracking detector.

ELECTROMAGNETIC CALORIMETRY

The CMS electromagnetic calorimeter, or ECAL, will consist of a cylindrical barrel and two endcaps, with lead tungstate crystals as the active medium; the total number of crystals will be approximately 100000. The barrel crystals will be read out using avalanche photodiodes (APDs), while various technologies are being considered for the endcaps, where the high radiation doses may rule out the use of APDs. The UK groups are involved in the mechanical design of the calorimeter, and in studies of the readout electronics; in addition, the RAL and Imperial College groups made major contributions to the 1995 test beam work, equipping the test crystals with APDs and preamplifiers, and constructing a temperature-controlled enclosure to hold the complete crystal array, as well as coordinating the data taking and analysis. The Brunel group is carrying out GEANT modelling of energy deposition in the test beam array. In the future, the UK groups propose to form a 'Regional Centre' for the ECAL construction, with the task of building one quarter of the calorimeter.

Test beam work in 1995 concentrated on achieving a performance using fast APD readout similar to that obtained with photomultipliers in 1994. Specifically CMS declared the achievement of an energy resolution of 0.6 % at 100 GeV as a milestone to their referees. Figure 1 shows the energy distribution measured for 120 GeV electrons in 1994 and 1995. In the 1994 tests there was a significant tail on the high side of the distribution. Several improvements were made in 1995 to eliminate this tail: the energy equivalent APD response to ionising radiation has been significantly reduced by the APDs having a thinner sensitive layer before the gain region; the 1995 crystals had a somewhat larger scintillation light yield, and were longer than those used in 1994, reducing the shower leakage.

A high degree of temperature stability was achieved and continuously monitored by sensors on the back and front of each crystal, and on each APD. A small residual diurnal

fluctuation with a peak-to-peak magnitude of between 0.2 and 0.3 degrees was observed. Some of the crystals in the test matrix were equipped with 2 APDs, each with an independent preamplifier, doubling the light collected and thus reducing the photostatistical contribution to the stochastic term of the energy resolution. With this setup the energy resolution was 0.6 % at 50 GeV. Figure 2 shows the energy resolution as a function of energy for single and double APD readout. When the fast, low noise preamplifiers (custom designed and provided by RAL) were used in conjunction with the E G & G diodes the energy equivalent electronics noise was less than 15 MeV per crystal at an APD gain of 50.

By the end of the year, a fully equipped 7 x 7 crystal matrix had been tested in front of a full depth hadron calorimeter prototype, with both electron and pion beams. The data from this test, now being analysed, will provide information about the longitudinal containment of hadron showers and the $e\pi$ ratio. This information is needed to assess the response of the combined calorimeter system to hadronic jets. We have also measured the rejection power against charged pions faking electrons. Preliminary results suggest that rejection factors of several thousand can be obtained by combining information from the tracker and the ECAL.

Detailed studies have been carried out, at both RAL and Brunel, on the avalanche photodiodes which were used in the beam tests. Their properties and characteristics are now well understood and have been compared to theoretical models. This has enabled thorough specifications to be drawn up for the next generation of APD's. The UK has played a central role in this area. New APD prototyping contracts have recently been placed with Hamamatsu and E G & G.

The light yields and radiation hardness of $PbWO_4$ crystals have been investigated using the ISIS facility at RAL, and the cobalt-60 cave and optical fluorescence spectrometer at Brunel University. This work will continue in the future, and will form part of the crystal testing programme for the UK regional centre. A special, dedicated spectrophotometer that can measure the transmission of full-length crystals with precise control over the optical polarisation has been designed and is currently under construction at Brunel.

The engineering and design of the ECAL has evolved through the year. After conducting detailed FEA work on the 'Basket' structures which were initially proposed for the design, the UK has suggested a new procedure for the construction of the ECAL. This involves the grouping of small numbers (6 - 12) of crystals into sub-units. These sub-units are light enough to be handled without special equipment, and can be fully equipped with photodetectors and front end electronics before incorporation into modules of about 600 crystals. The concept of the sub-unit is important for the logistics of building one quarter of the ECAL at the UK 'Regional Centre'. Important tasks can be separated and undertaken separately at each of the four UK institutes.

CMS TRACKER

CMS tracker activities in the UK

The CMS central tracker is based on silicon and gas microstrips plus an inner pixel detector system. The detectors will be operated in a 4T solenoidal magnetic field contained in a cylindrical volume of radius 1.3 m and length 7 m. The total number of channels to be read out is 11×10^6 MSGC and 3×10^6 silicon. As only two, basically similar, detector technologies are used a single electronic readout system is envisaged for both. This offers the opportunity of constructing a well-integrated system in a single support structure with a low material budget and economical data acquisition architecture. The basis of the electronic readout of the CMS tracker is front end electronics developed for LHC in the RD20 R & D programme. The UK groups are responsible for the overall system design and two major elements of the system: the front end readout electronics and the VME module which is the interface to the data acquisition system.

At Imperial College, in collaboration with RAL Electronics Division, most of the effort in the last year has been devoted to development of the APV5 chip, which is a radiation hardened version of the RD20 front end chip. A 32 channel version of the RD20 chip, the APV3, comprising amplifier-shaper, full length pipeline and analogue signal processor, was produced at Harris in their 1.2 mm AVLSIRA bulk CMOS process. The chip was tested in 1994 with silicon detectors in a beam. A 128 channel chip, the APV5, was delivered in 1995 which also contains a multiplexer and therefore embodies all the operations required for CMS. IC and Brunel University tested the chip on a CERN beamline in 1995. It is fully functional but there are some weak points in the performance which require further attention and a new submission is planned for Spring 1996.

In parallel with the chip development, several versions of the RD20 amplifier have been fabricated at Harris and in the DMILL process which have been evaluated. Individual transistors, as well as complete amplifiers, were characterised before and after irradiation up to 15 Mrad with special emphasis on threshold voltage shifts and noise performance. The PMOS transistors, which are most important in the design, show little change in noise and transconductance after irradiation. With the DMILL process, individual transistors show noise characteristics and radiation hardness very similar to the Harris devices. This work forms the subject of a thesis in its final stage of preparation.

An analogue optical fibre link provides the data path between front end chips and DAQ. The proposed system employs passive reflective modulator technology with external lasers providing the optical power based on the modulator technology being developed in the RD-23 collaboration. It exploits semiconductor multi-quantum-well (MQW) electro-absorptive structures (produced by GEC-Marconi in the UK) operated around 1.55 mm wavelength. A link is now operating at Imperial College after use in tests at CERN. Modulators and fibres have been irradiated in a Cobalt source at Imperial to 20 Mrad levels and further studies continue.

Simulation studies of the physics performance of the CMS tracker continue. A thesis is in preparation on time dependent and independent asymmetries in the B system.

A joint CMS/ATLAS workshop (3 - 4 October 1995) on radiation hardening of silicon detectors was organised at CERN by S Watts (Brunel), F Lemeilleur (CERN) and G Lindstroem (Hamburg). The meeting included representatives from the silicon wafer and detector industry in Europe, groups working on radiation effects, and academic semiconductor specialists. The workshop resulted in a clear plan of action for future work and showed the need for collaborative effort between the various groups and industry if radiation damage effects are to be understood and minimised at the LHC.

CMS DATA ACQUISITION

The CMS data acquisition system (DAQ) will have to handle unprecendented rates in data flow and event selection. At the nominal LHC design luminosity of 10^{34} cm 2 sec^{-1}, there will be approximately 10^9 interactions/sec. Some 10^7 electronics channels are anticipated to produce around 100 MBytes of raw digitised information at 40.08 MHz. The task of the DAQ will be to reduce this flow of data to 1 MByte sized events recorded at approximately 100 Hz for subsequent analysis. This will be achieved by using a combination of custom designed micro-electronics together with state of the art commercial hardware.

As reported last year, RAL engineers are designing a common architectural structure for the integration of all front-end electronics systems into the DAQ framework. Data will be read out in parallel from the front-end subsystems into around one thousand fast dual ported memory devices, each capable of buffering 1 kByte packets at a rate of several hundred MBytes/second. The tracking readout system, being developed by several UK groups, provides the greatest data throughput, and hence the biggest test for this environment. Together with collaborators from CERN and the U.S, the aim is to have a single CMS data acquisition prototype chain, from front-end through to filter-farm, implemented within the

next three years. This will enable key technology decisions, such as the event building switch matrix, to be carefully appraised and understood in good time for the ultimate commissioning of the final system in 2004. Already a pre-prototype Front-End Driver has been designed and test benches are being developed by RAL physicists and engineers using PowerPC micro-processors, PCI and VME busses.

SIMULATION STUDIES AND TRIGGER

Significant progress has been made in 1995 on the design of the Global Calorimeter Trigger Processor, which is a UK responsibility. This device will bring together information on electron/photon and jet candidates found in 18 regions of the calorimeter, and find the highest energy candidates for transmission to the CMS global trigger. It will also complete the sums of total and missing transverse energy over the calorimeter. The design uses modern high-density connector technology to concentrate all the input information together in one crate, as shown in figure 3. The design of a Sort ASIC is in progress: this is needed in both the Global Processor and in the regional processing to find the highest energy candidates. Algorithms have been identified which can perform the required sort in one LHC bunch crossing interval, resulting in a significant reduction in the overall trigger latency. Prototype runs in 1996 will test ideas on the ASIC and on high-speed data transmission, which are crucial to the system design.

A programme of detector simulation studies is under way to investigate the effect on the physics performance of various mechanical design schemes. Individual crystals in the ECAL must be separated from each other, to avoid damage and to allow for reflective wrapping. The effect of such inter-crystal gaps is that some fraction of particles entering the ECAL are reconstructed with less than their full energy. These low-energy tails can reduce the detection efficiency for the Higgs particle in the important two-photon decay channel. Figure 4 shows the variation of the low-energy tail (defined here as events with 1 GeV of energy lost for a 70 GeV incident photon) with gap size. The tail varies linearly from about 5.5 % of events at 0.3 mm to about 8 % for a 1 mm gap. This implies that, while the gaps should be kept as small as possible, there is no threshold in the gap size where the calorimeter performance degrades dramatically.

The RAL sub-unit design, and a similar proposal from Ecole Polytechnique, have also been simulated. In these schemes, material is placed between the crystals to form a strong alveolar structure. The materials which have been proposed are titanium and a glass-fibre/epoxy composite. The energy resolutions obtained are shown in figure 5, with a 0.5 mm air gap for comparison. It will be seen that placing 0.5 mm of glass-fibre/epoxy composite, or 0.2 mm of titanium, in the gap has no visible effect on the resolution, while 0.5 mm of titanium produces a very slight broadening of the peak. This figure demonstrates that the alveolar designs do not compromise the physics performance of the calorimeter.

Physics simulation work on the Higgs two photon decay channel, the main justification for a high resolution electromagnetic calorimeter, was continued with detailed studies of pizero rejection and the problem of locating the vertex at high luminosity.

SUMMARY

The CMS project has made substantial progress in 1995, both globally with the recommendation by LHCC that the experiment be approved, and more particularly in those areas where the UK institutes are involved.

The tracker groups have made a great deal of progress in developing radiation-hard readout electronics, leading to a successful test of the 128-channel APV5 front-end chip, and the fabrication and radiation testing of the RD20 amplifier. In addition, an optical fibre link has been demonstrated and radiation tested up to 20 Mrad.

The ECAL test beam array exceeded the resolution milestone of 0.6 % at 100 GeV with fast APD readout, while the electronics noise was reduced to less than 15 MeV per channel using new preamplifiers designed in the UK. A new mechanical design of the ECAL has been proposed, based on an alveolar structure, which would facilitate handling and construction. Simulation studies have shown that the proposed designs should achieve the physics performance demanded of the calorimeter.

CMS PUBLICATIONS

Results of tests on matrices of lead tungstate crystals using high energy beams.
J E Bateman et al. CMS TN/95-177.

Test beam results on position and angular resolution using a $PbWO_4$ calorimeter and silicon preshower.
D Barney. CMS TN/94-315.

Test beam results on e-pi discrimination using a $PbWO_4$ calorimeter.
D Barney. CMS TN/94-314.

Investigation of Avalanche Photodiodes for EM Calorimetry at LHC.
J E Bateman, S R Burge, R Stephenson et. al. CMS TN/95-135.

Gain and noise measurements on two avalanche photodiodes proposed for the CMS ECAL.
J E Bateman, S R Burge, R Stephenson. CMS TN/95-023.

CMS ECAL Basket 3 Finite Element Analysis.
M Brown. CMS TN/95-105.

CMS ECAL Basket 4 Finite Element Analysis.
M Brown. CMS TN/95-046.

An algorithm using tracks to locate the two photon vertex at high luminosity.
D J Graham. CMS TN/95-115.

The effect of limiting the pseudorapidity coverage of the ECAL angle measurement of photons from an intermediate mass Higgs.
C Seez. CMS TN/94-290.

The Higgs two photon decay in CMS : an update.
C Seez. CMS TN/94-289.

Pizero rejection with $PbWO_4$ crystals as a function of crystal size.
C Seez. CMS TN/94-288.

Study of the Shashlik response uniformity.
RAL, ICSTM, et. al. CMS TN/94-311.

Measurements of transistors and silicon microstrip detector readout circuits in the Harris AVLSIRA rad-hard CMOS process
M Raymond, G Hall, M Millmore, R Sachdeva, M French, E Nygaard, K Yoshioka.
Nucl. Instr. & Meths. **A351** (1994) 449-459.

Radiation hard electronics for LHC
M Raymond, G Hall, M Millmore, R Sachdeva, M French, E Nygaard, K Yoshioka.
Nucl. Instr. & Meths. **A360** (1995) 162-165.

Analogue lightwave links for detector front ends at the LHC
A Baird, J Dowell, P Duthie, K Gill, M Glick, N Green, G Hall, R Halsall, G Jarlskog, I Kenyon, A Moseley, S Quinton, G Stefanini, N Try, F Vasey, K Webster.
IEEE Trans in Nucl. Sci. **42** (1995) 873-881.

Beam test of a prototype readout system for precision tracking detectors at LHC
M Millmore, M French, K Gill, G Hall, G Howell, L Jones, W Langhans, B MacEvoy, J Matheson, R Payne, M Raymond, G Stefanini, F Vasey, D Vite, S Watts, R Wheadon.
IC/HEP/95-3 May 1995. To be published in Nucl. Instr. & Meths.

APV5RH: a 128 channel radiation hard pipeline chip for LHC tracker applications
M French, L Jones, P Murray, P Seller, M Raymond, G Hall
Proceedings of 1st Workshop on Electronics for LHC Experiments,
CERN/LHCC/95-56 (1995) 120-126.

The CMS tracker readout system
G Hall
Proceedings of 1st Workshop on Electronics for LHC Experiments,
CERN/LHCC/95-56 (1995) 114-118.

Study of the bunch crossing identification at LHC using Microstrip Gas Chambers
Angelini, R Bellazzini, A Brez, M Masai, F Raffo, G Spandre, M Spezziga, A Toropin, N Bacchetta, A Giraldo, M Loreti, D Bon, J C Caldero, J F Clergeau, D Contardo, G Guillot, R Haroutunian, D Kryn, J C Mabo, M Miguet, M Rebouillat, G Smadja, A Bondar, M Bozzo, A Morelli, F Parodi, O Runolfsson, J M Brom, T Kachelhoffer, A Pallares, S Qian, J L Riester, M French, L Jones, G Hall, B. MacEvoy, M Millmore, M Raymond, R Sachdeva, D Vite, R Hammarstrom, T Ladkinski, V Nagaslaev, A Peisert, L Shekhtman, C Vander Velde, P Vanlaer.
CMS/TN/95-048 (May 1995). To be published in Nucl. Instr. & Meths.

Front-End Driver in CMS Data Acquisition
S Cittolin, J F Gillot, R Halsall, W J Haynes, A Racz,
CMS TN /95-020.

Conference Contributions

The Front-End Driver of the CMS Tracker
R Halsall
Presentation at the First Workshop for Electronics at LHC Experiments, Lisbon,
11-15 September 1995.

Theses by UK Students

Signal processing algorithms and radiation hard electronics for the CMS tracking detector.
R. Sachdeva, Ph. D. thesis, University of London, September 1995.

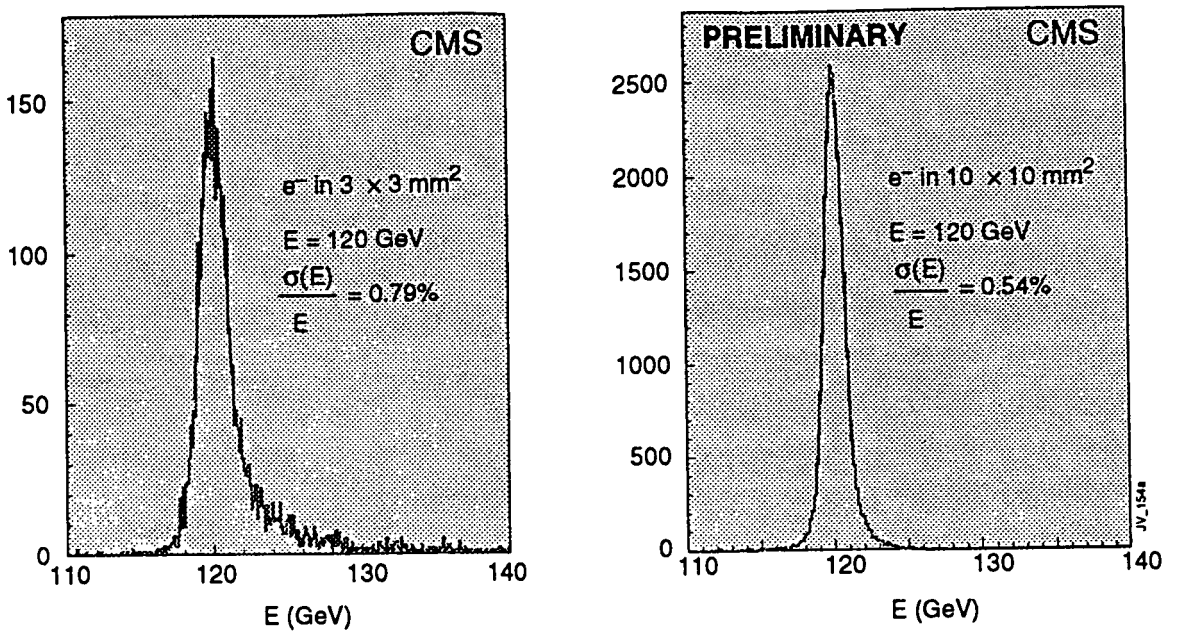

Figure 1 Energy distribution measured for 120 GeV electrons in the 1994 (left) and 1995 (right) beam tests.

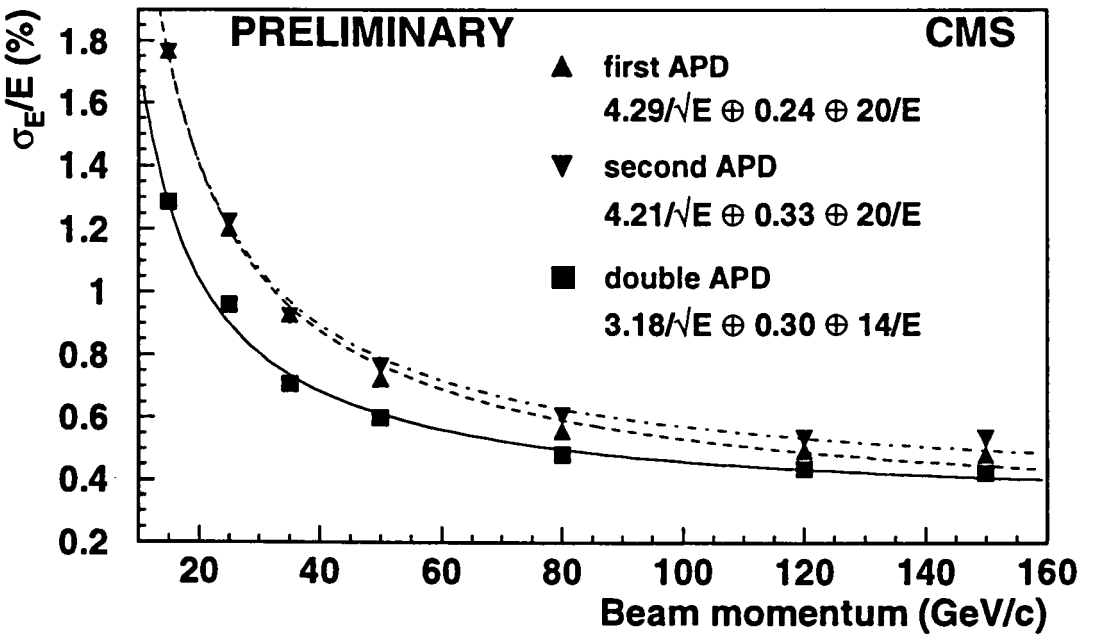

Figure 2 Energy resolution as a function of beam energy for crystals with single and double Hamamatsu-hc APD readout.

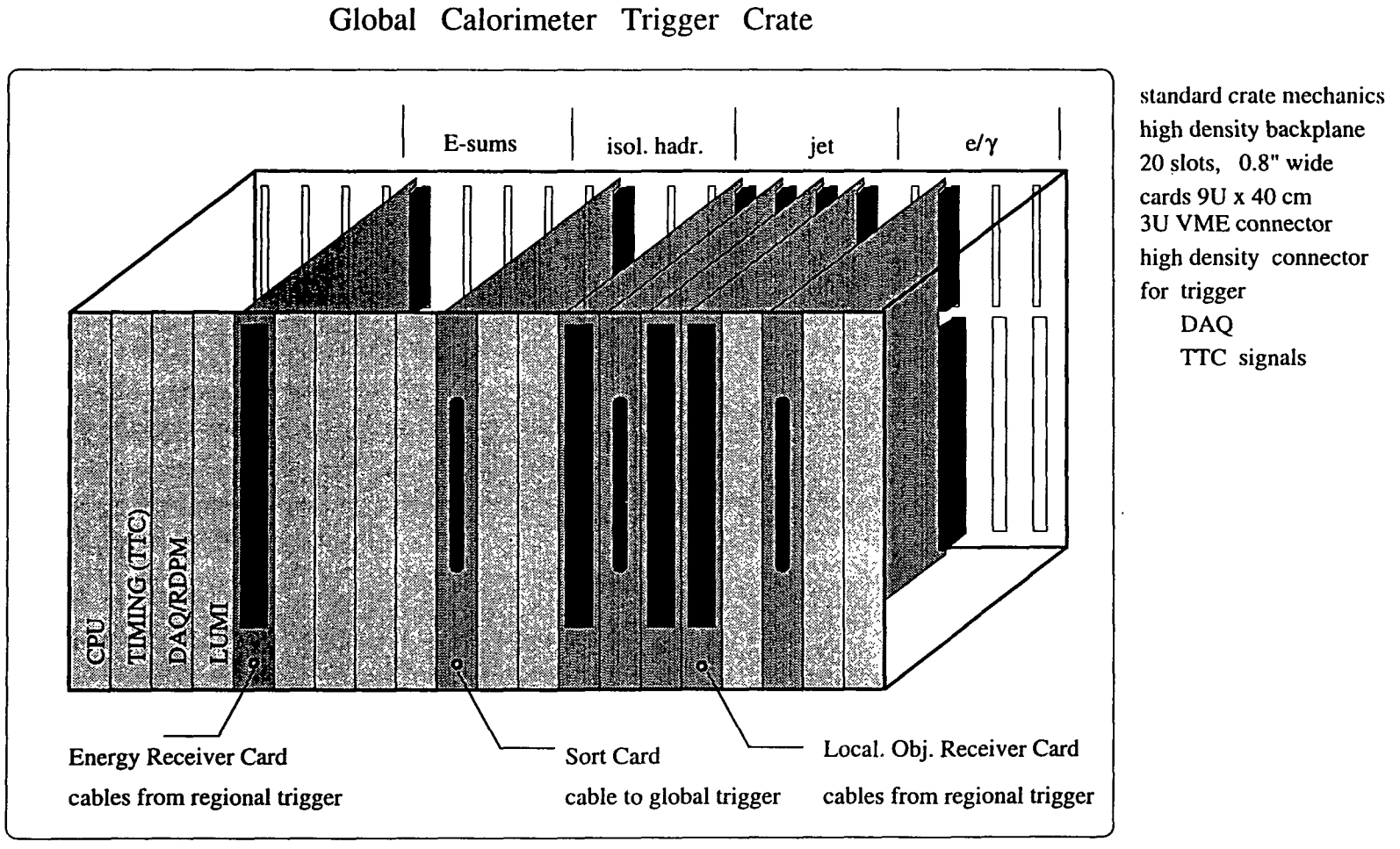

Figure 3 Schematic diagram of Global Calorimeter Crate design.

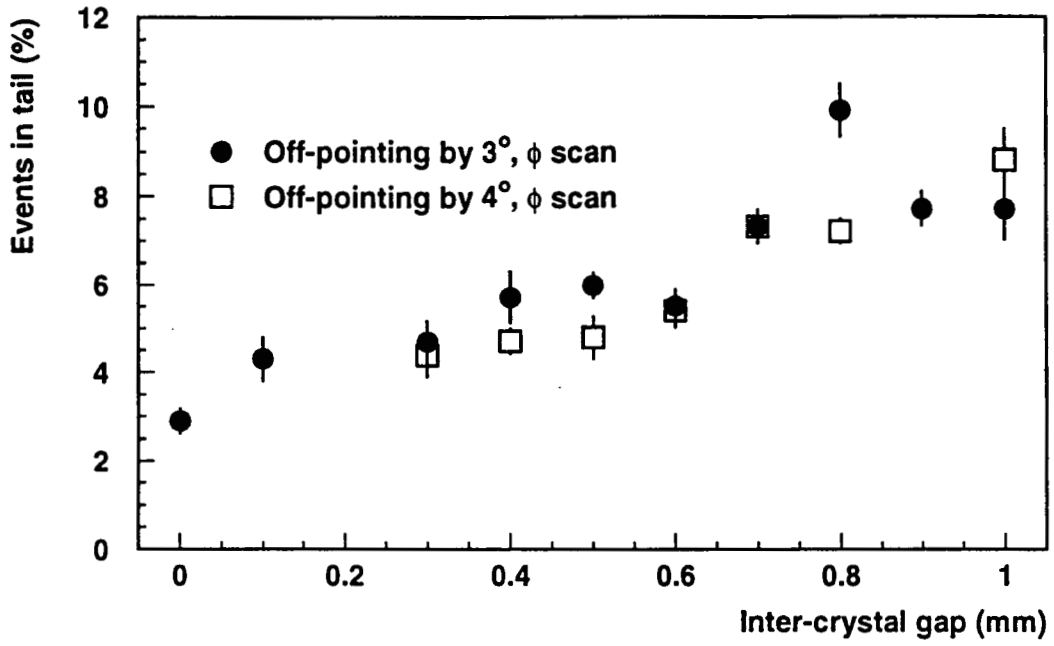

Figure 4 GEANT simulation of low-energy tail as a function of gap size, for 70 GeV incident photons. The two sets of points correspond to the crystal axes pointing away from the interaction vertex by 3 degrees and 4 degrees. The tail is defined as events with reconstructed energy more than 1 GeV below the energy of the incident photons.

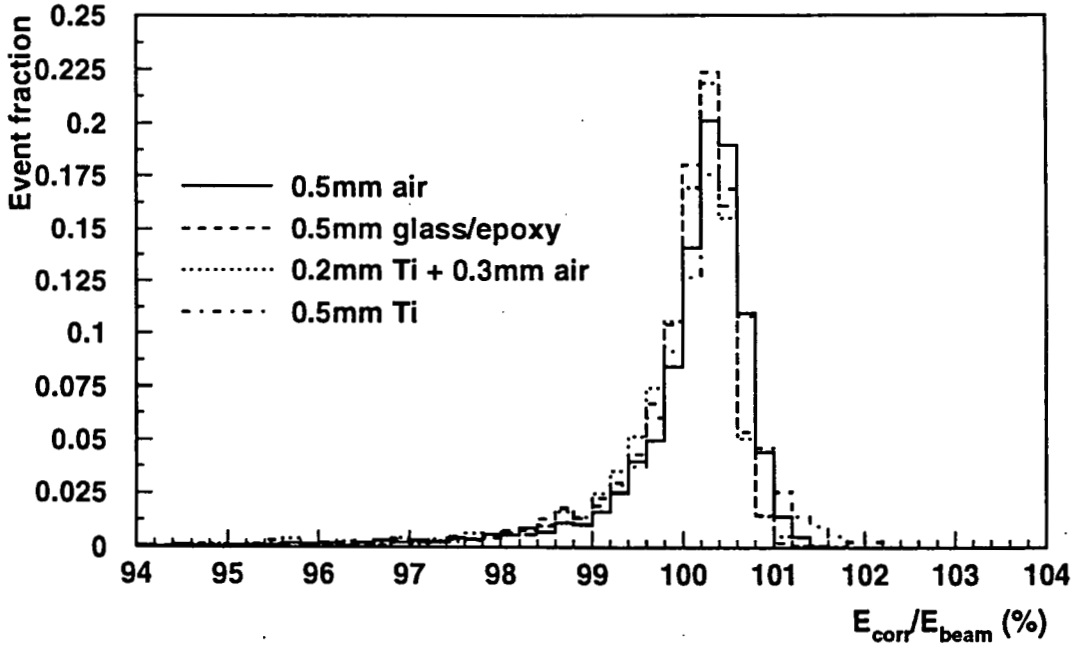

Figure 5 Simulated energy resolution for 70 GeV photons, with various materials between the crystals.

MEASUREMENTS OF THE SPIN STRUCTURE OF THE NUCLEON AT HERA

THE HERMES COLLABORATION **Proposal 780**

Alberta, Argonne, Caltech, Colorado, DESY, Erlangen, Frascati, Illinois-Urbana, INFN-Rome, Liverpool, Mainz, Marburg, MIT, MPI-Heidelberg, München, NIKHEF, New Mexico State, Pennsylvania, St. Petersburg, TRIUMF, Wisconsin, Yerevan.

Introduction

The HERMES collaboration was set up to make high precision measurements of the spin structure of the nucleon by means of deep inelastic lepton scattering. It uses the 27 GeV polarised positron beam available at the HERA electron storage ring in conjunction with internal polarised gas targets. A magnetic spectrometer, with gas microstrip, proportional and drift chambers for particle tracking, is used for momentum measurement of scattered positrons and hadrons. A calorimeter, Cherenkov detector and transition radiation detector provide particle identification. The experiment was installed in the HERA East Hall during the 1994-95 winter shutdown and was in full data taking mode for the whole 1995 running period.

Polarised Targets

A gaseous He-3 polarised target was used during the 1995 running period. This is effectively a polarised neutron target. The He-3 atoms are polarised by metastability exchange optical pumping and fed at a rate of 2×10^{17} atoms. s^{-1} into a storage cell located in the positron beam. The polarisation is around 50% and the target thickness is maximised by operating the cell at low temperatures, which are normally in the range 15 to 40K. The Liverpool Group designed and commissioned the cell cooling system. The group was also involved in the design, development and construction of the components which minimise the beam wake field interaction on the target components.

Experimental Programme

The HERMES detector system was commissioned during the first phase of the running period. There were initially severe background problems due to synchrotron radiation generated in the positron beam focusing and steering components. This was cured after intensive effort by HERA to optimise the beam steering parameters. The primary purpose of the data taking phase of the 1995 running period was to make a precise measurement of the neutron structure function [g_1^n] over as wide a range of Bjorken x as possible. A total of 5.5 million deep inelastic events was recorded, with a mean beam polarisation over 50% and Bjorken x values in the range 0.015 to 0.6. These data are currently being analysed. The HERMES spectrometer has excellent particle identification facilities [see fig. 2] and the Liverpool Group is involved in a preliminary study of semi-inclusive hadron asymmetries which should provide unique information on the flavour dependence of quark helicity distributions in the nucleon.

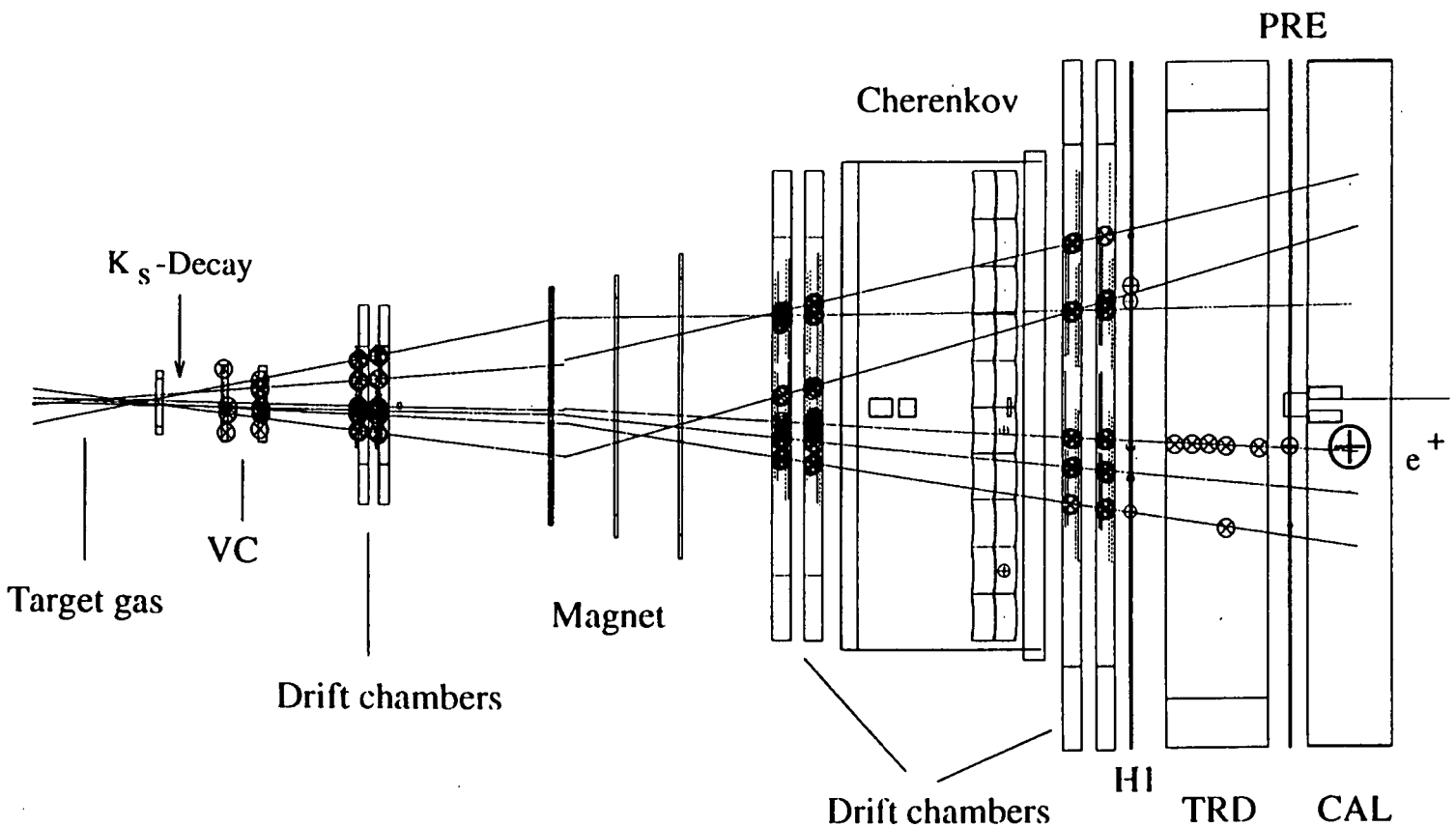

Fig 1. HERMES event display showing a K_S decay and a scattered positron.
VC = Vertex chambers, TRD = Transition radiation detector, CAL = Calorimeter,
H1 = Hodoscope, PRE = Preshower detector.

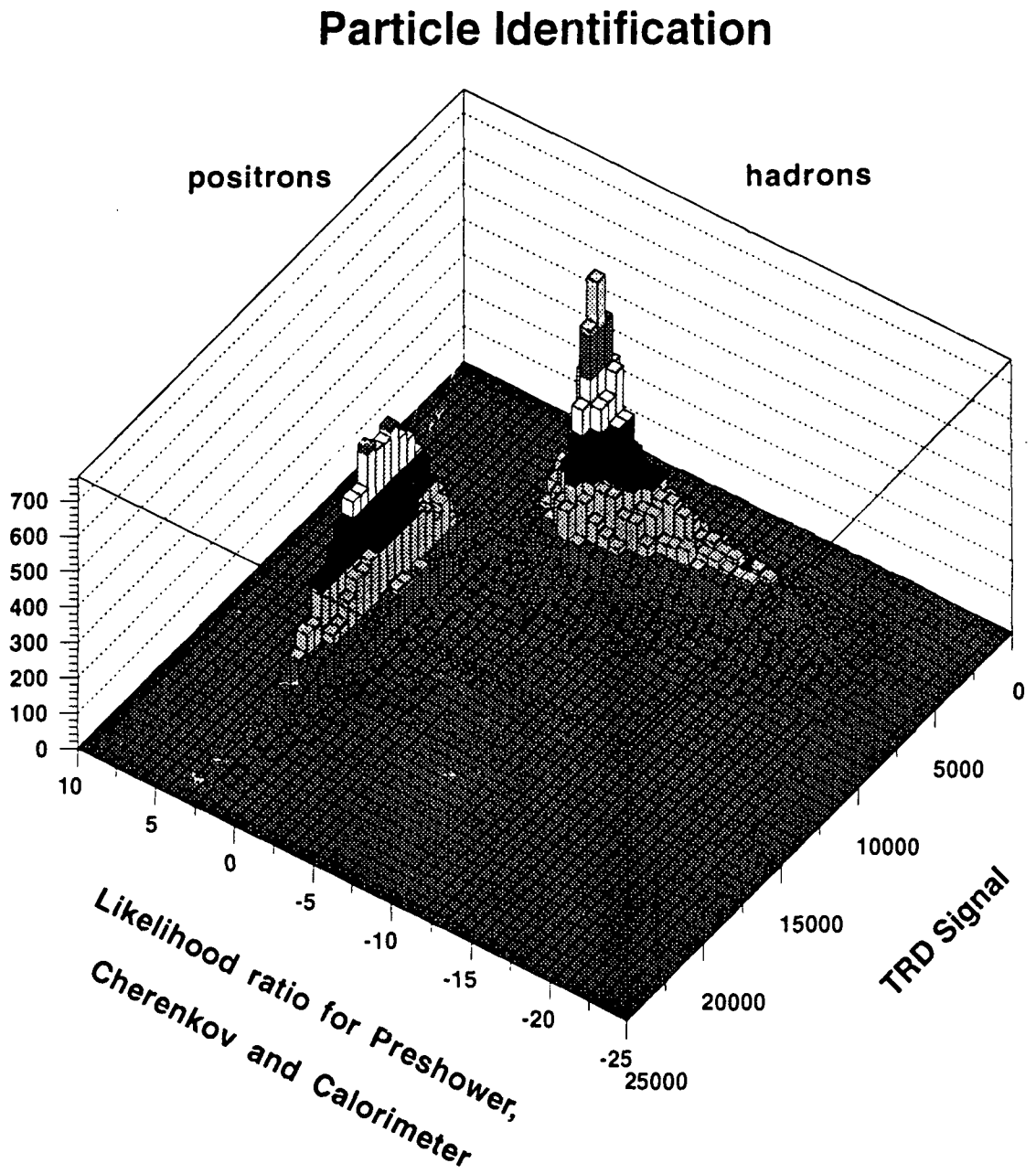

Fig 2. HERMES particle identification.

OptoElectronic Modulator Readout for LHC Tracking Detectors. P803

I.Dawson, J.D.Dowell, R.J.Homer, I.R.Kenyon, S.J.Oglesby, H.R.Shaylor, J.A.Wilson.

School of Physics and Space Research, University of Birmingham, PO Box 363, Birmingham B15 2TT.

Introduction

Data transfer from the frontend of LHC experiments is only feasible via optical fibre links which, compared to copper twisted pairs, reduce the volume of material by a factor of ten and the number of radiation lengths by a factor one hundred. In addition; ground loops, electronic pickup between channels and the need for high power drivers are eliminated. Possible means of converting the electronic signals at the frontend to optical signals rely on either active elements (lasers or LEDs) or passive modulators. In the case of modulators, the light source is a laser at the electronics barrack and is transmitted by fibre to the modulator. Electronic signals applied to the modulator affect the light level it transmits (or reflects) and this amplitude modulated light signal is returned to a photodiode in the electronics barrack for conversion back into electrical signals. The design, construction and proving of passive modulator technology has been carried by the RD23 collaboration (spokespersons: G. Stefanini and F. Vasey) which includes nine academic institutes and two industrial partners. Of the two possible modulator technologies investigated by the RD23 collaboration [1,2,3], that based on reflective Multi Quantum Well (MQW) modulators is preferred because the device is compact, uses negligible power and is polarization insensitive.

Proposed System

A proposed optical link for the readout of an inner tracker detector module is illustrated in Fig.1. Data transfer from the frontend uses monomode fibre ribbon, with the conversion from electrical to optical signals being performed at the frontend by MQW modulators at an optical wavelength of 1550nm. At the backend a tranceiver module, comprising lasers and photodiodes, mounted on a readout board and connected via optical splitters and couplers, transmit and recover the optical and electronic signals. As the link is reflective, a single fibre carries light from the laser to the the modulator and also returns the reflected (modulated) light to the photodiode. In the near future, the transceiver will be hybridised with the lasers and photodiodes mounted directly on substrates containing waveguides that form the splitters and couplers. Another possibility is to integrate the lasers, photodiodes and light guides into compact Opto-Electronic Integrated Circuits (OEICs). Although an attractive solution, timescale and cost factors disfavour this option.

To ease the installation and maintenance of the frontend and backend equipment, three optical link breakpoints are foreseen, two at the detector and the other at the readout board interface.

Modulator Characteristics

The modulators are designed and built by GEC-Marconi Materials Technology [4]. They are vertical cavity semi-conductor structures operated in reflection mode, thus suitable for fabrication as compact arrays which can be coupled directly to optical fibre ribbons.

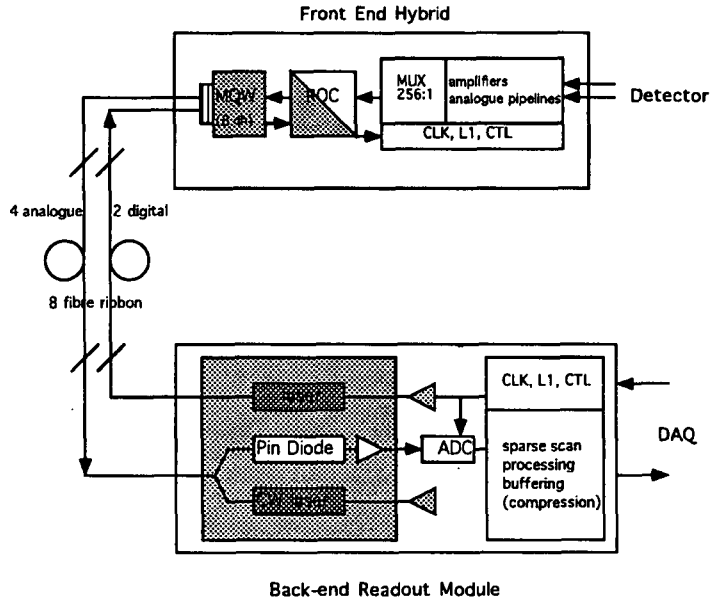

Figure 1: *Schematic diagram of proposed RD23 optical link.*

Reflectivity changes of $\Delta R \sim 10\%$ have been measured at $\lambda \sim 1540$ nm for an input voltage swing of $\Delta V \sim 3V$, corresponding to the linear range of the transfer function. As well as being used as transmitters, the MQW devices can also be used reversibly as photodetectors operating at $\lambda \sim 1300$ nm. This useful feature allows the proposed RD23 optolink to be used bidirectionally, that is, to send timing, trigger and control information as well as reading out analogue data.
Criteria that any frontend electro-optical device must satisfy for use on the inner tracker are as follows:

1. Radiation hard to 10 Mrad of γ radiation; $\sim 10^{14}$ neutrons cm^{-2} (similar rate for charged hadrons).

2. Operate satisfactorily in magnetic fields of 2 Tesla and at temperatures around -10degC.

3. Restrictions on cooling and power supplies limit power consumption at frontend, hence device must be low power.

4. Must have high degree of reliability due to minimal access to inner tracker.

All these points have, or are being, investigated. Irradiation of the MQW chips has been performed with neutrons (fluence $\Phi \sim 1.3 \times 10^{14}$ n cm^{-1}) and Co^{60} γ rays (accumulated dose D $\sim$ 20 Mrad) [5]. The spectral reflectance characteristics measured before and after irradiation did not show any significant change. Similar tests have been done on optical fibre and radiation hard fibres have been identified. Also based on spectral reflectance measurements, the induced effects of temperature and magnetic field variations on MQW chips has been modelled. Studies at Birmingham [6] have shown that for fields up to 4T there is negligible change in the MQW characteristics.

System Performance

The overall link performance is evaluated by measuring its transfer function (transceiver voltage output vs. frontend modulator input), linearising it around its quadrature point and determining the linear range of operation for a $\pm 1\%$ maximum deviation from linearity. The peak signal to noise ratio (SNR) can then be defined as the maximum linear output voltage range divided by the output rms voltage noise. The overall performance is dependent on all individual components, including fibre ribbons and optical connectors. Results have been obtained using a 4-channel transceiver assembled with discrete fibre couplers, giving a gain of $G_t \sim 0.43$ V/μW in a bandwidth B $\sim$ 30 MHz. The link uses a 100m length of non rad-hard monomode fibre, with two breakpoints based on angle-polished MT-8 connectors. All modulators used to date are 4-channel but future versions will contain 8-channels.

Measurements made by both Birmingham and CERN have revealed that for some of the better modulators, SNR values of $\sim$ 150 are possible. However, looking at all the channels on all the modulators reveals a wide spread in performance, with only 70% of the channels having a signal to rms noise ratio greater than 100:1. This is expected to improve with the next phase of modulator development as the assembly process becomes more mature. Also, the chips used in the current modulator packages have a 50% modulation efficiency deficit compared to devices issued from previous growths, so a factor of two improvement is expected by using the original chip growths.

The optical link has also been integrated into a complete readout chain in the 1995 Atlas-SCT tests in the H8 beam at CERN. The set-up incorporated a silicon strip detector and APV5 frontend readout chip; an MQW modulator mounted near the APV5; 100m of fibre ribbon, transceiver and readout using Sirocco modules. Off-line analysis is still under way but preliminary results are encouraging. Figure 2 shows a typical comparison of the default (LED based) readout with the MQW based readout. They agree well. The signal is seen at 10 units and is measured by summing the (pedestal subtracted) pulse height information from two adjacent strip pairs and comparing with the noise from those channels. The noise peak at zero is removed by a 2.5 σ cut.

Future Developments

Birmingham's role within the RD23 collaboration [6,7,8,9,10,11] will be to continue testing and evaluating various aspects of the MQW-modulator optical link. In particular, a team comprising GEC/Marconi and the Birmingham group will be modelling and measuring noise on optical links to understand how this would affect performance of LHC readout. Studies will also continue on alternative modulator technologies, notably the silicon-based modulators being produced by Bookham Technology Ltd.

In parallel, the RD23 collaboration will be addressing some of the main questions concerning the fully integrated analogue optical link which can be summarised as: (*i*) does it offer the required performance and reliability, and (*ii*) can it be produced by industry in volume quantity at affordable cost.

The Birmingham group also intends to extend its expertise by studying links using active sources (LEDs or Laser Diodes) on the detector. In particular the MQW laser diodes are inherently very efficient in terms of optical output power/electrical input power and share the radiation resistance of the MQW modulators; so it is likely that the choice between devices on the detector could be confined to MQW based devices.

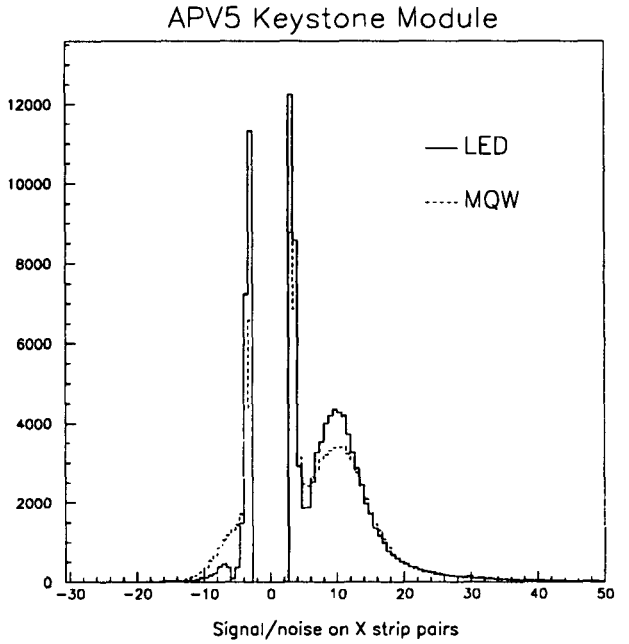

Figure 2: *Comparison of pulse height distributions using LED and MQW based readout.*

References

(1) CERN/DRDC 93-38 (1993)
(2) CERN/DRDC 94-38 (1994)
(3) CERN/DRDC 95-61 (1995)
(4) M.J.Goodwin et al., "The application of optoelectronic technologies to high performance electronic processor interconnects", Optical and Quantum Electronics, Vol 26, pp455-70, 1994.
(5) K.Gill et al., "Ionising radiation damage of optical fibre data link components in the CMS Inner Tracker", CMS TN/95-005.
(6) "Applications of Optoelectronics in High Energy Physics", M.S.Haben, PhD Thesis, University of Birmingham (1993).
(7) "Optoelectronic readout for LHC detectors", I.R.Kenyon, Proceedings of the International Conference on Computing in High Energy Physics pp 693-696 CERN 92-07, December 1992.
(8) "Lightwave Analogue Links for LHC Detector Front Ends" I.Kenyon, M.Haben, J.Dowell, K.Webster and CERN, EPFL (Lausanne), Imperial College, Lund, RAL and GEC- Marconi, Nuclear Instruments and Methods A344 199-212, (1994)
(9) "Analogue optical links for the front end at LHC"; J.D.Dowell (for RD23), 22nd International Conference on High Energy Physics, Glasgow July 1994.
(10) "Investigation of the Use of Optical Modulators for Analogue Data Readout from Particle Physics Detectors", K.Webster, PhD Thesis, University of Birmingham (1995).
(11) "AnalogueSignal Transfer Using MQW-Modulator Based Optical Links", I.Dawson et al., ATLAS SCT Workshop; Oxford (1995).

Development of High Resolution Silicon Strip Detectors for Experiments at High Luminosity at LHC

RD20 **Proposal 807**

NCSR Demokritos Athens, Bonn University, Comenius University Bratislava, CERN, INP Cracow , FNPT Cracow, MPI Heidelberg, Liverpool University, Brunel University, Imperial College London, CPPM Marseille, Oslo University, SINTEF Oslo, INFN Padova University ,INFN Roma Sanità , Rutherford Appleton Laboratory, LEPSI Strasbourg, INFN Torino, Uppsala University, IHEP Vienna, PSI Würenlingen

1 Introduction

The aim of this project has been to develop the elements of a high spatial precision tracking detector for use in LHC experiments based on silicon microstrip detectors and radiation hard front end electronics. The project is now reaching a conclusion and the final status report is due to be presented in January 1996. For this reason, the current report is a brief summary of progress in the last year. A final summary will be prepared after the concluding status report.

The emphasis in the UK in the last year has been on the completion of the front end electronics chip, now in a working 128 channel radiation hard form, and on bulk radiation damage studies of silicon where significant progress has been made in understanding the microscopic origins.

2 Bulk damage studies of detectors

The origin of bulk damage in silicon at the microscopic level has been poorly understood as, although some defect complexes have been identified in many irradiation studies, there are a large number of less well understood defects and some of these may be implicated in the observations. Recently, however, a combination of experimental measurements of primary defect introduction rates and a numerical model of the evolution of complex defects, has shed more light on the phenomena which underly the experimental data and may offer real possibilities of hardening the detector material if the concentration of various impurities, such as oxygen and carbon, can be altered. A model based on deep acceptor states in the material appears to explain most of the experimental results on bulk damage in high resistivity silicon detectors. Candidates for the traps have been tentatively identified as vacancy-oxygen complexes with the aid of numerical simulations. The concentration of oxygen and carbon in the silicon is important in influencing the concentration of deep traps and may allow the possibility of improving the hardness of detectors. The model provides a semi-quantitative explanation of the observed data but needs further extensions and tests to be fully verified.

Some time ago the suggestion was made that type inversion in silicon could be explained by means of the creation of deep acceptor states. Deep levels are states found near the centre of the band gap, while shallow levels are found closer to the band edges. Deep levels can exist in different charge states depending on other conditions in the material. In unbiased material in thermal equilibrium the occupation of a state depends on Fermi-Dirac statistics and is calculable if the concentration of states and their energy levels are known. In biased material the situation is more complex because the charge state depends on the energy level but also on the density of free carriers. Thus it is necessary to solve Poisson's equation for the electric field, satisfy the current continuity conditions and include the correct occupancy statistics.

Such calculations were first carried out by Watts and collaborators at Brunel University. They hypothesised that after high particle fluences the bulk material was close to intrinsic silicon and, to simplify the calculations, assumed a single deep acceptor level at the middle of the forbidden energy gap. Using the measured value of current density as a function of fluence and Shockley-Read-Hall statistics, they carried out a numerical semiconductor simulation in which they calculated the depletion voltage as a function of fluence.

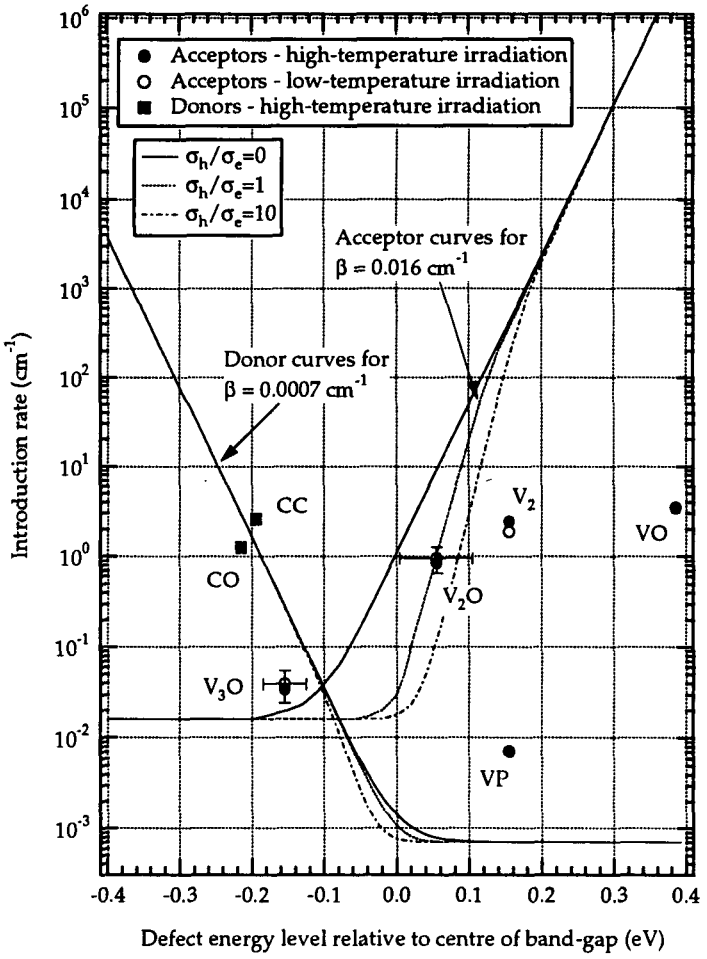

Fig. 1. The lines ascending to the right show the introduction rate for an acceptor state at a given energy level required to give β = 0.016 cm^{-1} for different assumptions of electron and hole cross-sections. Circles show known or possible acceptor state introduction rates from the model, squares show known donors. The lines ascending to the left show the introduction rate of donor states required to be consistent with the presence of CO and CC states. They correspond to β_{donor} = 0.0007cm^{-1}.

In this calculation there is only one free parameter, which is the introduction rate of the acceptor state. This was adjusted to ensure that effective doping at high fluence conformed with data. Changing the assumption that the acceptor is not at mid-gap leads to a simple scaling of the result so that the required introduction rate can be plotted as a function of the energy level of the state (fig.1). With these simple assumptions it is possible to explain the observed behaviour of silicon diodes after neutron irradiation: detectors show effective type-inversion when under bias and the trend of effective doping concentration with fluence is explained well (fig. 2).

The essence of the hypothesis has been verified by observing the depletion behaviour of diodes under illumination; it is clearly observed that irradiated detectors behave differently to non-irradiated ones in a manner consistent with deep traps being filled by photo-generated carriers.

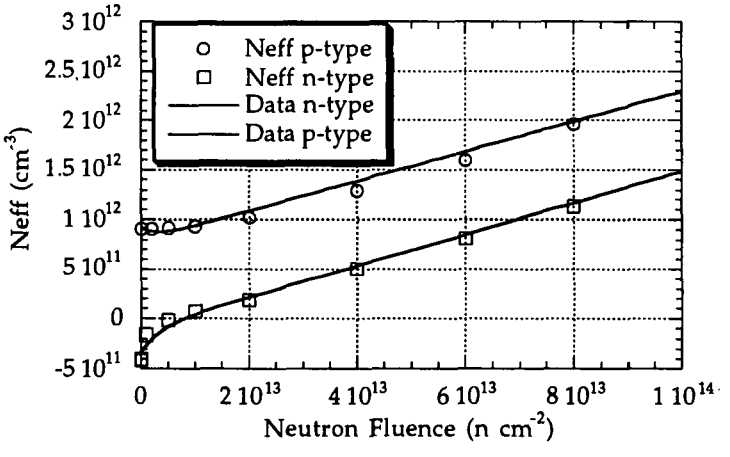

Fig. 2. N_{eff} vs 1 MeV neutron flux for n- and p-type silicon. Lines represent fits to data from the RD2 collaboration and symbols are from model calculations.

A computer model of defect evolution which was developed to explain optical absorption data from electron irradiated silicon has been applied by MacEvoy et al. at Imperial College to attempt to understand better the concentrations of important defect species during irradiation. Measured

introduction rates of interstitials, vacancies and primary divacancies from electron and neutron irradiation were used as input and the model was applied to investigate the evolution of defects in high resistivity detector material during neutron and gamma irradiation to levels expected at the CERN LHC. The results were compared in several cases with experimental data in the literature and found to be in good agreement. Two strong candidates for deep acceptors were identified - V_2O and V_3O.

3 Electronics

The RD20 front end chip is based on a 50-75nsec time constant amplifier and a pipeline memory followed by an analogue signal processor, which implements a deconvolution algorithm, to limit the output pulse to a single beam crossing interval. The pulse processing is carried out by forming a weighted sum of consecutive temporal samples of the amplifier output voltage using a switched capacitor circuit.

The chip has now been implemented in the Harris AVLSI-RH 1.2μm bulk CMOS radiation hardened process. The APV5 chip contains 128 channels of amplifiers, pipeline and signal processing along with a multiplexer. The wafers containing the chips were received in May 1995 and several beam tests for both CMS and ATLAS were carriedo ut over the summer. The chip is fully functional but there are a number of areas where improvements are required: gain and pedestal variations, multiplexer speed and excess noise. The origin of each of these has now been understood and layout is under way for the next submission: the APV6 which should be delivered in summer 1996. The development continues in the context of the CMS experiment.

Publications since October 1994

Measurements of transistors and silicon microstrip detector readout circuits in the Harris AVLSIRA rad-hard CMOS process M. Raymond, G. Hall, M. Millmore, R. Sachdeva, M. French, E. Nygård, K. Yoshioka. Nucl. Instr. & Meths. A351 (1994) 449-459

Radiation hard electronics for LHC M. Raymond, G. Hall, M. Millmore, R. Sachdeva, M. French, E. Nygård, K. Yoshioka. Nucl. Instr. & Meths. A360 (1995) 162-165.

*Radiation damage studies of field plate and p-stop silicon microstrip detectors*J. Matheson, H-G. Moser, S. Roe, P. Weilhammer, S. Moszczynski, W. Dabrowski, P. Grybos, M. Idzik, A. Skoczen, K. Gill, G. Hall, B. MacEvoy, D. Vite, R. Wheadon, P. Allport, C. Green, J. Richardson, R. Apsimon, L. Evensen, B. Avset, P. Giubellino, L. Ramello. Nucl. Instr. & Meths. A362 (1995) 297-314.

A microscopic explanation for type inversion and the annealing behaviour of radiation damaged silicon detectors. J. Matheson, M. Robbins, S. Watts, G. Hall, B. MacEvoy. Submitted to Nucl. Instr. & Meths.

Defect evolution in irradiated silicon detector material. B. MacEvoy, G. Hall, K. Gill. To be published in Nucl. Instr. & Meths.

Radiation damage to silicon detectors. G. Hall. To be published in Nucl. Instr. & Meths.

APV5RH: a 128 channel radiation hard pipeline chip for LHC tracker applications
M. French, L. Jones, P. Murray, P. Seller, M. Raymond, G. Hall. Proceedings of 1st Workshop on Electronics for LHC Experiments, 120-126.

Further experimental support for the deep-acceptor model K. Gill, G. Hall and B. C. MacEvoy. Paper presented at 2nd International Conference on Large Scale Applications and Radiation Hardness of Semiconductor Detectors, Florence, May 1995. To be published in Il Nuovo Cimento.

CERN-RD42 Diamond Detectors Proposal 812

MPI-Heidelberg; LEPSI, Strasbourg; Rutgers University; CPPM, Marseille;
IHOAW, Vienna; Ohio State University; Bristol University; Los Alamos National Lab.;
CERN; Sandia National Lab.; Lawrence Livermore National Lab.;
Universita di Pavia; University of Toronto

The physical properties of diamond are exceptional in many ways, in particular they are well suited to its use as a solid-state detector in radiologically harsh environments. The available evidence is that diamond is extremely resistant to radiation damage while silicon undergoes substantial changes at the fluences expected after a few years operation of a vertex detector at the LHC. Cosequently devices similar to silicon microstrip or pixel detectors but made of diamond are very attractive, and are feasible because the Chemical Vapour Deposition process makes it possible to manufacture microcrystalline diamond in thin sheets of adequate area.

The principal drawback of diamond is the small signal size. This is in part an unavoidable consequence of the smaller number of electron/hole pairs created by minimum-ionising particles travelling through diamond, but is also a result of the trapping of moving electrons and holes within the material. The performance of a particular sample may be characterised by quoting a "charge recombination length" which is the mean separation of electrons and holes before they become trapped. Over several years the RD-42 group has collaborated with a commercial producer of CVD diamond in the USA (the Norton Steel Company, now owned by the French multi-national St. Gobain) to improve this parameter, which is now about 120 μ-metres in the best samples.

Over the last year this program has continued, and has been supplemented by successful production of detector-grade CVD diamond by the de Beers company. Diamonds from both manufacturers have been tested using energetic β-rays in "characterisation stations" at Ohio, CERN and Strasbourg, and information on their performance fed back to the manufacturers. Some samples have been remetallised with microstrip electrodes and tested in pion beams at the CERN SPS with encouraging results.

In parallel with this work, RD-42 has been further investigating the radiation hardness of diamond by exposing some of the test pieces to very intense low energy pion beams at the Paul Scherrer Institute, to neutron fluxes at ISIS, to α particles at a van-der-Graaf facility in the USA and at the Max Planck Institute in Heidelberg, and to powerful gamma sources. So far the results of these tests have been very encouraging. The signal size is found to *increase* by about a quarter during initial radiation exposure under high voltage and thereafter to remain constant up to the highest fluences tested, with the exception of the α studies which show some degradation at fluences beyond likely LHC exposures.

Publications:

F. Borchelt et al., "First Measurements with a Diamond Microstrip Detector", Nucl. Instr. and Meth. **A354** (1995) 318.

C. Bauer et al., "Pion Irradiation Studies of CVD Diamond Detectors" submitted to Nuclear Instruments and Methods A.

C. Bauer et al., "Recent Results from the RD-42 Diamond Detector Collaboration" invited paper to Hiroshima conference on Vertex Detectors, 1995

W. Dulinski et al., "Recent Results from CVD Diamond Trackers", in the Proceedings of the 1995 Vienna Wire Chamber Conference to appear in Nuclear Instruments and Methods A.

RD-42: DETECTOR CURRENT versus PION FLUENCE

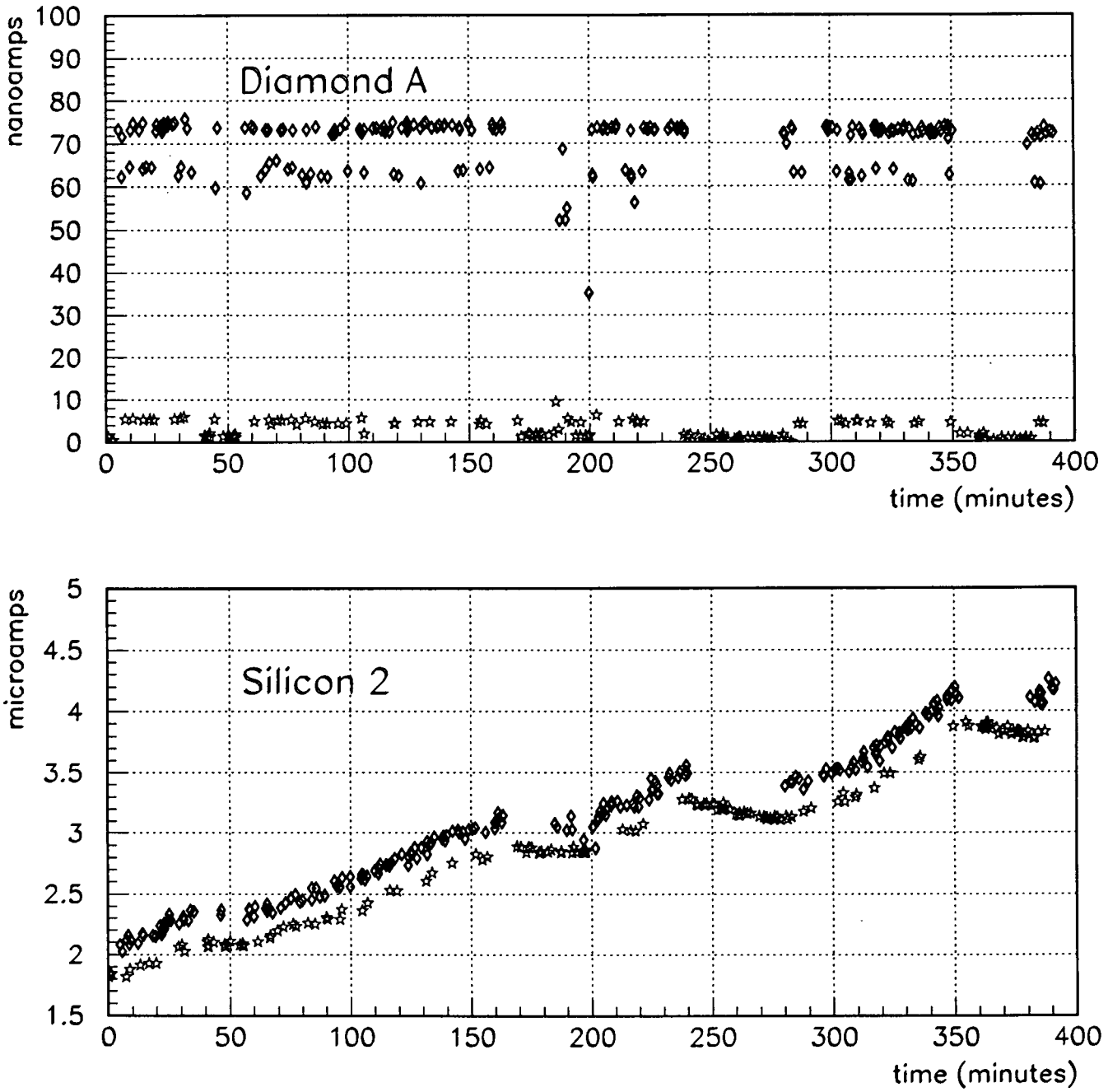

The diagram shows the current in a diamond detector and a silicon diode simultaneously exposed to an intense pion beam at the Paul Scherrer Institute. The pion beam fluctuates between two different intensities (both shown as diamonds in the diagram), and is sometimes off (stars). The pion fluence is 4×10^{12} pions/cm^2 on the left-hand side of the diagram and 1.4×10^{13} pions/cm^2 on the right. The cumulative effect of radiation damage in the silicon is clearly visible, although it is partly reversed by annealing during the beam off periods. Note the difference in the current scales.

DENSE, FAST, RADIATION-TOLERANT FLUORO-HAFNATE GLASS SCINTILLATORS FOR ELECTROMAGNETIC CALORIMETERS IN HIGH ENERGY PHYSICS

PROPOSAL 883

Brunel University; Rutherford Appleton Laboratory; University of Sheffield

INTRODUCTION

Work has continued on the development of fluoride glasses with a view to understanding their strengths and limitations as an alternative to crystals in homogeneous calorimeters. A priority in the work over the last year has been the need to develop techniques for manufacturing larger blocks, but also, more detailed studies have been carried out to determine the effects of various dopant concentrations.

GLASS PRODUCTION

The initial hafnium glass formulations used, could only be cast to a maximum of 10 mm thick. Research has lead to the development of new formulations which can now be cast to 21 mm thick. A block of high quality 21 mm by 30 mm by 140 mm has now been manufactured at Sheffield University and preparations are underway to construct an array of 6 calorimeter cells 20 mm by 30 mm by 280 mm for beam line tests.

The work on the development of large blocks was aided by PIPSS grants and there has been close collaboration with industrial partners from Merck and Johnson Matthey. An important outcome of this close collaboration has been the demonstration that it is possible to simplify the processing of the raw materials, and hence reduce their cost, yet still produce high quality glass by carefully controlling the production conditions, Figure 1 shows the critical dependence of optical transmission on the atmosphere under which the glass is prepared.

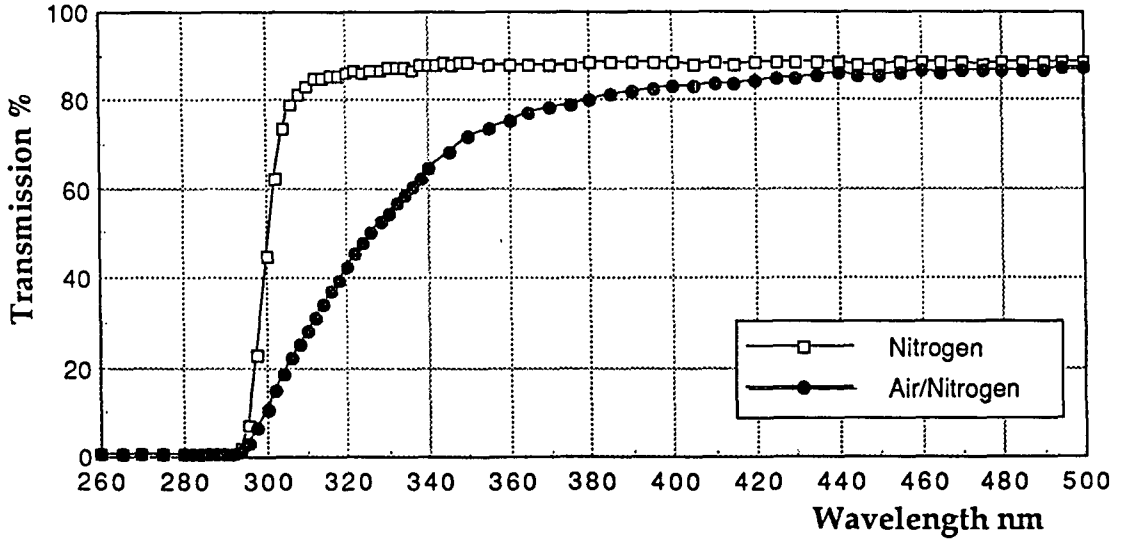

Fig. 1 Showing the effect of melting atmosphere schedule on UV transmission

LIGHT YIELD

The scintillation yields were measured relative to a CeF_3 crystal using a secondary charged-particle beam at the proton synchrotron accelerator of the ISIS neutron spallation source at the Rutherford Appleton Laboratory. The beam line was tuned to accept protons with a

mean momentum selected in the range from 540 to 750 MeV/c. At these momenta the protons are below threshold for directly producing Cherenkov light in the sample (the threshold is 840 MeV/c for a refractive index of 1.5). This is an important consideration since even a small contribution from Cherenkov photons can bias fits to scintillation decay curves. Scintillation light was detected by a Thorn EMI 9814QKB photomultiplier. The photomultiplier signal was recorded on a 1 G Sample/s digital oscilloscope, using a gate width of 500 ns.

For a given basic glass composition, the light yield was found to increase monotonically with cerium content up to the maximum concentration that could be incorporated into a stable glass. Typically, a glass containing cerium fluoride at a concentration of 5% (molar) gives a light output per MeV of energy deposited which is approximately 10% that of a cerium fluoride crystal. Figure 2 shows the variation of light yield with cerium fluoride concentration for a set of glasses with a composition HBCeAN.

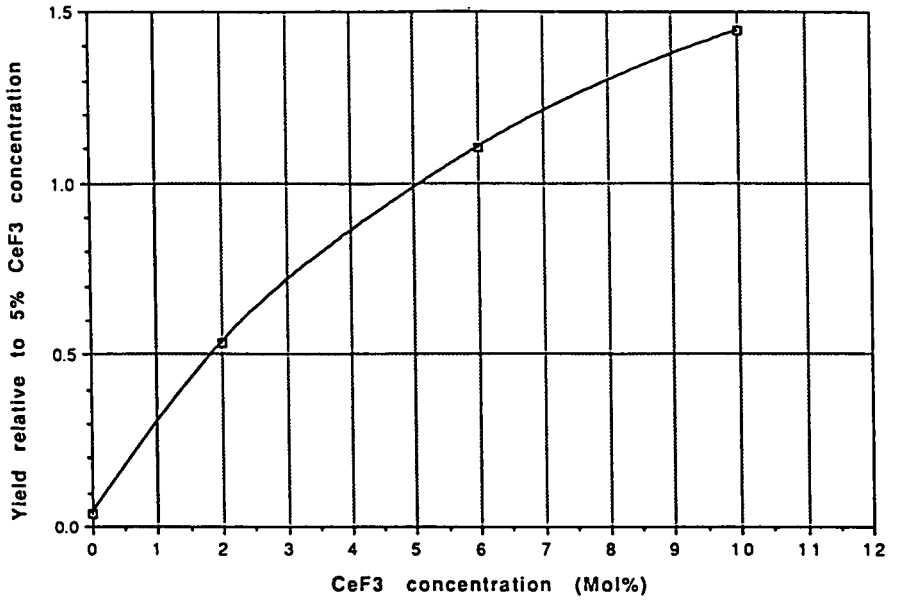

Figure 2 The measured light yield plotted against CeF_3 concentration, for a set of glasses of composition 'HBCeAN'. The yield has been normalised to unity for 5% CeF_3 concentration.

DECAY TIME SPECTRA

Scintillation decay time spectra were obtained by two methods. In one approach, several thousand individual digitised wave forms, recorded with protons at ISIS, were summed to give an average pulse shape. The other measurement, performed at Brunel University, used a standard delayed single-photon technique, with an additional multi-photon veto logic. The sample was excited by an annihilation photon from a 10 mCi Na^{22} positron source, the other photon was detected in a BaF_2 crystal which started a fast time-to-amplitude converter. The data were collected over a time window of 2000 ns, with a single-photon timing resolution of 1.40 ns.

Figure 3 shows a typical decay time distribution obtained with protons. In the range from 0 to 250 ns, the curve is well fitted by the sum of three exponentials:

$$I(t) = I_0(ae^{-t/\tau_1} + be^{-t/\tau_2} + ce^{-t/\tau_3})$$

where $\tau_1 = 11$ ns, $\tau_2 = 25$ ns, $\tau_3 = 62$ ns and the coefficients a, b and c are in the ratio 0.16:1.0:0.26.

Since the three terms are strongly correlated in the fit, the decay spectrum is more usefully characterised by considering the fraction of the light yield contained within a given time interval. Integrating under the curve, one finds that 53% of the light is emitted in the first 25 ns. This result is very similar to that obtained with a single crystal of CeF_3.

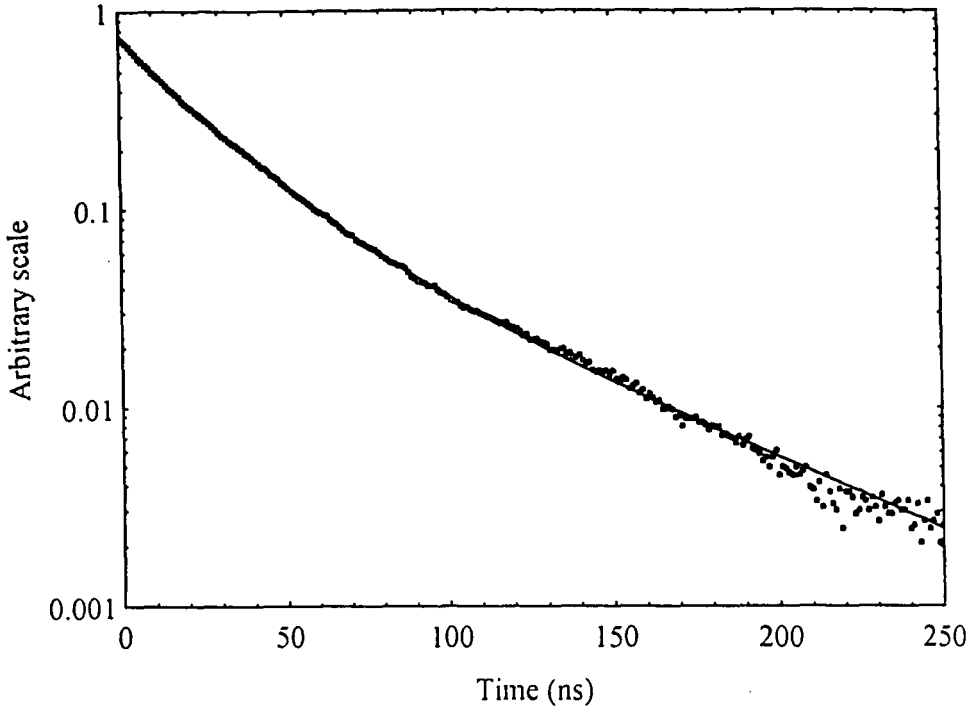

Figure 3 The measured decay time spectrum for scintillation light from a sample of Ce doped fluorohafnate glass (HBCeALi). The smooth curve is a fit to the data and is the sum of three exponential terms: $I(t) = I_0(ae^{-t/\tau_1} + be^{-t/\tau_2} + ce^{-t/\tau_3})$ where $\tau_1 = 11$ ns, $\tau_2 = 25$ ns, $\tau_3 = 62$ ns and the coefficients a, b and c are in the ratio 0.16:1.0:0.26.

TRANSMISSION AND EMISSION SPECTRA

Emission spectra have been measured using X-ray (~ 9 keV) and ultraviolet light (284 nm) excitation, with similar results. Figure 4 shows the fluorescence spectrum obtained for a fluorohafnate glass (HBCeA) containing CeF_3 at a concentration of 8% (molar). The spectrum is dominated by an emission band centred at 320 nm, which is attributed to radiative transitions from the lowest excited 5d-level of Ce^{3+}, to the 4f ground state.

The optical transmission as a function of wavelength is shown on the same plot. It can be seen that the emission spectrum lies close to the band-edge. Good optical transmission just above the cut-off is therefore crucially important for detectors using large blocks of glass, if significant self absorption of scintillation light is to be avoided.

RADIATION DAMAGE

Radiation damage in glasses is characterised by the development of optical absorption bands which result from the creation and population of defects known as colour centres. The development of these absorption bands is consistent with the irradiation creating and populating new defect sites and the sites relaxing either spontaneously or as a result of irradiation, or both. The absorbance at a particular wavelength saturates as a function of dose.

In an LHC experiment the radiation dose in the electromagnetic calorimeter will be dominated by electromagnetic showers produced by high energy photons from p^0 decays. As a result, the dose will vary with depth in the calorimeter (being greatest at the position of

the average shower maximum) and will be higher close to the direction of the colliding beams (the 'forward' regions) than at larger angles with respect to this axis (the 'central' region). The estimated dose in the central region, averaged over the first eight radiation lengths of the detector, is 0.4 kGy/year. In order to investigate the ability of our glasses to withstand these large radiation levels, samples were irradiated with a 4 Ci Co^{60} source at Brunel. Doses of up to 6 kGy were delivered in 5 days (at a dose rate of 12 m Gy/s), corresponding to more than 10 years of operation in the central region at LHC.

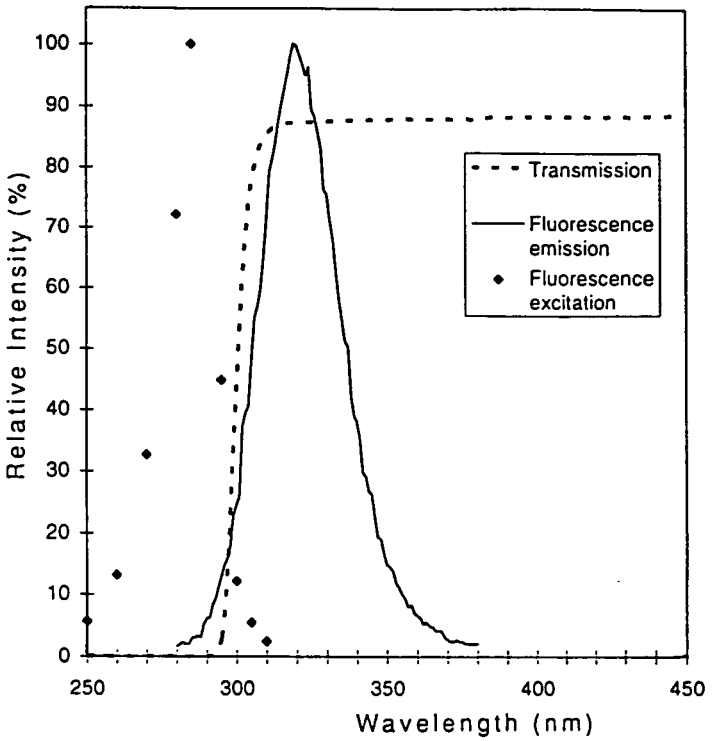

Figure 4 Fluorescence excitation and emission spectra for a cerium doped fluorohafnate glass together with the optical transmission measured for the same sample.

All undoped fluorohafnate glasses studied proved to be quite susceptible to radiation damage, the internal transmission at 325 nm of a 5 mm thick sample typically falling to 5% of its initial value after 6 kGy. Studies were therefore made to determine the effect of various dopants (Fe, Ga, Nb, In, Pr, Nd, Sm, Eu, Gd, Ho, Er, Yb, Lu) on radiation hardness. In some cases the effect was quite dramatic. Thus for example adding 1.5% (molar) of EuF_3 to HBLA resulted in a glass which exhibited negligible damage at wavelengths above 400 nm for doses in excess of 6 kGy. Unfortunately strong damage was still observed in the Ce^{3+} emission region from 300 to 350 nm.

The dopant which was found to minimise radiation damage in the Ce emission region is indium, the magnitude of the effect depending quite sensitively on the concentration (figure 5). Curve II in this figure shows how the radiation-induced optical attenuation (at 350 nm), measured immediately after a dose of 2.4 kGy (Co^{60} g-ray), varies with indium concentration. The addition of indium has the undesired effect of reducing the light yield from Ce doped glass, as can be seen from curve I. However, for an indium concentration of 0.5%, which maximises the radiation hardness, the loss in light yield (from a small sample) is only 30%.

Since the radiation dose received by a calorimeter at LHC would be spread over the ten year lifetime of the experiment, the effect of thermal annealing over a long interval at room temperature should also be taken into account. Curve III in figure 5 shows how the radiation-induced attenuation length varies with indium concentration for a much larger dose (7 kGy delivered in 7 days) followed by storage for 4.5 months in the dark at room temperatures. Comparing curves II and III it can be seen that self annealing largely offsets

the effect of the bigger radiation dose for indium concentrations of 0.8% and above. At lower indium concentrations self annealing occurs to a greater degree and this is particularly evident for the point at 0.2% concentration. However, the optimum indium concentration still appears to be close to 0.5%, even allowing for self annealing.

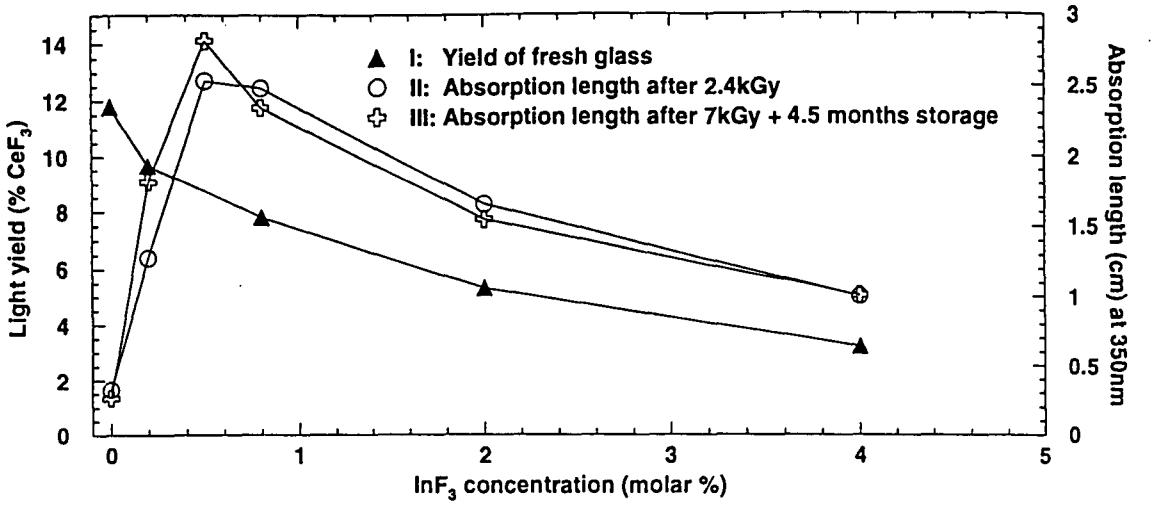

Figure 5 The effect of InF_3 doping on the light yield and radiation hardness of a glass with basic composition 'HBCeAN', containing 5% (molar) CeF_3.
Curve I (triangles) shows the variation of light yield versus InF_3 concentration. The yield is normalised to the yield obtained from a crystal of CeF_3 of similar dimensions to the glass samples.
Curve II (open circles) shows the variation of radiation-induced optical attenuation at 350 nm, measured immediately after a dose of 2.4 kGy. (Co^{60}-γ).
Curve III (crosses) shows the optical attenuation induced by a dose of 7 kGy, followed by 4.5 months storage in the dark at room temperature.

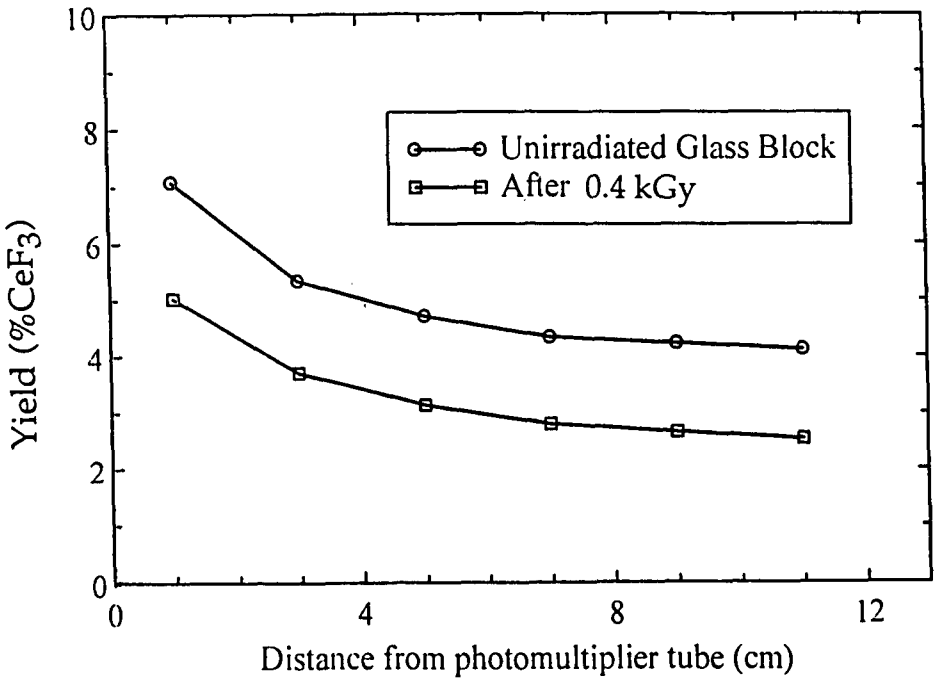

Figure 6 The light yield as a function of position along the length of a block (dimensions 13 x 3 x 1 cm^3) of fluorohafnate glass (HBCeALi) doped with 0.5% (molar) InF_3.
The upper curve was obtained before irradiation. The lower curve was measured immediately following a 0.4 kGy dose (Co^{60}-γ) delivered approximately uniformly over the volume of the block.

The above studies were performed using small samples of glass (typically 1 cm^3). In order to obtain a better understanding of how the results would translate to the performance of a glass calorimeter, the effect of irradiation on light yield was measured using a much larger block of glass (HBCeALi doped with 0.5% InF_3). The block was 13 cm (8.2 radiation lengths) long with a rectangular cross section (3 x 1 cm^2). For the light yield measurements it was wrapped in Tyvek and a 2" phototube wasmounted on one end. The proton beam was directed through the 1 cm dimension at several points along the length. The block was then irradiated with a dose of 0.4 kGy in 40 hrs (~ 1 year dose at LHC), delivered approximately uniformly over the whole volume, and the light yield remeasured.

The results are shown in figure 6. Both before and after irradiation the light yield shows a strong variation as a function of distance from the phototube in the region close to the tube, whereas further from the tube the yield varies rather slowly. The loss of light from the far end following irradiation is 35%. A full sized detector would be 3 times longer than the block tested, however, the radiation dose at LHC falls off rapidly after the first 8 radiation lengths. On the basis of these data we conclude that this particular glass would satisfactorily survive one year of operation in the central rapidity region at LHC. However, ten years of operation would require some method of *in situ* annealing to be devised.

OPTICAL ANNEALING

All the glasses were stored and irradiated in complete darkness to avoid any possibility of photo-induced bleaching. After spontaneous recovery of absorbance had stabilised, several glasses were illuminated with light from a 150 W Hg arc lamp. Interference filters were used to select the 365 nm, 435 nm and 577 nm lines in the Hg spectrum. Lines above 400 nm were observed to cause little measurable change in absorbance, but the 365 nm line was extremely effective in reversing the radiation induced optical damage in some fluoride glasses. Some glasses were found to recover fully (figure 7); whereas others, including those doped with indium, recovered only partially.

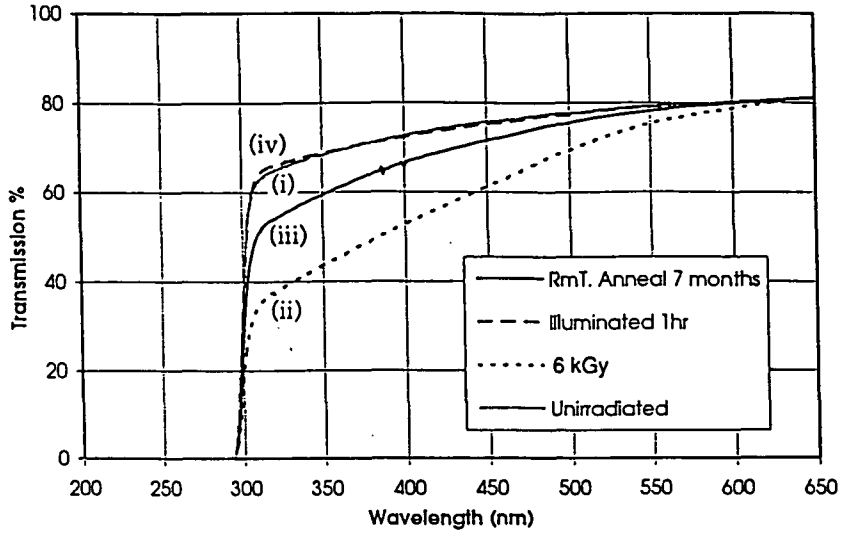

Figure 7 The measured external transmission of a fluoro-hafnate glass; (i) unirradiated, (ii) after 6 kGy, (iii) after annealing in the dark at room temperature for 7 months (where strong recovery is observed), and (iv) after illuminating with a mercury arc lamp for one hour. The glass has fully recovered after one hour of optical annealing.

CONCLUSIONS

We have demonstrated that cerium doped fluorohafnate glass could be used as the active medium in a high performance electromagnetic calorimeter for many particle physics applications. Radiation damage would be a limitation to use in the harsh environment at LHC although this might be overcome by optical annealing *in situ*.

PUBLICATIONS

[1] Dense, fast, radiation-tollerant fluoro-hafnate glass scintillators for electromagnetic calorimetry in high energy physics.
P R Hobson, D C Imrie, T Price, K W Bell, R M Brown, D J A Cockerill, P S Flower, G H Grayer, A L Lintern, M Sproston, K J McKinlay, J M Parker.
RAL Preprint RAL-P-95-003
To be published in the proceedings of Scint 95, International Conference on Inorganic Scintillators and Their Applications, Delft 1995.

[2] The industrial production of large, inexpensive blocks of scintillating fluoro-hafnate glass.
P R Hobson, T Price, D Bowen, T Cliff, B Kinsman, R Smith, R M Brown, D J A Cockerill, P S Flower, P W Jeffreys, K J McKinlay, J M Parker.
To be published in the proceedings of Scint 95, International Conference on Inorganic Scintillators and Their Applications, Delft 1995.

[3] Emission properties of cerium-doped fluoro-hafnate glasses studied by synchrotron radiation excitation.
E G Devitsin, N Yu Kirikova, V E Klimenko, V A Kozlov, V N Makhov, S Yu Potashov, L N Dmitruk, P R Hobson, T Price, K W Bell K W, R M Brown, D J A Cockerill, P S Flower, P W Jeffreys, B.W. Kennedy, G H Grayer, A L Lintern, M Sproston.
To be published in the proceedings of Scint 95, International Conference on Inorganic Scintillators and Their Applications, Delft 1995.

Laser/Plasma Particle Acceleration Experiments
Observation of Electron Acceleration from the Breaking of Relativistic Plasma Waves

Proposal 895

Imperial College, Blackett Laboratory, Prince Consort Road, London, UK
University of California at Los Angeles, Los Angeles, California, USA
LULI, Ecole Polytechnique, Palaiseau, France
Lawrence Livermore National Laboratory, Livermore, California, USA
Rutherford Appleton Laboratory, Chilton, Didcot, UK

Electrons in a plasma undergo collective wave-like oscillations near the plasma frequency. These plasma waves can have a range of wavelengths and hence a range of phase velocities. Of particular note are relativistic plasma waves[1], for which the phase velocity approaches the speed of light. The longitudinal electric field associated with such waves can be extremely large, and can be used to accelerate electrons (either injected externally or supplied by the plasma) to high energies over very short distances. The maximum electric field, and hence maximum acceleration rate, that can be obtained in this way is determined by the maximum amplitude of oscillation that can be supported by the plasma. When this limit is reached, the plasma wave is said to 'break'. Here we report observations of relativistic plasma waves driven to breaking point by the Raman forward-scattering instability induced by short, high-intensity laser pulses using the VULCAN laser at the Rutherford Appleton Laboratory. The onset of wave-breaking is indicated by a sudden increase in both the number and maximum energy (up to 44 MeV) of accelerated plasma electrons, as well as by the loss of coherence of laser light scattered from the plasma wave.

For these experiments VULCAN was used in its ultra-high power mode using the technique of Chirped Pulse Amplification (CPA)[2]. The system typically generated 25TW, 0.8 ps pulses on target with a 20 μm diameter laser spot using *f*/5 optics. The effective Rayleigh length was 350 μm. The laser was focused onto the well-defined edge of a 4 mm diameter, laminar plume of helium gas from a pulsed, supersonic gas jet located 2 mm below the focal region. The maximum intensity of 6×10^{18} W cm^{-2} is sufficient to doubly-ionise the helium gas producing a fully-ionised plasma over at least 2 mm into the jet. The exponentiation rate $ln(G(\phi, x))$ of the Raman instability, and therefore of the electron plasma wave, is approximately proportional to n_e. (the plasma density). The plasma density was controlled by varying the backing pressure of the jet and was measured (through the frequency shift of the anti-Stoke sidebands) to be linear with backing pressure from 5 bar to at least 18 bar where the electron density was 1.5×10^{19} cm^{-3}. Calculations have shown that by varying the density by a factor of 3 results in enormous changes in the final electron plasma wave amplitude.

Figure 1 shows the electron energy spectrum measured using a magnetic field dispersive spectrometer in the forward f/60 cone centred on the laser axis for three different plasma densities: 1.5×10^{19}cm^{-3} (a-c), 1.0×10^{19}cm^{-3} (d) and 0.54×10^{19}cm^{-3} (e). The number of accelerated electrons at a given energy and the maximum electron energy both show a dramatic increase as the plasma density is increased to 1.5×10^{19}cm^{-3}. The number of electrons above 20 MeV increases by at least two orders of magnitude and the accelerated electron distribution is rather flat up to 30 MeV where it begins to decrease. The highest electron energies observed were 44 MeV, the instrumentation limit. We interpret the sudden increase in electrons and maximum energy, together with broadening of the electromagnetic spectrum, as the signature that wave-breaking has occurred. The large increase in the number of electrons accelerated at the highest plasma density is consistent with the wave trapping the bulk of the plasma thermal distribution function rather than a few tail particles at low plasma densities. Indeed the (spectrometer-limited) maximum electron energy of 44 MeV is not too far from the absolute maximum of 70 MeV that a test electron would obtain, limited by dephasing in an ideal plasma wave with $\alpha=1$ which is near the relativistic warm-plasma wave-breaking limit expected for our plasma conditions.

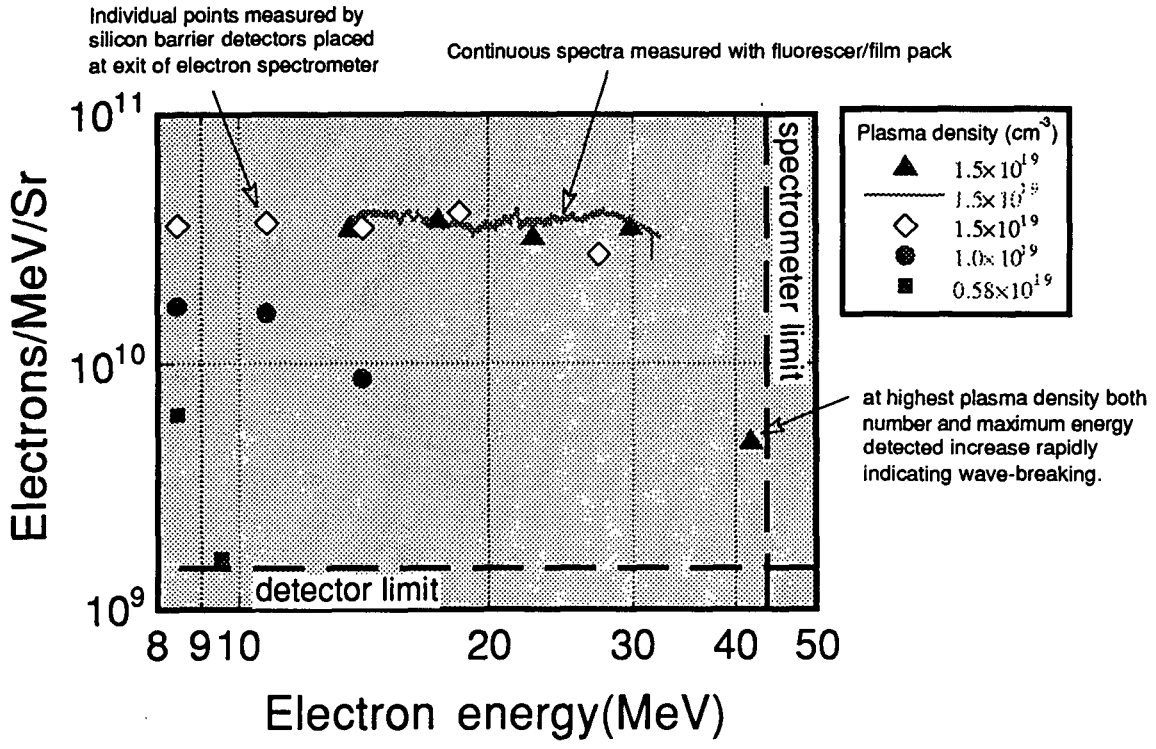

Figure 1. Energy spectra of electrons emitted due to the Stimulated Raman Forward Scatter instability resulting from the interaction of high power (35 TW) Vulcan laser with a variety of densities of plasma.

We note that the normalised transverse emittance $\varepsilon_n=\gamma\sigma\delta\theta$ of any particular energy group from this experiment is quite small. Here γ is the relativistic Lorentz factor for that energy group, σ is the source size (~10 μm), and $\delta\theta$ the angular spread (~8 mrad due to the f/60 collection cone). At 30 MeV, $\varepsilon_n=5\pi$ mm mrad which is low enough to be competitive with modern photoinjector based linacs.[3] However, the beam current measured here (~1 A in a ± 1% bandwidth around 30 MeV) is roughly 10-100 times lower than present-day photoinjector technology. The tremendous advantage over conventional linacs is the extremely short distance over which this energy is obtained. As dephasing limits the acceleration length to $\pi\gamma^3_\phi/\kappa_0\approx300$ μm, the 44 MeV that the electrons gain indicate a peak electric field of over 100 GVm^{-1} which would represent the highest collective wave-field ever produced in a laboratory. Laser technology is advancing very rapidly and it is reasonable to expect that the average current can be increased through a combination of higher laser frequencies and plasma densities as well as by increased repetition rate. Thus, one could envisage in the not-too-distant future a new class of compact accelerators based, on the breaking of relativistic electron plasma waves which may find applications where 2-200 MeV electrons or photons are needed.

References

1. T Tajima and JM Dawson, Phys Rev Lett. 45, 267-270 (1979)
2. P Maine et al., SPIE Vol. 913, 140 (1988)
3. JS Fraser and R Sheffield, IEEE J Quant Electr. 23, 1489-1496 (1987)

A more detailed account of this experiment can be found in:
A Modena, Z Najmudin, AE Dangor, CE Clayton, KA Marsh, C Joshi, V Malka, CB Darrow, C Danson, D Neely and FN Walsh. "Electron Acceleration from the breaking of relativistic plasma waves." Letters to Nature, Vol 377, 606-608, 19 October 1995.